THE TRIASSIC REPTILE *HYPERODAPEDON* FROM ELGIN: FUNCTIONAL MORPHOLOGY AND RELATIONSHIPS

By M. J. BENTON†

Department of Geology, The University, Newcastle upon Tyne NE1, 7RU, U.K.

[Plates 1 and 2]

CONTENTS

† Present address: Department of Zoology, University Museum, Parks Road, Oxford, OX1 3PW, U.K.

The rhynchosaur *Hyperodapedon gordoni* from the late Triassic of Elgin, northeast Scotland, was a squat 1.3 m long reptile with a specialized skull. The partial remains of about 35 individuals were studied largely from casts. There is a broad size range (? age), and two morphs may be distinguished on the basis of proportions (? sexual dimorphism).

Hyperodapedon had a large nasal capsule and a large eye with sclerotic plates. These indicate a good sense of smell and diurnal vision. There was no tympanum, but *Hyperodapedon* could probably detect sound via skin behind the quadrate, and via its throat and large hyoids.

Evidence from the jaw articulation and tooth wear shows that *Hyperodapedon* had a precision-shear bite. Food was probably scraped up with the premaxillary beak and manipulated by a powerful tongue. The batteries of teeth on maxilla and dentary retained open roots throughout their functional life with no normal reptilian replacement. The hindlimb was adapted for scratch-digging, from a comparison of its claws with those of modern mammals. The diet probably consisted of tough, but not hard, plant material.

The forelimb may have been held in a semi-sprawling pose with humerus rotation important in locomotion. The hindlimb was adapted for a semi-erect gait and the femur moved back and forwards with little rotation.

Hyperodapedon is found in aeolian sands, and its skeletons show little physical disturbance, although there is evidence of scavenging.

The late Triassic rhynchosaurs from Elgin, India, Brazil and Argentina form a close taxonomic group quite distinct from those of the middle Triassic, on the basis of univariate and multivariate analyses. The Indian form is returned to the genus *Hyperodapedon* as *H. huxleyi* since it is so similar to the Elgin form. *Hyperodapedon* differs from the South American *Scaphonyx* in the presence of lingual teeth on the dentary.

The early Triassic *Mesosuchus* probably belongs to a separate family rather distinct from the true Rhynchosauridae. Rhynchosaurs have no special relationship with the sphenodontids, and they form a distinct, and important, lineage within the Permo-Triassic diapsid radiation.

1. INTRODUCTION

Rhynchosaurs were a widespread group of reptiles restricted to the Triassic Period. Representatives of the group are known from the early, middle and late Triassic of southern Africa, South America, India, North America, England and Scotland (Chatterjee 1980a). The ecological role of the rhynchosaurs is currently controversial, their diet being described as rhizomes and fruit (Sill 1971a) or molluscs (Chatterjee 1974). It is important to assess the adaptive zone occupied by the group because of their dominance of many middle and late Triassic terrestrial faunas.

The relationships of the rhynchosaurs to other reptiles, and to each other, are currently under discussion. They have normally been classified as Lepidosauria, closely allied to the living tuatara *Sphenodon* (Romer 1966), but there are now arguments for closer affinities with Prolacertiformes and Thecodontia (Cruickshank 1972; Benton 1983c). Current classifications of the rhynchosaur group include a stratigraphically based scheme (Chatterjee 1969, 1974; Sill 1971b) and a geographic arrangement (Chatterjee 1980a).

The Elgin rhynchosaur, *Hyperodapedon gordoni*, was described briefly by T. H. Huxley in 1859 on the basis of a partial skeleton and skull collected by the Reverend Dr George Gordon. Huxley (1869) described this specimen and others, and concluded that *Hyperodapedon* was closely related to *Rhynchosaurus* Owen, 1840 from the middle Triassic of England, and ascribed material to *Hyperodapedon* from the Triassic of the English Midlands and Devon, and from India. The English material is apparently one or more large species of *Rhynchosaurus* (Walker 1969), and the Indian material is now named *Paradapedon* (Huene 1938; Chatterjee 1974). The Elgin reptile beds had been considered to be Devonian in age until 1859, and most doubts were removed when Huxley (1869) demonstrated the close affinities of *Hyperodapedon* to undoubted Triassic rhynchosaurs (see Newton (1893) and Benton (1977, 1983b) for details of the history of the question of the age of the Elgin reptile beds).

Further material of *Hyperodapedon* was described by Huxley (1887), Burckhardt (1900),

Boulenger (1903) and Huene (1929, 1938, 1939 b). Because of the poor preservation of the bone, these authors disagreed about the location of important suture lines, and their accounts were rather generalized. Boulenger (1903) also erected a new genus, *Stenometopon*, based on a specimen that supposedly differed from *Hyperodapedon*.

Specimens of *Hyperodapedon* have been collected from three quarries near Elgin: Lossiemouth (East), Lossiemouth (West) and Spynie. The sediments belong to the Lossiemouth Sandstone Formation (Warrington *et al.* 1980), and they indicate aeolian conditions of deposition. The associated fauna consists only of reptiles (procolophonid *Leptopleuron*, rhynchocephalian *Brachyrhinodon*, thecodontians *Stagonolepis*, *Ornithosuchus*, *Erpetosuchus* and *Scleromochlus*, and coelurosaurian dinosaur *Saltopus*), and indicates an age assignment probably in the early Norian (Walker 1961). In several respects, the Elgin fauna closely resembles that of the Maleri Formation, India (Chatterjee & Chowdhury 1974).

The aims of the present study have been to:

(i) describe the osteology of the Elgin rhynchosaur *Hyperodapedon* on the basis of much unstudied material and with use of new casting techniques, and to reconstruct soft parts where possible;

(ii) assess the functional morphology of *Hyperodapedon*, and of other rhynchosaurs, from the large amount of new data derived from the anatomical study;

(iii) establish the most likely niche occupied by *Hyperodapedon* and other large rhynchosaurs, and to reconsider their ecological significance in the Triassic;

(iv) consider the relationships of *Hyperodapedon* to other rhynchosaurs, and to assess the relative merits of the current schemes of classification.

Repository abbreviations are: American Museum of Natural History, AMNH; British Museum (Natural History), BMNH; Elgin Museum, EM; Geological Survey Museum, London, GSM; Glasgow Museum, Kelvingrove, KM; Museum of Comparative Zoology, Harvard, MCZ; Manchester Museum, MM; Newcastle University, Geology Department, NUGD; Royal Scottish Museum, Edinburgh, RSM.

2. MATERIALS AND METHODS

2.1. *Preparation*

Information could be derived from positively preserved specimens, like BMNH R699. However, in most cases, the bone was so soft and the sandstone matrix so hard that standard preparation techniques were not successful. Thus, the remaining bone was removed from certain specimens with dilute hydrochloric acid, and casts were produced from the natural rock moulds. Casting materials had to be flexible and tough because of the complex nature of the moulds, and they included polyvinylchloride and Silastic rubber compounds. These methods produced high-fidelity replicas of the original bone, showing details of surface textures and vessel openings, and the rock moulds were still available for further casting. Full details of these casting techniques are given in Benton & Walker (1981).

Dr A. D. Walker made casts of NUGD A and several BMNH, EM and RSM specimens and prepared BMNH R4780 in 1967. In the course of the present study, further casts of these and other specimens were made between 1978 and 1981, and they form the basis of the description of *Hyperodapedon*.

2.2. *Number of individuals*

There are apparently 31–37 individuals present (34 from Lossiemouth, 3 from Spynie), most being represented by parts of the skull, or skull and skeleton. There is no evidence of the breaking up of individual specimens between museums. Within each collection attempts were made to combine material into the minimum number of individuals represented by fitting blocks together. Other clues to the association of material include collection and repository data, type of matrix, and manner of preservation.

The specimens are listed below together with brief indications of the portions preserved and the date of collection. Full details are given in Benton (1981, appendix 1).

(i) EM 1978.566.1, 2. Partial skull, cervical, dorsal, and sacral vertebrae, anterior ribs, interclavicle, forelimb, pelvis, femur. Some elements mislabelled by Huxley on the specimen ('R.U.' = rib; 'Crd.' = interclavicle; 'Sc.' = scapula; 'Scp?' = rib(?); 'Hu?' = radius). Collected by Reverend George Gordon, 1858, from Lossiemouth. Labelled 'type specimen'; described by Huxley (1859, 1869); 1978.566.2 = Huxley's 'block No. 1'.

(ii) EM 1978.567.1–3. Partial skull, dorsal vertebrae, gastralia, pectoral and pelvic girdles. Mislabelled 'type'. Collected by G. Gordon from Lossiemouth. 1978.567.2 = Huxley's 'block No. 2'.

(iii) EM 1886.3. Dorsal vertebrae, ribs, gastralia, shoulder girdle, humeri, partial pelvic girdle, hindlimb. Lossiemouth.

(iv) EM 1926.6. Maxillary tooth plate. Collected by D.M.S. Watson(?), from Lossiemouth.

(v) RSM 1952.10.4. Small partial skull. Lossiemouth.

(vi) RSM 1966.43.1. Snout tip. Lossiemouth.

(vii) RSM 1966.43.2. Dentary tip of juvenile. ?Lossiemouth.

(viii) RSM 1967.10.1A–D. Dorsal vertebrae, anterior caudals, ribs, gastralia, shoulder girdle, right forelimb, pelvis, both hindlimbs. ?Lossiemouth.

(ix) RSM 1967.10.2A, B. Partial skull. ?Lossiemouth.

(x) RSM 1967.10.3A, B. Small partial skull. ?Lossiemouth.

(xi) RSM 1967.10.4. Dorsal vertebrae, ribs, ?forelimb. ?Lossiemouth.

(xii) BMNH R699. Skull, cervical, dorsal, sacral and anterior caudal vertebrae, ribs, gastralia, both girdles, forelimbs, left hindlimb. From Lossiemouth; presented by Reverend George Gordon, 1886. Described by Huxley (1887, pp. 676–688, pl. 26), Lydekker (1888, pp. 297–298, figs 67, 68), Woodward (1898, p. 188, fig. 116), Burckhardt (1900, pl. 19), Huene (1929, pp. 38–40, pl. 8, fig. 1, 3–8), Hughes (1968, p. 470).

(xiii) BMNH R3137. Partial skull. From Lossiemouth; collected by R. Grant, *ca.* 1865; donated by William Taylor, 1903.

(xiv) BMNH R3138. Snout region of skull. From Lossiemouth; collected by R. Grant, *ca.* 1865; donated by William Taylor, 1903. Described by Huxley (1869, p. 140; 1887, pp. 685–686, figs 7, 8).

(xv) BMNH R3140. Partial skull. From Lossiemouth (East Quarry); collected by William Taylor in 1900. Described by Boulenger (1903, pp. 175–178, fig. 1, pl. 11), and Huene (1929, pp. 38–40, pl. 8, fig. 2; 1938, p. 113).

(xvi) BMNH R3141. Partial skull. Type of *Stenometopon taylori*. From Lossiemouth (West Quarry); collected by William Taylor in 1902. Described by Boulenger (1903, pp. 178–182, figs 2, 3, pls 12, 13), and Huene (1938, p. 113; 1939b, pp. 512–514, fig. 9).

(xvii) BMNH R3148. Dorsal, sacral, anterior caudal vertebrae, ribs, gastralia, radius, ulna of left side. From Lossiemouth; presented by 'Reverend Dr G. Gordon, July 1885'.

(xviii) BMNH R3150. Partial skull (small). From Lossiemouth; collected by William Taylor, 1903.

(xix) BMNH R3151. Partial right maxilla. From Lossiemouth; collected by William Taylor, 1903.

(xx) BMNH R3153. Isolated left surangular. ?Lossiemouth; collected by William Taylor, 1903.

(xxi) BMNH R3560. Dorsal vertebrae, ribs, fore- and hindlimbs. ?Lossiemouth (originally registered as *Stagonolepis*).

(xxii) BMNH R3563. Skull, dorsal vertebrae, gastralia, ribs, crushed shoulder girdle. From Lossiemouth; donated by William Taylor, 1907.

(xxiii) BMNH R3932. Partial skull, ribs, right forelimb, ?shoulder girdle. From Lossiemouth; donated by William Taylor, 1911.

(xxiv) BMNH R3933. Partial skull, dorsal vertebrae, ribs, left and right forelimbs, shoulder girdle. From Lossiemouth; donated by William Taylor, 1911.

(xxv) BMNH R4780. Large left dentary. From Lossiemouth; donated by William Taylor, 1915. Described by Huene (1929, p. 40).

(xxvi) BMNH R4781. Maxilla, dorsal, sacral vertebrae, proximal caudals, ribs, gastralia, pelvis, right femur. From Lossiemouth; donated by William Taylor, 1915.

(xxvii) BMNH R4782. Skull, cervical, dorsal vertebrae, ribs, shoulder girdle and forelimb of right side. From Lossiemouth; donated by William Taylor, 1915.

(xxviii) BMNH R4791/4805. Dorsal, sacral, proximal caudal vertebrae, ribs, gastralia, left forelimb, hindlimb. From Lossiemouth; donated by George Gordon, 1885.

(xxix) BMNH R4795. Dorsal vertebrae, ribs, right shoulder girdle, humerus. From Lossiemouth; donated by George Gordon, 1885.

(xxx) BMNH R4806. Dorsals, gastralia. From Lossiemouth; donated by George Gordon, 1885.

(xxxi) BMNH R9250. Partial skull. No collection data.

(xxxii) GSM 69764–71. Skull, cervical vertebrae, interclavicle, ?humerus. ?Lossiemouth.

(xxxiii) GSM 90922–4. Partial skull, cervical and anterior dorsal vertebrae, forelimb. ?Lossiemouth.

(xxxiv) GSM 90925–59. Skull, cervical and anterior dorsal vertebrae, ribs, gastralia, left forelimb, hindlimb. ?Lossiemouth.

(xxxv) GSM 90960–2. Limb bone, isolated maxilla. ?Lossiemouth.

(xxxvi) GSM 91067–71. Seven dorsal vertebrae. Spynie; collected by J. Horne, 3.vi.1901.

(xxxvii) MM L8269, L8272. ?Jaw fragment (labelled 'tibia'), maxillary tooth plate. Lossiemouth (West Quarry); collected by D. M. S. Watson.

(xxxviii) KM G66, 41as. Ribs and gastralia. ?Lossiemouth.

(xxxvix) NUGD A. Skull (lacks posterior part). Spynie Quarry; collected by Professor T. S. Westoll, 1948.

(xl) NUGD B. Skull and anterior cervical vertebrae. Spynie Quarry; collected by Professor T. S. Westoll, 1948.

Several specimens may be combined, namely: RSM 1967.10.2 (?) and RSM 1967.10.4; BMNH R3933 and R4781; and BMNH R4791/4805 and R4806. This would give 37 individual animals. However, six specimens (EM 1926.6; BMNH R3153, R4780;

GSM 90960–2; MM L8269, L8272; KM G66, 41as) are isolated jaw elements, or other fragments, and they could be excluded from the estimate of numbers of individuals. Thus the total number ranges from 31 to 37.

2.3. *Individual variation*

There is a range in size of specimens on a scale similar to that found in *Stagonolepis* by Walker (1961), but not as great as in *Ornithosuchus* (Walker 1964). Very few specimens yielded more than a few key measurements, but these were tabulated and skull lengths were estimated by comparing dimensions with more complete material (table 1). There are no clearly distinct size groups, except for the one very small animal (?juvenile). However, we may recognize a

TABLE 1. KEY MEASUREMENTS (IN MILLIMETRES) FOR ALL SPECIMENS OF *HYPERODAPEDON*

(Actual skull lengths are marked with an asterisk, and others are estimated from known measurements.)

	coracoid length	humerus length	radius length	ilium length (crest)	pubis length	femur length	maxillary plate width	estimated skull length (±10 mm)
RSM 1966.43.2								70
BMNH R3933	57	90	72					125
BMNH R4781				58	25		20	130
BMNH R4782	55	95	73				20	130*
RSM 1952.10.4								?130
RSM 1967.10.1		95		62				140
GSM 90960–2								?140
RSM 1967.10.3							20	145
EM 1978.567.1–3				65				145
BMNH R3150							21	145
BMNH R4795	65	113						165
BMNH R3560		115						165
EM 1886.3	75	116	81	77				165
MM L8272/L8269							24	170
GSM 90922–4								?175
GSM 69764–71								175
RSM 1966.43.1								?175
EM 1978.566.1–2					45	119		175
NUGD A							25	175*
NUGD B							25	175*
BMNH R3153								?175
BMNH R3932								?175
BMNH R3141								180
BMNH R4791/4805	80					125		180
BMNH R699	81	130	86		53	125	30	180*
GSM 90925–59								180
EM 1926.6							30	180
BMNH R3138								180
BMNH R3563								180
BMNH R4806								?180
BMNH R9250								?180
GSM 91067–71								?180
KM G66.41as								?180
BMNH R3148								180
RSM 1967.10.4								?190
BMNH R3140							31	190
BMNH R3151							33	?200
RSM 1967.10.2								?210
BMNH R3137							34	210
BMNH R4780								?210

typical animal from either end of the normal range. Several individuals have skull lengths averaging 130–140 mm, and a large number cluster around measurements of 170–180 mm. These may reach 210 mm on the basis of estimates from some large partial specimens. Von Huene (1929, p. 40) suggested that BMNH 47800, a partial dentary, was 'from a skull approximately or more than twice as large as R699', but careful measurements suggest that it is no more than 25% larger than the average 170 mm skull.

TABLE 2. MAIN MEASUREMENTS (IN MILLIMETRES) OF HYPERODAPEDON

(Estimates are marked with an asterisk. A typical small, and a typical large specimen are shown.)

	(BMNH R4782)	(BMNH R699)
skull length in midline (premaxilla–quadrate)	130	180
skull width across quadratojugals	190	240
maximum width of maxillary tooth plate	25	30
mandible length	185	200*
presacral column length	430*	600
scapulocoracoid height	80	140 (R4795)
scapula height	50	105 (R4795)
coracoid length	50	81
coracoid breadth	30	40*
interclavicle length	85 (GSM 69764–71)	100 (EM 1978.566)
humerus length	95	130
humerus, proximal breadth	55	70
humerus, least diameter of shaft	18	19
radius length	73	86
ulna length	73	87
metacarpal II length	15	16
ilium, crest length	58 (R4781)	77 (EM 1886.3)
ilium, breadth of neck	25 (R4781)	30 (EM 1886.3)
ilium height	55 (R4781)	70 (EM 1886.3)
pubis length	25 (R4781)	53
pubis breadth	52 (R4781)	80
ischium length	30 (R4781)	65 (R4791)
femur length	90*	125
tibia length	75*	95
fibula length	75*	95
metatarsal IV length		40
pes length including tarsus		150 (R3560)
estimated length of presacral and sacral vertebral column	470	650
estimated length of tail	330	460
estimated total length	930	1290

The main measurements of a well preserved small animal (BMNH R4782) and of a larger one (BMNH R699) are given in table 2. A complete tail is not preserved in any specimens, but a comparison with the body proportions of Scaphonyx (Huene 1942) and Paradapedon (Chatterjee 1974) suggests that the tail was about 0.7 times the length of the combined presacral and sacral column. Huxley (1887, p. 676) estimated a length of 6–7 ft (2 m) for BMNH R699 on the assumption that Hyperodapedon had a tail proportionately as long as Sphenodon.

The preserved material of Hyperodapedon displays a far smaller size range than has been recorded in Paradapedon (skull lengths, 110–460 mm: Chatterjee 1974) or Scaphonyx (skull lengths, 60 mm (MCZ 1664) to 400 or 500 mm: Huene 1942). Little can be said of changes in proportion of the skull or skeleton of Hyperodapedon with growth, since the only juvenile specimen (RSM 1966.43.2) is no more than the anterior portion of a dentary. Nevertheless,

the main allometric changes in the skull were probably a progressive relative widening of the posterior portion with associated changes in orbit and temporal fenestra shape, as suggested in *Scaphonyx* by Barbarena (1971).

Although size groups have not been distinguished in the preserved material of *Hyperodapedon*, there appear to be two well defined forms based on proportions. In skulls of the same midline length, for example, 'critical' elements (e.g. occipital condyle, maxillary tooth plate) are always the same size, while all other bone plates and all bone bars between skull openings (e.g. frontal, postorbital) show distinct thin and thick forms (figure 4c). These may be termed 'robust' and 'gracile'. Some representative measurements are given in table 3, and it can be seen that 'non-critical' elements have gracile:robust ratios within the range 0.33–0.84. Skulls BMNH R699, R4782, and NUGD A are robust forms, and BMNH R3141 and NUGD B are gracile forms. Similar relationships arise from measurements of postcranial elements (e.g. robustness of long bones and girdle bones). There is no relation between overall size and robustness.

TABLE 3. MEASUREMENTS (IN MILLIMETRES) OF A ROBUST (NUGD A) AND A GRACILE (NUGD B) SKULL, AND GRACILE:ROBUST RATIO FOR EACH MEASUREMENT

	robust	gracile	ratio
midline skull length	1750	1750	1.00
length, anterior nasal–posterior frontal	700	700	1.00
width of two premaxillae below naris	290	210	0.72
maximum depth of anterior orbital wall at anterolateral angle of orbit	240	200	0.83
minimum interorbital width of frontal	380	320	0.84
minimum width of postfrontal/postorbital bar	90	65	0.72
length of jugal/postorbital contact laterally	320	260	0.81
thickness of jugal below lower temporal fenestra	60	20	0.33
maximum width of maxillary tooth plate	240	240	1.00
width of midpalatal ridge in front of interpterygoid vacuity	23	10	0.43
maximum width of occipital condyle	180	170	0.94
maximum ventral width of angular at splenial contact	220	220	1.00
thickness of upper edge of prearticular	40	25	0.62

It may be concluded that the size distribution corresponds to age, and that the variations in proportions correspond to sexual dimorphism. It cannot be said whether the robust forms are male or female, since either sex may be the larger or more robust among different groups of living reptiles.

3. TAXONOMY

Class Reptilia Laurenti, 1768

Subclass Diapsida Osborn, 1903

Order Rhynchosauria (Gervais, 1859) Osborn, 1903

Family Rhynchosauridae Huxley, 1887

HYPERODAPEDON GORDONI HUXLEY, 1859

(figures 1–41)

1859 *Hyperodapedon gordoni* Huxley, *in* Murchison, p. 435.

1869 *Hyperodapedon gordoni* Huxley; Huxley, pp. 138–144.

1887 *Hyperodapedon gordoni* Huxley; Huxley, pp. 675–689.

1903 *Stenometopon taylori* Boulenger, pp. 178–182.

Lectotype (designated here): EM 1978.566. 1, 2 partial skull and skeleton. Triassic,

Lossiemouth, near Elgin. Described by Huxley (1859, 1869), and figured here for the first time (figure 1, plate 1).

3.1. *The holotype of Hyperodapedon gordoni*

Huxley (1859, 1869) regarded the two individuals EM 1978.566 and EM 1978.567 as the single holotype specimen. A brief review is necessary in support of the lectotype designation given here.

Huxley's original note (1859, p. 435) mentioned one specimen showing vertebrae, ribs, fore- and hindlimbs, and skull. He noted the concave articular surfaces of the vertebrae and the 'numerous series of subcylindrical palatal teeth'. All of these features are seen in EM 1978.566.

In his first full description of *Hyperodapedon*, Huxley (1869, pp. 142–144) described 'the specimen on which the genus was founded'. He stated that 'the remains of the specimen are exhibited by the opposed faces of broken blocks of sandstone, some of which have been separated by splitting along the plane in which the fossil lay' and went on to describe (pp. 141–142) the 17 vertebrae and ribs, clearly EM 1978.566.2 ('block No. 1'). There is no evidence that a counterpart was collected, although it is implied by Huxley's remarks. Further, on p. 142, he stated that the 'abdominal ribs...are better shown in another slab' (probably EM 1978.567.2; figure 3). Huxley (1869, pp. 142–143) went on to describe EM 1978.566.1, containing 'the anterior cervico-dorsal vertebrae and the skull...bent round so that its axis is nearly at right angles with that of the body'. Much of the description seems to suggest that the skull was better preserved in 1869 than now (e.g. the 'downwardly curved, beak-like anterior termination of the snout, which appears to be formed altogether by the premaxillae' (p. 143) is no longer present). The remaining description of limbs and girdles (pp. 143–144) refers mainly to EM 1978.566.2 ('block No. 1'). Huxley (p. 143) referred to a cast of the 'scapula' of 'block No. 1' on 'block No. 2' which also showed 'sundry scattered imperfect impressions on limb-bones', probably the broad anterior dorsal ribs, partial humerus (?), and hindlimbs of EM 1978.567.2. The final comments on teeth (Huxley 1869, p. 144) may refer partly to EM 1978.566.1 and partly to EM 1978.567.1. In later accounts, Huxley (1887, p. 675) continued to refer to a single 'type specimen, now in the Elgin Museum'.

It is clear that Huxley regarded EM 1978.566 and EM 1978.567 as counterparts of one specimen. This is surprising since the former is preserved on its side, and the latter in a dorsoventrally flattened orientation, there is no way that the two specimens can be matched, each has similar portions of the skull preserved, and EM 1978.567 is about three-quarters of the size of EM 1978.566. Every block is numbered in red paint, and some bones are outlined in red, all most probably done by Huxley himself (A. D. Walker, personal communication, 1981), and the blocks remaining are 1A–C, 1E (11B), 2 (EM 1978.566.1, 2) and 3, 3', 3", 3''', 4, 4', 5, 7, 8 (EM 1978.567.1–3). It seems most likely that George Gordon sent all of the blocks of EM 1978.566 to Huxley in 1858, and may have sent EM 1978.567 then or later. By 1869, Huxley had numbered all the pieces and considered that they all belonged to one individual. However, the original brief description, and the bulk of the 1869 account clearly refers to EM 1978.566, and this specimen shows most anatomical features. It is designated as lectotype with EM 1978.567 as paralectotype.

Phil. Trans. R. Soc. Lond. B, volume 302

Benton, plate 1

FIGURE 1. The type specimen of *Hyperodapedon gordoni*, EM 1978.566. Skull and skeleton (cervical and dorsal vertebrae, ribs, gastralia, forelimb, hindlimb) in ventral and left lateral views respectively (magn. ×0.4). The blocks are shown slightly separated since they do not fit together tightly now. Photographs by A. D. Walker.
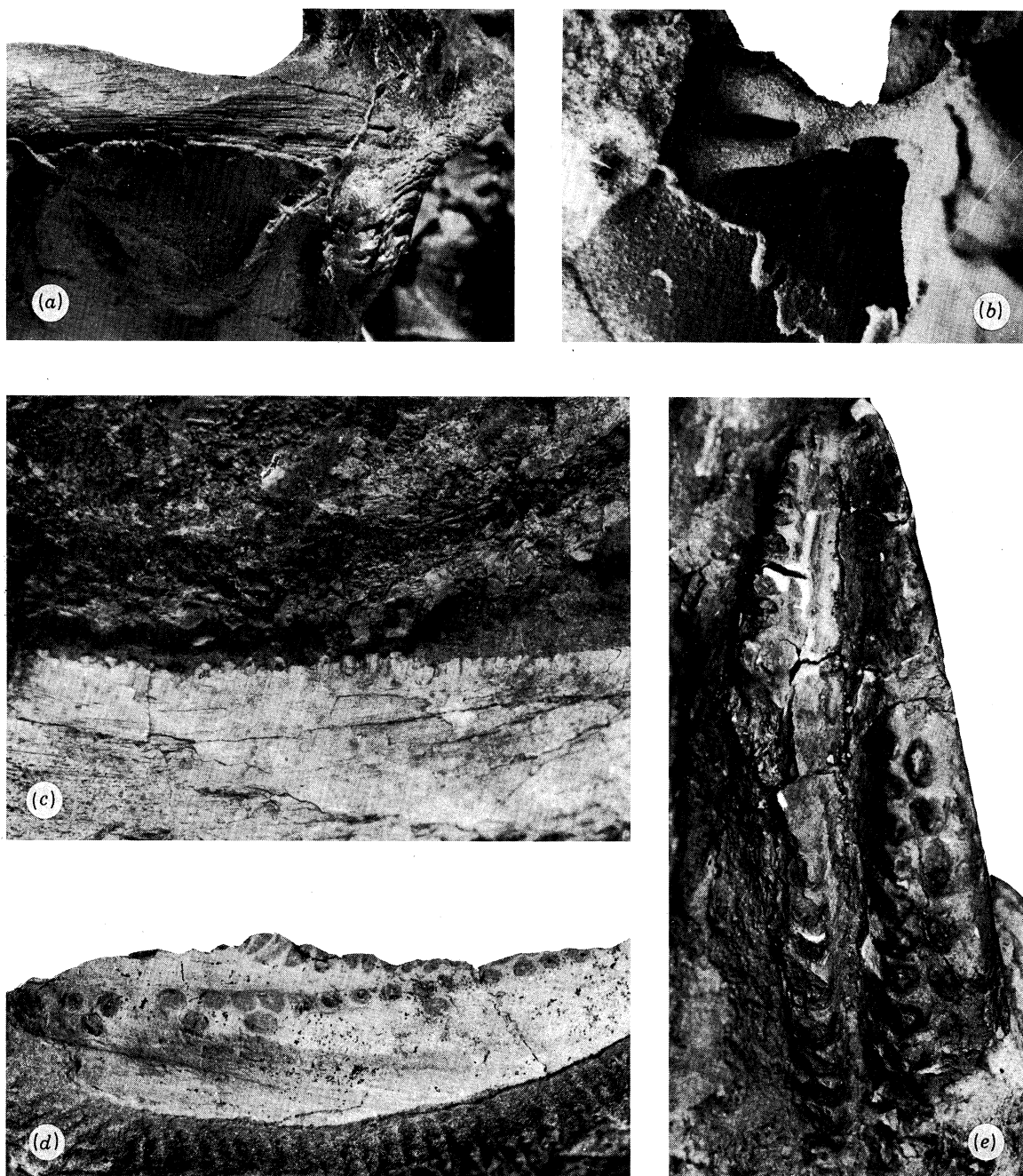
FIGURE 2. Details of the skull and teeth. (*a*) Anterodorsal view of proximal end of the premaxilla, prefrontal and maxilla, showing bone surface textures; cast of NUGD A (magn. × 1.3). (*b*) Lateral view of a natural rock cast of the lacrimal duct, NUGD A (magn. × 3.0). (*c*) Lateral view of the right dentary and maxilla, jaws slightly open, showing complete and broken teeth, NUGD B (magn. × 1.5). (*d*) Palatal view of small left maxillary tooth plate, BMNH R3140 (magn. × 1.5). (*e*) Medial view of middle portion of a large dentary, showing buccal and lingual teeth, BMNH R4780 (magn. × 2.0).
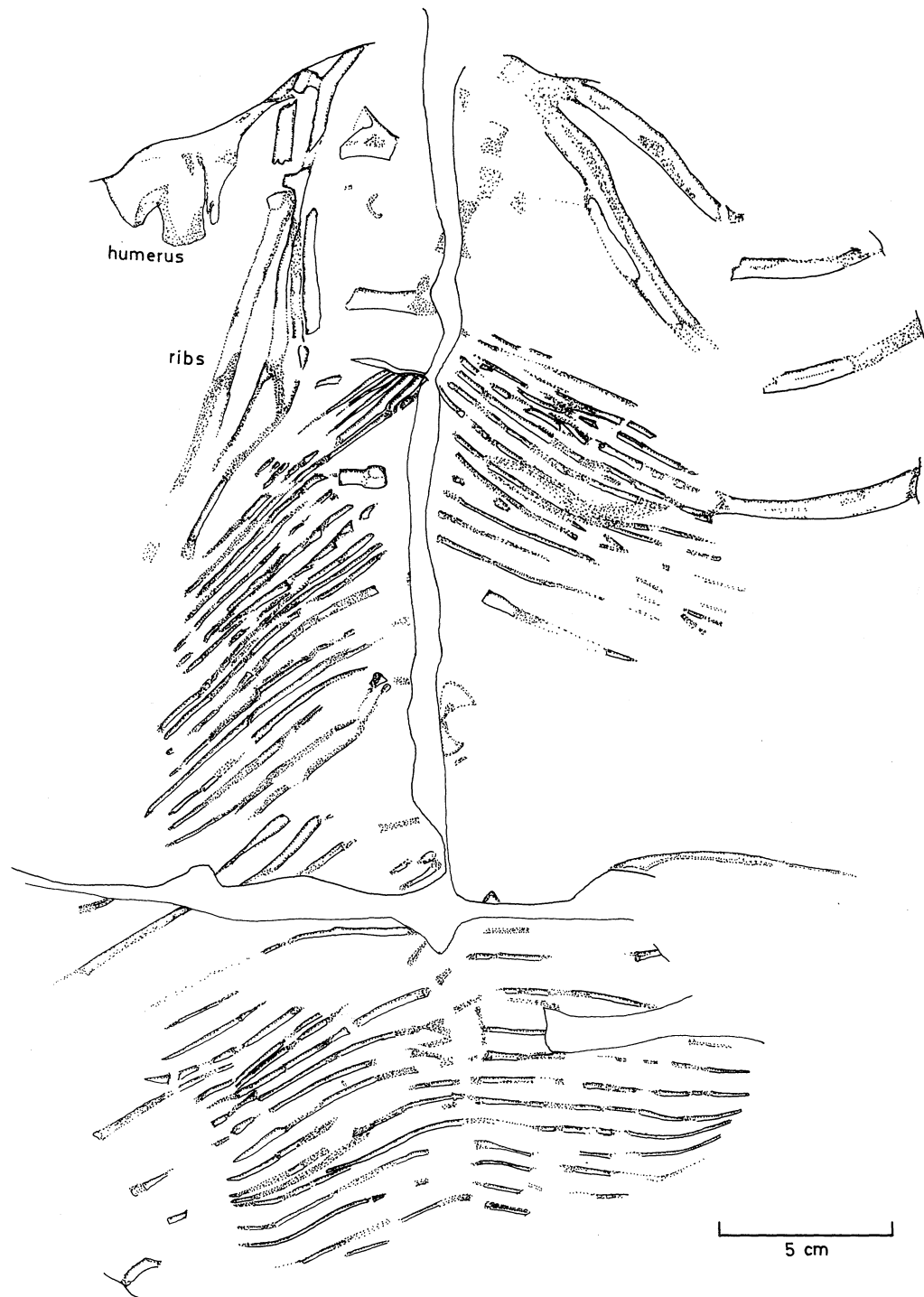
FIGURE 3. EM 1978.567.2. Specimen showing ribs, gastralia, and parts of the forelimb; dorsal view of ventral part of the skeleton.

3.2. The status of Stenometopon Boulenger, 1903

Boulenger (1903, pp. 178–182) described a new genus and species of rhynchosaur, *Stenometopon taylori*, based on a specimen from Lossiemouth. He gave the differences from *Hyperodapedon* as:

(i) premaxillae directed nearly horizontally, instead of diagonally down;

(ii) nasal opening longer;

(iii) nasal bones absent;

(iv) lower temporal fossa larger;

(v) interorbital part of frontal narrower.

Huene (1938, p. 113; 1939b, pp. 512–513; 1942, p. 319) pointed out some mistakes in Boulenger's reconstruction, and suggested that the holotype of *Stenometopon* was just a damaged specimen of *Hyperodapedon*.

The type material (BMNH R3141) was initially collected in three blocks which Boulenger had divided and prepared, and it now consists of six blocks. The critical areas where Boulenger identified differences between *Stenometopon* and *Hyperodapedon* lie over cracks. His suggestion that the premaxillae are nearly horizontally directed (e.g. his restoration, fig. 3) is not supported by the material. Indeed, his photograph of the left side of the skull (Boulenger 1903, pl. 12) shows this. The longer nasal opening and lack of nasals is easily explained because of the poor preservation of the skull in that region: much of the bone of the maxillae, lacrimals and vomers has also been lost at this major crack. The lower temporal fossa is identical with that of other *Hyperodapedon* material, although BMNH R699 (see, for example, Huxley 1887, pl. 26, fig. 2) is rather distorted.

The question of interorbital distance, and the overall width of the skull, was stressed by Boulenger. He gave a measurement of 16 mm for least distance between the orbits, compared with 40 mm in BMNH R699. However, again, the critical area lies over a crack and bone has been lost on both orbital edges of the frontal. The apparent orbital edges are only impressions of the ventral descending lamellae of the frontals which lie about 10 mm medial to the true dorsal orbital edge. A careful refit of the blocks yields a minimum interorbital width of 29–32 mm. The well preserved bones surrounding the lower temporal fossa show that the type specimen of *Stenometopon* is a gracile form of *Hyperodapedon* with a skull length of about 180 mm and its true interorbital width is very close to that of NUGD B.

The evidence presented here, and that given by Huene (1938, 1939b, 1942), makes it clear that there is no generic or specific distinction between the holotype of *Stenometopon* (BMNH R3141) and *Hyperodapedon*, and *S. taylori* should be synonymized with *H. gordoni*. Other BMNH material labelled *S. taylori*, but never described as such (e.g. BMNH R4781, R4782), is also clearly *H. gordoni*, and will be considered as such in the description.

4. SKULL

4.1. General description

Most of the skull description is based on casts of NUGD A and B. Additional information is derived from a cast of BMNH R4782 and casts of two maxillary tooth plates (EM 1926.6; BMNH R4781). Other good skull remains include: RSM 1967.10.2, 3; BMNH R699, R3137, R3138, R3140, R3141, R3563; GSM 69764–71, 90925–59. The
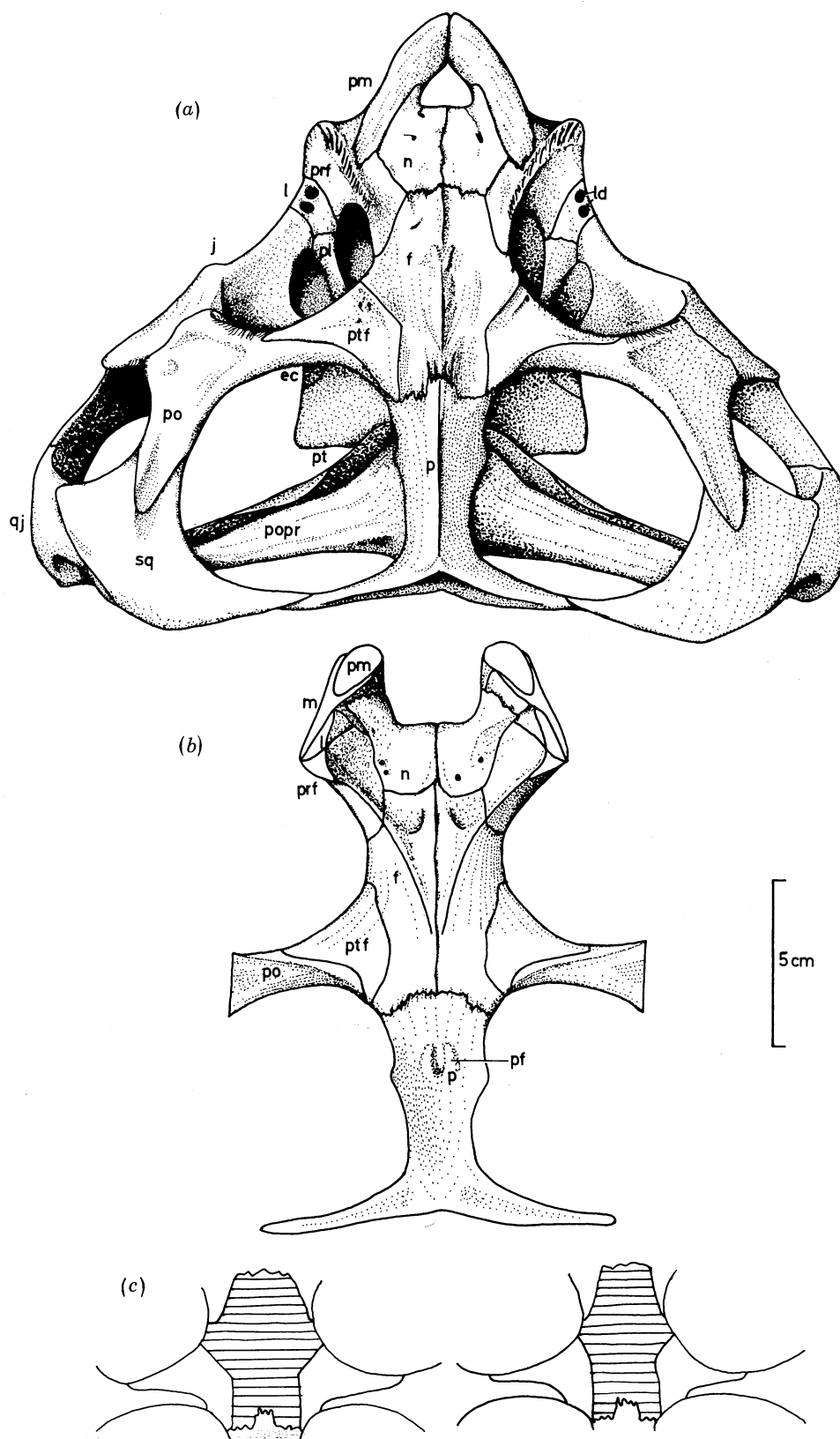
FIGURE 4. Composite restoration of the skull. (*a*) Dorsal view; (*b*) ventral view of underside of skull roof. All figures are of robust individuals unless otherwise stated. Abbreviations used in figures are listed at end of paper. (*c*) Comparison of middle of skull roof of a robust (left) and a gracile (right) animal, based on NUGD A and B respectively. Frontal bone is shaded.

general skull drawings (figures 4–7) are based on NUGD A and B and are standardized to represent a robust individual with a skull length of 175 mm.

The skull is roughly triangular when viewed from above. In lateral view, the skull and lower jaw are deep and a long premaxillary 'beak' curves down between the rising processes of the lower jaws. The orbits are mainly dorsal in position with a strong anterior rugose ridge. The striking feature of the palatal view is the pair of triangular tooth plates with a midline groove in each to receive the lower jaw. Internally, the skull is divided into nasal, orbital and temporal compartments by bony walls in front of the orbit and behind the orbit. These are composed of prefrontal, lacrimal and palatine, and postorbital, jugal and ectopterygoid respectively, and may be termed 'anterior orbital septum' and 'posterior orbital septum'.

4.2. *Dermal bones of the skull roof* (figures 4–7)

The paired *premaxillae* curve down to form a prominent 'beak'. Each bone originates near the anterior edge of the orbit but is excluded from the orbital border by the prefrontal. The premaxilla is clamped between two ascending processes composed of maxilla, nasal and vomer (figure 5a, b). The premaxilla is laterally flattened in its posterior part but becomes more pear-shaped in cross-section anteriorly in the border of the single narial opening. The flat inner surfaces of the premaxillae touch below the naris, but they are not suturally linked. The surface of the bone is striated longitudinally (figure 2a, plate 2), especially near the proximal end, and this may indicate the presence of a horny sheath, as suggested by Huxley (1887, p. 680). The tips of the 'tusks' are fairly sharp, but there is no evidence for terminal teeth, as suggested initially by Huxley (1869, p. 142).

The *maxillae* are barely visible from above, and they will be discussed later as part of the palate.

The paired *nasals* meet on an irregular suture. The nasal overlaps the medial side of the premaxilla, and runs further forwards into an expanded lobe of thin bone on the inside, just meeting the maxilla (figures 4b, 5b). Each nasal is pierced by a pair of small foramina, visible in dorsal and ventral views (figure 4a, b).

The paired *frontals* occupy the middle third of the length of the skull roof, and border the orbit for a short distance. Huene (1929, pl. 8, fig. 1a) mistakenly showed the frontals separated from the orbital margin by a long anterior process of the postfrontal. The two frontals meet medially along a straight suture, poorly marked in places, which is raised on a slight ridge just behind the nasals. It passes back into a groove, and then runs up onto the apex of a sharp median ridge which continues into the sagittal crest of the parietal (figure 4a). The median suture is more clearly marked on the ventral surface of the skull roof (figure 4b). The internal ridges running anteroventrally round the front of the orbit (cristae cranii frontales) originate posteriorly on the ventral surface of the frontals as low ridges near the midline (figure 4b). In dorsal view (figure 4a), the frontal is pierced by one or more small foramina.

The *parietals* are fused to form a T-shaped element that separates the upper temporal fossae medially and expands laterally into a posterior cross-bar. The anterior contact with the frontal and postfrontal is a firm suture of complex interdigitating bone tongues, and there is no sign of a parietal foramen. The postorbital may barely touch the parietal in some specimens. The parietal rises to a sharp crest and is triangular in cross-section with a ventral concavity and two oval pits (parietal fossae, pf, figure 4b) to receive the supraoccipital. The narrow posterior wings contact the squamosals lightly. A dorsal ridge runs the width of this posterior cross-bar and defines a long backwardly facing concavity (figure 7).
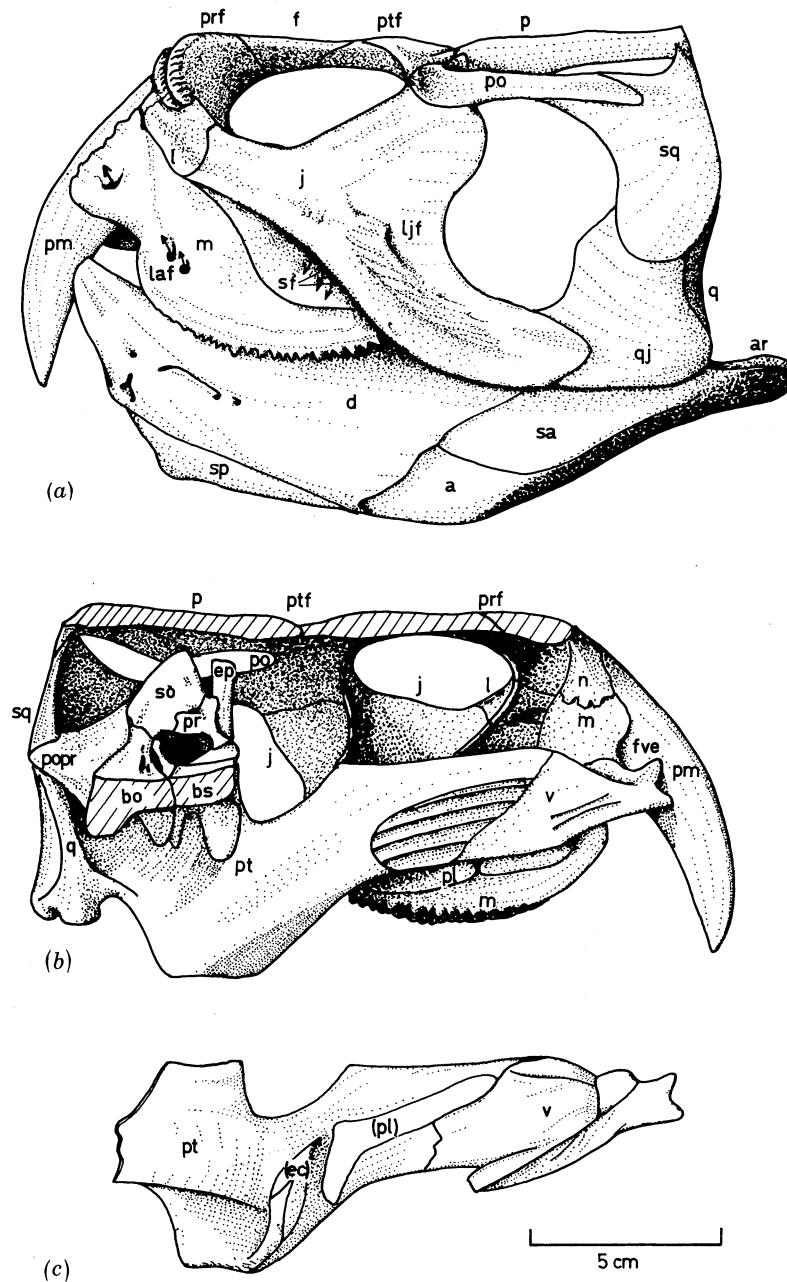
FIGURE 5. Composite restoration of the skull. (*a*) Left lateral view with the mandible in place; vessel openings indicated by arrows. (*b*) Medial view of the left half of the skull sectioned sagittally; cut surfaces shaded diagonally. (*c*) Lateral view of right pterygoid and vomer complex; attachment surfaces of palatine and ectopterygoid left unshaded.

The *lacrimal* is a small rounded rectangle of bone visible laterally at the anterior edge of the orbit, and it transmits the lacrimal duct medially (ld, figures 4*a*, 9*a*). The lacrimal and prefrontal together form a short stretch of the raised rugose anterior orbit margin. The small posterior internal section of the lacrimal bears two large openings just below the orbit edge, and meets the ascending process of the palatine. The lacrimal canal passes forwards to its exit below a half-spiral ridge on the small anterior medial lacrimal segment (figure 5*b*). As with his South American rhynchosaurs, Huene (1929, pp. 37–42, pl. 8, figs 1*a*, *b*) misinterpreted the

lateral extent of the lacrimal in *Hyperodapedon*. He labelled the anterior rising portion of the maxilla as lacrimal, and the lacrimal itself as part of the jugal.

The *prefrontal* forms most of the strong rugose ridge at the front of the orbit (figure 2a). It meets the maxilla and lacrimal laterally, forms a groove for the extreme posterior root of the premaxilla, and is bordered by the nasal and frontal medially. The prefrontal forms most of the bony 'anterior orbital septum' internally where it is bounded by lacrimal and palatine behind, and nasal, lacrimal and maxilla in front.

The *postfrontal* is a three-pronged bone which forms the posteromedial border of the orbit. An anterior process runs under the frontal and a lateral process is met by the postorbital. The posterior process runs beside the frontal and touches the anterior margin of the parietal with a point. It does not quite reach the margin of the upper temporal fossa. The postfrontal–postorbital junction seems to be a 'tongue and groove joint' in cross-section, where a tongue of the postfrontal fits into a groove of the postorbital. Dorsally, the prefrontal is pierced by one to three small foramina near the orbit edge (figure 4a).

The *postorbital* is also a three-pronged bone. The medial process meets the postfrontal, and barely touches the parietal in the anteromedial margin of the upper temporal fossa (figure 4a). It meets the jugal laterally along a broad suture. The middle part of the postorbital is depressed, and the posterior process runs between upper and lower temporal fossae in a long tongue overlapping the squamosal. Huene (1929, pl. 8, fig. 1a) shows the suture between postorbital and postfrontal too far forward.

The *jugal* is a large four-pronged bone that forms the middle part of the side of the skull. The anterior process borders the orbit, contacts the lacrimal on a broad margin, and runs sinuously over the maxilla to the back of the tooth row. More prominently in lateral view (figure 5a), a heavy ledge runs above this from the anterior tip of the jugal backwards and downwards. The ledge is supported by a series of small columns that are separated by four or five large suborbital foramina, visible in ventral view (sf, figure 6a). On the inside, the anterior process is seen to meet the lacrimal and the ascending process of the palatine (figure 4a). There is a strong horizontal internal ledge along the middle of the jugal, exactly opposite the outside ledge (figures 4a, 6b). The jugal runs forwards as far as the anterior lacrimal duct opening, and fits into a groove in the posterior margin of the ascending process of the maxilla. At this point, the bony plate covering the cheek area is very thin.

The inner ledge swings posteromedially to share a long serrate suture with the ectopterygoid, and it partially surrounds a large opening in the floor of the orbital cavity, termed here the medial jugal foramen (mjf, figure 6b).

The dorsal process of the jugal meets the postorbital on a strong irregular suture surface between orbit and lower temporal fossa. The posterior process runs below the lower temporal fossa and overlaps the quadratojugal with a long thin pointed tongue of bone. Burckhardt (1900, p. 489) figured the jugal–quadratojugal contact too far forward, and the jugal–postorbital contact too far medially. The jugal is rugose, bearing a second large lateral ridge which runs parallel to the main ledge, and this conceals a major vessel opening (termed here the lateral jugal foramen, ljf, figure 5b) and several smaller ones. A similar mediolaterally running jugal canal is seen in *Sphenodon* (foramen zygomatico-temporale, Osawa 1898a, p. 501) and in *Paradapedon* (Chatterjee 1974, fig. 4b).

The *quadratojugal* is an L-shaped bone which forms the posterolateral angle of the skull and lower posterior margin of the lower temporal fossa. The anterior arm runs into a long tongue

inside and below the jugal and the rising arm is overlapped by the squamosal. It meets the quadrate medially along a broad interdigitating suture line that surrounds a large quadrate foramen and a smaller opening ventrally (figures 7, 9*b*).

The *squamosal* is a broad triradiate bone forming much of the posterior margin of the skull and of the temporal openings. An anterior tongue runs under the postorbital and posterior elements meet the parietal with a narrow contact and the quadratojugal with a broad contact. In posterior view (figure 7), the squamosal has a face that expands ventrolaterally to a broad triangle to receive the end of the paroccipital process and extracolumella, as in *Sphenodon* and other rhynchosaurs (e.g. isolated squamosal of *Scaphonyx* (Huene 1929, pp. 19, 20, pl. 2, fig. 3)). This articulation surface is stepped out from the remainder of the posterior margin of the squamosal which supports the upper parts of the quadrate firmly.

4.3. *Dermal bones of the palate* (figures 5, 6)

The *maxilla* consists of a heavy tooth-bearing portion in the palate and a lateral ascending thin sheet of bone. The ascending part forms a groove in which the premaxilla is held firmly. It covers the premaxilla laterally for half its length, but it is separated from the orbital margin by the lacrimal. In lateral view, the maxilla bears a small opening in a fold below the lacrimal, three major foramina (lateral alveolar foramina, laf, figure 5*a*) and a series of striations running parallel to the tooth row. A vertical ridge runs down the medial surface of the ascending maxillary process (figures 6*b*, 9*d*). A large canal (superior alveolar canal) runs in the floor of the nasal cavity here through the bone of the maxilla, entering just in front of the palatine (posterior alveolar foramen) and exiting in front of the ridge just mentioned (anterior alveolar foramen) (paf, aaf, figure 6*b*).

The tooth-bearing portion of the maxilla is attached firmly to the vomer, palatine, jugal and ectopterygoid. There is a deep groove between the back of the tooth plate and the jugal and ectopterygoid. The alveolar margin is convex, curving gently upwards, but it does not reach the premaxilla, as shown by Boulenger (1903, p. 176). The palatal surface is split by a deep V-shaped furrow to receive the lower dentition, and teeth are present on the flat surfaces on each side. Further details of the dentition are given below (§6.1).

Previous authors (Huxley 1869, 1887; Lydekker 1885; Boulenger 1903; Huene 1929) thought that the V-shaped groove in the tooth plate marked the boundary between maxilla and palatine. Burckhardt (1900, p. 491) thought that the suture lay laterally to the tooth plate and he considered that it was formed entirely by the palatine. Huene (1938) showed that the tooth plate is entirely maxillary.

The paired *vomers* are three-pronged bones. The anterior process of each runs to an ascending point where it contacts the premaxilla. Laterally, between the anterior tip of the vomer and the anterior edge of the medial maxillary process is a square gap in the medial cover of the premaxilla. *Paradapedon* has a similar notch (Chatterjee 1974, fig. 4*b*), and it may be homologous with the fenestra vomeronasalis externa of the lizard *Ctenosaura* (Oelrich 1956, p. 24) (fve, figures 5*b*, 6*b*).

Posteriorly, each vomer has two processes which fork laterally and medially around the choana, and just touch equivalent anterior forks of the palatine (figures 5*c*, 6*a*, *b*). The lateral process also clamps the maxillary tooth plate, and the medial processes of both vomers meet and rise to form a low median septum. These vertical plates of the vomer are grooved laterally (figures 5*c*, 6*b*), and the bone runs well back in contact with the pterygoids. In medial view

(figure 5*b*), the ascending lamella bears a pair of curved ridges that slot into those of the other vomer. Towards the front of this ascending part is a long pit or foramen, and the lateral suture with the maxilla contains a tube (figure 9*d*), possibly homologous with the lacrimal groove of lizards (Oelrich 1956, p. 24).

Huxley (1887, p. 681, pl. 26, fig. 3) indicated the position of the choanae ('posterior nasal opening', 'p.n.') as possibly just behind the premaxillae, but Burckhardt (1900, p. 491) noted this error. Boulenger (1903, p. 176) showed the vomers extending too far posteriorly.
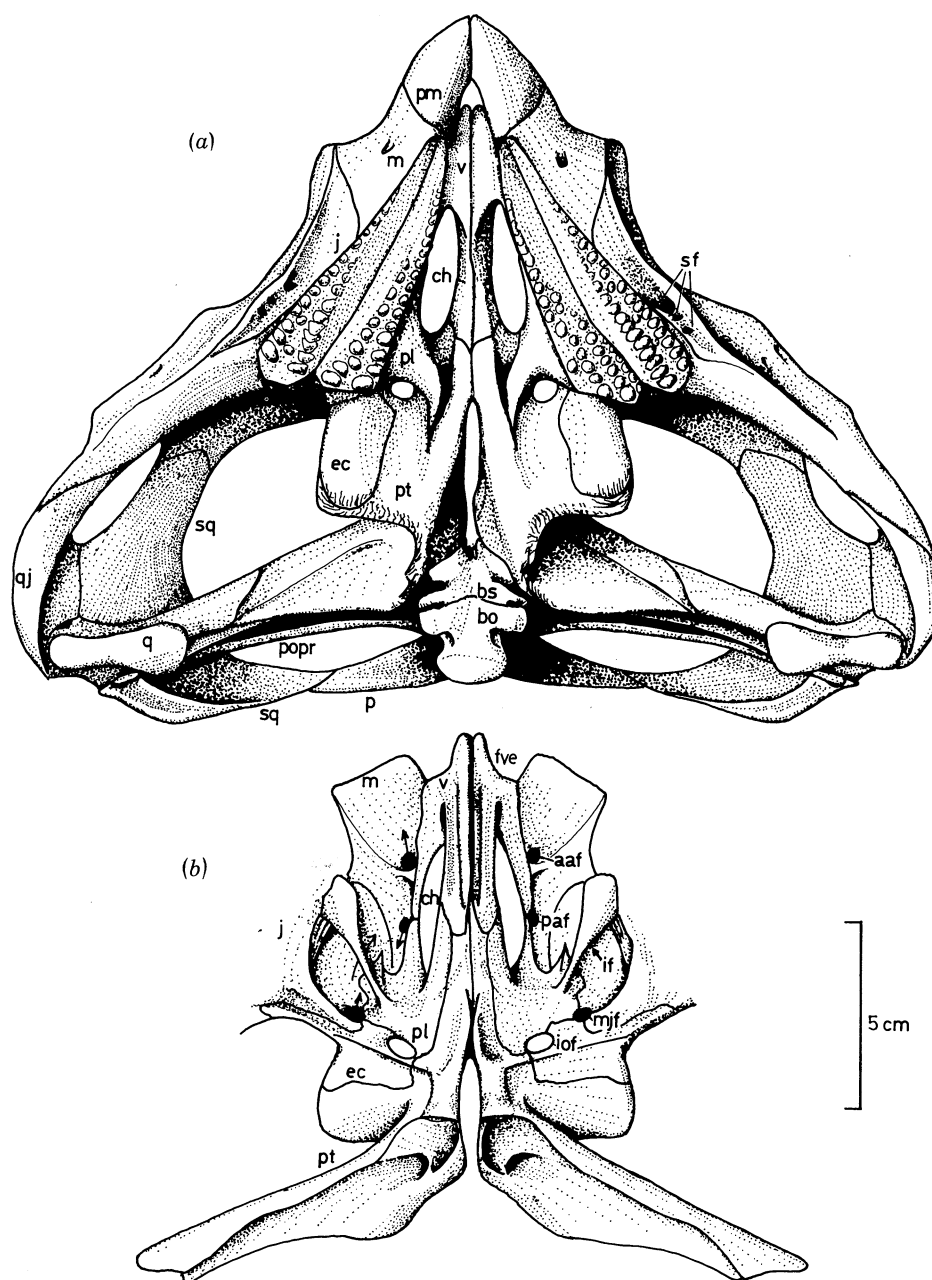

FIGURE 6. Composite restoration of the skull. (*a*) Palatal view; (*b*) dorsal view of the palate with the skull roof and braincase removed.

The *palatine* is a complex five-pronged bone at the posterior angle of the choana. An anterior process forms part of the median septum between vomer and pterygoid, but does not reach the midline as suggested in *Paradapedon* by Chatterjee (1974, fig. 4b). This segment splays out laterally to form the posterior margin of the choana and the palatal canal. In palatal view (figure 6a), a second strong anterior process meets the maxilla on the lateral side of the choana and runs back in contact with the jugal round the median jugal foramen to meet the ectopterygoid (figure 6b). The fourth, posterior, process passes round the inferior orbital foramen to meet the pterygoid posteriorly (figure 6b). The fifth process is a long anterolaterally ascending process that meets the jugal, lacrimal and prefrontal distally (figures 4a, 6b). This process spans the floor of the orbital cavity and cheek, leaving a large passage below which is presumably the homologue of the infraorbital foramen of lizards and *Sphenodon* (if, figure 6b).
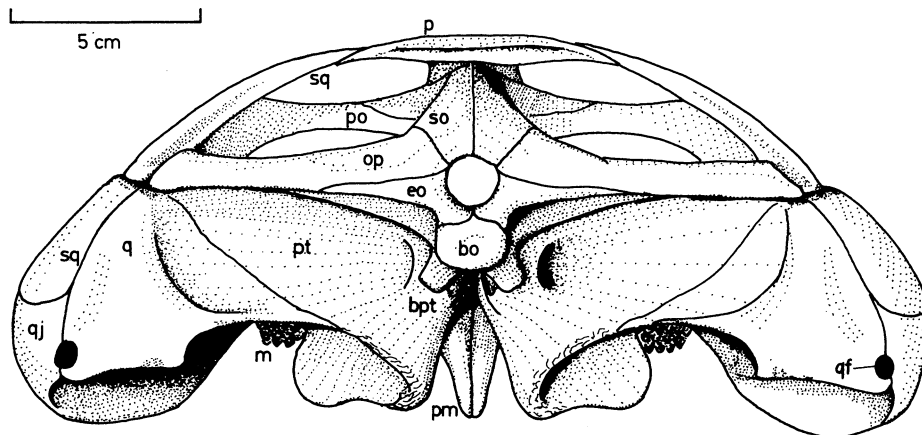

FIGURE 7. Composite restoration of the skull in occipital view. Distal ends of paroccipital processes restored from other rhynchosaurs.

The *ectopterygoid* is an approximately L-shaped bone. The laterally running arm forms part of the posterior orbital septum and borders the jugal and maxilla in front (figure 6a, b). The posterior arm curves over the pterygoid for a short distance when viewed dorsally, but on the ventral surface runs into a long tongue which becomes rugose at its distal end (figure 6a, b).

The *pterygoids* are long elements that occupy more than half the length of the palate. They meet anteriorly, and each expands backwards into a ventral (ectopterygoid) and a dorsal (quadrate) ramus which form a partial spiral when viewed from behind (figure 7).

The anterior rami rise vertically in contact on a pair of remarkable corrugated medial plates (figure 5b). These suture plates run well forward between the vomers and they are partially flanked by processes from the palatine (figures 5c, 6b). The pterygoids diverge backwards to surround the deep interpterygoid vacuity (pyriform recess). Viewed from above (figure 6b), the pterygoids descend and broaden around the interpterygoid vacuity and rise into broad plates (postcolumellar process) behind the columellar fossa (attachment of epipterygoid). Behind these, the deep basipterygoid pits nearly meet in the midline (figure 6b).

Behind the maxillary tooth plate, the ectopterygoid ramus of the pterygoid expands laterally as a thick slab of bone behind the palatine and above the ectopterygoid. The posterior part of this ramus is highly rugose.

The quadrate ramus swings dorsolaterally from the ventral part and becomes thin. In

46-2

NUGD A and B there is a clear 'step' in the angle of the curve (figure 6a) and a diagonal ridge also on the anterior face which extends towards the quadrate (figures 5c, 6a). The quadrate ramus shows a deep concavity running laterally on the posterior surface from the pit that lies in front of the basipterygoid pit (figures 6b, 7). The pterygoid lies behind a long medial tongue of the quadrate and the junction runs dorsolaterally to the end of the paroccipital process (figure 6).

4.4. Quadrate and epipterygoid

The *quadrate* is a strong vertical element in the plane of the occiput. Dorsally, the quadrate lies in a deep groove on the posterior side of the squamosal and the contact runs down the squamosal and the quadratojugal. Here it is pierced by a large quadrate foramen just above the condyle, as in *Stenaulorhynchus* (Huene 1938, p. 89, pl. 8, fig. 2), *Scaphonyx* (Huene 1942, p. 270, pl. 31, fig. 1d), and *Paradapedon* (Chatterjee 1974, p. 221, fig. 5). Above the condyle there is a strong rounded vertical pillar (posterior crest) at the lateral end of the thin curved pterygoid ramus (figure 7).

The articular condyle extends directly mediolaterally and is slightly twisted and constricted in the middle (figure 6a). Further details are given below (§6.2).

The right *epipterygoid* is preserved in NUGD A (figures 5b, 10d). The broad triangular base is firmly applied to the anterior face of the pterygoid just lateral to the contact with the basisphenoid. The lower edge cannot be clearly distinguished from the pterygoid, but it runs anteromedially down into a deep columellar fossa, which is seen on the left side where the epipterygoid is absent. The rod-like epipterygoid narrows rapidly as it rises and it is flattened in a posterolateral–anteromedial plane. Halfway up, it twists into an anteroposterior (parasagittal) plane before terminating in a spatulate process which lightly contacts the parietal. The shape and relationships of the epipterygoid are very like that of *Sphenodon*, and probably *Stenaulorhynchus* (Huene 1938, fig. 5).

4.5. Soft part anatomy of the head (figures 2, 8, 9)

The following account of soft part anatomy of the snout covers the nasal and orbital cavities, and the region of the quadrate, but excludes the temporal region, the braincase, and the musculature, which are dealt with later. No attempt is made to reconstruct all blood vessels, nerves, and cartilaginous structures since there is no evidence for many of these. The aim of this section is to explain the well preserved rugosities, foramina, channels and ridges in the skull roof and palate by comparison with the anatomy of the head of living reptiles. Much of this is based on dissections of the head of *Sphenodon* and of the skink *Mabuya*, as well as major published accounts of the head of lizards and *Sphenodon*, such as Osawa (1898a), Watkinson (1906), O'Donoghue (1920), Wettstein (1931), Bellairs & Boyd (1947, 1950), Oelrich (1956) and Jollie (1960). It should be stressed that *Sphenodon* is used as a model generalized diapsid, and no close relationship with rhynchosaurs is implied.

4.5.1. External surface of snout and palate

The outer surface of the skull of *Hyperodapedon* is highly rugose or ridged in some areas, but smooth in others (figure 2a, plate 2; figures 4a, 5a). The curved longitudinal ridges that lie just above, and parallel to, the maxillary tooth row, probably indicate the boundary between close attachment of the skin above and the fleshy lips below, as in *Sphenodon*. The ridging of the premaxilla has already been mentioned, and it may indicate the presence of a horny sheath.

The edges of the external naris (nasal, premaxilla) are smooth which may indicate fleshy areas partially enclosing the opening (as postulated for *Procynosuchus* (Kemp 1980a, p. 95)). The frontal, parietal and central parts of the jugal bear strong longitudinal ridges and small vessel openings which suggest closely adhering 'reptilian' skin, possibly composed of rather large scales as in lizards and snakes.

There are several areas on the rims of the orbit and temporal openings that display radial incisions on thickened bone edges; for instance, the anterior prefrontal edge of the orbit, the anterior edge of the postorbital (behind the orbit), and the higher part of the posterior jugal edge (anterior rim of the lower temporal opening (figures 2a, 4a)). The remainder of the orbit rim is less rugose. These are probably all attachment sites for tough connective tissue crossing the orbit and lower temporal opening, exactly as in *Sphenodon*.

Some of the posterior skull roof elements (e.g. jugal, quadratojugal, postorbital, squamosal, pterygoid) display fine radiating ridges (some are sketched in figure 5a) which presumably reflect the direction of growth of the various skull elements from the initial ossification centres. Some of the more obvious centres are the major rugosity of the jugal, the posterior ventral corner of the quadratojugal, the central concavity of the postorbital, the paroccipital process (and extracolumella) process of the squamosal, and the basipterygoid recess of the pterygoid.

Bone surface textures possibly indicative of jaw muscle attachments are described below (§6.3).

4.5.2. *Blood vessels of the orbital and nasal cavities* (figures 2b, 8a, 9a)

Foramina in the roof of the palate of *Hyperodapedon* indicate a pattern of blood vessels similar to *Sphenodon* (O'Donoghue 1920) and generalized lizards like *Ctenosaura* (Oelrich 1956), and comparisons are made with these accounts.

The palatine artery (pla, figure 8a) proceeded forward from the basisphenoid region and probably crossed the pterygoid dorsally, as in *Ctenosaura*, rather than ventrally, as in *Sphenodon*, because of the relatively high position of the basisphenoid and the deep ventral keel of the pterygoid. It may have given off a lateral artery that ran over the ectopterygoid towards the coronoid recess. The major part of the palatine artery then probably passed through the inferior orbital foramen to run over the ventral surface of the palatine to supply the roof of the mouth. A dorsal (or medial) palatine artery (mpla, figure 8a) continued forwards over the dorsal surface of the palatine bone probably in grooves near the midline.

The temporal artery branch from the stapedial artery descended behind the postorbital, and probably sent frontal artery branches to the small foramina in the frontal bone (figure 4), as in *Sphenodon*. The frontal artery descended into the orbital cavity and gave off a ventral branch, the inferior nasal artery (ina, figure 8a), part of which passed over the dorsal surface of the vomer, probably in the groove medial to the choana, and pierced the vomer, possibly through the long foramen below the dorsal groove. A small anterior branch passed dorsally again, possibly through the fenestra vomeronasalis externa (fve, figure 6b).

The temporal artery also gave off a further ventral branch, the inferior orbital artery, which doubtless passed through the infraorbital foramen (figure 6b) and became the maxillary artery (ioa, ma, figures 2b, 8a, 9a). This large artery continued through the superior alveolar canal in the maxilla, giving off ventral branches to the maxillary teeth (figures 8a, 9a). Other branches probably passed laterally to the lips and skin through some large foramina (figures 5a, 9a), as in *Sphenodon*. One long thick branch passed far forwards within the maxilla and exited
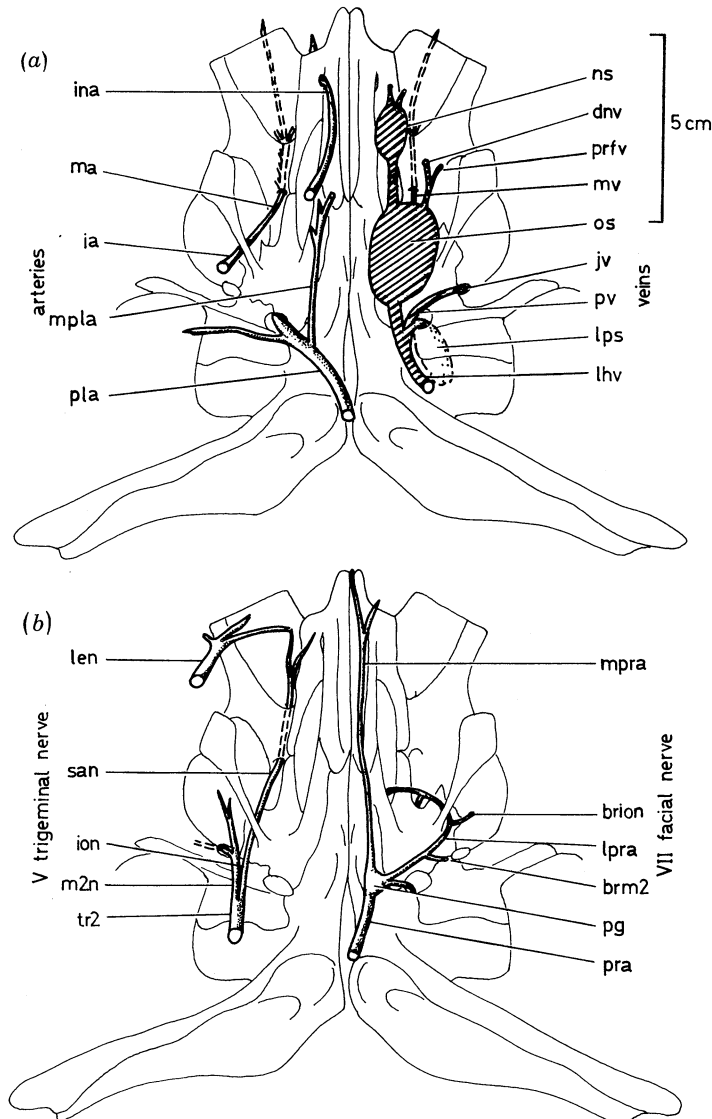
FIGURE 8. Reconstruction of selected soft parts of the skull, drawn on a dorsal view of the palate. (a) Arteries (left) and veins (right). (b) Nerves: divisions of the trigeminal (left) and the facial (right).

just below the premaxilla (figure 4a), probably supplying the tissue round the base of the 'tusk' and the external nasal tissues. This anterior maxillary foramen is present in *Stenaulorhynchus* (Huene 1938, p. 87, pl. 9, fig. 1) and *Scaphonyx* (Huene 1942, p. 268, pl. 31, fig. 10).

Certain aspects of the venous system of *Hyperodapedon* may be inferred. *Hyperodapedon* probably had an extensive nasal sinus (ns, figure 8a) and an orbital sinus (os, figure 8a) that filled an unknown volume of the high orbital cavity. A dorsal nasal vein (dnv, figure 8a) probably passed through the nasal bone and into the orbital sinus from above, and it may have been joined by a prefrontal vein (prfv, figure 8a) draining through small openings in the orbital wall of the prefrontal (Bruner 1907). The orbital sinus also received veins from the jugal and posterior lips, probably through the medial jugal foramen (mjf, figure 6b; jv, figure 8a). The maxillary vein (mv, figure 8a), draining the lateral snout and maxillary tooth plate, probably passed back

through the superior alveolar canal into the orbital sinus from below (cf. *Lacerta* (Bruner 1907)). Ventrally, in the large cavity between pterygoid and ectopterygoid (figure 6a) there probably lay a large lateral palatine sinus (lps, figure 8a). This sent a large branch dorsally through the inferior orbital foramen (figure 6a, b) to the pterygoid vein which drained back into the lateral head vein (lhv, figure 8a).

Thus, the canals on the dorsal aspect of the palate and in the maxilla suggest rich vascularization of the maxillary tooth plate, lips, and narial tissues.

4.5.3. *Nerves of the orbital and nasal cavities* (figure 8b)

This account deals with some of the branches of both the trigeminal nerve (V) and the facial nerve (VII) of *Hyperodapedon*, and the foramina indicate closest similarity with *Sphenodon* (Osawa 1898a; Werner 1962) and lizards (Watkinson 1906; Oelrich 1956).

The maxillary division (trigeminal 2) split into two branches high in the temporal region: maxillary 2 (+1) and the infraorbital nerve (tr2, m2n, ion, figure 8b). Maxillary 2 (+1) innervated the posterior orbital elements and gave off a lateral branch which entered the medial jugal foramen (figure 6b) and passed through the bone to the skin as a series of infraorbital cutaneous branches through the lateral jugal foramen (?and suborbital foramina) (ljf, sf, figure 5a), as in *Sphenodon*. The infraorbital nerve entered the infraorbital foramen to become the superior alveolar nerve (san, figure 8b). This continued through the superior alveolar canal (figure 6b), giving off dental and labial branches to the teeth and lips, as in *Varanus* and *Sphenodon*. Anteriorly, it innervated the naris and joined the lateral ethmoidal nerve coming from above.

The ophthalmic division (trigeminal 1) innervated the dorsal region of the orbit and nasal capsule. An anterior branch, the lateral ethmoidal nerve (len, figure 8b), gave off a small dorsal cutaneous branch that pierced the nasal bone (figure 4a) (cf. *Ctenosaura* (Oelrich 1956, p. 63)). It also sent branches through the nasal process of the maxilla to supply the skin there (through the foramen between maxilla and lacrimal, figure 5a), and finally anastomosed with the superior alveolar nerve.

The palatine ramus (pra, figure 8b) of the facial nerve (VII) branched above the pterygoid, possibly at a palatine ganglion (pg, figure 8b) resting in a slight concavity as in *Sphenodon*. A ventral branch probably passed through the inferior orbital foramen to innervate the tissues of the roof of the mouth. The medial palatine ramus (mpra, figure 8b) ran in a groove anteriorly over the palatine process of the pterygoid and the palatine. It innervated the oral surface of the palate, possibly through the choana and pyriform recess between the pterygoids, and travelled anteriorly in the median vomerine groove (figures 5c, 6b) to innervate the ventral surface of the vomer and anterior nasal capsule. The lateral palatine ramus communicated with the maxillary division of the trigeminal and with the inferior orbital nerve, before passing through the infraorbital foramen (lpra, brm2, brin, figure 8b). The lateral palatine ramus then passed to the ventral surface of the palatine and maxilla, possibly through the posterior angle of the choana as in *Sphenodon* (Wettstein 1931).

4.5.4. *Quadrate foramen* (qf, figures 7, 9b)

The large foramen between quadrate and quadratojugal probably conducted the mandibular vein and internal mandibular vein to the neck region as in *Sphenodon* (O'Donoghue 1920, pl. 7, fig. 2). The secondary small opening below the quadrate foramen may have guided a

small quadrate vein down to the mandibular vein, as in lizards (Bruner 1907, p. 23) and possibly also *Sphenodon* (O'Donoghue 1920, pl. 7, fig. 2).

4.5.5. *Cartilaginous nasal capsule* (figure 9c)

In the anterior snout area are various ridges and processes that indicate the nature of the cartilaginous nasal capsule. Again, *Sphenodon* (Pratt 1948) and lizards (Oelrich 1956) are used as models. The nasal septum was supported between the vomers and probably rose to divide the single nasal opening. The division between nasal septum and interorbital septum is probably marked by the change in angle of the median ridge at the vomer–pterygoid junction (figures 5b, c, 6b).

The cupola (anterior and dorsal roof of anterior nasal tube) probably formed a pair of tubes facing anteriorly, one on each side of the nasal septum, and attaching on the nasal and pre-maxillary border of the naris (cu, figure 9c). The division between zona annularis (surrounding the anterior chamber of the nasal sac) and paranasal cartilage (surrounding much of the olfactory chamber of the nasal sac) (za, pc, figure 9c) is probably marked by the vertical ridge on the inside of the maxilla (figure 6b). The lateral cartilaginous lacrimal ridge (lr, figure 9c) probably coincided with the remarkable semi-spiral ridge on the lacrimal (figures 5b, 9a) and conducted the lacrimal duct anteroventrally.

Ventral to the paranasal cartilage was the cartilaginous maxillary process (mp, figure 9c) which probably inserted into the broad space below the ascending process of the palatine (figure 6b). This appears to correspond to the position between prefrontal, palatine and maxilla in *Ctenosaura*.

Ventrally, the paranasal cartilage surrounded the choana and formed part of a tube to the naris, via the cupola. Above this, there may have been an additus conchae, marked by the vertical ridge on the maxilla, although *Sphenodon* has no conchal formation (Pratt 1948, p. 191). Ventral to this, the paranasal cartilage probably rested on the vomer and palatine, well below the level of the base of the nasal septum, giving rise to a very large, deep olfactory chamber.

The cartilages of the vomeronasal organ of Jacobson (cJo, figure 9c) probably opened ventrally at the end of the lacrimal groove at the fenestra vomeronasalis externa (fve, figure 9d) and posteriorly for passage of the vomeronasal nerves. A septomaxilla was probably present, protecting Jacobson's organ and the anterior olfactory chamber, but none has been found. The so-called septomaxilla described in *Scaphonyx* by Huene (1929, p. 8, fig. 6) is in fact the internal ascending process of the maxilla.

Thus, because of the deepening of the skull, the anterior position of the naris and far posterior position of the choana, the olfactory chamber within the zona annularis and paranasal cartilage was remarkably long and deep. Even if the olfactory epithelium did not cover the entire internal surface of the chamber, it was probably larger than that of a lizard of the same size. The olfactory nerves passed to the olfactory bulbs which probably lay directly above in the relatively large circular pits under the frontal (figure 4b). The evidence of the size of the olfactory chambers and of the olfactory bulbs of the brain suggest that *Hyperodapedon* had a good sense of smell.

4.5.6. *Lacrimal duct and Jacobson's organ* (figures 2c, 4a, 9c, d)

The lacrimal duct passed from the tissues of the anterior part of the eye as two separate canaliculi which entered the lacrimal bone through two large foramina, of which the upper
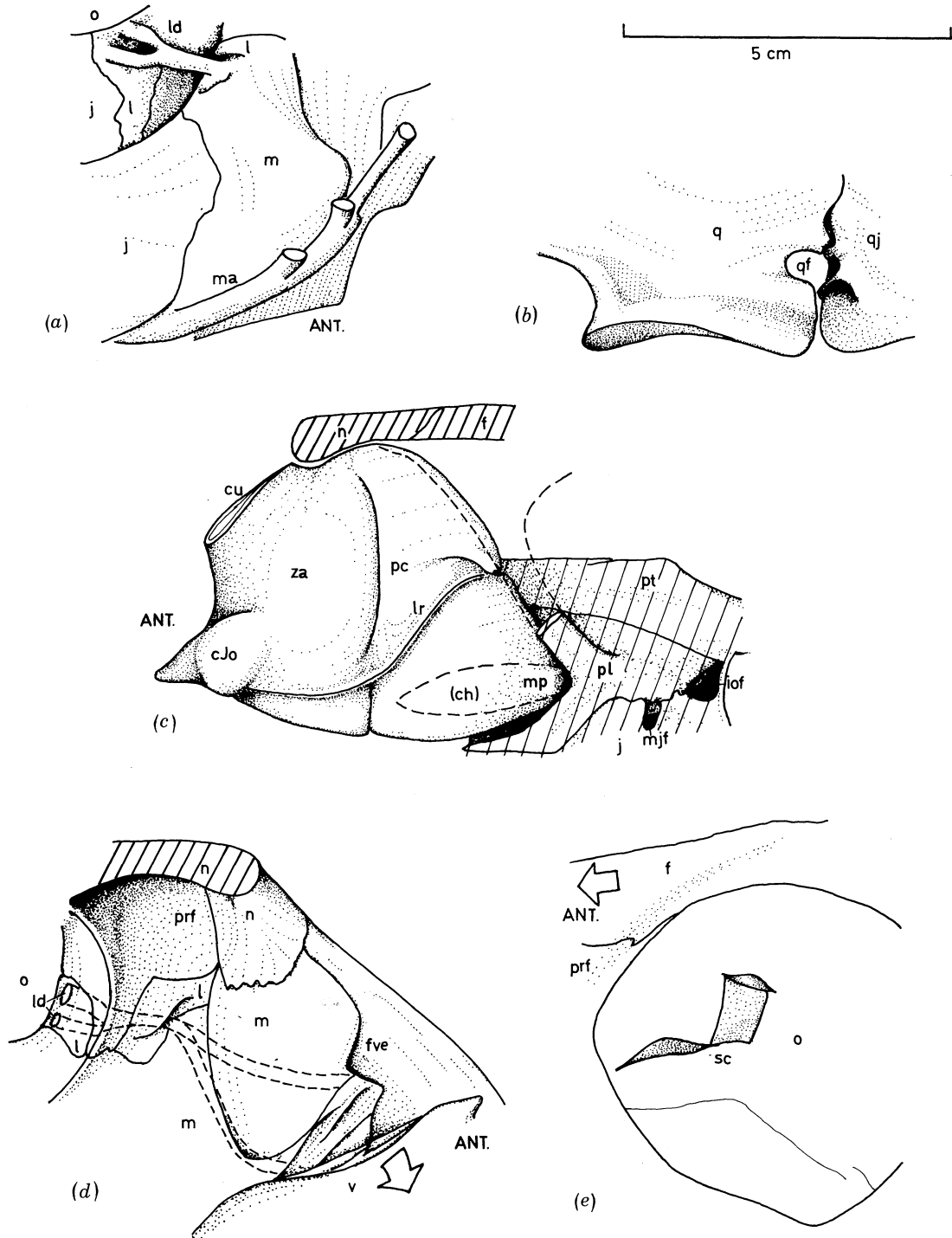
FIGURE 9. Details of the skull. (*a*) Lateral view of an internal rock mould of the anterior part of the skull, showing the lacrimal duct and palatal vessel canals, NUGD A. (*b*) Internal view of the left quadrate and quadratojugal showing the complex suture and the quadrate foramen; based on casts of NUGD B. (*c*) Reconstruction of the cartilaginous nasal capsule in left lateral view; bone of the anterior palate diagonally shaded, and part of skull roof sectioned; lacrimal ridge tentative; based on casts of NUGD A and B. (*d*) Medial view of anterior side wall of the skull showing two possible courses of the lacrimal duct (dashed lines) after it passes through the lacrimal bone; the vomer is pulled aside slightly to show the complex suture; based on casts of NUGD A and B. (*e*) Scleral ossicles as preserved within the orbit on the natural rock mould of NUGD A.

is the larger (figures 2 c, 4 a, 9 a, d). These soon fuse to a single flattened canal which enters the nasal capsule well anteriorly. This condition is similar to that of most lizards and *Sphenodon* (Bellairs & Boyd 1947, type A). In medial view, the bony lacrimal canal is roofed by a diagonal twist of lacrimal bone which conceals the opening (figure 9 d). The cartilaginous lacrimal ridge must trend steeply downwards across the medial surface of the maxilla, and it may enter the region of Jacobson's organ laterally, as in *Sphenodon* (Bellairs & Boyd 1950, pp. 289–290, 299). Alternatively, it may enter medially and ventrally, as in lizards (Bellairs & Boyd 1950, pp. 272, 274), having run down inside the maxilla and through a tube formed in the medial suture of maxilla and vomer (figures 5 c, 6 b). This lacrimal duct could then pass to the fenestra vomeronasalis externa (fve, figure 9 d) where it would enter the region of Jacobson's organ anteromedially.

In lizards, Jacobson's organ (vomeronasal organ) lies anteriorly within the cartilaginous nasal capsule and is roofed by the septomaxilla. In *Sphenodon*, the organ lies in the nasal septum (Parsons 1970). It communicates with the buccal cavity by a duct, and its function generally appears to be to detect the smell of food in the mouth (Romer 1956, p. 31). It is concluded that the Jacobson's organ in *Hyperodapedon* was set far forward and isolated from the rest of the nasal capsule because of the suggested course of the lacrimal duct and the presence of the large lateral notch which seems to be homologous with the fenestra vomeronasalis externa of lizards. The lacrimal duct to the buccal cavity may have passed through the gap between this notch and the premaxilla as in lizards (naso-palatine canal, e.g. *Anguis* (Jollie 1960, p. 29)), or back and through the anterior part of the choana, as in *Sphenodon* (Bellairs & Boyd 1950).

4.5.7. *Orbit and eye* (figures 4, 5, 9 e)

The orbit faces largely dorsally and anteriorly. It is composed of the prefrontal and rising palatine process in front (anterior orbital septum), the interorbital septum medially, the postorbital, jugal and ectopterygoid behind (posterior orbital septum) and jugal and lacrimal laterally. This bony housing of the eye is far more highly developed than in *Sphenodon* or lizards and, because of the remarkable posterior extent of the nasal capsule, the orbit is relatively rather restricted in *Hyperodapedon*, especially below. This suggests that the eye was placed high in the orbit, and probably bulged outside the bony rim. This would suggest in turn that scleral ossicles were probably necessary to maintain the shape of the eyeball, as in *Prolacerta*, *Sphenodon* and certain lizards with large orbits (Underwood 1970). Indeed, in NUGD A, three rectangular, gently curved plates are preserved high in the left orbit (sc, figure 9 e), and they are probably the remains of an extensive sclerotic ring. The best preserved plate measures 8 mm × 6 mm, but was probably larger. One other is 15 mm long.

This is the first record of scleral ossicles in rhynchosaurs. The plates are slightly curved which, according to Underwood (1970, pp. 79–81), suggests 'good powers of accommodation and probably diurnal habits' in a terrestrial reptile. Unfortunately, no complete ring is preserved, so that an estimate of the relative size of the cornea cannot be made. The large orbit and orbit walls, well defined by prefrontal and postorbital, indicate a large eye and suggest 'that vision is important in the life of the animal' (Underwood 1970, p. 81). The eye was probably surrounded and roofed by connective tissue and integument, and looked partly sideways, and mainly anteriorly over the dorsal prefrontal ridge when the head was lowered in its probable natural position (figure 40; Chatterjee 1980, pp. 63, 64).

4.6. *Endocranium and middle ear* (figures 7, 10, 11)

The bony portions of the braincase give good evidence of the form of its cartilages, and offer information on the shape of the brain and the distribution of cranial nerves and cranial blood vessels and ear structure. The braincase of *Hyperodapedon* seems to be very like that of *Sphenodon* and the interpretation is based upon a dissection of the latter animal and upon published accounts (Dendy 1909; Säve-Söderbergh 1946, 1947).
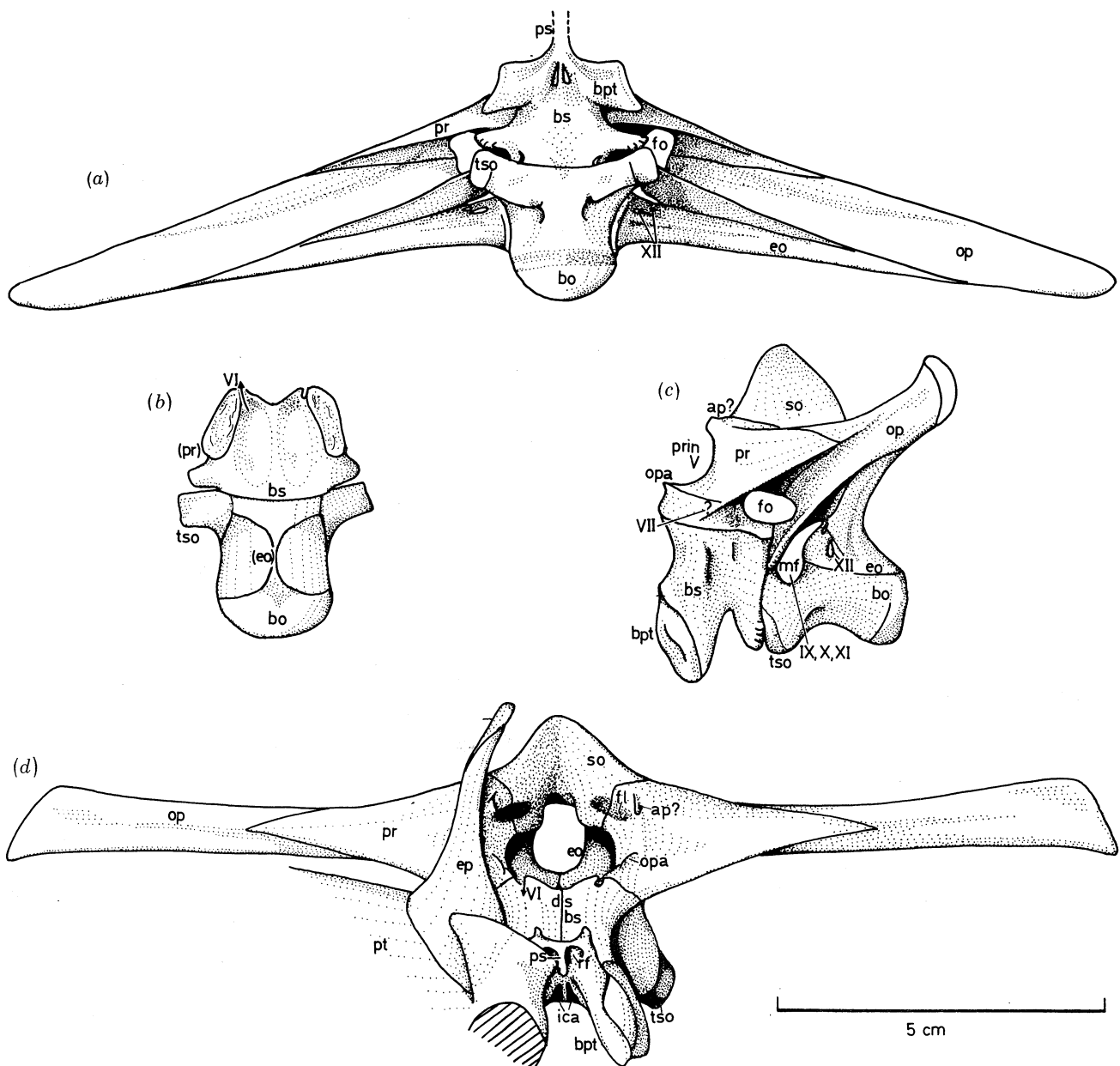

FIGURE 10. Composite restoration of the endocranium; distal ends of paroccipital processes restored from other rhynchosaurs. (*a*) Ventral view; (*b*) dorsal view of the basioccipital and basisphenoid with other elements removed; (*c*) left lateral view; (*d*) anterior view, with the pterygoid and epipterygoid indicated on the left side only.

4.6.1. *Ossified elements of the endocranium*

The most complete endocranium of *Hyperodapedon* is a cast of NUGD A. Additional information is derived from a partial disarticulated braincase in casts of NUGD B. Because of the poor preservation of bone material, braincases have not been preserved in any other specimens. Only BMNH R3140, which is broken fortuitously, shows some features in outline.

As with other rhynchosaurs, the ossified elements of the braincase include robust median elements: basioccipital, basisphenoid (+parasphenoid – no clear suture is seen) and supra-occipital, and paired exoccipitals, opisthotics and pro-otics. The cultriform process is not seen complete, and the distal end of the paroccipital process is not preserved in any specimen.

The *basioccipital* forms the major part of the hemispherical occipital condyle (figure 7) and, in front of this, expands into two lateral blunt-ended processes (tubercula spheno-occipitales, tso, figure 10a). Behind these are two deep pits facing posteroventrally. The basioccipital forms a small part of the middle of the braincase floor (figure 10b) and has two large areas of attachment for the exoccipitals. The floor of the metotic foramen is formed by the anterior dorsal part of the basioccipital (figure 10b, c).

The *basisphenoid* lies anterior to the basioccipital. Two blunt rugose processes press close to the tubercula spheno-occipitales (figure 10a). In front, the long basipterygoid processes are separated by a deep furrow containing the paired carotid foramina, and they contact the pterygoids on ridged facets (bpt, figure 10d). In anterior view, the basisphenoid rises high above the basipterygoid processes and forms a flat vertical dorsum sellae which bears a pair of shallow fossae (ds, rf, figure 10d). Each fossa is bounded ventrally by the pterygoid and dorsally by a raised ridge and small anterior process. Following Chatterjee (1974, p. 221), these are interpreted as retractor fossae for attachment of the retractor bulbi eye muscles, as in *Sphenodon* (Säve-Söderbergh 1946, figure 10). Between these lies a short anterior process, probably the base of a delicate cultriform process. In Chatterjee's illustration (1974, figure 6c), the structure labelled 'ic' is probably equivalent. The upper part of the dorsum sellae is divided by a weak median ridge and in the dorsal margin shows a pair of openings which may be just closed dorsally. The basisphenoid forms the anterior floor of the braincase (figure 10b), and shows two elongate depressions. Laterally, there are large ridged facets for the pro-otics.

The paired *exoccipitals* rest on the basioccipital and meet medially over the occipital condyle (figures 7, 10b). The medial portion is broad and narrows upwards. It forms the posterior part of the braincase wall and the ventral and lateral walls of the foramen magnum (figure 11a). It is perforated by two or three hypoglossal foramina, and forms the posterior margin of the metotic foramen (XII, mf, figures 10c, 11a). The exoccipital sends a lateral ascending process along the posterior margin of the paroccipital process, and its firm suture with the opisthotic may be detected dorsally and ventrally, but is not seen in *Paradapedon* (Chatterjee 1974, p. 223).

The *opisthotics* form the bulk of the long paroccipital processes, the posterior wall of the otic capsule, and the roof of the stapedial canal. The opisthotic contacts the basioccipital by a narrow pillar (the lagenar crest, lc, figure 11a) which forms the anterior margin of the metotic foramen. This pillar extends laterally into a long ridge that is bounded behind by the exoccipital and which forms the posterior margin of the stapedial canal (figure 10a, c).

The *pro-otic* forms the medial half of the anterior edge of the paroccipital process, and the anterior wall of the braincase, otic capsule and fenestra ovalis (figure 11b). The pro-otic rests on two large horizontal processes of the basisphenoid (figure 10b), and rises as a narrow pillar

to meet the supraoccipital. In medial view, the pro-otic bounds a large opening into the otic capsule, and encloses a large floccular recess (fl, figure 11*a*). As in *Sphenodon*, there is no typical ala pro-otica, but it may be represented by a small anterior process just above the trigeminal incisure in *Hyperodapedon* (ap?, figure 10*c*, *d*). The small anterior process at the ventral margin of the pro-otic incisure is probably the ossified proximal portion of the pila antotica, as in *Sphenodon* (opa, figure 10*c*, *d*).

The *supraoccipital* is a dorsally arched element that forms the roof of the braincase. It contacts the pro-otic, opisthotic and exoccipital with broad ventral surfaces (figure 11*b*). In medial view
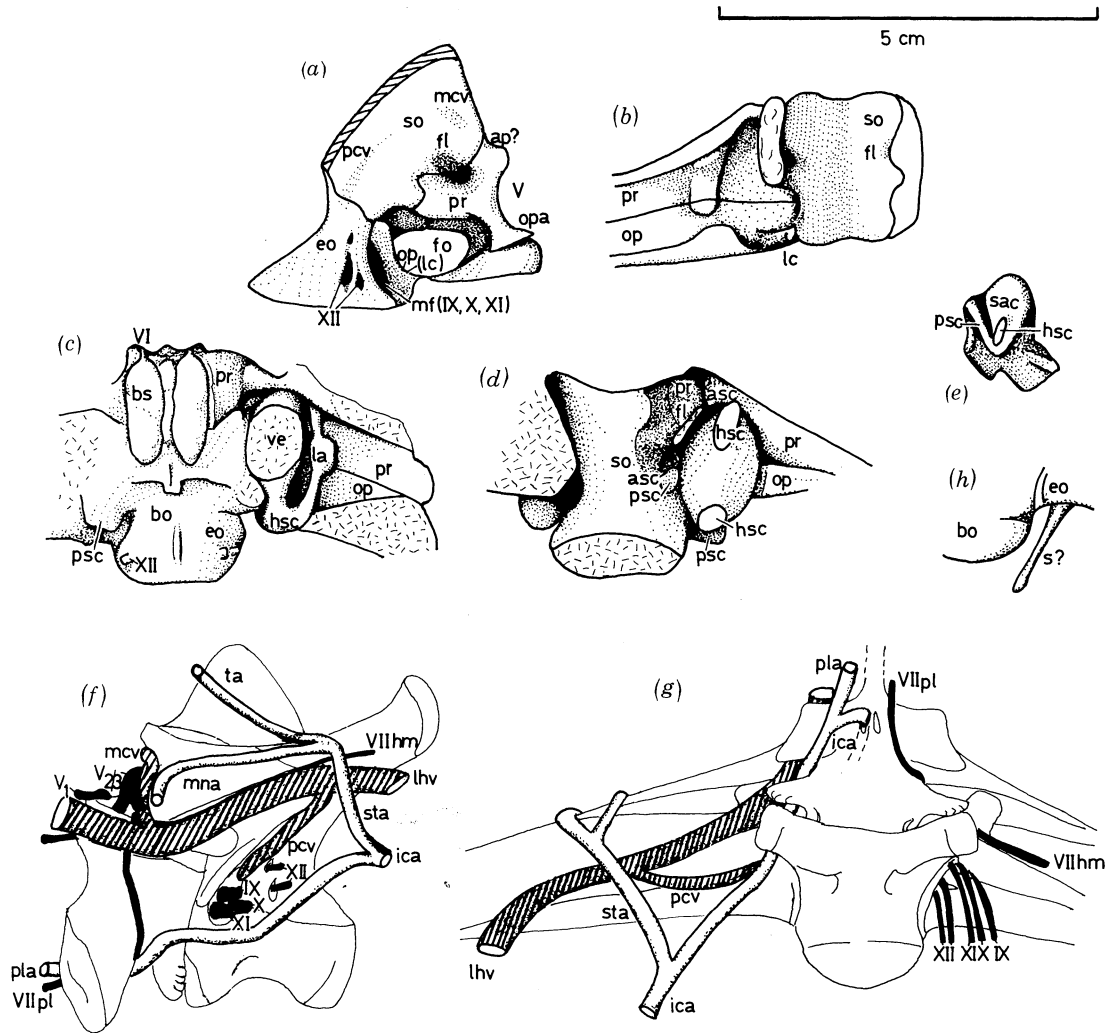

FIGURE 11. Endocranium. (*a*) Composite restoration of the side wall of the braincase in medial view; supraoccipital split in the midline. (*b*) Composite restoration of the supraoccipital, pro-otic and opisthotic in ventral view. (*c*) Ventral view of a natural rock mould of the braincase (NUGD A), showing impressions of the brain, cranial nerves and semicircular canals of the left-hand side. (*d*) Dorsal view of a natural rock mould (NUGD A) of the braincase, showing the inner ear of the right-hand side; the horizontal semicircular canal is broken. (*e*) Posterodorsal view of a natural rock mould (NUGD B) of part of the inner ear of the left-hand side; the horizontal semicircular canal is broken. (*f*) Restoration of the blood vessels and nerves of the braincase region, drawn in left lateral view; arteries unshaded, veins striped, nerves black. (*g*) Restoration of the blood vessels and nerves of the braincase, drawn in ventral view; arteries unshaded, veins striped, nerves black. (*h*) Possible distal end of a stapes, drawn from a cast of the left-hand side of the braincase, NUGD A.

(figure 11a), it bounds the floccular recess and medial portion of the otic capsule. The supraoccipital forms the dorsal margin of the foramen magnum and the proximal part of the paroccipital process, and it meets the parietal with a small contact (figures 7, 10c).

4.6.2. Orbitotemporal cartilages and membranes

The orbitotemporal membranes enclosed the anterior portion of the brain, and associated structures. Some evidence of the nature of these unfossilizable parts may be obtained by comparing Hyperodapedon with Sphenodon (Säve-Söderbergh 1946, 1947) and lizards (e.g. Ctenosaura (Oelrich 1956, pp. 19–22)).

The cultriform process of the parasphenoid was presumably short, because of the shortness of the interpterygoid vacuity (pyriform recess). It supported the posterior parts of the interorbital septum. Two cartilaginous bars, the pila antotica and the taenia marginalis, probably arose from the small ossified ala pro-otica (ap, figure 10c) and the anterolateral face of the supraoccipital respectively and extended forwards along the sides of the parietal. They supported the pituitary body, and the pro-otic membrane which surrounded the cerebrum and cerebellum. Because of the great width of the temporal region of the skull, the ossified and unossified sections of the endocranium in Hyperodapedon were limited to a narrow medial area.

4.6.3. The brain

The reptilian brain does not always fill the cranial cavity and, for that reason, a detailed reconstruction of the brain of Hyperodapedon is not attempted. However, some features are evident. The paired olfactory lobes were probably housed in the depressions on the ventral surface of the anterior part of the frontals (figure 4b). The cristae cranii form lateral borders to this region and partially surrounded the olfactory stalks. There is no evidence for the extent of the cerebral hemispheres, optic lobes or pineal organ. There is no parietal foramen, and thus no pineal eye, but a median depression on the ventral surface of the parietal, just in front of the parietal fossae, may represent the site and extent of the pineal organ (figure 4b).

The cerebellum probably occupied the upper anterior part of the braincase, surrounded by the supraoccipital and pro-otics. Part of it was doubtless accommodated in the large floccular fossae (fl, figure 11a, d).

As in Sphenodon and Paradapedon (Chatterjee 1974, pp. 221–3), there is no sella turcica, and the pituitary body was probably raised and separated from the dorsum sellae by a membrane, as a result of the invasion of the retractor bulbi eye muscles (Säve-Söderbergh 1946). The ridges and processes above the retractor fossae may have been for attachment of strong membranes separating the muscle mass from the pituitary.

The medulla oblongata was probably approximately cylindrical, and filled most of the braincase below the level of the supraoccipital. The paired oval-shaped depressions on the dorsal surface of the basisphenoid may reflect the ventral shape of the medulla (figure 10b).

4.6.4. Cranial nerves (figures 10c, d, 11a, f, g)

As in Sphenodon (Säve-Söderbergh 1946) and rhynchosaurs generally (Huene 1929, 1938, 1942; Chatterjee 1974), the exits for cranial nerves I–IV were through unossified anterior parts of the endocranium. The trigeminal (V) was probably a large nerve that exited through the shallow pro-otic incisure (prin, figure 10c), and it passed medial to the epipterygoid

(figure 10*d*). The maxillary and ophthalmic divisions (V_1, V_2) have been described above (§4.5.3) and the mandibular division (V_3) is described below (§5.2).

The abducens nerve (VI) probably passed forwards through the small lateral openings on the dorsal margin of the dorsum sellae (figure 10*d*).

The facialis nerve (VII) presumably exited through a small foramen in the pro-otic, behind the pro-otic incisure, but this has not been located in the casts. As in *Sphenodon* (Säve-Söderbergh 1946, p. 9), a palatine branch of the facialis (VIIpl, figure 11*f, g*) probably ran ventrally and medially in the groove at the proximal end of the basipterygoid process (equivalent to the vidian canal of lizards), and its further course is described in §4.5.3 above. Before passing around the basipterygoid process, the facialis probably gave off a major ramus hyomandibularis (VIIhm, figure 11*f, g*) which ran back over the pro-otic and into the stapedial canal above the stapes. A major branch here is the chorda tympani which, as in *Sphenodon* (Wyeth 1924, pl. 17, fig. 45), probably ran to the lateral end of the paroccipital process, behind the quadrate, and into the lower jaw (see §5.2 below).

The acoustic nerves (VIII) passed into the otic capsule through the large opening in the middle of the medial braincase wall which was probably covered by a membrane in life. The metotic foramen (including jugular foramen, glossopharyngeal foramen, vagus foramen, fenestra rotunda), passing posterolaterally between opisthotic and exoccipital, probably transmitted cranial nerves IX, X and XI. Finally, cranial nerve XII was transmitted through two or three small hypoglossal foramina in the exoccipital.

4.6.5. *Cranial blood vessels* (figure 11*f, g*)

The interpretation of the cranial blood vessels of *Hyperodapedon* is based on *Sphenodon* (Dendy 1909; O'Donoghue 1920; Säve-Söderbergh 1946, 1947), since the braincases are so similar. The internal carotid artery (ica) probably passed from the neck region below the paroccipital process, and then split into two branches. The stapedial artery (sta) passed under the stapes and split into two arteries of similar size, the temporal and the mandibular (ta, mna). The temporal artery ran up over the opisthotic and supraoccipital, probably in the slight grooves on these bones, and forward below the postorbital to supply the snout (see §4.5.2 above). The mandibular artery ran down along the upper surface of the pro-otic and turned outwards at the back of the pro-otic incisure to pass through the temporal region and into the lower jaw (see §5.2).

The internal carotid ran forward on the side of the braincase and then medially round the base of the basipterygoid process. One branch continued forwards as the palatine artery (pla) whose course through the rest of the skull is described in §4.5.2. The internal carotid probably supplied anterior parts of the brain, and the vessels from each side passed through the paired openings between the basipterygoid processes (figures 10*a, d*, 11*g*).

The brain region was drained by a complex of veins that probably passed into a sinus longitudinalis lying just below the supraoccipital, as in *Sphenodon*. A large posterior cerebral vein (pcv) probably left the braincase through the metotic foramen above the cranial nerves IX, X and XI. Further anteriorly, a large sinus transversus may have been drained through the pro-otic incisure by a large median cerebral vein (mcv). This vein is guided by a process and a groove in *Sphenodon*, and similar features are seen in *Hyperodapedon* (?ala pro-otica; shallow groove behind pro-otic incisure; figures 10*c*, 11*f*). Both the posterior and median cerebral veins drain into the lateral head vein (lhv) portion of the jugular vein. As in *Sphenodon*, this probably

ran back over the pro-otic in a groove below the incisure and into the stapedial canal (figures 10c, 11f).

4.6.6. *The inner ear* (figure 11 a–d)

Evidence for the structure of the inner ear comes from casts and natural rock moulds of NUGD A and B. The general structure is similar to that of *Paradapedon* (Chatterjee 1974), but the preservation in *Hyperodapedon* offers much new information.

The vestibular cavity is separated from the metotic foramen by a deep ridge of the opisthotic (lagenar crest, lc, figure 11 a, b). The vestibule is roughly triangular with anterior, posterior and dorsal apices in the pro-otic, opisthotic and supraoccipital respectively. The three semicircular canals link these apices and they are entirely surrounded by bone. Excellent natural rock moulds are seen when the bone is removed. The horizontal semicircular canal (hsc, figure 11c) is broad anteriorly and posteriorly, but narrows and then expands halfway along its length (at the junction of pro-otic and opisthotic) into an ampulla horizontalis (or lateral ampulla, la). The anterior and posterior vertical semicircular canals are rather shorter (asc, psc, figure 11 d, e), and they run from the dorsal surface of the anterior and posterior apices of the vestibule (ve) through pro-otic and opisthotic respectively to meet in a deep recess in the supraoccipital. The anterior and posterior ampullar recesses do not appear to be distinct from the vestibule in the rock casts, and they are probably represented by the slightly drawn out anterior and posterior extensions that pass deep within the pro-otic and opisthotic respectively (figure 11 b–d). The form of the utricle is concealed on the medial surface of the vestibule, but the sacculus (sac) seems to have been rounded. This is rather different from the situation in lizards (e.g. *Ctenosaura* (Oelrich 1956, figs 54–56) and *Sphenodon* (Osawa 1898b, p. 315)).

The medial wall of the braincase (figure 11 a) has a very large opening, presumably covered by a membrane in life, through which the auditory nervous rami and endolymphatic duct passed. The vestibule is underlain by a deep lagenar recess which is bounded below by the basioccipital and basisphenoid. The perilymphatic sac lay at the base of the medial entrance to the metotic foramen in the recessus scala tympani. The perilymphatic duct passed round the base of the lagenar crest and into the perilymphatic cistern below the vestibule. The perilymph system may have ended blindly in a cavity in the pro-otic, as in *Paradapedon* (Chatterjee 1974, fig. 7b ('per.')), but this is not seen in *Hyperodapedon*, and there is no evidence of a separate fenestra rotunda. The fenestra ovalis lies at the lateral side of the lagenar recess.

4.6.7. *The middle ear*

No stapes has been found *in situ* among the material of *Hyperodapedon*, nor of any other rhynchosaur. A slender rod with a bulbous end is preserved beside the occipital condyle in NUGD A (figure 11h), and this might be the distal end of a stapes. Because of the length of the stapedial canal in *Hyperodapedon*, the stapes must have been long and, if it was shaped like that of *Sphenodon*, it would have tapered considerably towards the contact with a cartilaginous extrastapes. The fenestra ovalis is large and elliptical (figure 10a, c), and the footplate of the stapes was probably large, as in *Sphenodon* (Wever 1978, p. 819).

The quadrate–squamosal area of the rhynchosaur skull is very similar to that of *Sphenodon* in the absence of a curved tympanic crest on the quadrate. In lizards, this crest marks the

anterior and dorsal margins of the tympanum, while *Sphenodon* has no external ear opening or tympanum. Thus, rhynchosaurs also probably had no tympanum.

Many reptiles other than *Sphenodon* lack a tympanum; and these include some lizards, amphisbaenians and snakes. These animals receive air-borne sound through the skin covering the auditory meatus, an expanded depressor mandibulae muscle, or through the quadrate (Wever 1978). The extrastapes in *Hyperodapedon* was probably linked to the large epihyal element of the hyobranchial skeleton (see §4.7), as in *Sphenodon*. This provides an additional auditory pathway for reception of ground- and air-borne sound in the throat muscles and hyoids (Tumarkin 1955). The sensitivity of these ears is often surprisingly good, and *Sphenodon* can detect a range of about three octaves in the low frequency for air-borne sound (Wever 1978, p. 831).

Hyperodapedon probably detected ground-borne sound via the hyoid apparatus but also, because of the delicacy of the stapes (if the fragment in figure 11*h* is indeed a stapes), it may have had a secondary mechanism for detection of air-borne sound through the skin without a tympanum.

4.7. *Hyoid apparatus* (figure 12)

Some *Hyperodapedon* skulls have strap-like bony elements associated with the mandibles. EM 1978.566.1A, B (counterparts) have an 80 mm segment of gently curved bone, about 6 mm wide and 1 mm thick (figure 12*a*). EM 1978.567.1C and GSM 90929 show similar fragments. NUGD B (a full-size gracile skull) has a narrower rod-like element (4–5 mm wide) just medial to the articular.
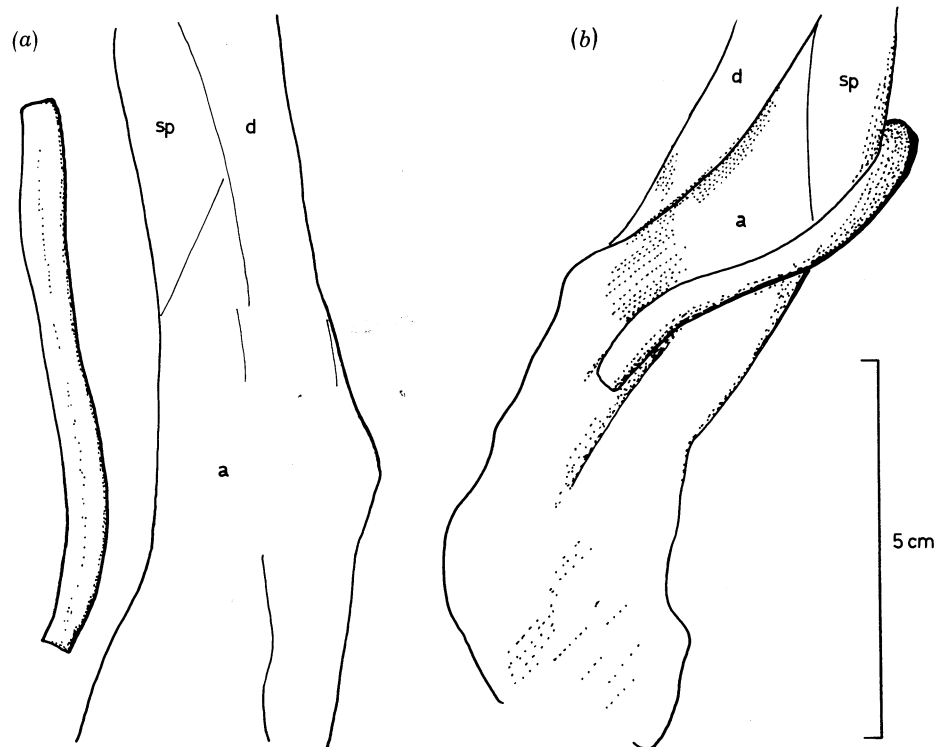

FIGURE 12. Ossified hyoid elements. (*a*) Ventral view of left mandible and hyoid of *Hyperodapedon gordoni*, EM 1978.566.1 A/B; (*b*) ventral view of right mandible and hyoid of *Scaphonyx fischeri*, München '18/4 (136)'.

It is suggested that these are examples of the epihyal portion of the ceratohyal which forms a similar curve below the mandible in *Sphenodon* (Rieppel 1978, fig. 1*b*). This is a dorsal cartilaginous element of the hyobranchial skeleton which joins the extracolumella (extrastapes) in *Sphenodon* (Wever 1978, p. 820) and may have done so in *Hyperodapedon*.

It could be argued that these elements in *Hyperodapedon* are parts of ceratobranchial 1 which is ossified in most reptiles, whereas the epihyal usually is not. However, the ceratobranchials are more ventral in position, and evidence from other rhynchosaurs with more completely preserved elements tends to confirm the identification given here. At least three specimens of *Scaphonyx* (MCZ 3641, 3642; Bayer. Staatsamml., München '18/4'('136'); figure 12*b*) preserve segments of hyoid elements. The hyoid element starts medially below the interpterygoid vacuity, curves laterally and then backwards across the flattened underside of the angular. It may then pass up to the paroccipital process, as in *Sphenodon* and some lizards (Romer 1956, p. 422), or it may end freely in the tissues of the throat region. Rhynchosaurs thus had a strong hyoid skeleton rather like that of *Sphenodon*, and this would aid hearing (see §4.6.7) and provide a base for the attachment of a large tongue.

5. Mandible
5.1. *Bone descriptions* (figures 13, 14)

Detailed information is available on the mandible of *Hyperodapedon* from casts of NUGD A, B, BMNH R3153 and R4782, and from a large dentary, BMNH R4780. The lower jaws are deep boat-shaped elements which rise to anterior pointed processes that lie lateral to the premaxillary 'tusks' when the jaws are closed. In dorsal view (figure 13*a*), these processes diverge from the symphysis, but the true rostra are not as long as indicated by Huxley (1887). Posteriorly, the jaws diverge widely and a slight sigmoid curvature is developed as in *Paradapedon* (Chatterjee 1974). The posterior half of the mandible is occupied by a large adductor fossa which is bounded laterally by the surangular and medially by the prearticular and is floored by a flattened angular. The fossa leads into a large meckelian canal that is enclosed entirely by the dentary, splenial and angular. The canal narrows forwards and runs into a meckelian groove and several large vessel openings.

The *dentary* occupies the anterior two-thirds of the mandible. Behind the tapering edentulous rostrum, a single row of palisade teeth (the buccal teeth) runs along the sharp occlusal margin back to the coronoid (figure 13*b, c*). In lateral view, the posterior margin of the dentary runs into a long tongue over the surangular, and descends anteriorly in an irregular edge over the surangular and angular.

In medial view (figure 13*c*), the dentary is partially overlain by the splenial ventrally and the coronoid and prearticular behind. A strong ridge runs back above the meckelian groove into an overhanging lamina that roofs the meckelian canal for its whole length (mg, mc, figure 14*a, b*). The lamina continues back to a point which fits into a pit on the upper edge of the prearticular near the front of the adductor fossa (figures 13*a*, 14*a*). A series of large conical lingual teeth runs above the meckelian canal up to the dorsal edge some distance behind the rostrum. Lingual teeth have not been described in *Hyperodapedon* previously, although A. D. Walker (personal communication), quoted in Chatterjee (1969, 1980*a*), notes their presence.

The *splenial* consists of a thick basal portion with a large thin ascending medial lamella. The
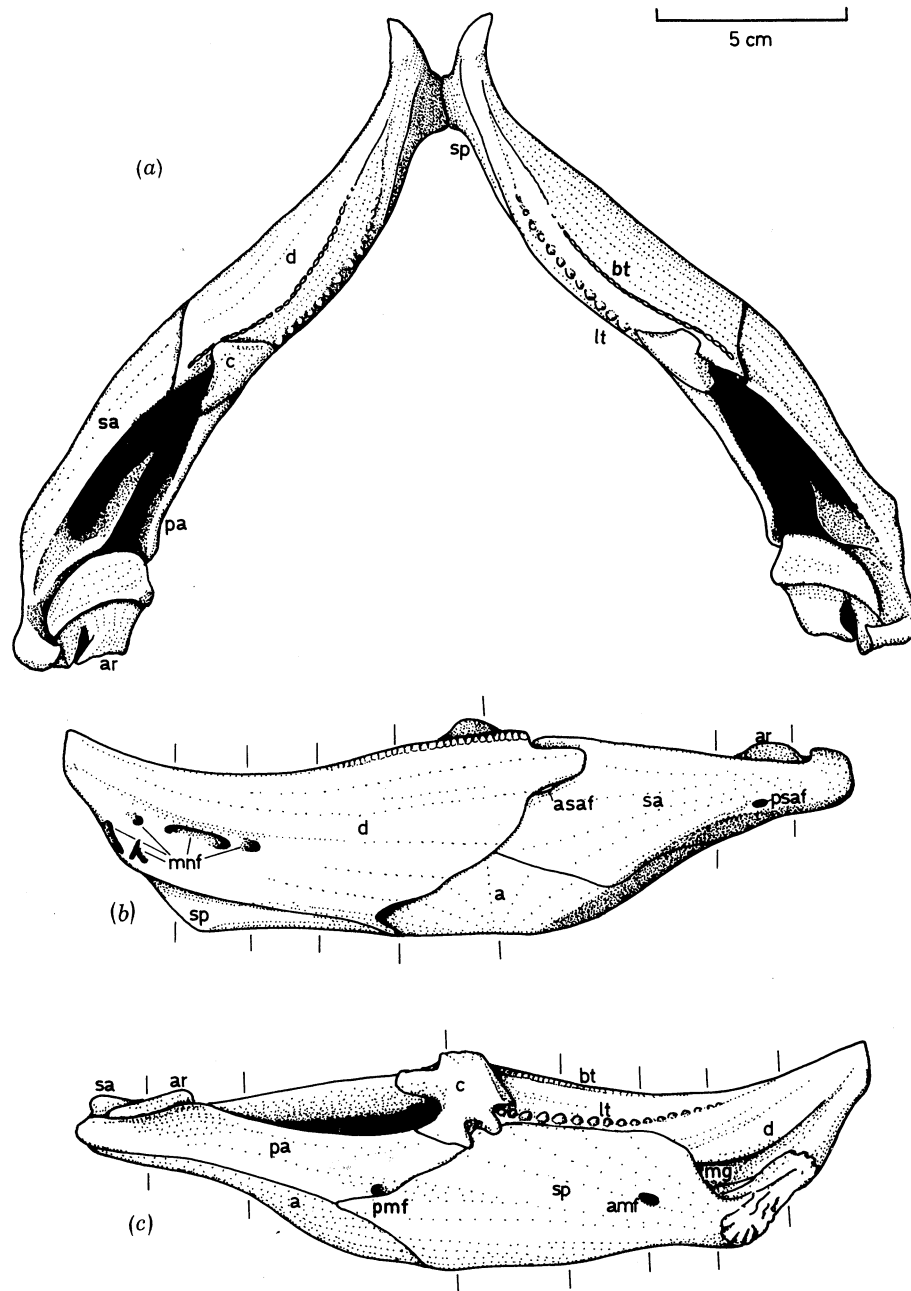
FIGURE 13. Composite restoration of the mandible. (*a*) Occlusal view; (*b*) left lateral view; (*c*) left medial view. The vertical lines indicate the locations of the sections shown in figure 14*b*. Note that the mandible is foreshortened in the lateral view of the skull (figure 5*a*) because of the high angle between the two elements, and its true full length is shown here.

anterior medial tongue rests on a large facet of the dentary and bears a large rugose facet which forms the symphysis. The splenial runs forwards for a short distance from the symphysis into a thin tongue of bone that rests in a shallow medial depression on the dentary (figure 14*a*). The medial ascending wing rises above the posterior margin of the symphyseal facet, and covers most of the medial lamella of the dentary below the lingual tooth row. It is bounded posteriorly by the prearticular and angular, and passes just in front of the posterior meckelian foramen

in the prearticular. Burckhardt (1900, p. 489) figured a separate element forming the symphysis and anterior part of the splenial which he termed 'praesplenial', but there is no evidence for a distinct bone here.

The single *coronoid* is a small complex bone that lies medially at the back of the tooth rows and forms the anterior border of the adductor fossa. The ventral margin overlaps the prearticular and a short anteroventrally directed lobe of the coronoid interlocks with the prearticular (figure 13c). The coronoid runs up round the last lingual tooth and then in a straight line to the dorsal margin where a small process conceals the posterior three or four buccal teeth in medial view (figure 13c). From here, the coronoid forms a posterior process that interfingers with the surangular and then swings medially over the anterior margin of the adductor fossa.

The *angular* is a canoe-shaped bone which forms most of the floor of the meckelian canal (figure 14a, b). The anterior section is concealed between the dentary and splenial, and it broadens posteriorly, maintaining a dorsal groove, until if forms the base of the mandible in its posterior half (figure 13b, c). The posterior part of the angular is bounded dorsally by the surangular and prearticular which meet and form the floor of the adductor fossa, excluding the angular on which they rest (figure 14b). The angular terminates in a narrow point in the midline below the glenoid fossa, but does not extend to the back of the mandible or contact the articular.

The *surangular* forms the lateral margin of the posterior half of the mandible, floors the lateral part of the glenoid fossa and forms a retroarticular process. The anterior end runs into a point between dentary and coronoid (figure 13b), and surrounds a foramen, probably equivalent to the large 'articular' foramen of *Sphenodon* (O'Donoghue 1920, p. 190), or anterior supra-angular foramen of lizards (Oelrich 1956, p. 35) (asaf, figure 13b). In lateral view (figure 13b), the rising lamina of the surangular is at right angles to the ventral portion and the angle is marked by a strong ridge. Inside the adductor fossa, the surangular forms a thin vertical lamina at the contact with the prearticular, and it rises backwards to the level of the glenoid fossa. The lateral sheet and the central lamina join here and run back as a solid unit, forming a strong lateral and ventral margin to the articular. The surangular wraps round behind the articular as a small retroarticular process, as in *Sphenodon*. Just lateral to the glenoid fossa in the lateral wall of the surangular is a posterior supra-angular foramen (psaf, figure 13b; cf. *Ctenosaura* (Oelrich 1956, p. 35)).

The *prearticular* forms the wall on the medial side of the adductor fossa and underlies the articular. It meets the dentary and coronoid and runs down to the angular well forward of the coronoid and concealed by the splenial in medial view (figure 13c). The prearticular runs back on top of the angular and meets the surangular in the floor of the adductor fossa. In ventral view, the prearticular meets the surangular at the posterior tip of the angular and runs to the back of the jaw as an expanded plate beneath the articular (figures 13c, 14b). The posterior meckelian foramen (pmf) is surrounded completely by the prearticular both inside and out, even though the channel is directed steeply ventrolaterally through the bone.

The *articular* is a small solid element that forms the glenoid fossa and the medial part of the retroarticular process. It is bounded ventrally and medially by the prearticular and laterally by the surangular, but does not rise much above these (figure 13b, c). The glenoid fossa is directed nearly mediolaterally when the mandibles are in position (figure 13a). The fossa has two slight depressions on either side of a raised middle portion and there is a marked posterior ridge. Behind this, the articular descends steeply to a lower platform in the retroarticular process, and it forms a vertical plate at the contact with the surangular.

5.2. *Blood vessels and nerves* (figure 14c, d)

The mandibular artery passed down through the temporal cavity and into the adductor fossa of the mandible (see §4.6.5), and its course through the lower jaw was probably like that of *Sphenodon* (O'Donoghue 1920) and lizards (Oelrich 1956). A small posterior branch (articular artery) probably ran to the articular region between prearticular and articular where there is a cavity, and it may have passed laterally through the well developed posterior supra-angular
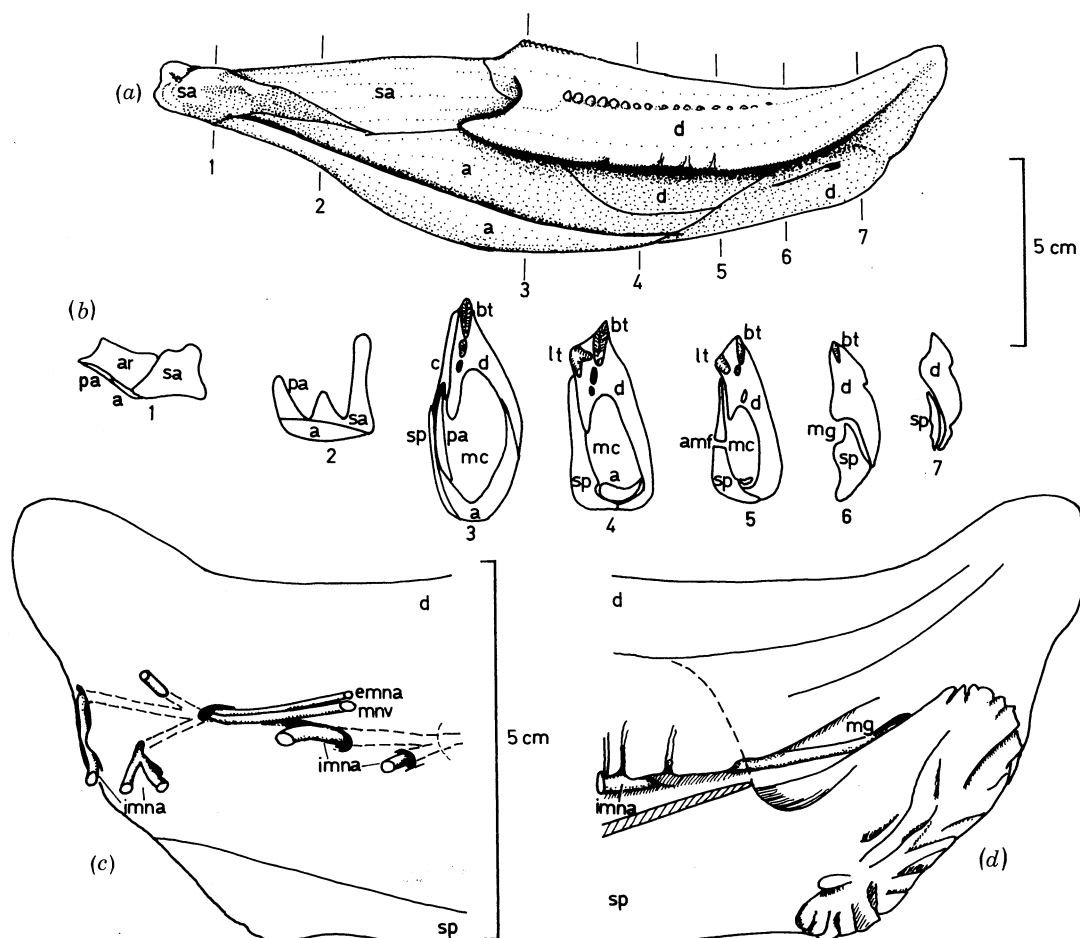

FIGURE 14. Details of the mandible. (*a*) Medial view with the splenial, coronoid and prearticular removed; the numbered vertical lines refer to the sections shown in (*b*). (*b*) Vertical sections through the mandible, showing the complex relations of the bones and teeth; from casts of NUGD A. (*c*) Restoration of the superficial blood vessels at the front of the mandible, in left lateral view; based on NUGD A. (*d*) Restoration of the blood vessels at the front of the mandible, and detail of the meckelian groove and the symphysis, in left medial view; the splenial is cut; based on NUGD A.

foramen (psaf, figure 13*b*). There was probably an internal and external mandibular division, as in *Sphenodon*. The internal mandibular artery doubtless ran dorsally in the large meckelian canal since there is no evidence of a separate canal through coronoid and dentary, as in *Sphenodon*. It gave off several branches to the tooth row, probably running in several vertical grooves on the medial surface of the dentary (imna, figure 14*a*, *d*). The internal mandibular artery passed into a large canal in the dentary (figure 14*a*) which split to reach the lateral surface through two large foramina mentales (mnf, figure 13*b*). Another branch of the internal

mandibular artery may have continued forward into the meckelian groove and through an anterior opening, concealed in medial view by the splenial symphysis (figure 14a), to an anterior set of foramina mentales. The most posterior lies at the front of a superficial longitudinal groove, and the three others form a complex pattern halfway up the rostrum (imna, figures 13b, 14c). The courses of these canals in the bone have been followed by inserting wires into the first cast of the left dentary of NUGD A (figure 14c, d).

A small external mandibular artery probably passed through the anterior supra-angular foramen and ran forward on the lateral surface of the dentary. A small dental artery may have re-entered the dentary, as in *Sphenodon*, from the longitudinal groove (emna, figure 14c).

The mandibular vein passes over the lateral surface of the dentary in *Sphenodon* (O'Donoghue 1920, pp. 211–212). The anterior portion lies within the bone and passes out into a groove, possibly equivalent to the groove seen in *Hyperodapedon* (mnv, figure 14c). The vein passed into the adductor fossa through the anterior supra-angular foramen and up through the quadrate foramen (see §4.5.4) to join the internal jugular vein in the neck. An internal mandibular vein may have drained the medial region of the adductor fossa, as in *Sphenodon*.

The mandible was innervated by the mandibular ramus of the trigeminal nerve (V_3). It probably split into several branches in the adductor fossa region, as in *Sphenodon* (Poglayen-Neuwall 1952, pp. 70–73, fig. 5). Two rami (n. cutaneus recurrens, n. cutaneus externus) passed laterally through the posterior and anterior supra-angular foramina respectively to innervate the skin (pmf, amf, figure 13b). The mandibular nerve then branched into three. The n. intermandibularis caudalis (= n. mylohyoideus) probably exited medially through the posterior meckelian foramen to innervate the tongue, lingual glands and mouth. A lateral branch (n. dentalis et n. labialis) probably ran dorsolateral to the meckelian cartilage, although there is no trace of a separate alveolar canal as in *Sphenodon*. It innervated the lips and teeth up to the symphysis. The third branch (n. intermandibularis medius) ran laterally to the meckelian cartilage, passed below it, and may have exited medially through the anterior meckelian fossa to innervate the anterior mouth and tongue.

The chorda tympani branch of the facialis nerve (VII) passes behind the quadrate and normally enters the mandible through an opening in the articular in lizards (Watkinson 1906), or enters the angular directly in *Sphenodon* (Osawa 1898a, p. 611). In *Hyperodapedon* there is a canal between surangular and articular, lateral to the glenoid fossa, which probably conducted the chorda tympani into the floor of the adductor fossa (figure 13a). It then passed forward into the meckelian canal, and probably fused with the mandibular nerve, as in *Sphenodon*.

The lower jaw of *Hyperodapedon* appears to have been well supplied with blood vessels and nerves when one considers the relative size of the openings. There is evidence then of well vascularized skin and lips at the front of the mandible, and a well innervated tongue and mouth region.

6. DENTITION AND FEEDING
6.1. *Dentition* (figures 2d–f, 15, 16)

The rhynchosaur dentition has always excited interest because of its specialized nature. Chatterjee (1974, p. 229) noted three peculiarities: an edentulous beak-like premaxilla and rostrum of the dentary; deeply rooted, rather than acrodont, teeth (but cf.: Romer 1956, p. 450; Edmund 1969, p. 153); and the multiple rows of teeth on the maxilla. Maxillary

dentitions of *Hyperodapedon* are well displayed in the following specimens: BMNH R699, R3140, R3565, R4781 (cast), R4782 (cast); EM 1926.6 (cast); MM L8272 (cast); NUGD A (cast), NUGD B (cast). Lower jaw dentitions may be seen in BMNH R4780, R4782 (cast); NUGD A (cast), NUGD B(cast).

During the course of this project, a large number of microscopical and serial sections were made which offered a great deal of information on the histology, implantation and replacement of the teeth (Benton 1981). This work will be reported elsewhere. Only a brief summary is given here, but with some detailed comments on patterns of tooth wear in relation to feeding.
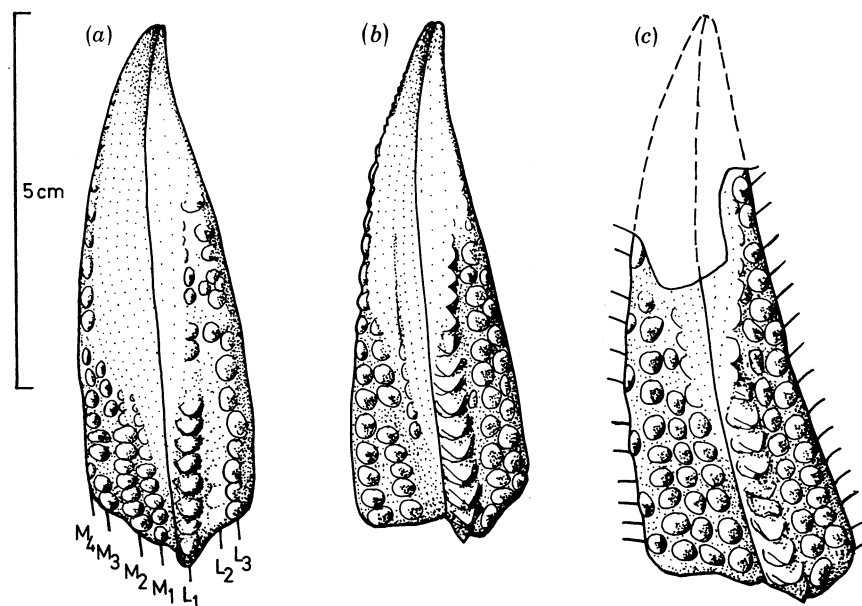

FIGURE 15. Maxillary dentition. Palatal views of left maxillae. Medial (M) and lateral (L) longitudinal tooth rows are marked. Courses of diagonal tooth rows are suggested. (*a*) NUGD A; (*b*) NUGD B; (*c*) EM 1926.6.

6.1.1. *Maxillary teeth* (figures 6*a*, 15)

The maxillary tooth plates are each divided by a central groove, and the teeth on each side are arranged in approximately longitudinal and diagonal rows (figure 15). Most specimens show a medial field with three or four longitudinal rows that is wider than the lateral field with two or three rows. Very old, large, specimens of *Hyperodapedon* maxillae are not known, and it cannot be said whether it added many extra rows posteriorly as in other rhynchosaurs (six or seven in some (Lydekker 1885; Huene 1942; Chatterjee 1974, 1980*a*)).

The maxillary teeth have two forms, both of which appear as pointed pyramids when unworn. The teeth on the lateral side of the groove are triangular in cross-section, with the longest flat plane facing forwards, and shorter slightly curved planes facing medially and laterally. The teeth in the other rows are more conical and irregular.

6.1.2. *Dentary teeth* (figures 13, 14)

The buccal teeth and lingual teeth of the dentary have already been described (§5.1). The buccal teeth are tightly packed, and the exposed portion is flattened to a chisel-shape by tooth

wear. The teeth are deeply rooted cylindrical forms which slope up, forwards and laterally. They become shorter towards the front of the jaw.

The lingual teeth are regular in arrangement and occur in a single well spaced row. They are far more regular than those of *Paradapedon* which are rather scattered (Lydekker 1885; Chatterjee 1974). However, occasional abnormalities occur in *Hyperodapedon*, where an extra tooth appears below the row, as in BMNH R4780 (figure 2*f*). The lingual teeth are broader and shaped like thickened thimbles with a deep pulp cavity. They are spaced differently from the buccal teeth (five lingual to nine buccal teeth longitudinally).

6.1.3. *Longitudinal groove and tooth wear* (figures 15, 16)

The groove in the maxillary tooth plate was initially homologized mistakenly with that of *Sphenodon* which occurs between maxilla and palatine (Huxley 1869). However, the groove is an inherent part of the rhynchosaur maxilla and is not simply produced by wear from the dentary (Chatterjee 1974).

The effects of wear by jaw movement may be seen in the maxilla, dentary and premaxilla. The medial surface of the rostrum of the dentary rubs against the lateral surface of the premaxilla and this action produces a slight depression on both elements. There are no clear wear striations, possibly because of a tough integument or horn cover on the premaxilla and dentary tip. The food may have caused some wear, but this was not significant since teeth not in tight occlusion show little sign of attrition.

As shown by Chatterjee (1974, p. 231), the curvature of the maxillary tooth plate is greater than that of the dentary. Thus, when the jaws close, only the middle portions come into tight contact. The posterior and most anterior parts of the maxilla do not contact the dentary at all. The dentary is worn medially and laterally in arc-shaped areas (figure 16*a*, *b*) and the eight or nine posterior lingual teeth do not contact the maxilla, and are completely unworn. The more anterior lingual teeth occlude with maxillary teeth of the two most medial rows and, because of different longitudinal spacing patterns in the lower and upper jaw, some fit between maxillary teeth, and some meet them directly (figure 16*c*). In the latter case, the crowns of the lingual and maxillary teeth are flattened (figure 16*d*, *e*). In some specimens, the lingual teeth have worn deep pits on the maxillary tooth plate that correspond accurately to individual teeth (figure 16*d*). This shows rather well that the jaw action in *Hyperodapedon* was of the 'precision shearing' type seen in *Uromastix* (Robinson 1976), rather than the propalinal sawing type of *Sphenodon*, as suggested by Sill (1971*b*) for *Scaphonyx*.

The maxillary tooth plate is worn extensively on either side of the groove (figure 16*d*, *f*) in a pattern that matches dentary wear. Both tooth-bearing elements are worn smooth which suggests equal rates of wear, and there are no striations indicative of propalinal movement, such as interpreted by Sill (1971*b*, pl. 4A) in *Scaphonyx*. The buccal teeth meet the bone of the maxillary groove and wear it rather further back in its deepest part. This is marked by a 'step' in the groove (figure 16*d*, *f*).

The anterior triangular teeth on the lateral side of the groove are worn flat, which produces a regular zig-zag saw-like pattern of cutting edges (figures 15, 16*f*), as observed in *Paradapedon* by Lydekker (1885, p. 6, pl. 2, fig. 1*a*).

The teeth in anterior portions of the maxilla and dentary are generally heavily worn and they are hard to distinguish from the bone in casts. This wear must have occurred in juvenile stages, since these teeth do not occlude in the adult. Relative growth causes the maxilla to curve
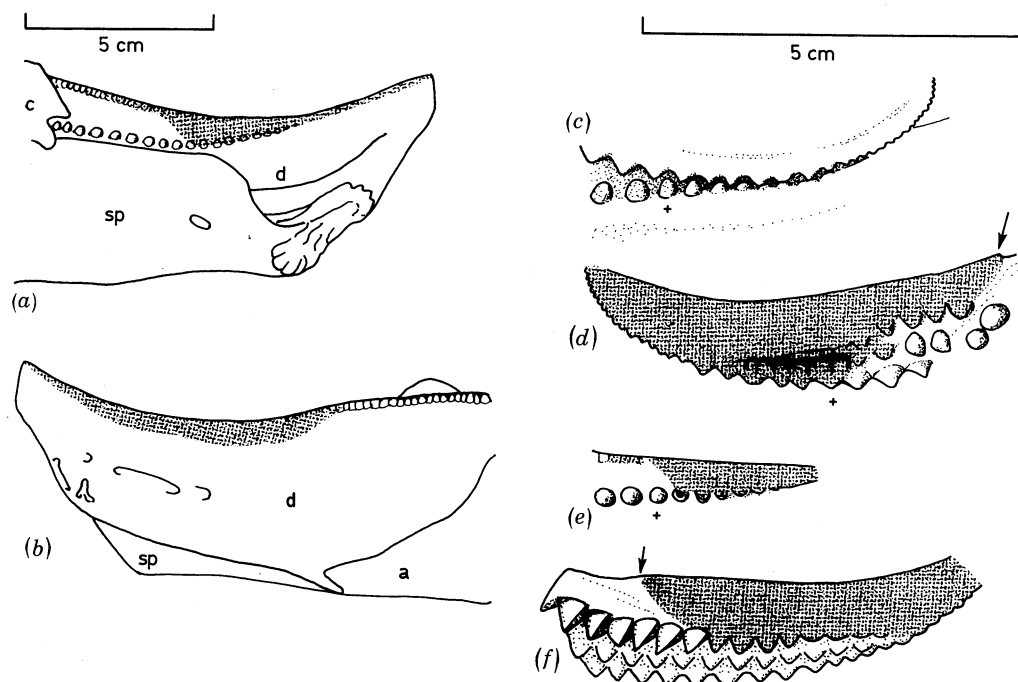
FIGURE 16. Wear patterns on tooth-bearing elements. Areas of war indicated by irregular shading. (*a*) Medial surface of the left mandible. (*b*) Lateral surface of the left mandible. (*c–f*) Details of occluding regions on the left dentary and maxilla; one dentary lingual tooth, and its site of occlusion on the maxilla, is marked by a ' + ' for ease of comparison. (*c*) Medial view of maxilla and dentary in occlusion. (*e*) Occlusal view of area of wear on the dentary. (*d*) Inner view of the medial half of the maxillary tooth plate. (*f*) Inner view of the lateral half of the maxillary tooth plate. In (*d*) and (*f*) the upper boundary is the apex of the groove, and the arrow marks the posterior limit of wear by the dentary in the groove. All based on NUGD B. Note the two scales for (*a*, *b*) and (*c–f*).

upwards away from the dentary and progressively more posterior portions of the tooth plate come into occlusion. The posterior buccal and lingual dentary teeth and maxillary teeth do not occlude. These are unworn in *Hyperodapedon* and *Scaphonyx* (Sill 1971 *b*, p. 308), although some tooth wear is seen here in *Paradapedon* (Chatterjee 1974, p. 233). It should be noted that the degree of tooth wear is not related to skull size (figure 15), and probably depends on the individual's diet, as in *Sphenodon* (Robinson 1976).

6.1.4. *Tooth replacement and function of the dentition*

Typical reptilian tooth replacement did not occur in *Hyperodapedon*. There is no evidence of unerupted successional teeth, nor of teeth falling out. Diagonal tooth families, or individual teeth, were added posteriorly to each series with growth of the dentigerous bones. The teeth of maxilla and dentary were tightly held by the growth of secondary bone, as in *Paradapedon* (Chatterjee 1974) and *Scaphonyx* (Sill 1971 *b*). Chatterjee (1974) introduced the term 'ankylothecodont' to describe the mode of attachment of rhynchosaur teeth, a combination of features of both the thecodont and acrodont systems.

The peculiar anatomical and histological features of the ankylothecodont rhynchosaur teeth may be understood by a comparison with living acrodont reptiles, in which teeth are also not replaced, but are added posteriorly. Such teeth must have a longer functional life than those of a typical polyphyodont reptile. *Uromastix* displays various mechanisms that contribute to this

(Throckmorton 1979): enamel and dentine layers are thickened; secondary dentine grows to fill the pulp chamber; a bony core in the pulp chamber facilitates its eventual obliteration; the jaw bone is able to perform a shearing function once the teeth are completely worn away; the teeth may move through the jaw bones to remain in good occlusion. *Hyperodapedon* displays a thick dentine layer and the slow obliteration of the pulp chamber by the growth of secondary dentine (Benton 1981). However, the enamel layer is not well developed and a bony core in the pulp chamber has only been reported in *Paradapedon* (Chatterjee 1974, p. 230). The bone of dentary and maxilla clearly performs the same function as the teeth and, in fact, most occlusion is between tooth and bone. Because of this, precise tooth–tooth occlusion and extensive remodelling of the bone was probably not necessary.
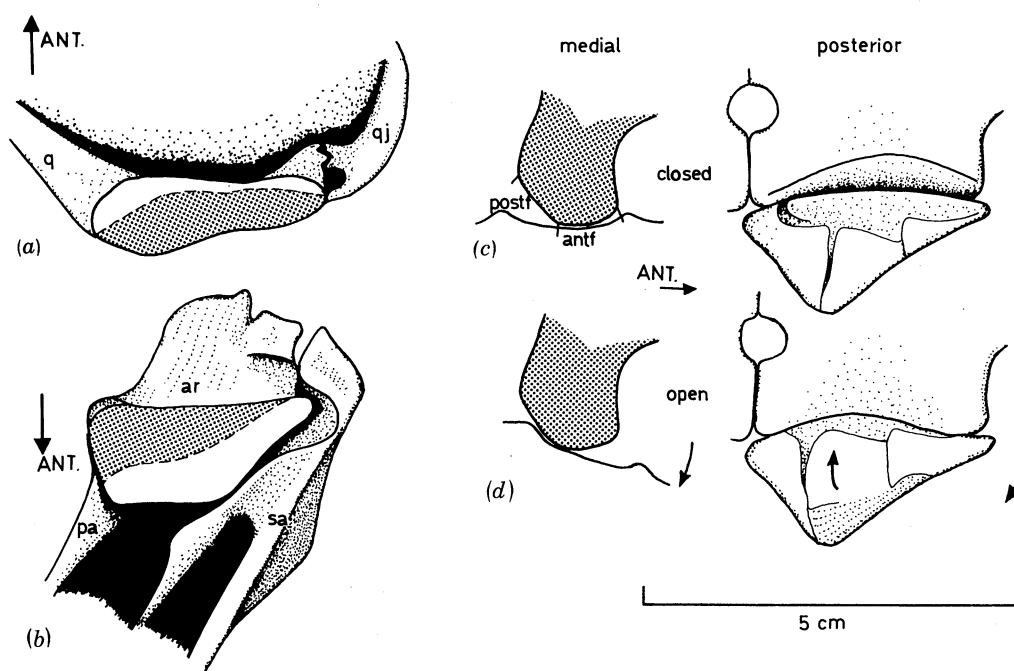

Figure 17. Jaw articulation. (*a, b*) Details of left quadrate condyle (ventral view) and glenoid of the mandible (dorsal view). The posterior articulating field is shaded, and the 'ANT.' arrows run parallel to the midline of the skull. (*c, d*) Jaw opening movements in medial view (diagrammatic) and in posterior view. When the jaw is closed, the anterior fields (antf) are in contact, and the quadrate is prevented from sliding forwards by an anterior lip on the articular. When the jaw opens (drops relative to the skull), the posterior fields (postf) come into contact, the small retroarticular process rises, and the quadrate is prevented from sliding backwards by a posterior lip on the articular.

6.2. Jaw articulation (figure 17)

The skull of *Hyperodapedon* appears to have been akinetic, and the quadrate is firmly fused to the quadratojugal, squamosal and pterygoid (figures 5a, 6a, 7). Thus, the only joint that need be considered in feeding is that between the quadrate condyle and the articular glenoid fossa.

The main axis of each condyle runs nearly transversely (figure 17a, b). The articular condyle is set at a slight angle to the main axis of the mandible, but this corresponds to the broad angle between both jaws (figure 13a). Both quadrate and articular condyle are divided into anterior and posterior fields which are well shown by casts of NUGD B (figure 17a, b). When the jaws are closed, the anterior fields are in contact (figure 17c), and when the jaws open, the contact rolls back smoothly onto the posterior field (figure 17d) so that maximum

gape is about 45°. Thus the 'fields' represent two extremes in the jaw opening cycle. There is no abrupt transition and the anteroposterior translation of the mandible relative to the skull is small and certainly nothing like that of dicynodonts (Crompton & Hotton 1967) which might be considered similar in some respects. Further protraction or retraction is prevented by raised anterior and posterior lips on the articular that fit tightly into depressions on the quadrate in the closed and open positions of the mandible respectively (figure 17 c, d). This confirms the evidence from tooth wear that propalinal or retractile movements were impossible, and that relatively little protraction or retraction occurred in a normal masticatory cycle. This is essential for a precision shear bite. Sill (1971 b, p. 304) noted that 'the glenoid cavity [of *Scaphonyx*] was approximately twice as wide as the condyle, thus a reduced fore and aft movement was possible'. The present work suggests that this movement was minimal in *Hyperodapedon*.

The angle of the condyles, and the sinusoidal curve of the mandibles when viewed from above (figure 13 a), minimize distortion about the symphysis when the jaws open. In *Sphenodon*, considerable rotation takes place about the long axes of the jaws at the symphysis because the jaws are straight when viewed from above, essential to permit propalinal jaw movements (Robinson 1976, p. 54).

6.3. *Jaw muscles* (figure 18)

Direct evidence of the sites of attachment of muscles in fossil vertebrates may be obtained from bone surface textures. The areas indicated are only approximate, and it is rarely possible to distinguish separate elements of a muscle block. Kemp (1979, p. 88) and King (1981, pp. 253–255) have reviewed various bone textures in mammal-like reptiles, and they conclude that irregular patterns of striations with some small foramina may indicate muscle attachment. First casts of NUGD B show surface textures well, and their pattern corresponds with the jaw muscles in *Sphenodon* (Haas 1973), which confirms that it is a suitable comparative model. The major elements of the jaw musculature of *Sphenodon* are summarized and used to reconstruct those of *Hyperodapedon*. Points of difference from Sill's (1971 b) account of *Scaphonyx* are indicated.

Adductor externus group (figure 18 a–c)

M. adductor mandibulae externus superficialis (mames): origin on medial face of postorbital–squamosal bar and internal parts of jugal; insertion on lateral face of surangular.

M. adductor mandibulae externus medialis (mamem): origin on lateral face of parietal, anterior face of parietal–squamosal bar, upper internal portions of squamosal; insertion on basal aponeurosis attached to top of surangular.

M. adductor mandibulae externus profundus (mamep): origin on internal face of squamosal, anterodorsal process of pro-otic; insertion on basal aponeurosis attached to top of surangular.

Adductor internus group (figure 18 b, c)

M. pseudotemporalis superficialis (mpsts): origin on posterior part of postfrontal and lateral face of parietal; insertion on basal aponeurosis attached to top of surangular.

M. pseudotemporalis profundus (mpstp): origin on parietal, epipterygoid, and cartilaginous braincase; insertion on medial surface of dentary and surangular (adductor fossa) and anterior articular.

M. pterygoideus typicus (mpt): origin on ectopterygoid, ventral faces of pterygoid, lower epipterygoid, medial and lateral face of pterygoid ramus of quadrate; insertion on angular and prearticular.
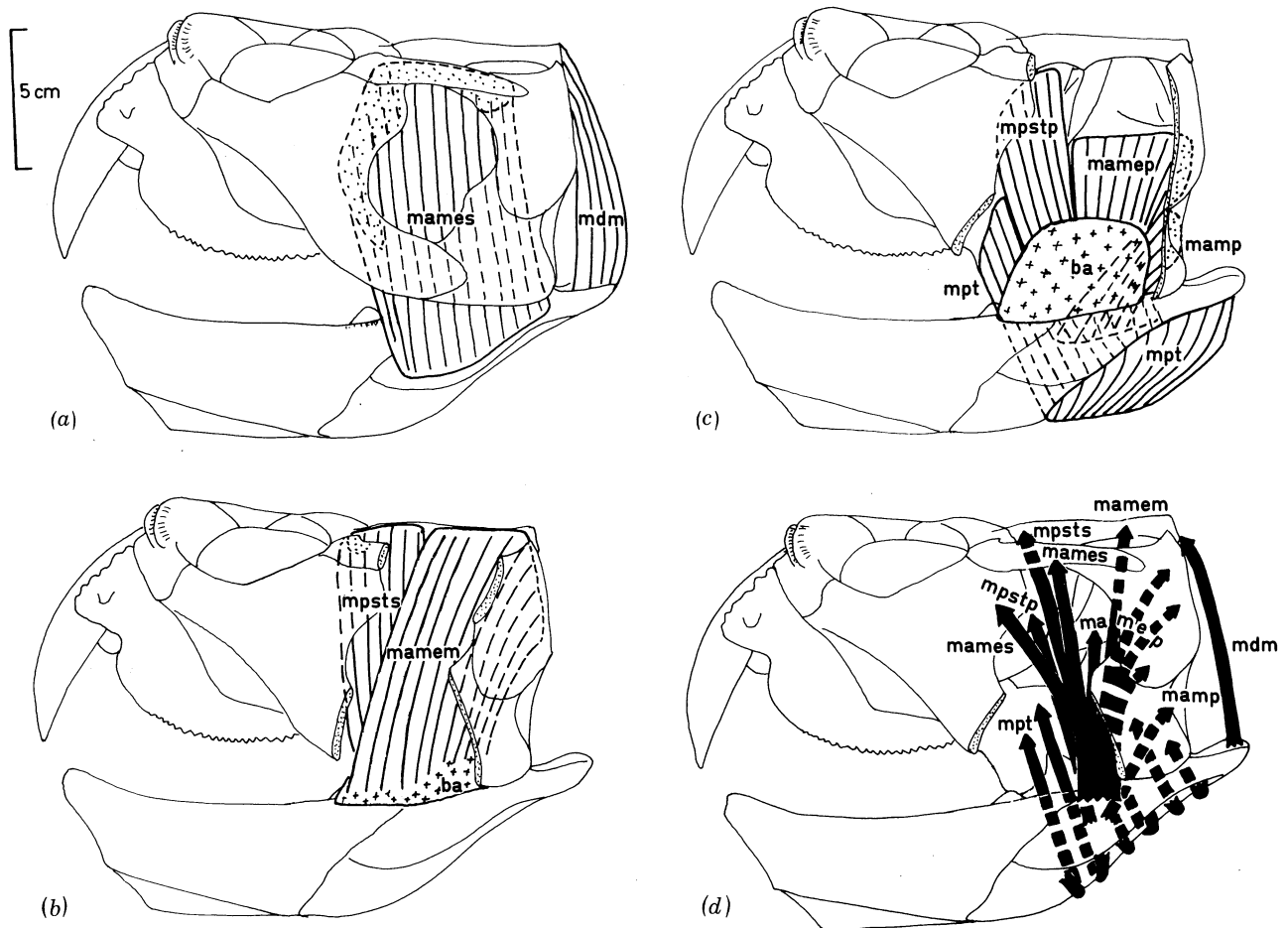
FIGURE 18. Reconstructions of the major jaw muscles of *Hyperodapedon*. (a) Superficial layer; (b) deeper layer (temporal bars removed); (c) deepest layer. Based on the musculature of *Sphenodon* and lizards. (d) Summary of the main jaw muscles, showing directions of maximum force, and the relative size of each.

Adductor posterior group (figure 18c)

M. adductor mandibulae posterior (mamp): origin on internal surface of quadrate, quadratojugal, lower squamosal; insertion on medial side of adductor fossa.

Depressor group (figure 18a)

M. depressor mandibulae (mdm): origin on posterior border of parietal and squamosal; insertion on retroarticular process (prearticular–surangular).

Some of the muscle fields are well marked by ridges on the bone in *Hyperodapedon*. The ventral zone of insertion of the large mpt is bounded laterally by a strong ridge between angular and surangular (figure 13b). The surangular ridge on the floor of the large adductor fossa (figure 13a) may have separated the insertions of a large mamp and a mamep (Sill 1971b, p. 315). The deep pocket on the posteromedial face of the quadrate ramus of the pterygoid, just lateral to the basipterygoid pit (figures 6b, 7) may mark the limit of origin of the mpt, and the diagonal ridge on the anterior face (figure 6a) may have had a similar function.

Sill (1971b) suggested that the mames included a major anterior slip that originated laterally below the jugal ridge, and he homologized it with the m. levator anguli oris of lizards. However,

this muscle originates from the medial face of the postorbital in *Sphenodon* (Haas 1973, p. 293) and from the postorbital or parietal in lizards and snakes (Haas 1973, p. 317). If rhynchosaurs had a muscle originating laterally on the jugal and inserting on the lateral face of the dentary, it is not matched by any known muscle in living reptiles. The surface texture of the bone in *Hyperodapedon* shows long striations below the jugal ridge, and there is no evidence of muscular attachment. The prominent jugal ridge may have supported a flexible muscular cheek to retain food, as in ornithischian dinosaurs (Galton 1973) and mammals.

Bone surface textures do not indicate any muscle attachments on the small coronoid. As in *Sphenodon*, it probably supported an anterior part of the basal aponeurosis upon which inserted parts of the mpsts.

6.4. *Jaw mechanics and feeding* (figure 18 d)

Ostrom (1964) used *Triceratops* as a model to interpret the lower jaw as a third class lever with the force (muscular contraction) applied at a point (or points) between the fulcrum (jaw articulation) and the resistance (dentition). The most efficient mechanical arrangement is to have the muscle fibres directed at right angles to the jaw ramus and attached as far forward of the articulation as possible. The muscles cannot attach too far forward or the effective gape is reduced.

Hyperodapedon and other rhynchosaurs appear to have had a simple muscle arrangement in terms of the lever model. The greatest force of the adductors acted somewhat behind the coronoid (figure 18 d). There were probably no major diagonal muscles, and the strongest adductive force at various stages of the bite were exerted vertically.

Different jaw muscles were brought into play during the different phases of jaw closure, and the major adductive force migrated backwards. The pseudotemporalis and pterygoideus probably exerted maximum force when the jaws were beginning to close, and the external adductor group became vertical, and thus more powerful, when the jaws were nearly closed (figure 18 d). The final force came from posterior elements of the external adductor group and the posterior adductor. The curvature of the maxillary tooth plate and dentary would have allowed the bite to take place with the jaws nearer to full closure, when the jaw adductors were working at their greatest mechanical advantage, a feature seen in some lizards (Rieppel & Labhardt 1979).

The evidence from tooth wear, articulation facets and probable muscle distributions points to a precision shear bite in *Hyperodapedon*, and probably in other rhynchosaurs as well. The sequence of jaw movements given by Sill (1971 b, p. 316) for *Scaphonyx* may be modified to the following.

(i)   Abduction by the m. depressor mandibulae.

(ii)   Simple adduction by the m. pterygoideus typicus and m. pseudotemporalis and manipulation of food material by the tongue.

(iii)   Increased pressure by the m. pterygoideus as food is cut at the back of the maxillary groove. The adductor externus group begins to contract.

(iv)   Full contraction of the adductor externus group with main force swinging from anterior to posterior elements as the cutting force moves forward. Final powerful occlusion by contraction of the m. adductor posterior.

Food material was probably gathered and manipulated by the premaxillary 'beak' and taken into the mouth by a powerful muscular tongue (suggested by the heavy hyoids: see above). The food was probably passed to the back of the tooth plate and held in place initially by the

tongue and sharp posterior maxillary and lingual dentary teeth. The closing jaw compressed and cut the food diagonally forwards along the maxillary groove, with maximum occlusal shearing force exerted towards the middle of the areas of wear (figure 16). This system forced the food material into a wedge that concentrated the force of the jaw (Sill 1971 b), but there was probably little sawing motion.

6.5. *Forces on the skull and lower jaw*

Structural aspects of the skull may be interpreted in mechanical terms in relation to the pattern of stresses set up during feeding. It is assumed that major compressional stresses are opposed by heavy cranial elements, and areas of no stress (neutral zones) may be characterized by the thinness of the bone or its complete absence (Alexander 1968; Frazzetta 1968).

The heavy mediolateral strut behind the orbital cavity, composed of postorbital, jugal and ectopterygoid (figure 5 b), probably braced the large internal areas of origin of the mames on jugal and postorbital. Similarly, the lateral and medial ridges on the jugal (figure 5 a, b) ran parallel to major anterior fibres of the mames and mpt (figure 28 a, c), and prevented compression of the orbit during early stages of the closure of the lower jaw. The bones of the cheek region, where maxilla and jugal overlap below the heavy jugal ridge, are very thin. There are no special forces acting here, and this is probably a functional homologue of the antorbital fenestra of the archosaurs.

The box-like cross-section of the adductor fossa region of the mandible with a sharp ventrolateral ridge between angular and surangular (figures 13, 14) would prevent distortion under muscular tension. The external adductor muscles pulled straight up while the pterygoideus pulled up and medially and slightly forwards. The posterior adductor pulled up and back. The resultant forces would readily twist a rounded element, and the sharp angles reduce this torsional stress, as in a box girder.

One final structural element in the skull that probably relates to feeding, and possibly also to defence or fighting, is the premaxillary 'beak'. This was pointed and could be used as a scraper or stabber. Impacts on the tip of the bone were evidently hard in some cases, since a large chip has broken off along the posterior margin of the left premaxilla in NUGD A. The force of an impact would pass straight up the premaxilla to the thickened prefrontal ridge in front of the orbit (figure 5 a). It is suggested that one function, at least, of this special rhynchosaur feature was to dissipate energy without fracturing the bone. This is rather different from the situation in dicynodonts, where the force from the tusk passes below the orbit into the jugal and squamosal, or in carnivorous mammals (e.g. sabre-toothed cats, walrus) where the compressional stress passes over the orbit and into the heavy frontal. The medial position of the rhynchosaur 'tusks' and the breadth of the orbital area mean that the stress could not pass below or above the orbit, and had to be dissipated before reaching the orbital boundary.

6.6. *Diet*

It has been suggested that rhynchosaurs ate plants (Huene 1939 a; Romer 1963; Sill 1971 a, b) or molluscs (Burckhardt 1900; Chatterjee 1974, 1980 a). The latter interpretation does not seem likely because of the relative lack of wear on non-occluding teeth, and the inappropriateness of the shearing jaw action for dealing with hard-shelled animals. Also in favour of a herbivorous diet is the barrel-shaped body (to accommodate a large gut for the slow digestion of plants), the large numbers of these animals present in all faunas, and the general absence, or rarity, of fossil mollusc shells in association.

In South America, the rhynchosaurs of the Santa Maria Formation are associated with remains of wood, and elements of the *Dicroidium* flora are found in the lower parts of the formation (abundant cycadophytes, rarer sphenopsids and coniferophytes) (Sill 1969). Some sphenopsids and coniferophytes have been found in the Ischigualasto Formation. The Bromsgrove Sandstone Formation of the English Midlands has yielded pteridophytes and coniferophytes in beds of the same age as some that yielded *Rhynchosaurus*. Clues to the rhynchosaur diet may also be obtained from the adaptations of the powerful jaw mechanism which indicate something tough, but probably not hard, because of lack of wear on non-occluding teeth. The plant materials suggested by Romer (1962) and Sill (1971 *a*, *b*) include the 'fruit' of lycopsids, sphenopsids and ferns, artichoke-like bennettitaleans, seed ferns and cycad rhizomes.

We may focus on the diet more closely by examining the distribution of the rhynchosaurs in time and space. Their rapid spread, massive local dominance, and apparently rapid extinction in the middle Norian suggest that important elements of their diet may have had a similar history. Rhynchosaurs are also commonest in southern continents (Gondwanaland), with the only important northern representative being *Hyperodapedon*. The Triassic plant record suggests a parallel in the *Dicroidium* flora. Triassic reptile evolution, plants and climates are discussed in more detail elsewhere (Tucker & Benton 1982; Benton 1983 *a*).

The pteridosperm (seed-fern) *Dicroidium* and its relatives radiated from the late Scythian to the Carnian to dominate many lowland environments in Gondwanaland (Anderson & Anderson 1970; Retallack 1977). Other elements of the *Dicroidium* flora include equisetaleans (e.g. *Neocalamites*), ferns, 'cycadophytes', ginkgoales (e.g. *Baiera*) and conifers (e.g. *Podozamites*) (Anderson 1974; Retallack 1977). *Dicroidium* and its relatives disappeared rapidly towards the top of the Norian and early Rhaetian. A new flora, dominated by diverse conifers and bennettitaleans, took over in the Rhaetic and Jurassic (Barnard 1973; Miller 1977). Northern hemisphere floras of the same time (e.g. Chinle, Arizona: Carnian–Norian) are dominated by cycadophytes, ferns and conifers, and contain no seed ferns. Plants have not been found at Elgin, but a *Dicroidium* flora of southern aspect may have occurred there.

It is difficult to assess the habit of the various elements of the *Dicroidium* flora. However, the equisetaleans were probably low bamboo-like swamp dwellers, *Dicroidium* was probably a low shrub, the cycads bore leaves and fruit on an elevated bole, ginkgos were small trees and shrubs, and the rarer conifers were probably large trees (Cruickshank 1978). Rhynchosaurs probably could not rear up on their hind legs, and would have had to feed in a height range of 0–1 m. This restricted their diet to *Dicroidium*, equisetaleans, ginkgos, and the fallen leaves or fruits of cycads and conifers.

Dicroidium and other seed ferns are associated with large seeds, possibly contained in a fleshy fruit, and reproductive structures (Retallack 1977). The primitive Triassic conifers and ginkgos had large open cones (Anderson 1978). These, in addition to fertile structures of equisetaleans and ferns probably formed the rhynchosaur diet. Cycads and bennettitaleans were not abundant and were probably of less importance.

7. Axial skeleton
7.1. *Vertebral column*

Several series of vertebrae of *Hyperodapedon* are preserved, but none is complete. The best column, in BMNH R699, shows much of the presacral series, and Huxley (1887) estimated

that it contained 23 or 24 vertebrae, and Huene (1929, p. 39) suggested 24. However, the most anterior vertebra on the main slab cannot be the second cervical, as Huxley assumed, because it has a large rib. Thus, *Hyperodapedon* probably had 25 presacrals, two sacrals (Huene 1929, pl. 8, fig. 7 shows three), and 25 or more caudals, as in *Stenaulorhynchus* (Huene 1938, p. 94), *Scaphonyx* (Huene 1942, p. 275) and *Paradapedon* (Chatterjee 1974, p. 236).

7.1.1. *Atlas–axis complex* (figure 19)

A fine axis and parts of the atlas complex are preserved in NUGD B. The single atlas centrum (figure 19*a*, *b*, *e*) is a small crescentic box-like element, slightly convex anteriorly, placed high on two ovoid facets on the axis centrum (figure 19*c*). On the dorsal, slightly concave surface of the atlas centrum are two small openings on either side of the midline (figure 19*e*), presumably for ventral branches of spinal nerve 1. Below, and slightly forward of this, the flattened, spatulate atlas intercentrum (figure 19*a*, *b*, *e*,*f*) articulates with the axis intercentrum. The latter element is not preserved complete, but seems to have been a small crescentic unit (figure 19*a*, *e*,*f*). The atlantal arch is not preserved in NUGD B, but casts from BMNH R4782 show the outline of the right neural arch of the atlas (figure 30*g*). The supposed atlas described by Huxley (1887, p. 677, pl. 26, fig. 7) in BMNH R699 is more probably the posterior face of the third cervical vertebra.

The axis centrum (figure 19*a*, *b*, *d–f*) is nearly circular in cross-section. The anterior ventral margin bears three small bulbous processes that have roughened edges and were probably originally linked by cartilage. The anterior face of the centrum is not clearly visible, but the posterior face is slightly concave. A small facet for the atlantal arch is developed above the atlas centrum facet, and the posterior section of the greatly expanded fan-shaped neural spine bears a low-angle postzygapophyseal facet. The neural spine was probably capped by cartilage which would have given it a shape rather more like that of *Scaphonyx* and *Paradapedon*, although probably not as elongate posteriorly as that of *Stenaulorhynchus*. There is no sign of a rib facet which is seen in these other rhynchosaurs.

7.1.2. *Cervical vertebrae* (figures 20, 21)

There are few remains of cervical vertebrae, but we may assume a total of eight, as in *Paradapedon*. The neural arch of cervical 3, preserved in NUGD B (figure 19*a*, *e*), shows a form similar to that of *Paradapedon*. The zygapophyses are large and the neural spine is very low, but probably had a cartilaginous cap. The zygapophyses become steeper and centrum length increases behind the axis (figure 20). Cervicals 3–6 are preserved in BMNH R4782, and comparison suggests that cervicals 4–8 are preserved in BMNH R699. These specimens display partial ventral views (figure 21*a*, *b*) which show a slight midventral keel. Casts of BMNH R4782 allow a partial reconstruction of vertebrae 7 and 8 (figure 21*c*). The zygapophyseal facets are now placed more nearly vertically (65°) and the neural spine is reduced. No information on parapophysis or diapophysis is available.

7.1.3. *Dorsal vertebrae* (figures 20, 22, 23)

Information for the description of the dorsal vertebrae is derived from casts of BMNH R4795 (dorsals 1–6), RSM 1967.10.1A (1–7), BMNH R4791 (5–17), RSM 1967.10.1B–D (2–17), BMNH R4781 (11–17) and GSM 90933–4 (16–17). The numbering of the dorsal vertebrae is subject to a possible error of ±1.
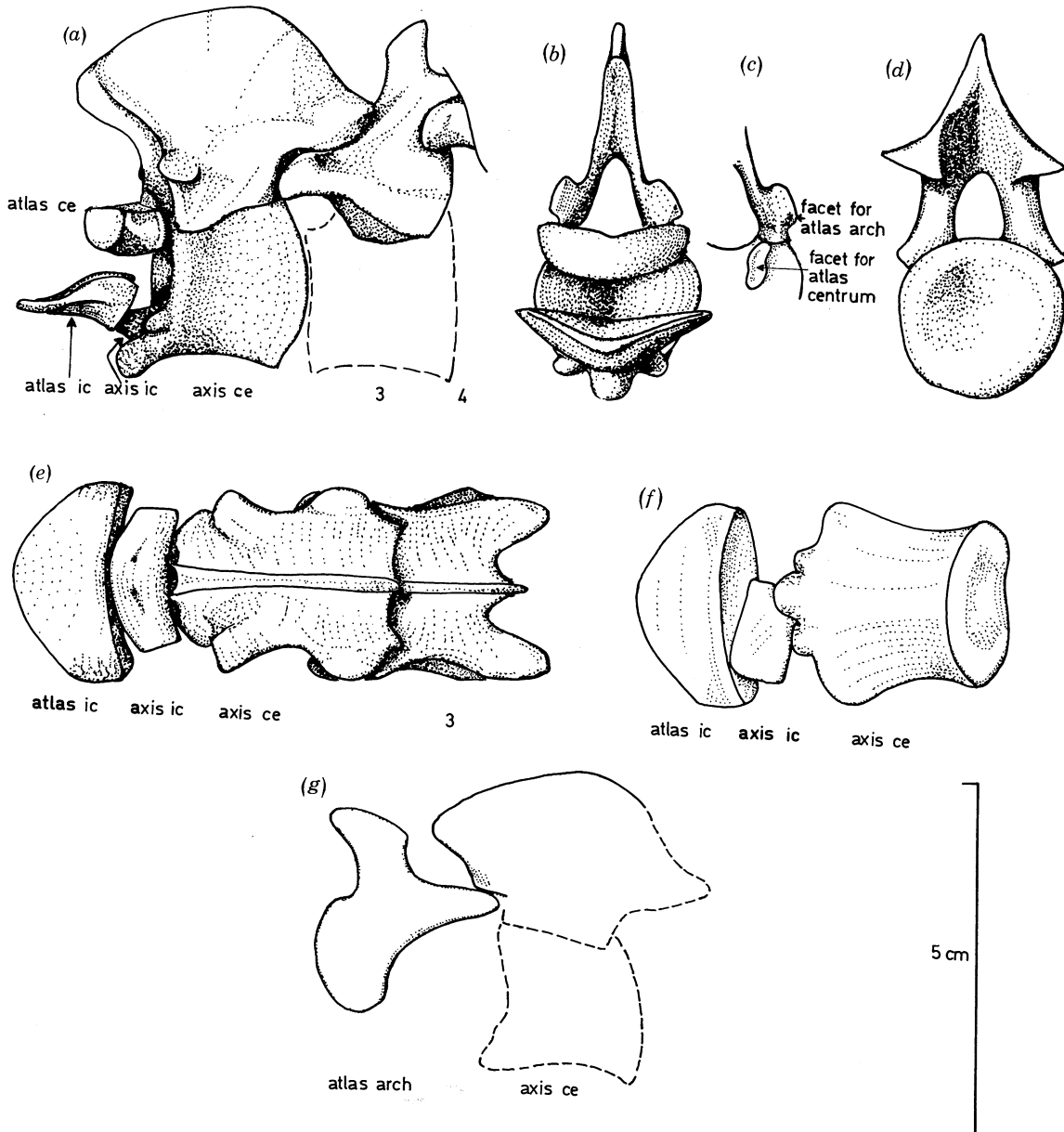
FIGURE 19. Atlas and axis. (a) Left lateral view of atlas, axis and cervicals 3 and 4, with atlas neural arch missing, NUGD B; (b) anterior view with atlas neural arch missing, NUGD B; (c) anterior view of part of axis, showing facets for atlas elements, NUGD B; (d) posterior view of axis, partially restored from NUGD B; (e) dorsal view with atlas neural arch missing, NUGD B; (f) ventral view of atlas intercentrum and axis, NUGD B; (g) left lateral view of atlas and axis neural arches, restored from casts of BMNH R4782.

The centra are roughly circular, constricted in the middle, and display a slight ventral keel (figure 22a). The terminal facets are amphicoelous. Dorsal 1 has a very short centrum; centrum length increases towards the middle of the back, and decreases slightly towards the sacrum, while the breadth remains roughly constant (figure 20).

The rib articulations are not well preserved in anterior dorsals, but in dorsal 1 (figure 22b) they are placed well anteriorly and seem to trend nearly vertically. Parapophysis and diapophysis cannot be distinguished. Further back, the oval diapophysis is projected horizontally on a broad flattened transverse process, placed centrally well above the centrum. The processes
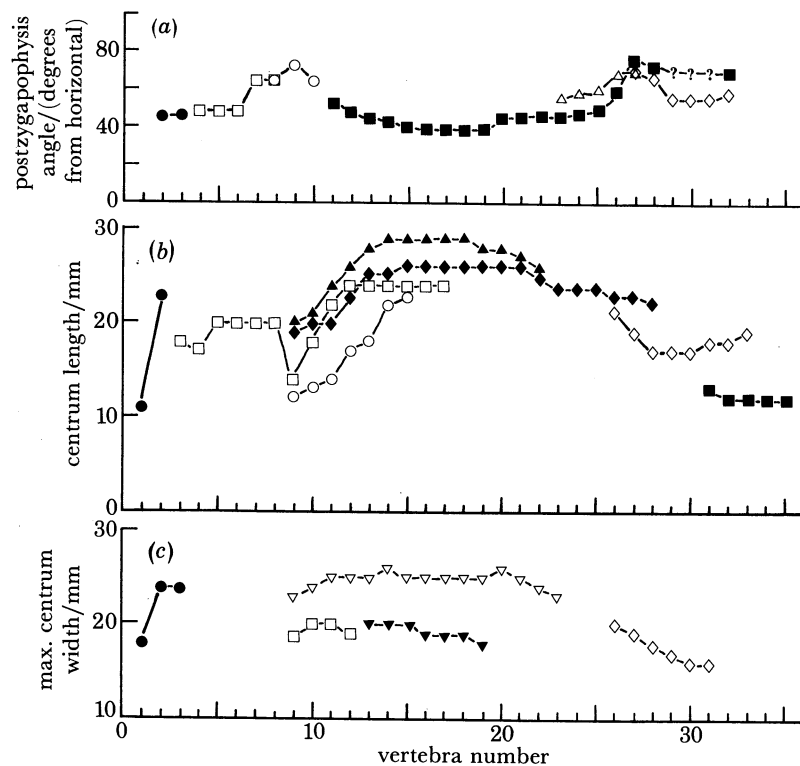
FIGURE 20. Variation in vertebral measurements throughout the series. Cervicals are 1–8, dorsals are 9–25, sacrals are 26 and 27, and caudals are 28–35. Measurements of series of vertebrae are taken from different individuals (represented by different symbols: ○, BMNH R4795; □, BMNH R4782; △, BMNH R4791; ◇, BMNH R3148; ●, NUGD B; ■, RSM 1967.10.1; ▲, BMNH R699; ◆, EM 1978.1; ▼, GSM 90933/4; ▽, EM 1886.3).
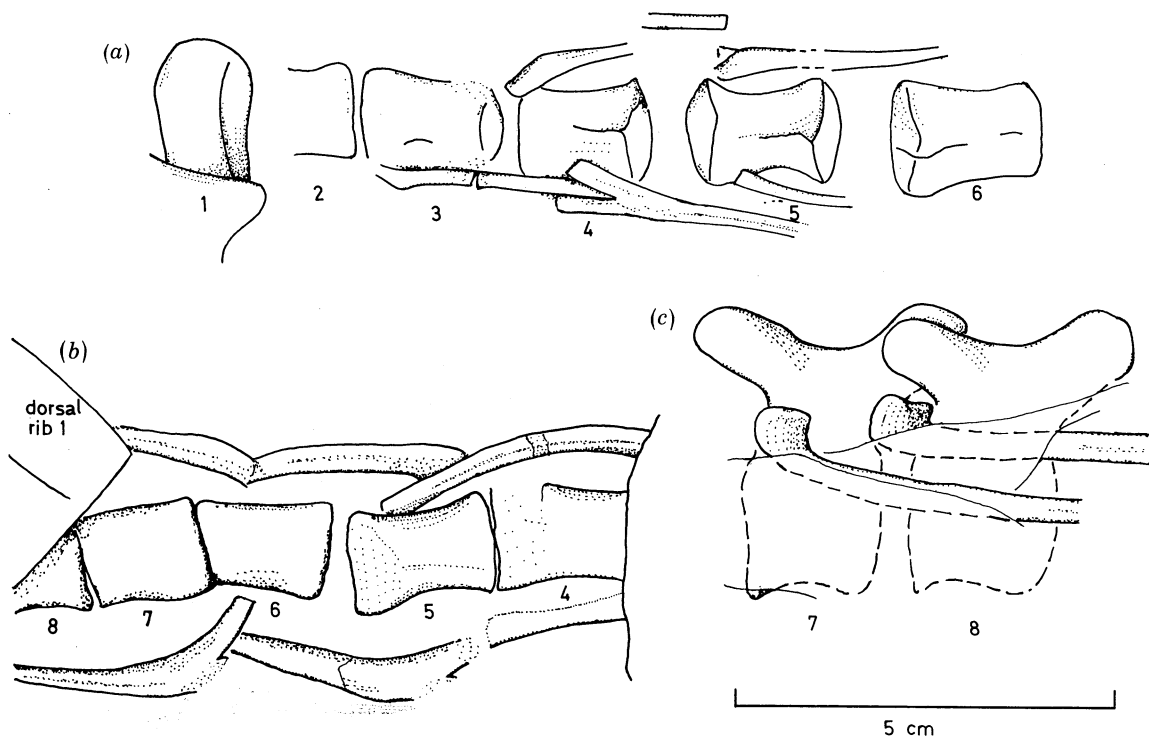

5 cm

FIGURE 21. Cervical vertebrae. (a) Ventral view of cervical vertebrae 1–6, including atlas intercentrum and axis centrum, and some ribs, BMNH R4782; (b) ventral view of cervical vertebrae ?4–8, with some ribs, BMNH R699; (c) left lateral view of cervical vertebrae 7 and 8, with associated ribs, restored from BMNH R4782.

become longer in dorsals 14–17 (figure 23*c*). The rib facets most resemble those of some specimens of *Scaphonyx* (Huene 1942, pl. 32, figs 2–4), but differ from *Stenaulorhynchus*, *Paradapedon* and large specimens of *Scaphonyx* which have heavy circular facets.

The zygapophyses are large in dorsal 1, and placed nearly vertically (figure 22*b*). The angle reduces to 30–40° in the region of dorsal 7, and maintains this value back to dorsal 11 or 12 (figure 23*b*, *c*). The angle then increases back to the sacrum (figure 20). The zygapophyses project beyond the ends of the centrum, and have well developed circular facets throughout the series.

All neural spines are compressed laterally and lie over the mid to posterior part of the centra. The anterior edge is thin, and the posterior is broad and bifurcates ventrally to form the postzygapophyses. In dorsal 1, the spine is narrow and the posterior edge runs parallel to the anterior (figure 22*b*). In other dorsals, the posterior edge is more or less vertical and the spine has a broad base. The neural spine appears to be lower in the mid-dorsals than behind or in front.

7.1.4. *Sacrum* (figure 24)

Information on sacral vertabrae is derived from casts of RSM 1967 . 10 . 1 B–C, GSM 90933–4, BMNH R3148, and R4781.

The two sacral vertebrae have centra of approximately equal length, but they are slightly shorter than the preceding dorsals (figure 20). The centrum of the first sacral vertebra is flat ventrally and rectangular in cross-section (figure 24*a*, *c*). The posterior face of the centrum slopes obliquely, forming a gentle S-shape in lateral view. The centrum of the second sacral vertebra (figure 24*b*) is rather rounder ventrally. The posterior faces of both centra are concave, but detailed information on the anterior faces is not available, and no comparison can be made with *Paradapedon* in which centrantra occur. However, despite slight compression, the centra of *Hyperodapedon* seem to be far lower than those of *Paradapedon* and *Stenaulorhynchus*.

The zygapophyses are well developed and are oval (figure 24*a*, *b*, *d*). The large prezygapophyses of sacral vertebra 1 slope at about 60°, the postzygapophyses of sacral 1 and pre- and postzygapophyses of sacral 2 at about 70–75° to the horizontal (figures 20, 24). The neural spine of the first sacral is similar to that of posterior dorsals, while that of the second sacral is rather shorter. Both are inclined a little backwards. The transverse processes project further laterally in the first sacral than the second. They are hard to interpret in the material available, but the diapophysis appears to be a thin plate oriented horizontally in the first sacral, and descending backwards in the second. The parapophysis of the first sacral is a large anteriorly protruding 'socket' occupying half the length of the centrum (figure 24*a*, *c*). That of the second sacral appears to be smaller and placed higher up and further back (figure 24*b*).

The sacral ribs are separate from the vertebrae, only one being preserved in articulation. The rib of the first sacral vertebra (figure 24*a*, *c*, *e*, *f*) is larger than that of the second. The ventral facet is broad where it articulates on the side of the centrum, and the rib narrows gradually to a thin plate above which articulates with the end of the transverse process. The rib slopes backwards when articulated, and presumably met the rib of the second sacral distally. The distal end is slightly concave (figure 24*f*). The proximal ventral portion projects anteriorly (figure 24*c*, *e*), and probably formed facets lateral to the centrum as in *Paradapedon* (Chatterjee 1974, p. 240) and *Scaphonyx* (Huene 1942, p. 279). The rib of sacral vertebra 2 (figure 24*g*) is shorter and is not so broad ventrally. There is no evidence of autotomy planes in the caudal vertebrae of *Hyperodapedon*.
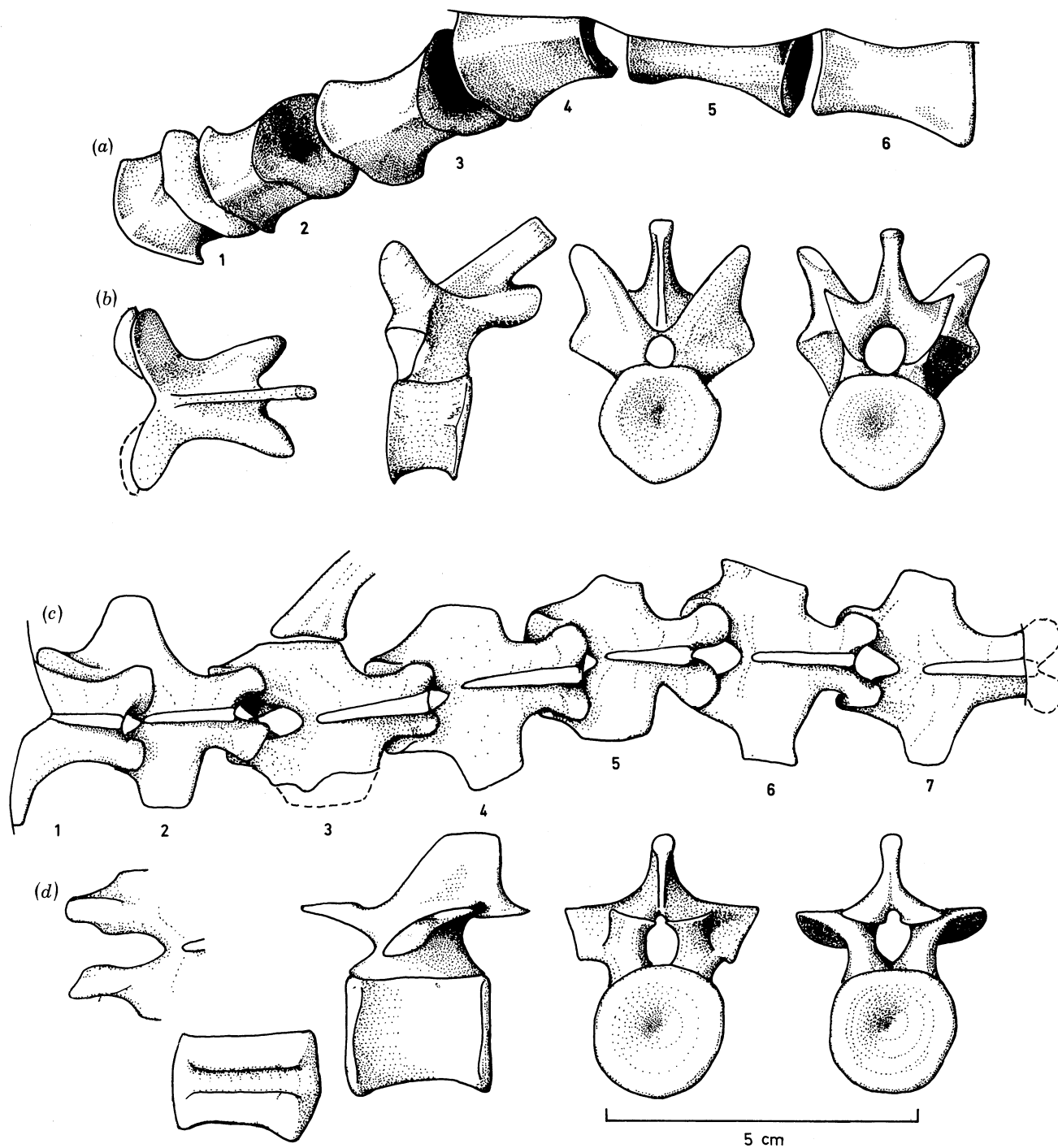
FIGURE 22. Anterior dorsal vertebrae. (a) Ventrolateral view of dorsal vertebrae 1–6 (?), BMNH R4795. (b) Dorsal vertebra 1 in dorsal, left lateral, anterior, and posterior views, restored from BMNH R4795. (c) Dorsal view of dorsal vertebrae 1–7 (?), RSM 1967.10.1A. (d) Dorsal vertebra 7 in dorsal view (anterior part only), dorsal view of centrum with neural arch removed, left lateral, anterior and posterior views; restored from RSM 1967.10.1A and BMNH R4791.
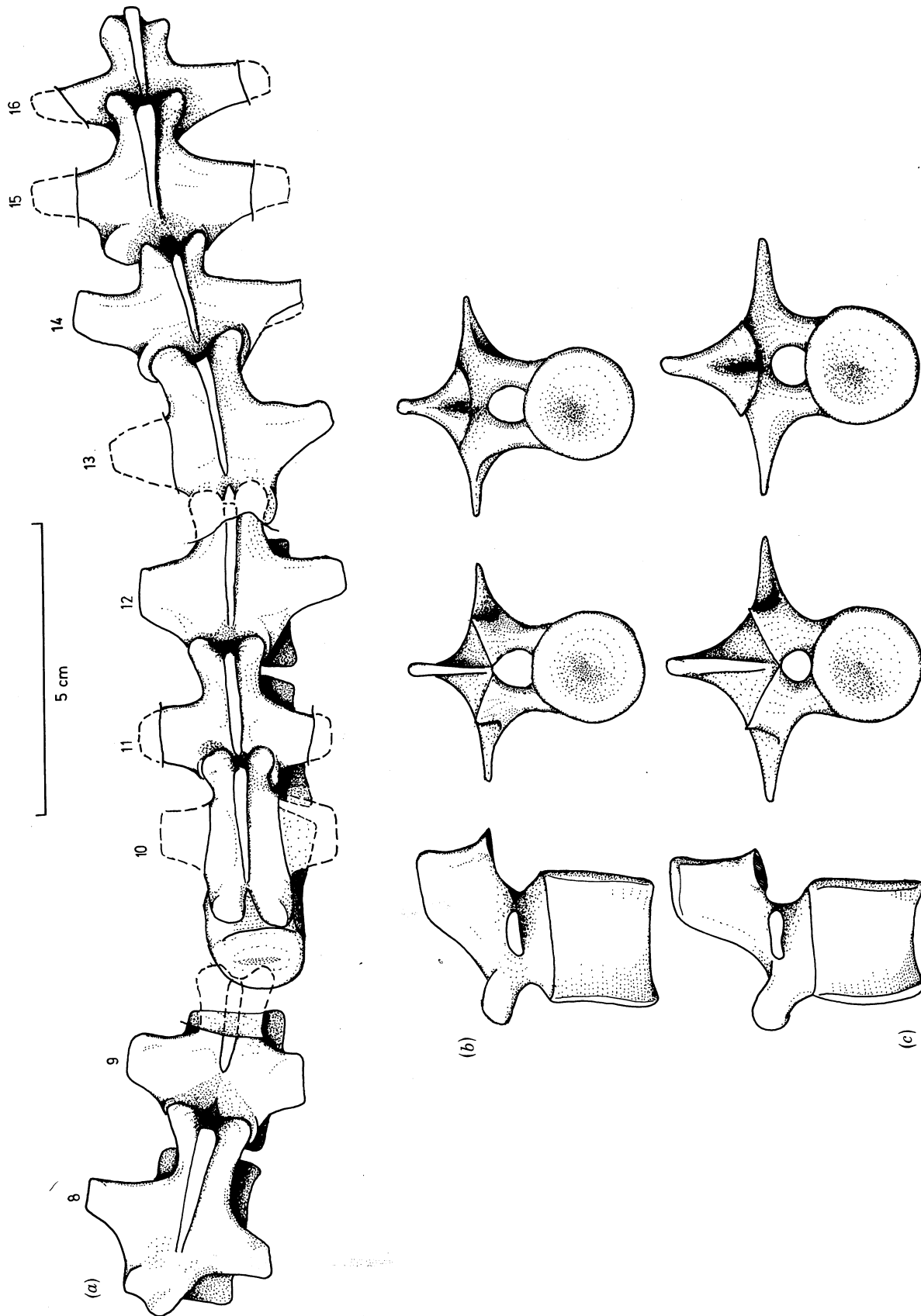
FIGURE 23. Posterior dorsal vertebrae. (*a*) Dorsal view of dorsal vertebrae 8–16 (?), BMNH R4791, slightly restored; (*b*) dorsal vertebra 11 in left lateral, anterior and posterior views, restored from BMNH R4791; (*c*) dorsal vertebra 16 in left lateral, anterior, and posterior views, restored from BMNH R4791.
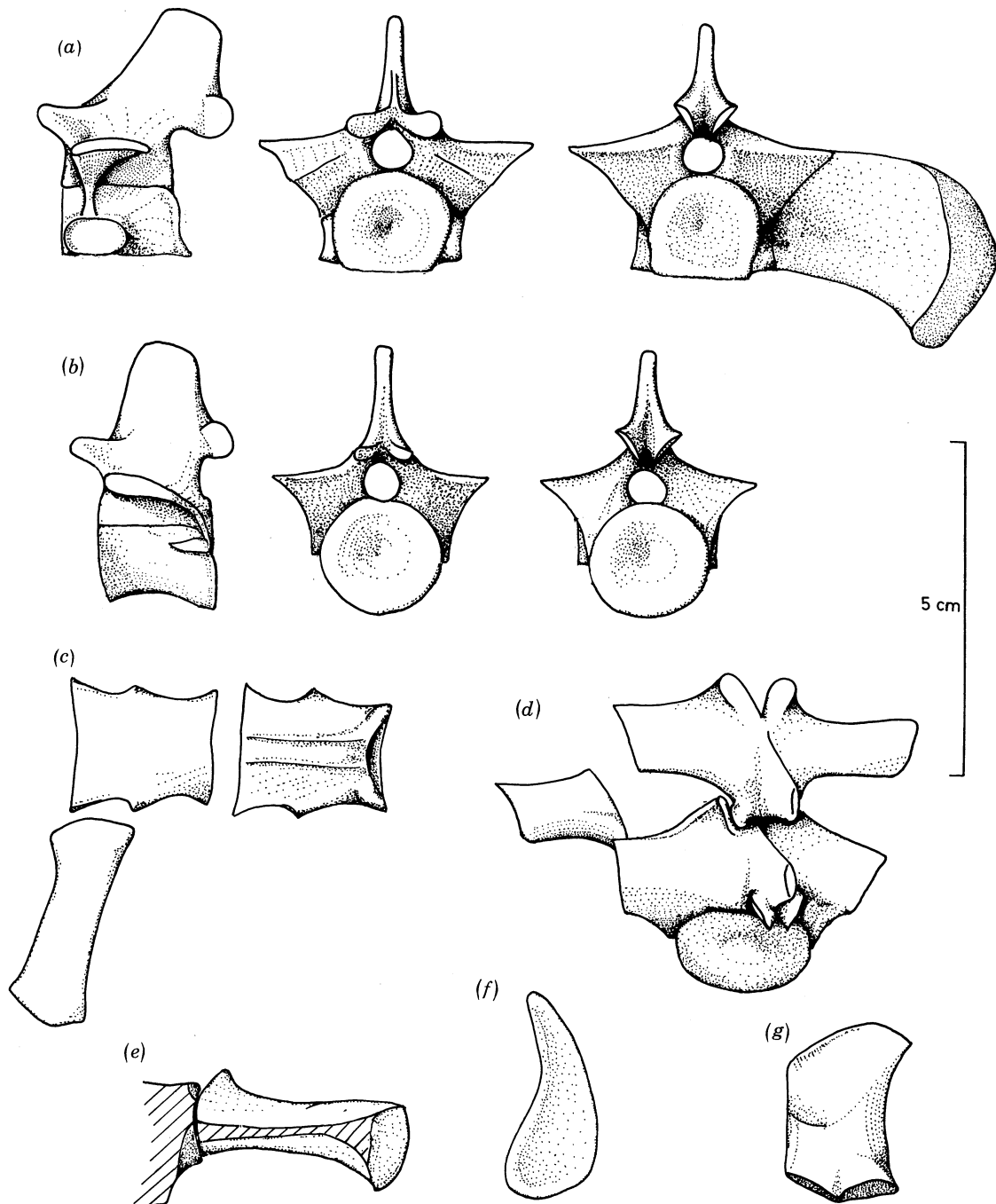
FIGURE 24. Sacral vertebrae. (a) Sacral vertebra 1 in lateral, anterior and posterior views (with left sacral rib); restored from BMNH R3148, RSM 1967.10.1B/C and GSM 90933/4. (b) Sacral vertebra 2 in lateral, anterior and posterior views; restored from BMNH R3148, RSM 1967.10.1B/C and GSM 90933/4. (c) Centrum of sacral vertebra 1 in ventral and dorsal views, and right sacral rib in ventral view, BMNH R3148. (d) Sacral vertebrae 1 and 2 in dorsal view with displaced left sacral rib 2, GSM 90933/4. (e) Dorsal view of horizontal section through sacral vertebra 1 and right sacral rib, near the base; restored from RSM 1967.10.1B/C. (f) Sacral rib 1, distal view; restored from GSM 90933/4. (g) Right sacral rib 2, posterior view, GSM 90933/4.

7.1.5. *Caudal vertebrae* (figure 25)

The number of caudal vertebrae is unknown, but may have been in the region of 25 or 30, as estimated for *Stenaulorhynchus*, *Paradapedon* and *Scaphonyx*. The longest series available for *Hyperodapedon* consist of caudals 1–8 (RSM 1967.10.1 B–D), and caudals 1–6 (BMNH R3418).

The first caudal vertebra (figure 25*a*) has a centrum as long as the second sacral, but centrum length reduces somewhat from the third vertebra (figure 25*b*) backwards (figure 20). The centrum is constricted laterally in ventral view in caudal 3, and appears to become more and more constricted further back, as in *Paradapedon*. The articular faces of the centrum are deeply concave, but information on the dorsal outline is limited.

The prezygapophyses in proximal caudal vertebrae (figure 25*a*, *b*) project far forwards, which is possibly partly the result of distortion, and the postzygapophysis just reaches the level of the posterior margin of the centrum, as in *Scaphonyx* and *Paradapedon*. The facets are steeply inclined, at about 60–70°. The neural spine is low, and has a broad base in caudal 3, and seems to become lower in succeeding vertebrae (figure 25*c*, *d*). The transverse processes from caudal vertebra 3 backwards are short.

Anterior caudal vertebrae bear small ribs on their large transverse processes. Long chevrons are preserved in two specimens, and appear first between caudals 3 and 4. Chevron facets are not clearly preserved anywhere.

7.2. *Ribs* (figures 21, 26–28)

Series of ribs are preserved in 17 individuals, of which the most useful for restoration were: EM 1886.3, 1978.567; BMNH R699, R3560, R4782, R4791, R4795; and RSM 1967.10.1, 4. Most of these display the overall form well, but articular heads are often not easy to see.

Ribs are present on all presacral vertebrae, except probably the atlas and axis, and on the anterior caudal vertebrae. The articular head of the rib is divided into two branches, a dorsal tuberculum and ventral capitulum, in the cervical ribs (figure 27). The two articular portions are still just visible in the first dorsal rib (figure 27 (9)), but unite in all ribs behind the second or third, as in *Stenaulorhynchus* and *Scaphonyx*. *Paradapedon* displays a division rather further back (Chatterjee 1974, p. 241).

The cervical ribs are strong, but short (Huxley 1887, p. 677), and taper towards a point ventrally. The anterior three dorsal ribs are broad and long (figure 27 (9, 10, 11)) and they are differentiated from those that follow behind. They appear to have bunched together and run down and backwards as a broad plate-like unit behind the shoulder girdle (figures 1, 2, 28), a feature apparently not present in other rhynchosaurs. The remaining dorsal ribs are oriented more laterally and decrease slightly in length and breadth backwards to the 11th or 12th (19, 20), after which the size reduces more rapidly (figures 26, 28). The articular head remains broad except in the most posterior dorsal ribs and the distal ends of all ribs are expanded (figures 27, 28). The shafts appear to be flattened in all ribs, although the proximal end may become rather rounded posteriorly.

Proximal caudal ribs were probably broad and short (figure 26), as in *Scaphonyx* (Huene 1942, pl. 32, fig. 5), and they may be represented by irregular plate-like elements scattered beside caudal vertebrae 2–4 in RSM 1967.10.1 D (figure 25*d*). Caudal vertebrae 4–6 in BMNH R3148 bear short straight rod-like ribs that trend laterally and backwards. The articulating heads are not visible.
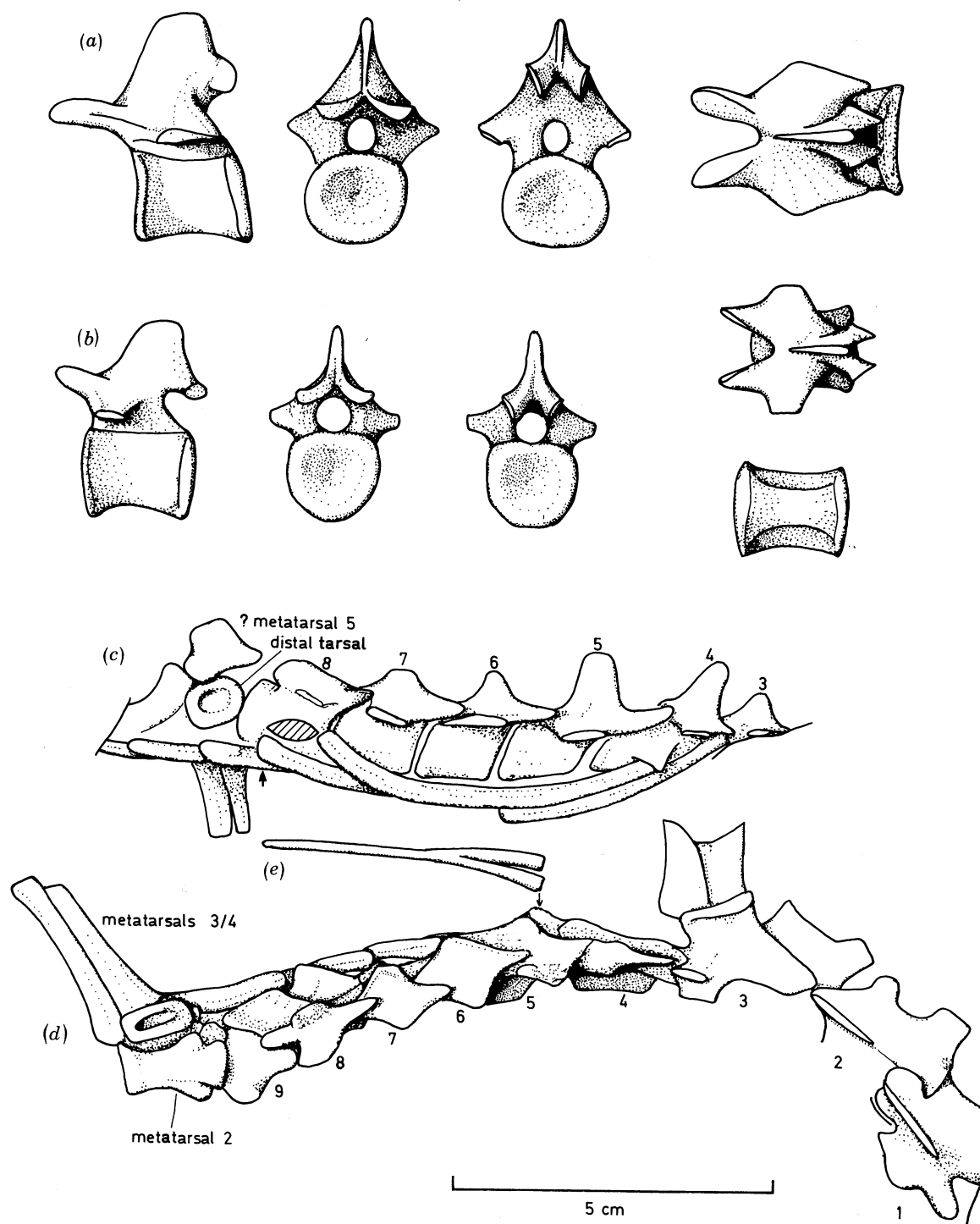
FIGURE 25. Caudal vertebrae. (a) Caudal vertebra 1, left lateral, anterior, posterior, dorsal views; restored from BMNH R3148. (b) Caudal vertebra 3, left lateral, anterior, posterior, dorsal, ventral views; restored from BMNH R3148. (c) Right lateral view of caudal vertebrae 3–8 with chevrons and foot bones mixed, RSM 1967.10.1D. (d) Dorsolateral view of caudal vertebrae 1–8 with chevrons and foot bones mixed, RSM 1967.10.1D. (e) Ventral view of chevron 5 or 6, RSM 1967.10.1D.
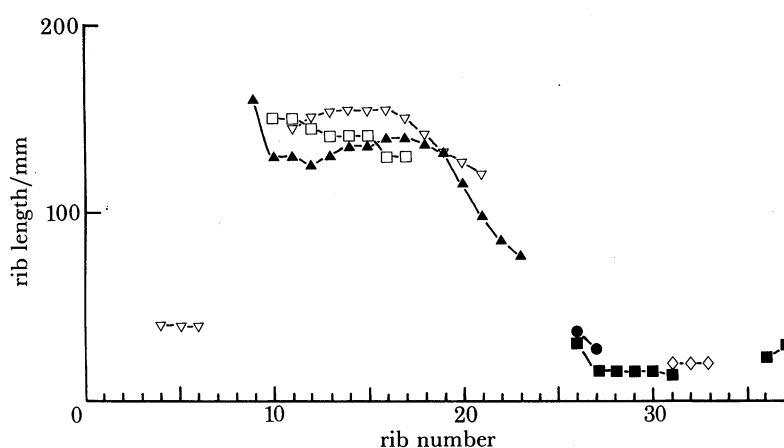
FIGURE 26. Variation in rib length in cervical (1–8), dorsal (9–25), sacral (26, 27) and anterior caudal vertebrae. Measurements of series of ribs are taken from different individuals, represented by different symbols: ▽, BMNH R699; □, BMNH R4782; ◇, BMNH R3148; ▲, EM 1886.3; ●, GSM 90933/4; ■, RSM 1967.10.1.

7.3. *Chevron bones* (figure 25 *c–e*)

Long chevron bones associated with caudal vertebrae 3–8 are preserved in casts of RSM 1967.10.1D (figure 25 *c–e*). They are long curved rod-like elements, flattened in a vertical plane, with clear double heads for articulation below the caudal vertebrae. In life, the chevron bones probably projected posteroventrally, and the anterior ones would have run back beneath three of four vertebrae. They are longer and flatter than those of *Stenaulorhynchus* and *Scaphonyx*.

7.4. *Gastralia* (figures 1, 3, 28)

Series of gastralia are preserved in many specimens, and especially well in: EM 1978.566 (figure 1), 1978.567 (figure 3), 1886.3 (figure 28); BMNH R699, R3148, R3563, R4781, R4782, R4791; and GSM 90933–4. An average-sized animal had 50 or more rod-shaped elements covering the entire ventral region of the trunk. The anterior gastralia are V-shaped (Huxley 1887, pp. 678–679) and lie below the shoulder girdle region. Further back, the gastralia become straighter, and then they begin to form a V-shape backwards, terminating below the sacrum. The mid-series gastralia are divided in the midline, but it is hard to tell if this applies to anterior and posterior gastralia because of the poor preservation. All longer elements appear to have extra lateral pieces that sometimes become slightly displaced (figure 28). The gastralia are narrow and of uniform width from back to front, but they are rarely perfectly straight. They are closely spaced and there are about three below each vertebra. However, they do not contact the ribs, and there is no evidence of a sternum, nor of sternal ribs.

The scale and pattern of the gastralia seems very like that of *Rhynchosaurus* (Woodward 1907). The set of V-shaped gastralia from the 'Keuper' sandstone (Bromsgrove Sandstone Formation) of Hollington, Staffordshire, ascribed by Woodward (1905) to *Hyperodapedon*, probably do not belong to a rhynchosaur, since the 27 elements are all tightly V-shaped with no sign of straightening out. They may belong to a thecodontian.
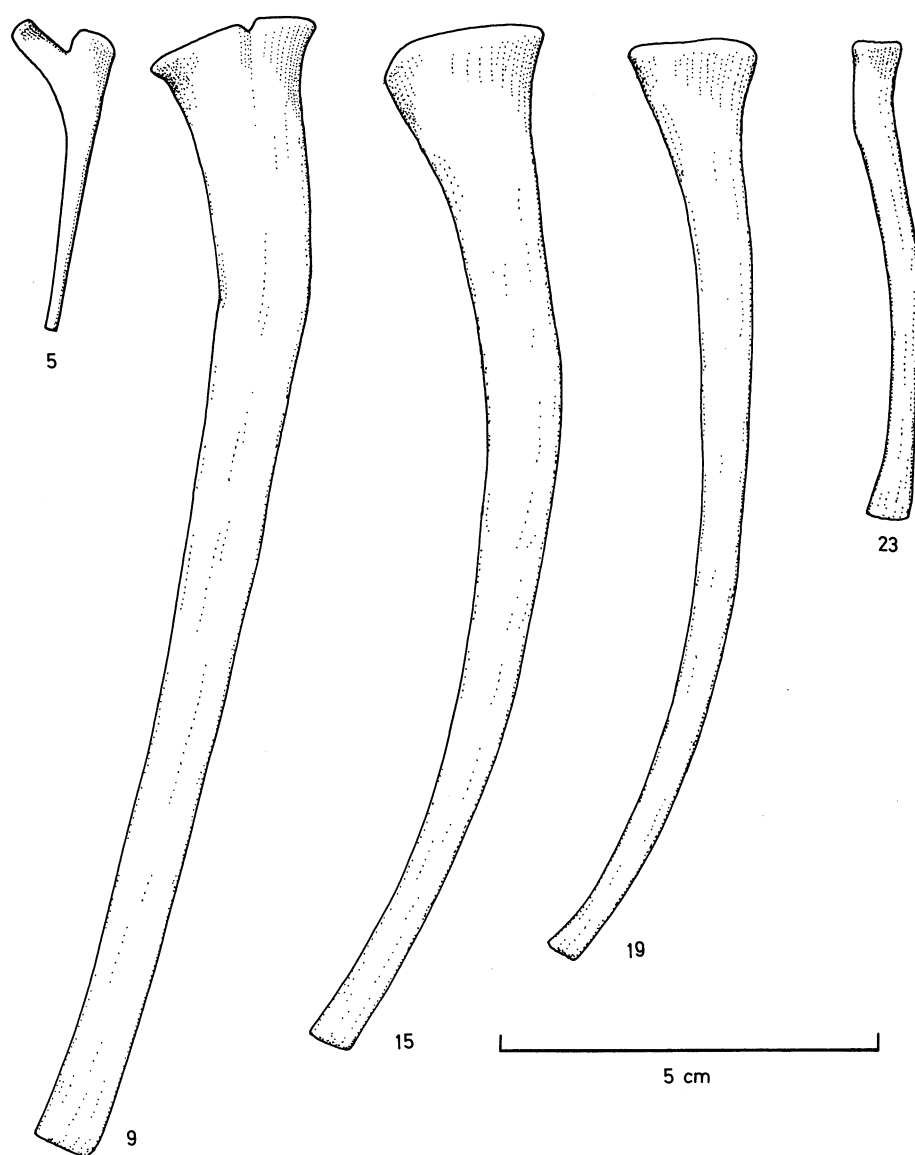
FIGURE 27. Left presacral ribs associated with vertebrae 5, 9, 15, 19, 23 (i.e. cervical 5, dorsals 1, 7, 11, 15). Restored as follows: 5 (BMNH R699, R4782), 9 (EM 1886.3; BMNH R4795; RSM 1967.10.1A), 15 (EM 1886.3; BMNH R4782, R4791), 19 (BMNH R4782, R4791; RSM 1967.10.1B/C), 23 (BMNH R4782, R4791; RSM 1967.10.1B/C).

7.5. Functional aspects of the axial skeleton

7.5.1. Intervertebral movements

Considerable rotation of the head was probably possible between the basioccipital and the atlas ring, although little was possible between atlas and axis. The atlas centrum rested firmly on facets of the axis, and the atlas neural arch elements were probably also firmly fixed. However, the atlas intercentrum formed a broad plate beneath the basioccipital which would allow lateral and vertical rolling.

Various forms of intervertebral movement could have occurred in the remainder of the vertebral column of *Hyperodapedon*. Rotation about a longitudinal axis was possible between nearly all vertebrae because the small postzygapophysis could slide across the broader

prezygapophysis of the vertebra behind. Only in the case of the sacral vertebrae are the prezygapophyses so small that they inhibited rotation.

We may assume that zygapophysis angles between 0° and 45° from the horizontal allow maximum bending of the vertebral column from side to side, and angles between 45° and 90° allow maximum bending up and down. Thus, the neck (45–50°) could bend in both horizontal and vertical planes. The vertebrae of the shoulder region (cervicals 7, 8; dorsals 1, 2), with angles of 60–70° (figure 20*a*), could rotate relative to each other mainly in a vertical plane. The dorsal vertebral column (40–45°) was again flexible in both planes, and particularly the horizontal. Zygapophysis angle in the sacral region (70–75°) suggests reduced lateral flexibility. The angles remain high in the anterior tail, so that it too was probably rather inflexible in a horizontal plane. Thus, lateral flexion of the vertebral column was much reduced in the shoulder and pelvis regions.

7.5.2. *Rib function*

The first three anterior dorsal ribs were broad, long and backwardly trending (figures 1, 3, 27, 28). They probably rendered the anterior trunk largely rigid because they ran parallel and straight beneath the scapula and met distally. This would have enhanced the effect of the anterior dorsal vertebrae in strengthening the trunk against lateral flexure, as in certain cynodonts (Jenkins 1971; Kemp 1980*b*).
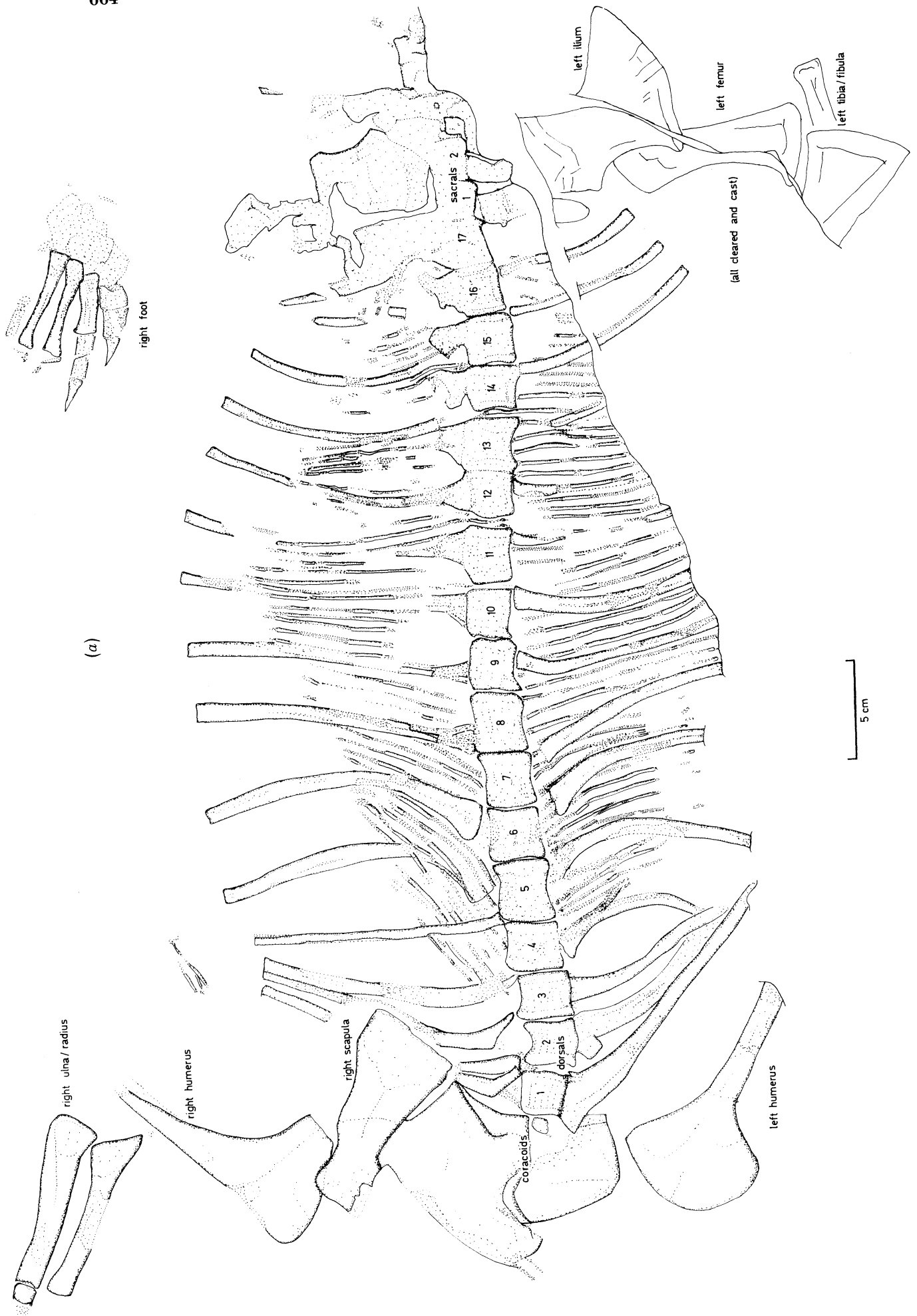
These specialized dorsal ribs do not seem to occur in other rhynchosaurs, although Huene (1938, p. 97) noted that the distal ends of the ribs of *Stenaulorhynchus* were broader in the most anterior dorsal region. Further, there is no clear evidence of a reduction of lateral flexion of the vertebral column in the shoulder region of *Paradapedon* since zygapophysis angle is about 45° throughout the presacral series (Chatterjee 1974, p. 239).

The remaining dorsal ribs of *Hyperodapedon* have a single articular head and horizontal diapophysis which would have permitted some flexibility, particularly in a vertical plane. This was probably connected with pulmonary ventilation. Upwards rocking of the ribs increases the volume of the body cavity and aids inspiration in the absence of a diaphragm, as in lizards (Wood & Lenfant 1976).

7.5.3. *Axial musculature*

It is clear that large muscles attached on the broad axis neural spine, but their areas of origin cannot be delimited. The m. rectus capitis posterior probably had its origin on the anterodorsal region and inserted on the supraoccipital. It would have functioned in flexing the head dorsally. The m. obliquus capitis magnus probably had a larger origin covering most of the centre of the axis neural spine, and inserted along the top of the opisthotic and exoccipital behind the temporal artery, as in *Sphenodon* (Byerly 1925; personal observation). The possible great length and lateral extent of this muscle in *Hyperodapedon* would have permitted it to turn its head from side to side over a wide arc. The m. longissimus transversalis cervicis, inserting ventrally along the paroccipital process, and the m. longissimus transversalis capitis, inserting on the spheno-occipital tuber, would assist in this motion.

The m. rectus capitis anterior ran ventrally, linking the anterior cervical vertebrae and inserted on the spheno-occipital tuber. It was probably well developed, and contraction would pull the ventral occiput back and would produce a sudden lowering of the head, possibly useful for operation of the premaxillae in scraping up food, or in fighting (?).

(a)

right foot

right ulna / radius

right humerus

right scapula

coracoids

dorsals

left humerus

sacrals 2

17

16

15

14

13

12

11

10

9

8

7

6

5

4

3

2

1

left ilium

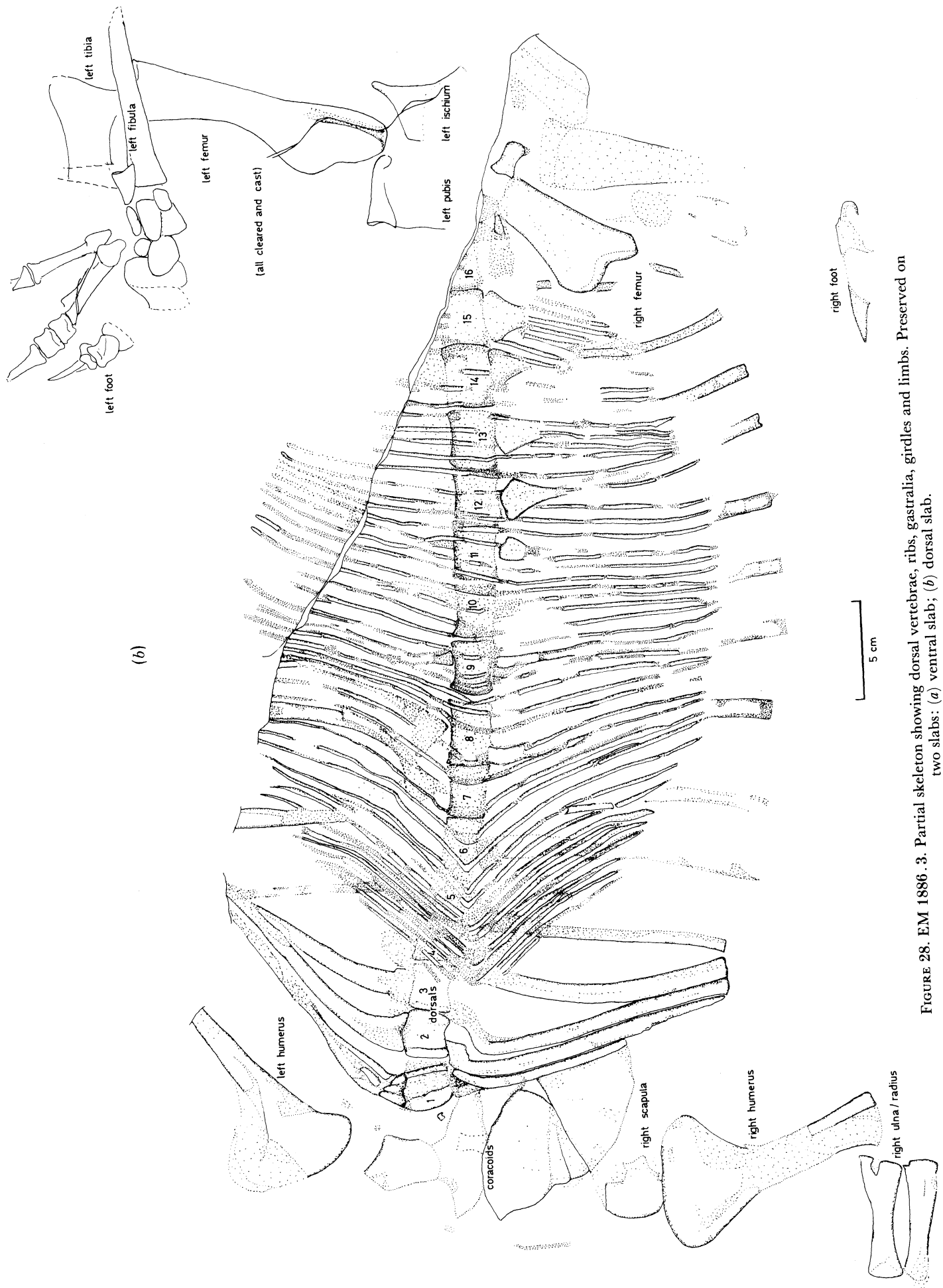left femur

left tibia / fibula

(all cleared and cast)

5 cm

FIGURE 28. EM 1886.3. Partial skeleton showing dorsal vertebrae, ribs, gastralia, girdles and limbs. Preserved on two slabs: (a) ventral slab; (b) dorsal slab.

The dorsal axial musculature of the neck (m. spinalis capitis and m. longissimus articulo-parietalis + trapezius, inserting on the posterior face of the parietal and squamosal respectively) had to support the weight of the head. There is a deep pit along the entire width of the posterior face of the parietal (figure 6) which increased the area for attachment of these important muscles.

The relatively large cervical ribs suggest a powerful neck musculature to support the heavy head. The broad anterior dorsal ribs may have given a large area of origin for medial muscles attaching the shoulder girdle. It is unlikely that they had any function in the development of an enlarged iliocostalis system of muscles for lateral flexure in locomotion, as suggested for some cynodonts (Jenkins 1971), since middle and posterior dorsal ribs are not expanded. The broad anterior caudal ribs and long chevrons would have offered extensive origins for the caudifemoral musculature.

8. APPENDICULAR SKELETON
8.1. *Shoulder girdle* (figure 29)

Elements of the shoulder girdle are preserved in several specimens and the best examples are: EM 1886.3; BMNH R699, R3933, R4782 (cast), R4795 (cast); RSM 1967.10.1A (cast); and GSM 69764.

The *scapula* shows a range of gracile and robust forms (figure 29 a, b), and the reconstructions are based on the former (figure 29 e, f). The true mediolateral curvature in many individuals (e.g. BMNH R4782, RSM 1967.10.1A) may be greater, but these specimens are almost certainly distorted. The scapula has a broad dorsal end (figure 29 b) which was doubtless finished with cartilage in life. The suprascapula may have become ossified in older animals, and this may also give rise to some of the variation in scapula shape as preserved. The upper portion of the lateral surface of the blade is rugose in several specimens, and it narrows and curves outwards on passing downwards. The anterior margin swells laterally into a small acromion process for the reception of the clavicle. The posterior margin expands to support a broad semicircular glenoid face which points posterolaterally.

The *coracoid* is a curved element, less than half as high as the scapula. It is attached to the scapula on a broad face and forms the lower part of the glenoid fossa, which makes an angle of 100–110° to the scapular portion. In ventral view (figure 29 c), the coracoids nearly touch on either side of the interclavicle, and they can be seen to lie in the region of presacral vertebrae 7–9. The coracoid appears to consist of a ventral and a lateral portion and the bend is marked by a lateral ridge in front of the glenoid. There is a fairly large coracoid foramen that appears to be present as an incisure in front of the glenoid face. Burckhardt (1900, p. 488) believed that he could divide the coracoid of *Hyperodapedon* (BMNH R699) into a coracoid and 'praecoracoid', but there is no evidence for this.

The *interclavicle* is preserved in EM 1978.566 (figure 1), BMNH R699, R4782 (figure 29 c) and GSM 69764 (figure 29 d). It is a three-pronged structure, with a long dagger-like plate extending horizontally between and behind the coracoids probably to the level of presacral vertebra 11. Part of the anterior cross bar is preserved, but the *clavicles* are not seen, except for a possible distal end in RSM 1967.10.1A. The elements identified as clavicles by Huene (1929, p. 39, pl. 8, fig. 5: 'r.Cl.', 'l.Cl.') in BMNH R699 are anterior broad dorsal ribs and displaced scapula respectively.
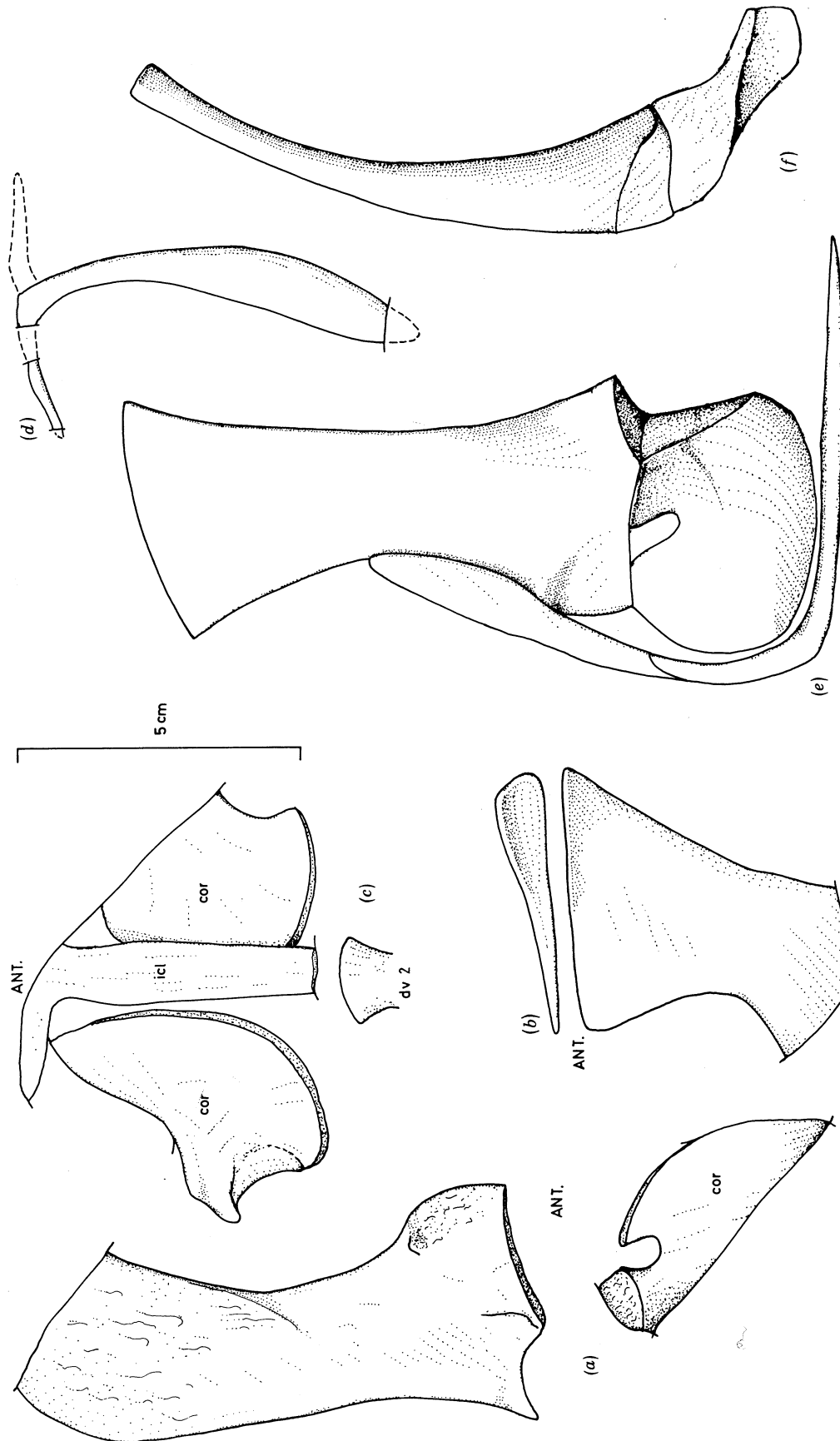
FIGURE 29. Shoulder girdle. (*a*) Lateral view of disarticulated right scapula and partial coracoid, BMNH R4795, showing roughened areas of muscle attachment on the scapula, and part of the glenoid surface and the coracoidal incisure. (*b*) Dorsal and lateral views of a distorted partial left scapula, BMNH R4782. (*c*) Ventral view of the two coracoids and the interclavicle, partially preserved; located just in front of dorsal vertebra 2, BMNH R4782. (*d*) Ventral view of interclavicle, partially restored from GSM 69764. (*e*, *f*) Scapulocoracoid with clavicles and interclavicle, lateral and posterior views of left side; restored from EM 1886.3 and BMNH R4795, with clavicles from other rhynchosaurs.

8.2. *Forelimb* (figures 30, 31)

Elements of the forelimb are preserved in 13 specimens, usually in articulation. The following were most useful for the description: EM 1886.3; BMNH R699, R4782 (cast), R4791 (cast), R4795 (cast); RSM 1967.10.1A (cast).

The *humerus* (figure 30) has expanded ends and a narrow shaft linking them. The proximal and distal articular regions are set at about 45° to each other. The proximal end consists of a broad posterior plate and a narrow anteroventral deltopectoral crest. These probably stood at about right angles to each other, but a complete uncrushed specimen of the proximal end is not available. The proximal articular surface (figure 30) is divided into a long posterior humeral convexity and presumably a short broad anterior humeral concavity on the deltopectoral crest (Holmes 1977).

The shaft is narrow and elliptical in cross-section, and the long axis of the ellipse changes its orientation as the shaft twists and expands. The distal end bears a deep rounded triangular depression on the ventral surface The entepicondyle is flat posteriorly, and the ectepicondyle bears a thin supinator crest and groove (for the radial nerve and blood vessels). The epicondyles show no foramina. The distal articular surface (figure 30*f*) is divided into a large anterior capitellum and posterior trochlea for separate articulation with radius and ulna respectively. These faces wrap round the sides of the humerus, and their shape is well shown in a cast from BMNH R4795. The surface is highly rugose and was probably capped with cartilage.

The *radius* (figure 31) is slightly shorter than the ulna and is expanded symmetrically at both ends. The shaft is elliptical in cross-section and is marked by a lateral ridge. The proximal articular surface is oval in outline and flat, or slightly concave, for articulation with the humerus. The distal articular surface is rather more circular in outline; it is slightly concave, and slopes up medially.

The *ulna* (figure 31) also has broad ends and a narrow shaft, but it is slightly larger than the radius in all dimensions. In medial view (figure 31*b*), the dorsal margin is straighter than the ventral margin, but this effect is apparently not so marked in *Paradapedon* (Chatterjee 1974, p. 245). The proximal articular facet curves down to meet the radius. The outline is convex and cordate, and the apex is matched with a short ridge on the proximal medial surface of the shaft. There is no clear olecranon process. The shaft is elliptical and flattened mediolaterally in cross-section. The distal articular surface has an irregular triangular shape and it slopes up medially. The articular facets are not well preserved and were probably finished with cartilage.

The hand of *Hyperodapedon* is incompletely known. Metacarpals and phalanges are preserved in BMNH R699 and R4782, but the carpal region is absent.

Carpals may be represented by one or two obscure fragments at the distal end of the ulna and radius of the right side in EM 1886.3 (figure 28*a*, *b*). Similarly, a few incomplete fragments appear in a cast of BMNH R4791+4805 at the distal end of the left radius. The only good carpal is a radiale adhering to the right radius in a cast from BMNH R4782 (figure 31*f*). The proximal facet slopes up medially and matches the distal facet of the radius. The radiale has similar diameters to the radius, and clearly acted as an extension of the latter. The distal face also slopes up medially and is slightly concave. The size and shape of the radiale suggest that an intermedium may not have been present, or if it was, it was probably small.

The five *metacarpals* in BMNH R699 are all present (figure 31*g*). Metacarpal I is short and broad, II–IV, as far as preserved, are longer and have distinct shafts and expanded heads, and
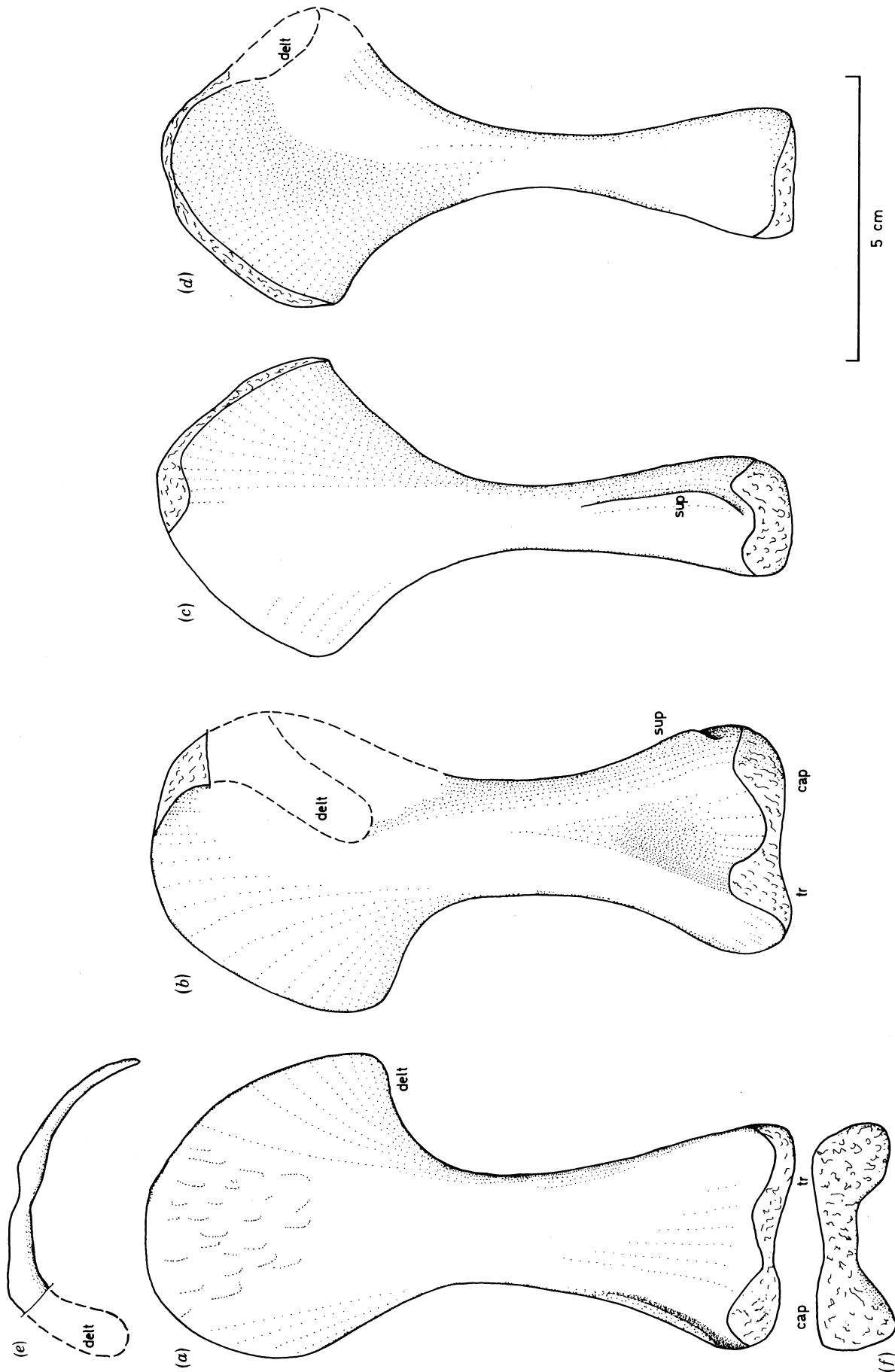
FIGURE 30. Restoration of the left humerus. (*a*) Dorsal; (*b*) ventral; (*c*) anterior; (*d*) posterior; (*e*) proximal; (*f*) distal views. Restored from BMNH R699, R4782, R4791, R4795, with deltopectoral crest from other rhynchosaurs.
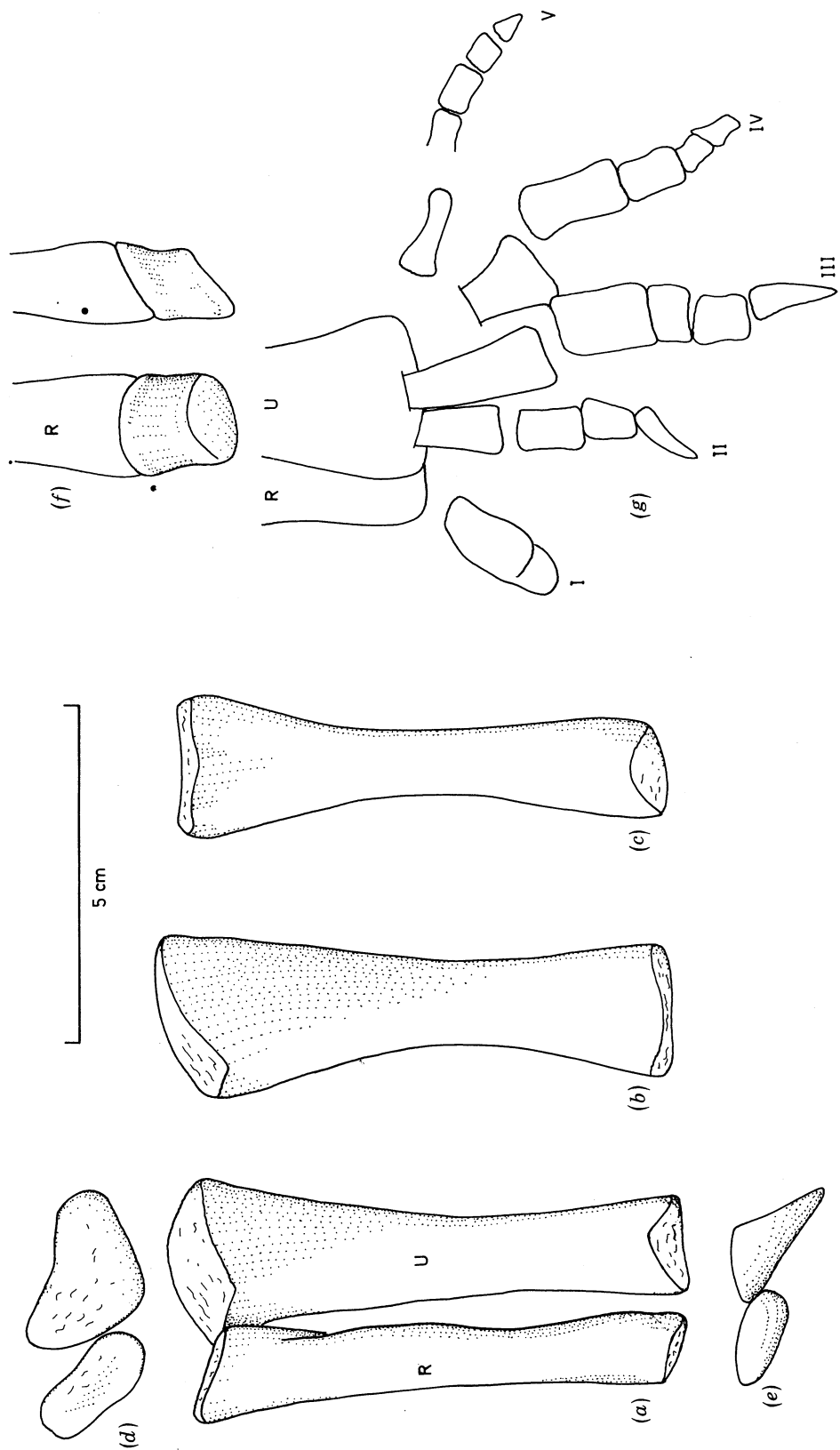
FIGURE 31. Lower forelimb. (a–e) Restorations of left radius and ulna in anterior, medial ulna, medial radius, proximal, and distal views; based on BMNH R4782 and RSM 1967.10.1A. (f) Left radiale in medial and anterior views, attached to radius, BMNH R4782. (g) Outline sketch of left hand in dorsal; view, BMNH R699; lacks carpals, and metacarpals displaced.

V is a small spindle-shaped element. The *phalangeal series* of digits II, III and V are complete, and the formula appears to be 2:3:4:5:4 (Huene 1929, p. 39). The claws of digits II and III are long and pointed, while that of digit V is rather shorter. Articular surfaces are not clearly visible. The fingers are relatively short and spread widely in a fan shape. Digit V appears to diverge rather further laterally than digit I does medially.

The hand is not fully known in any rhynchosaur. *Mesosuchus* (2:3:4:5:3) has a similar broad radiale that fits closely to the radius, and there is no intermedium preserved. It also has an ulnare and four distal carpals (Haughton 1921, p. 86, pl. 3, fig. 5). *Rhynchosaurus* (2:3:4:5:3) seems to have a small intermedium and two distal carpals in one specimen (Woodward 1907, p. 297, pl. 2, fig. 2; Huene 1929, pl. 6, fig. 9). *Stenaulorhynchus* has a radiale, ulnare and four distal carpals preserved (Huene 1938, p. 103, pl. 13, figs 1–3). One specimen of *Scaphonyx* (2:3:4:5:4) shows four small carpals interpreted tentatively by Huene (1942, p. 303, pl. 34, fig. 5) as radiale, distal carpal 4, ulnare and intermedium. However, all these elements are small and rounded, and they do not match the distal articular facets of radius or ulna. They are more probably distal carpals 2, 3 and 4 respectively, and the 'intermedium' may be correctly identified. Very few hand remains of *Paradapedon* are preserved.

The hand and wrist of *Hyperodapedon* and other rhynchosaurs was probably similar in pattern and proportions to the primitive reptile arrangement of captorhinomorphs, 'eosuchians' and early thecodontians. As in these groups, a scale effect is seen: smaller animals (e.g. *Rhynchosaurus*) have relatively longer fingers than the larger ones (e.g. *Hyperodapedon*). In all cases, the hand is shorter than the foot.

8.3. *Pelvic girdle* (figure 32)

Elements of the pelvis are shown well in: EM 1978.566, 1886.3 (cast); BMNH R699, R4781 (casts), R4795 (+R4805) (casts); RSM 1967.10.1B–D (casts); and GSM 90933/4 (casts). EM 1886.3 and BMNH R4781 were useful in reconstructing the proportions of the pelvic elements, but the lack of three-dimensionally preserved material makes it difficult to produce an accurate reconstruction of the anterior view of the pelvis.

The *ilium* (figure 32*a, d, e*) is a flat nearly vertical element, expanded dorsally and ventrally. The dorsal blade projects furthest posteriorly. The upper margin is thin and bowed, but thickens slightly at the angles. The iliac blade narrows ventrally to a neck with rounded anterior and posterior margins and expands to accommodate the rounded imperforate acetabulum. The acetabulum is bounded in front by a rounded pillar and it merges smoothly with the posterior margin. Centrally, above the acetabulum, there is a slight boss on the neck. The lower edge contacts the pubis and ischium, and the ischium contact seems to be slightly longer. The medial surface of the ilium is only seen in EM 1886.3 and it shows sacral rib facets, but they are not very well preserved.

The *pubis* (figure 32*b, d, e*) is a broad quadrangular element. The anterior margin is rounded and runs from the midline anteroventrally to the unfinished distal surface of the short vertically placed processus lateralis. The pubis meets its partner for a short distance in the midline. The posterior edge is in two parts: a broad lateral portion that meets the ischium, and a longer medial portion that forms the anterior margin of a large diamond-shaped space (figure 32*e*). A large foramen for the obturator nerve pierces the pubis near the middle of its posterior margin. Laterally, the pubis forms a small part of the acetabulum below the iliac contact.

The *ischium* (figure 32*c, d, e*) is a curved, thin, elongate plate-like element. The anterolateral angle expands into a broad facet that contacts the ilium and forms a small part of the
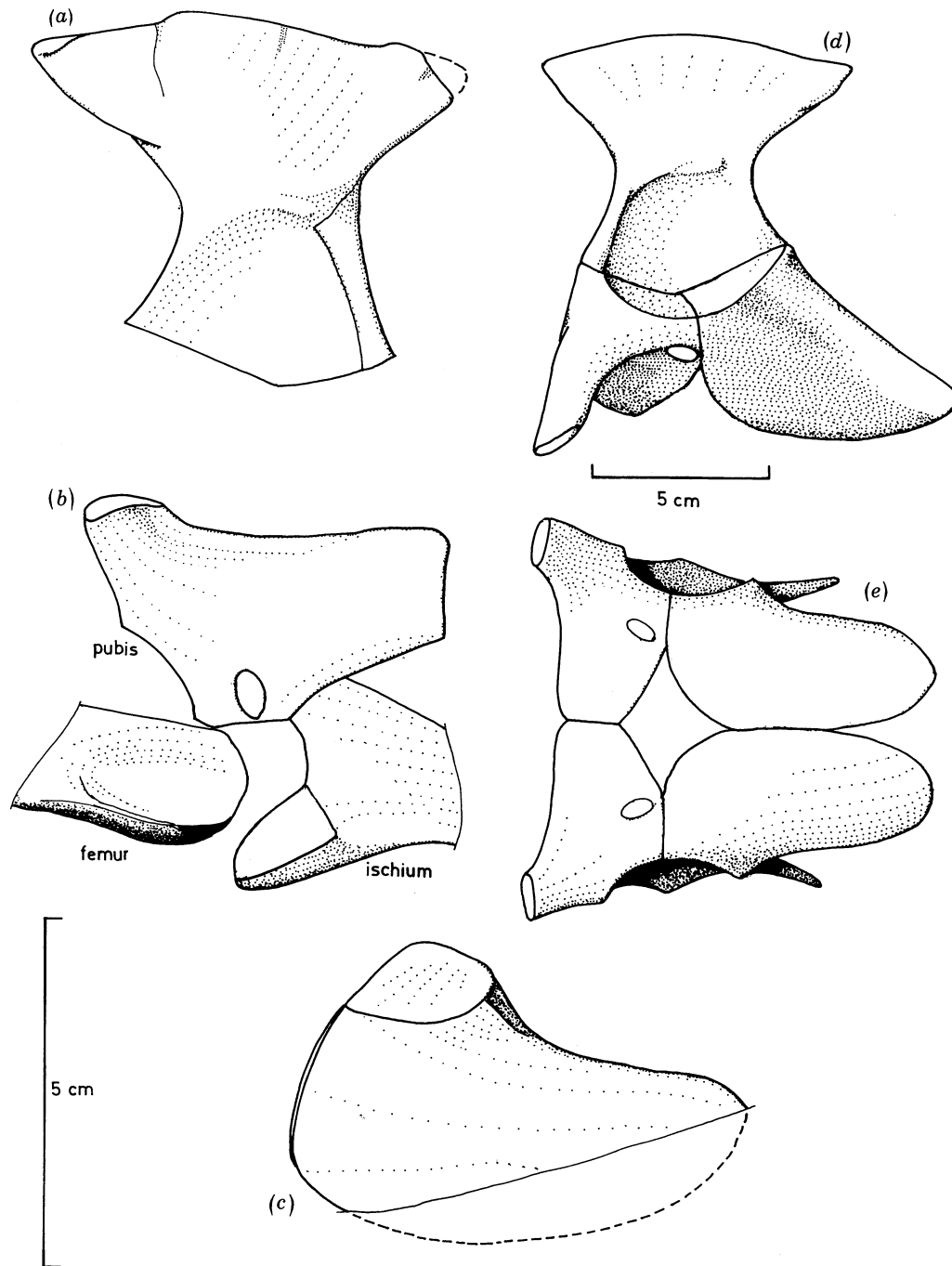
FIGURE 32. Pelvic girdle. (*a*) Right ilium in lateral view, RSM 1967.10.1B/C. (*b*) Right pubis, partial ischium and proximal end of femur in ventral view, BMNH R4781. (*c*) Left ischium in ventrolateral view, partially restored, BMNH R4791/4805. (*d*, *e*) Composite restoration of the pelvic girdle in left lateral and ventral views, based on EM 1886.3; BMNH R4781, R4791/4805. Note the different scales for (*a*–*c*) and (*d*, *e*).

acetabulum. The anterior margin passes medially in contact with the pubis and runs freely for some distance as the posterior margin of the ventral diamond-shaped space. The ischia meet for a short distance medially and curve posterolaterally to a rounded, thickened posterior margin.

8.4. *Hindlimb* (figures 33–35)

Several specimens preserve parts of the hindlimb. The most useful for reconstruction were: EM 1978.566, 1886.3 (casts); BMNH R699, R3560 (cast), R4791 (+4805) (cast); RSM 1967.10.1 B–D (cast); and GSM 90932/5 (cast).

The *femur* has a constricted shaft, and expanded ends set at a slight angle to each other. The proximal end has a marked ventral intertrochanteric fossa between two raised flanges (figure 33*b*). The anterior of these, the internal trochanter, forms a broad projection below the ovoid articular surface (figure 33*c*, *d*). The 'ridge' on the dorsal margin of the posterolateral view of EM 1886.3 (figure 33*c*) seems to have been produced partly by crushing and it is not a special process. There is no fourth trochanter and the adductor ridge is not pronounced. The distal end expands to slightly less than the proximal width. There is a depressed popliteal space in the middle of the ventral view of the distal portion, and the distal articular surface (figure 33*e*) is clearly divided into rounded medial and lateral condyles, both for the tibia. The fibula was received on a small condyle on the posterolateral surface.

The *tibia* (figures 33*a*, 34*a–d*) is extremely broad proximally and narrower distally. It is flattened and is clearly divided into an anterior (extensor) and posterior (flexor) surface. The proximal articular surface is elliptical and it is divided to receive the two femoral condyles. The shaft is oval in cross-section and arched médially away from the fibula. A low cnemial crest runs for a short distance from the anteromedial angle of the proximal articular surface (figure 34*b*, *d*). The shaft twists slightly and the anterior face is marked by a diagonal ridge and groove (figure 34*a*). The distal end is slightly expanded, and the articular surface is oval in outline. The shaft slopes up posteriorly and is divided into two flat facets (for centrale and astragalus) which are set at a slight angle to each other.

The *fibula* (figures 33*a*, 34*e–h*) is a long slender bone that arches laterally away from the tibia. It twists in such a way that the proximal and distal articular facets stand at right angles to each other. The proximal end is barely broader than the shaft and the articular facet is oval in outline. The flattened shaft twists and then expands to form a spatulate distal end. The distal articular facet is oval in outline and it curves round the medial and lateral sides of the shaft.

The *tarsus* is poorly preserved in several specimens, but there is enough material to produce a general reconstruction (figures 35, 36). As in other rhynchosaurs, there are three proximal elements and four distal. Hughes (1968) and Chatterjee (1974) called the three proximal tarsals of rhynchosaurs tibiale, intermedium and fibulare, while Carroll (1976*a*) gave strong evidence that these should be homologized respectively with the centrale, astragalus and calcaneum of primitive reptiles. The latter convention is used here.

The *centrale* (figures 35*a*, *c*, 36) is a rounded medial element that is attached firmly to the astragalus. The broad proximal facet contacts the tibia, and there is a small contact area for distal tarsal 1.

The *astragalus* (figures 35*a–c*, 36) is the largest of the proximal tarsals. The facets for the epipodials are deep and curved to fit firmly. The fibula rests in a deep pit on the posterior face of the astragalus (figure 35*a*), and the tibia is overlapped by a posterior process. The proximal articular surface is not clearly visible, but the tibial and fibular facets do not seem to lie at right angles to each other as in *Stenaulorhynchus* and *Scaphonyx* (Hughes 1968). The contact with distal tarsals 2 and 3 is also not preserved clearly.
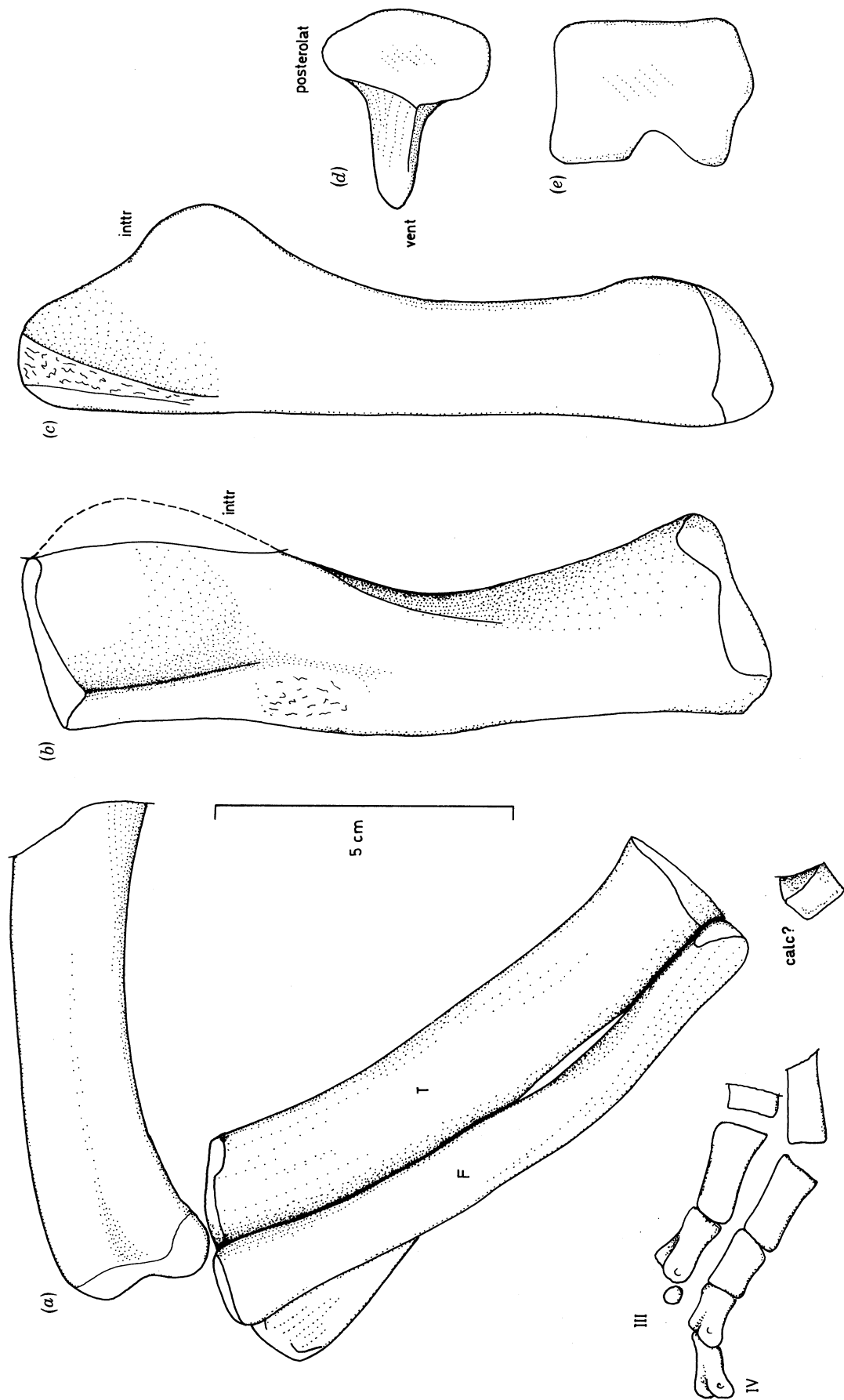
FIGURE 33. Hindlimb. (a) Left femur, tibia and fibula, and foot in posterior view, GSM 90932/5. (b–e) Restoration of the left femur in ventral, posterolateral, proximal, and distal views; based on EM 1886.3; BMNH R4791/4805; GSM 90932/5.

The *calcaneum* (figures 35 *a–c*, 36) is a smaller element, expanded medially where it is attached to the astragalus. It narrows and then expands again laterally in a broad descending process above metatarsal V. The proximal contact with the fibula, and the distal articular surface, are not visible.

The four *distal tarsals* (figures 35 *b*, *c*, 36) are small elements that form a row above metatarsals 1–4. They are circular to oval in dorsal and ventral view, and the first is the smallest, the fourth the largest. The proximal and distal articular surfaces of tarsal 1 are rounded, and those of tarsals 2–4 are rectangular in outline with a depressed centre (figure 25 *c*, *d*).
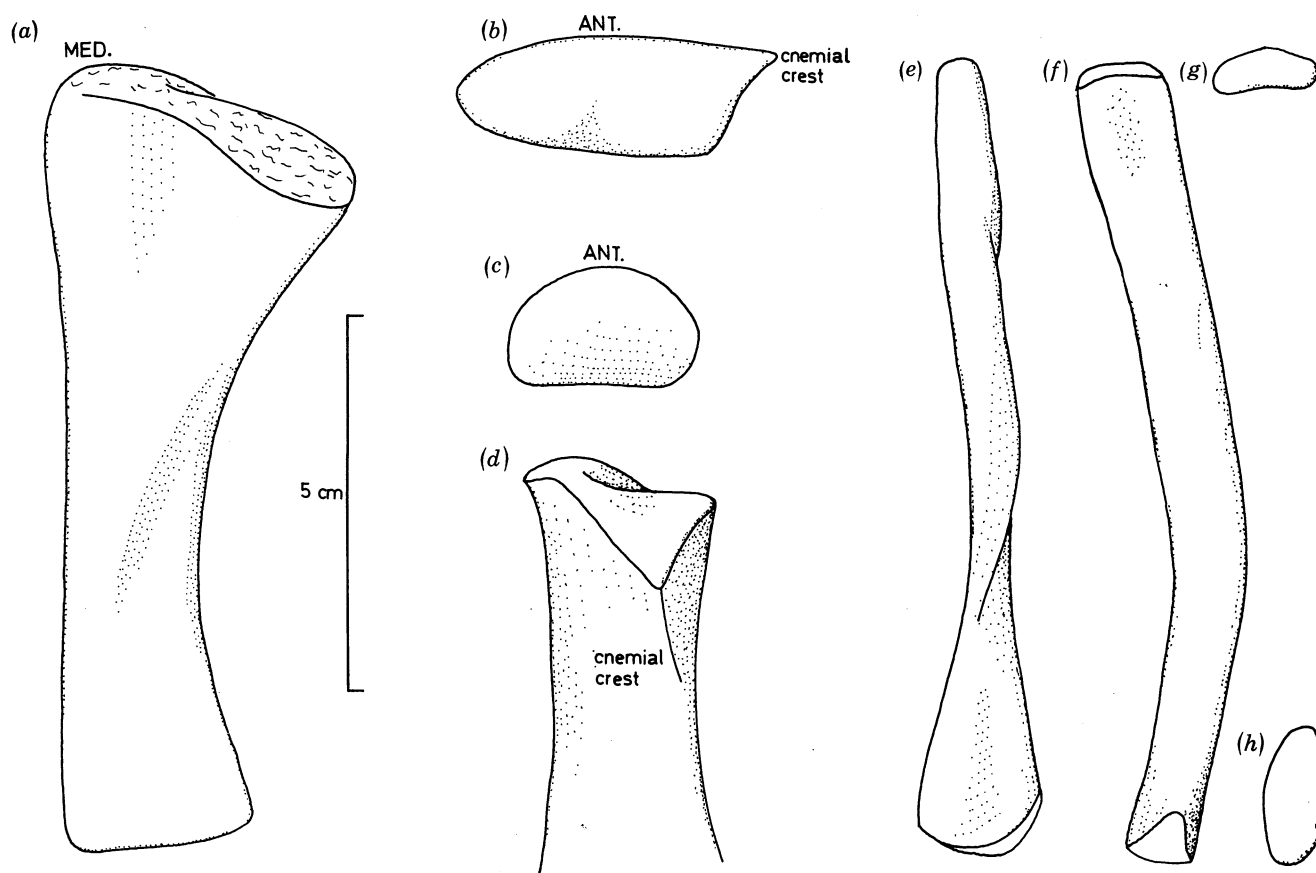
FIGURE 34. Hindlimb. (*a–c*) Restoration of the left tibia in anterior (extensor), proximal and distal views; based on EM 1886.3; RSM 1967.10.1. (*d*) Medial view of proximal end of right tibia, RSM 1967.10.1D. (*e–h*) Restoration of the left fibula in anterior, medial, proximal, and distal views, based on EM 1886.3 and GSM 90932/5.

The *metatarsals* vary greatly in shape (figures 35 *b–d*, 36). The first is short and broad with a greatly expanded proximal end. The length increases and the breadth decreases from the second to the fourth, and the fifth is L-shaped. Metatarsals II–IV have raised grooved portions at the distal end with collateral ligament pits on each side (figures 25 *d*, 35 *c*, 36).

The *phalanges* are all short and have expanded ends, and the phalangeal formula is 2.3.4.5.4. The phalanges reduce in length distally in each digit, except for the unguals. In side view (figure 35 *e*), they have roller-like convex distal facets with lateral depressions that indicate the
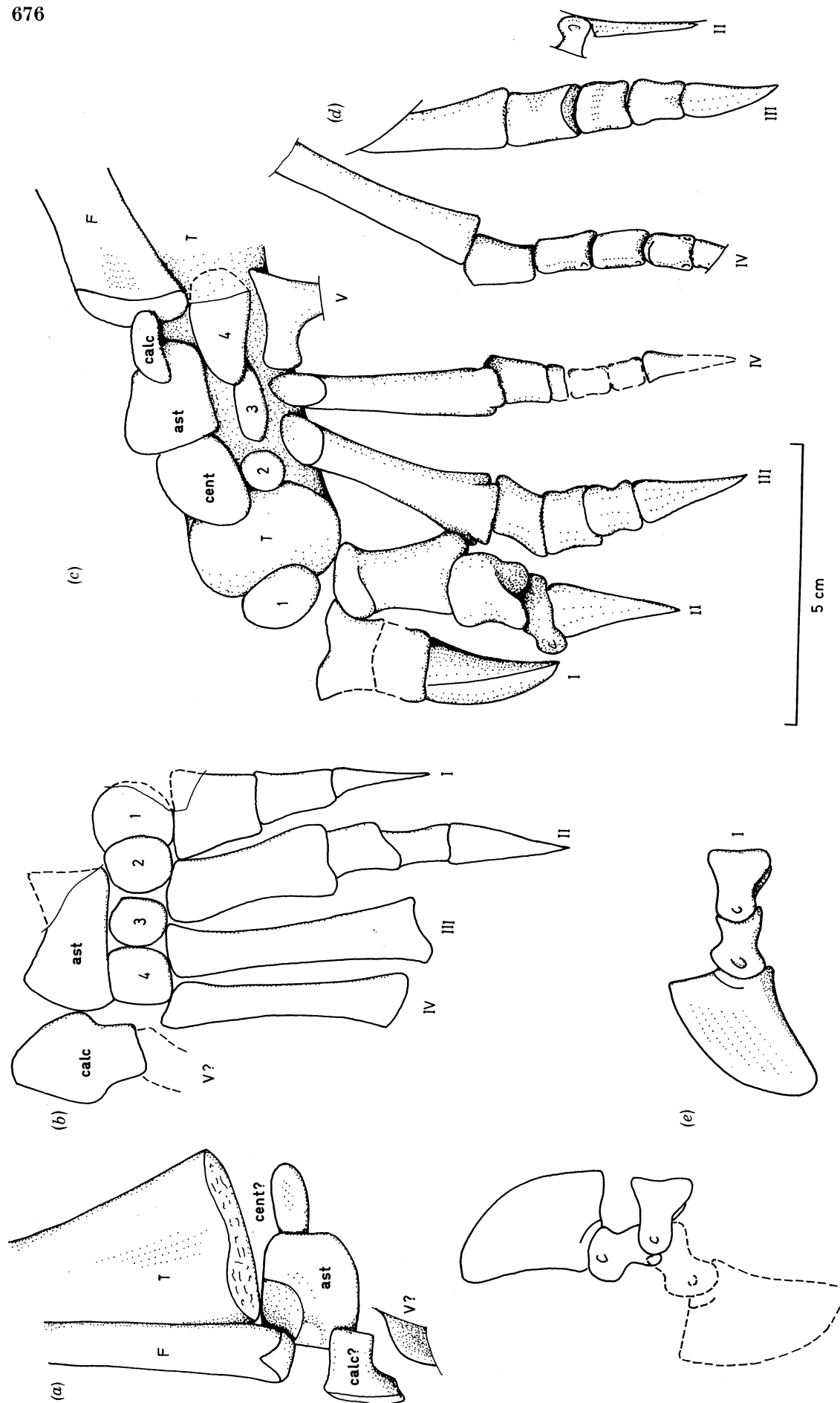
FIGURE 35. Foot. (a) Posterior (flexor) view of the distal ends of the tibia and fibula of the left side, with three proximal tarsals and a possible metatarsal, RSM 1967.10.1D. (b) Ventral (flexor) view of a partial left foot, restored from EM 1886.3. (c) Ventral (flexor) view of a partial right foot with ankle bones and distal ends of the tibia and fibula, partially articulated, EM 1886.3. (d) Dorsal view of three partial digits of the right foot, EM 1886.3. (e) Restoration of right digit I, and a sketch showing the maximum flexion and extension possible; based on EM 1886.3.
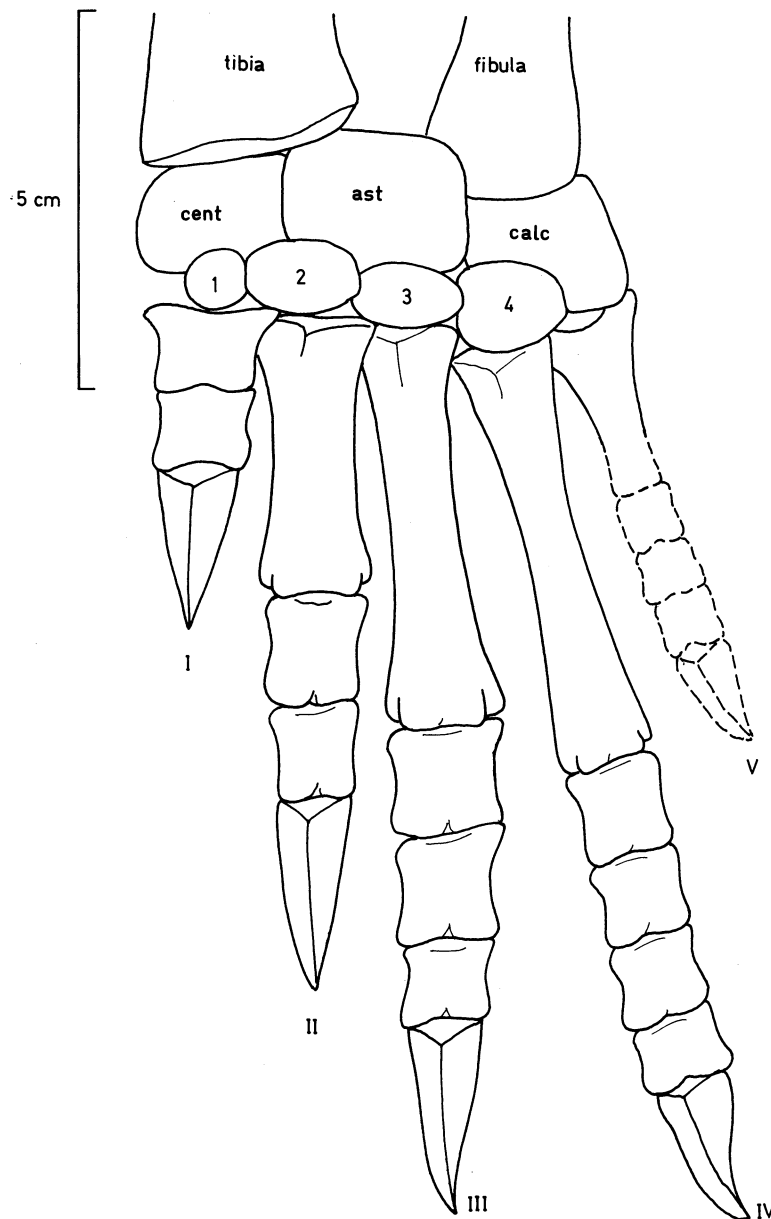
FIGURE 36. Reconstruction of left tarsus and pes. Dorsal view, based on BMNH R3560, and other specimens.

presence of strong collateral ligaments. The biconcave proximal facets may extend beneath the adjacent phalanx. Each digit bears a large claw, the size of which decreases from digit I to digit V. The claws are high, blunt-ended and bilaterally compressed, and they have a sharp dorsal peak. They were probably covered with a horny sheath in life. The high degree of flexion and extension possible is shown diagrammatically in figure 35e.

8.5. *Functional aspects of the forelimb*
8.5.1. *Joint mobility and stride* (figure 37)

The exact location and orientation of the shoulder girdle with respect to the vertebral column and ribs is not known because of compression in all preserved specimens. However, the coracoid

FIGURE 37. Reconstruction of forelimb movements. The shoulder girdle slopes backwards at 10° from the vertical. Muscles are indicated by areas of attachment and main lines of action. (a–c) Stages in the power stroke of a normal stride in left lateral view.

of *Hyperodapedon* is normally found below the region of presacral vertebrae 7–9 (e.g. EM 1886. 3; BMNH R699, R4782, R4795), and this seems to be the case in *Scaphonyx* (Huene 1942, fig. 65) and *Paradapedon* (Chatterjee 1974, fig. 27). The scapular blade probably sloped backwards at an angle of about 10°, as in these forms where the curvature can be seen clearly.

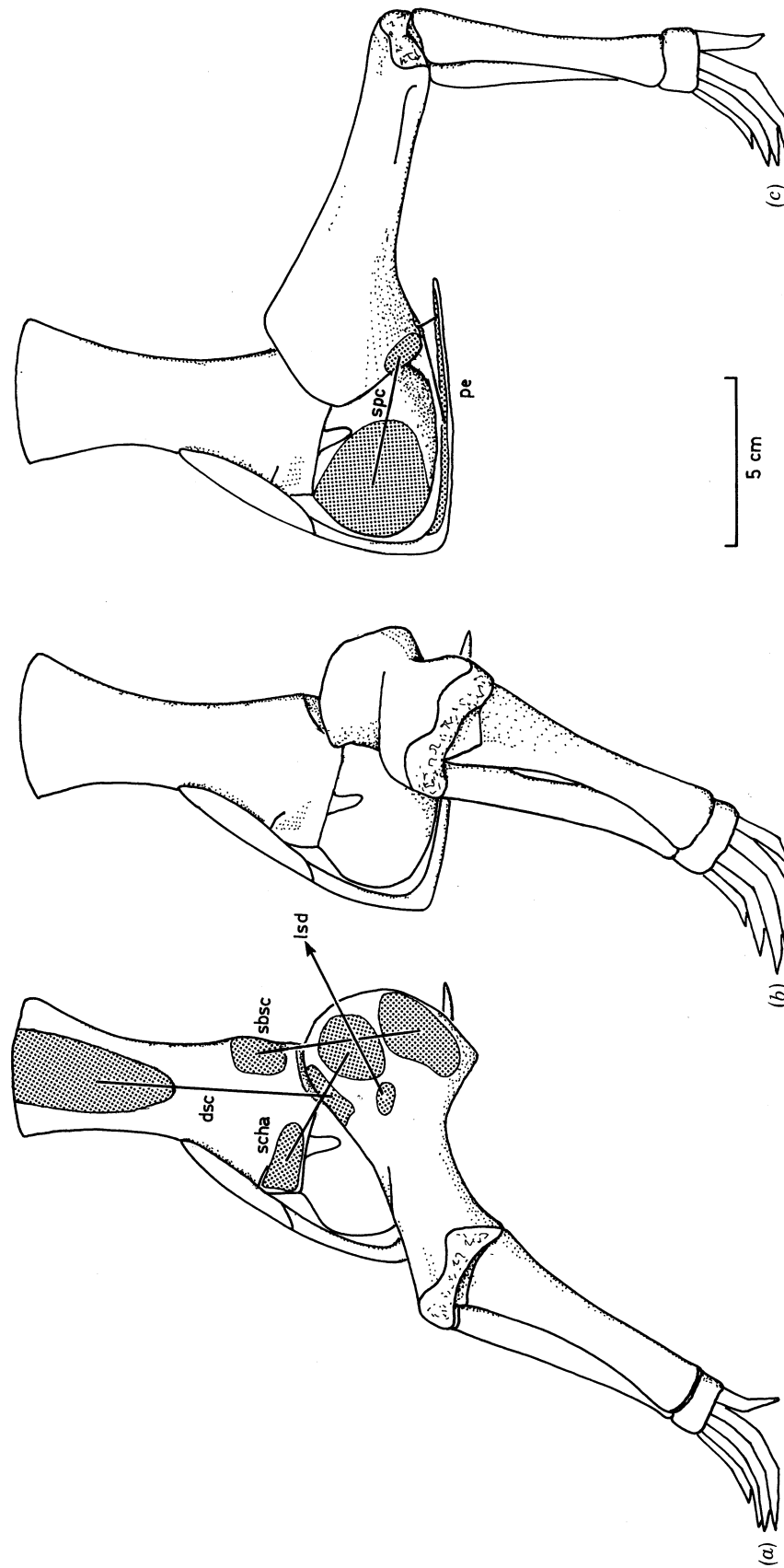In the reconstruction of forelimb movements, the shoulder girdle is set in this position, and this means that the glenoid fossa faces posterolaterally and slightly ventrally. For the sake of simplicity, it is assumed that the shoulder girdle was fixed relative to the axial skeleton during the stride (figure 37).

The range of movements of the proximal end of the humerus on the glenoid fossa is difficult to interpret because of the incongruity of the two faces. Although cartilage probably improved the fit, it seems that only small areas of the surfaces were in contact at any time. During a normal back-swing of the limb, the region of contact probably rolled, rather than slid, from anterior to posterior points of both faces, as suggested by Kemp (1980a, b) for some cynodonts.

Most evidence points to a modified sprawling forelimb gait for *Hyperodapedon*: the scapular portion of the glenoid is anterior to the coracoidal portion, the entepicondyle is still quite well developed, and the forearm elements are rather shorter than the humerus (criteria of Bakker (1971)). However, the vertical long axis of the glenoid and its posterolateral orientation is an advance over the condition seen in *Captorhinus*, an obligatory sprawler (Holmes 1977). The posterior portion of the coracoid in *Hyperodapedon* is also reduced and the humerus could end the power stroke tucked tightly against the side of the trunk. The arc of humerus swing was about 100° in *Hyperodapedon* (60° in *Captorhinus*). Thus, *Hyperodapedon* could probably adopt either a sprawling or semi-erect forelimb gait.

When the humerus was drawn fully forward, the humeral concavity (behind the deltopectoral crest) rested on the anterolateral margin of the glenoid faces of scapula and coracoid, and the humerus was oriented with the distal end far anterior to, and probably slightly below, the proximal end (figure 37a). The long thin humeral convexity was not in contact at this stage. As the humerus was drawn back during the power stroke, the deltopectoral crest rolled down, the humerus rotated about its long axis, and progressively more posterior portions of the humeral convexity came into contact with the glenoid fossa (figure 37b). The distal end of the humerus followed an arc slightly below the level of the proximal end during the power stroke. The humerus rotated further, and at the end of the swing it was nearly horizontal and directed backwards parallel to the side of the body.

During the power stroke, the radius and ulna rotated slightly in their ventral positions on the capitellum and trochlea respectively (figures 31a, 37). The proximal end of the radius was raised slightly initially, and the ulna rose considerably during the stride. The twist of the forearm with respect to the humerus allowed the hand to maintain its position as the humerus swung back.

The radius–radiale joint clearly allowed only limited movement, and it is likely that the main wrist joint in *Hyperodapedon* was between the carpals and metacarpals. The rotation of radius and ulna during the power stroke probably necessitated adjustments in the carpus also.

The reconstructed forelimb stride length of *Hyperodapedon* is 20–25 cm, thus 30–35 % of the presacral length. Small movements of the shoulder girdle and mid-trunk movements could add 10 % to this figure.

8.5.2. *Muscles*

It has been suggested above that the shoulder girdle was rather firmly attached to the anterior dorsal ribs and that the anterior trunk was inflexible. The muscles involved were probably the serratus superficialis (posterior), the serratus profundus (anterior) and the costosternocoracoideus (?and the sternocoracoideus) (Holmes 1977).

Rugosities on the lateral side of the scapula (figure 29*a*) indicate the general area of origin of a large scapular deltoid dorsally and the scapulohumeralis anterior near the lower anterior edge. Rugosities near the proximal end of the humerus on the posterodorsal surface (figure 30*a*), probably represent the areas of insertion of the scapulohumeralis anterior and subcoracoscapularis. It is uncertain whether there was a scapulohumeralis posterior. The supinator process, on the anterior distal margin of the humerus (figure 30*a–c*), bore the origin of the supinator muscles. Further muscle attachment sites are not indicated by unequivocal evidence, and a detailed reconstruction is not attempted. It may be assumed that the musculature was similar to that of *Sphenodon*, generalized lizards and primitive captorhinids (Fürbringer 1900; Romer 1944; Lécuru 1968; Holmes 1977), and main muscle directions are shown in figure 37.

Retraction and anterior rotation of the humerus were probably accomplished by the subcoracoscapularis, coracobrachialis (longus and brevis) and latissimus dorsi, with extension of the lower limb by the triceps. Protraction may have been accomplished by the pectoralis, supracoracoideus and scapulohumeralis anterior, with flexion of the lower limb by the biceps. However, in all cases, these muscles do not seem to be positioned in such a way as to provide a strong power stroke. Many would have acted more strongly as adductors or elevators (e.g. scapular deltoid, scapulohumeralis anterior).

The limitations of the muscles and the small area of contact between the glenoid fossa and the humerus indicate that the shoulder joint was weak and not associated with the main locomotory forces.

8.6. *Functional aspects of the hindlimb*

8.6.1. *Joint mobility and stride* (figure 38)

The pelvic girdle was firmly united with the axial skeleton and it was clearly virtually immovable. The relationships to the vertebral column in the region of the sacrum suggest that the pelvis was oriented in such a way that the upper margin of the ilium was tilted backwards at about 20° below the horizontal, as in other rhynchosaurs (Huene 1942, fig. 65; Chatterjee 1974, fig. 27). This position is used in the reconstruction of limb movements (figure 38).

The acetabulum faces laterally and slightly downwards and backwards. It is a broad shallow basin (figure 32) and the proximal articular head of the femur (figure 33*d*) is far smaller. Although cartilage doubtless improved the fit in life, it seems that *Hyperodapedon* could have had a wide range of femur positions from horizontal 'sprawling' to oblique 'semi-erect' stance. In both orientations, protraction was limited by the processus lateralis of the pubis and retraction by the internal trochanter coming into contact with the posterior margin of the acetabulum. Slightly greater protraction of the femur was possible in a near-horizontal orientation and greater retraction in a nearer vertical orientation. The latter additional movement would have added more to the stride length than the former, and a femur orientation of about 45° from horizontal was probably best for rapid locomotion.

The orientation of the knee and ankle joints tends to confirm this normal semi-erect gait. The two tibial facets of the femur are mainly distal, and not ventral, which suggests that a
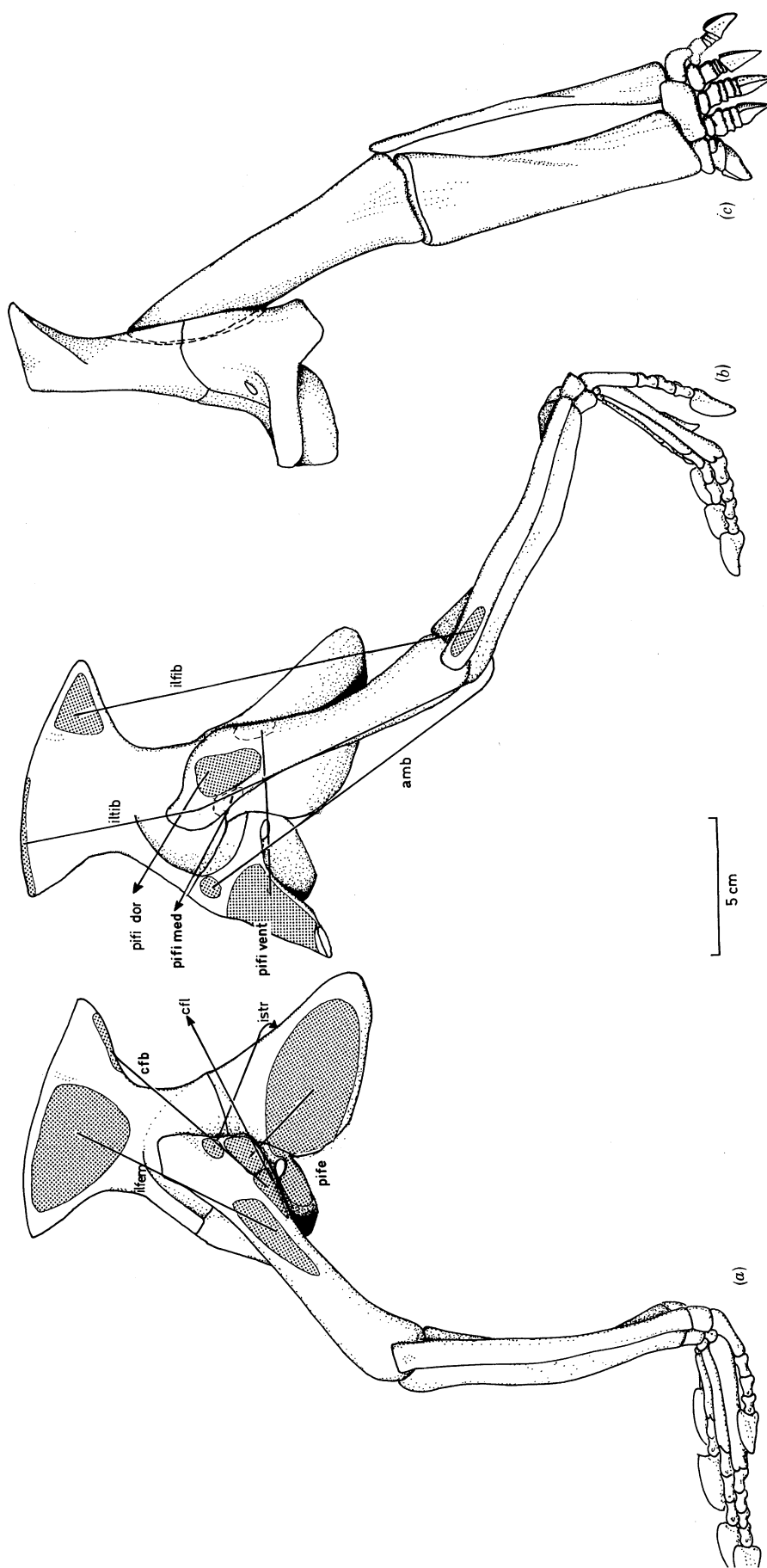
FIGURE 38. Reconstruction of hindlimb movements. The ilium blade is set at 20° below the horizontal. Muscles are indicated by areas of attachment and main lines of action. (*a, b*) Stages in the power stroke of a normal stride in left lateral view. (*c*) Left hindlimb and half pelvis in anterior view; this view of the pelvis is based on other rhynchosaurs.

horizontal position of the femur was unusual. Tibia and fibula are of nearly equal length, and the proximal tarsals were firmly united with each other and with the epipodials so that very little rotation of the crus was possible. Thus, the femur must have remained almost in a vertical plane during the stride, and that demands a semi-erect limb posture.

Further evidence in support of a semi-erect hindlimb gait for *Hyperodapedon* comes from studies of the evolution of archosaur locomotion (Bakker 1971; Charig 1972, p. 153). *Hyperodapedon* shares the following characters with semi-erect and erect archosaurs: two sacral vertebrae, ilium (anterior process well developed, weak supra-acetabular crest, acetabulum imperforate), pubis and ischium slightly elongated, femur (head inturned, shaft gently sigmoid, fourth trochanter weak or absent), tibia not 'twisted', tarsus characters uncertain, pes (plantigrade, phalangeal series equal in length to metatarsals, digits III and IV of similar length, V rather reduced).

A study of the joints in *Hyperodapedon*, and comparison with other rhynchosaurs, suggests that the pelvis–femur joint was rotatory and would have allowed considerable elevation and depression (abduction and adduction), the femur–crus joint was a simple hinge with little possibility of rotation, and the ankle joint was mesotarsal, with the main hinge and rotatory joint between the proximal and distal tarsals (Hughes 1968).

In lateral view, the femur begins the retraction stroke at an angle of 40–45° below horizontal and finishes at an angle of 45–50° below horizontal. Seen from above, the femur swings through an arc of about 90° and the posterior position lies more in a parasagittal plane than the anterior.

During the power stroke, femur rotation was probably far less than that of the humerus, and it had the effect of slightly elevating the internal trochanter. The distal tibial facets of the femur are oriented mediolaterally during the whole stride. The slight rotation and the more parasagittal orientation of the femur at the end of retraction were compensated for by the ventrolateral slope of the proximal articular head of the tibia (figure 34a) in maintaining the anteroposterior orientation of the crus and foot.

The reconstructed hindlimb stride length of *Hyperodapedon* is 20–25 cm, the same as that of the forelimb.

8.6.2. *Muscles*

The distribution of pelvic and hindlimb muscles is modelled on *Sphenodon* (Perrin 1895; Byerly 1925) and lizards (Romer 1942; Snyder 1954). The lateral surface of the iliac blade (figure 32a) is divided into two areas: a large anterior depression (for m. iliofemoralis) and a smaller posterior zone (for m. iliofibularis), presumably with m. caudifemoralis brevis at the posterior-most tip. The origins of the puboischial muscles cannot be seen clearly. The insertions of the mass of muscles near the proximal end of the femur also cannot be demarcated, although it may be assumed that the internal trochanter (figure 33c) supported large puboischiofemoralis externus and caudifemoralis groups. The iliofemoralis probably inserted anterior to the internal trochanter, possibly behind the slight ridge seen in posterolateral view (figure 33c), as in *Sphenodon*, rather than on the anteromedial side, as suggested by Huene (1938, p. 104, pl. 10, fig. 1a) for *Stenaulorhynchus*. The puboischiofemoralis internus group probably inserted dorsally, anteriorly and ventrally, and the intertrochanteric fossa and roughened ventral areas of the femur (figure 33b) may have accommodated elements of the puboischiofemoralis externus group.

The probable main muscle directions are indicated in figure 38a, b. Powerful retraction was

achieved by the large puboischiofemoralis externus group and the caudifemoralis group (origins: posterior part of iliac blade; haemal spines of anterior caudal vertebrae, already shown to be large). Main long axis rotation and some retraction during the power stroke were effected by the large iliofemoralis, and possibly also the ischiotrochantericus. The puboischiofemoralis internus (?ventral, medial and dorsal portions) effected the recovery stroke.

Extension of the lower limb was probably effected by the long ambiens (origin, dorsolateral portion of pubis), the iliotibialis (origin, upper border of iliac blade) and the femorotibialis (origin, shaft of femur), all of which may have united to a common tendon and inserted on the cnemial crest of the tibia. The iliofibularis (origin, posterior iliac blade; insertion, lateral trochanter on proximal fibula) was a lower limb flexor.

8.6.3. *Scratch-digging with the hindlimb* (figure 39)

Huene (1939a) interpreted the rhynchosaur hindlimb as a powerful digging tool, and he reconstructed *Stenaulorhynchus* digging roots by backwards scratching movements. He noted the following adaptations in support of his interpretation: strong hindlimb bones, huge claws, great development of hindlimb retractor muscles, strong foot flexors and strong rolling tarsus.

Further evidence from the pelvis, femur, crus and pes of *Hyperodapedon* tends to confirm Huene's view. The long posterior projection of the ischium would have increased the scope and extent of the posteriorly pulling puboischiofemoralis externus muscle block, and the posteromedial slope of the ischium would allow a large posterior movement of the limb. The strong pelvis, laterally inflexible vertebral column in the sacral region and strong caudifemoralis origins on the tail would have assisted in digging.

The nearly parasagittal movement of the femur during a normal stride would allow controlled digging. The power stroke in digging was produced by the femoral flexors (puboischiofemoralis externus, iliofemoralis, caudifemoralis longus, brevis) already mentioned. However, the hindlimb adductor muscles (puboischiotibialis group, adductor femoris), which inserted more distally, were probably also important femoral retractors. These originate on the pubo-ischiadic ligament in lizards (Romer 1942) and *Sphenodon* (Byerly 1925), which is clearly not preserved in fossil material. However, the strong processus lateralis of the pubis of *Hyperodapedon* may indicate its presence.

The broad tibia provided attachment sites for the powerful crus flexor muscles (iliofibularis, pubotibialis, flexor tibialis internus and externus) and extensor muscles (ambiens, iliotibialis, femorotibialis) described above.

The plantar flexors of the foot were also clearly important in digging. A strong gastrocnemius presumably ran from the broad ventral surface of the femur (popliteal cavity or flexor fossa at the distal end (figure 33b)) to the plantar aponeurosis on the posterior side of the tarsus and metatarsus, as in *Sphenodon* (Byerly 1925). The peroneus (origin, proximal lateral fibula; insertion, lateral fibulare, digit V) and the flexor digitorum group (origin, distal femur, medial fibula, slips from crus muscles; insertion, metatarsals and phalanges in *Sphenodon* (Byerly 1925)) were also presumably well developed, as suggested by the broad tarsals, metatarsals and phalanges. These muscles pull the foot back and would hold it firm during posteriorly directed scratching movements.

The pes of *Hyperodapedon* is very long (figures 36, 38) and the claws are relatively enormous when compared with living and fossil reptiles of similar size (see, for example, Romer 1956, figs 188–196). The claws are not pointed and were probably not weapons. The bilaterally

flattened shape, on the other hand, does suggest a dorsoventral action. The large collateral ligament pits on both sides of metatarsals and phalanges point to the need for bracing of these elements against dislocation. The manus claws are similar, but smaller, and the forelimb was weak, which suggests that it was probably not used so much in digging.

Huene (1939a) compared *Stenaulorhynchus* with moles and mole-like burrowers, anteaters and the aardvark. In the former group, digging is achieved by rotation of the humerus and thrusting of the broad hand, and this is not a suitable model for comparison with rhynchosaurs. Rhynchosaurs clearly fit into the category of scratch-diggers (Hildebrand 1974, p. 519): animals that cut and loosen the soil with the claws and push it back with the sole of the foot by alternate flexion and extension of the limbs. Living examples include some turtles and tortoises that scrape holes to bury eggs with the hindlimbs, or dig with the forelimbs, some birds, some carnivores that dig out prey or bury bones, ground squirrels, marsupial moles, and golden moles that scratch-dig burrows, and armadillos, pangolins and aardvarks.

A comparison of the digging digits of rhynchosaurs and scratch-digging mammals (figure 39) shows that similar adaptations are present:

(i)   One main digging digit with shortened phalanges and metatarsals (or metacarpals) in some powerful diggers. Some forms have the other digits reduced (e.g. golden mole, marsupial mole), or there may be a sequence of claw sizes (e.g. pangolin, anteaters, rhynchosaurs). The functional correlates of these different morphologies have not been studied in detail (Hildebrand 1974, p. 520).

(ii)   Large curved (but not trenchant, or recurved) bilaterally compressed claws.

(iii)   Broad curved phalangeal articular surfaces with interlocking tongue and groove systems to strengthen the joint and stop over-flexion or over-extension. Strong collateral ligaments to prevent dislocation.

(iv)   A wide arc of flexion and extension of the digit, to allow deep digging and to protect the claw while walking, respectively.

(v)   Metatarsal (or metacarpal) of main digging digit may expand proximally with curved lateral prominences.

Digging with one hindfoot requires a stable tripodal stance. The great range of movements of the femur in the shallow acetabulum would allow *Hyperodapedon* to swing over to place the main pelvic weight over one vertically placed flexed leg. The large fan of muscles originating all round the pelvis and inserting all round the femur would provide all the postural muscles required in order to maintain balance.

8.7. *General aspects of locomotion*

The forelimb of *Hyperodapedon* is believed to have been held in a partially sprawling position, while the hindlimb was semi-erect during normal and rapid progression. The stride length of both limbs was 20–25 cm.

Coombs (1978) has assessed the gaits and cursorial adaptations of dinosaurs by comparison with mammals. He distinguished various modes of locomotion osteologically in terms of foot structure, and by plotting ratios of lengths of various limb elements. *Hyperodapedon* falls in the subcursorial category on the basis of both criteria, and it probably had running ability like that of the dinosaur *Protoceratops*.

It is unlikely that *Hyperodapedon* could rear up on its hind legs and tail, either for digging, or for feeding at heights above 30–40 cm. The pelvis is narrow and long, the tail is short and
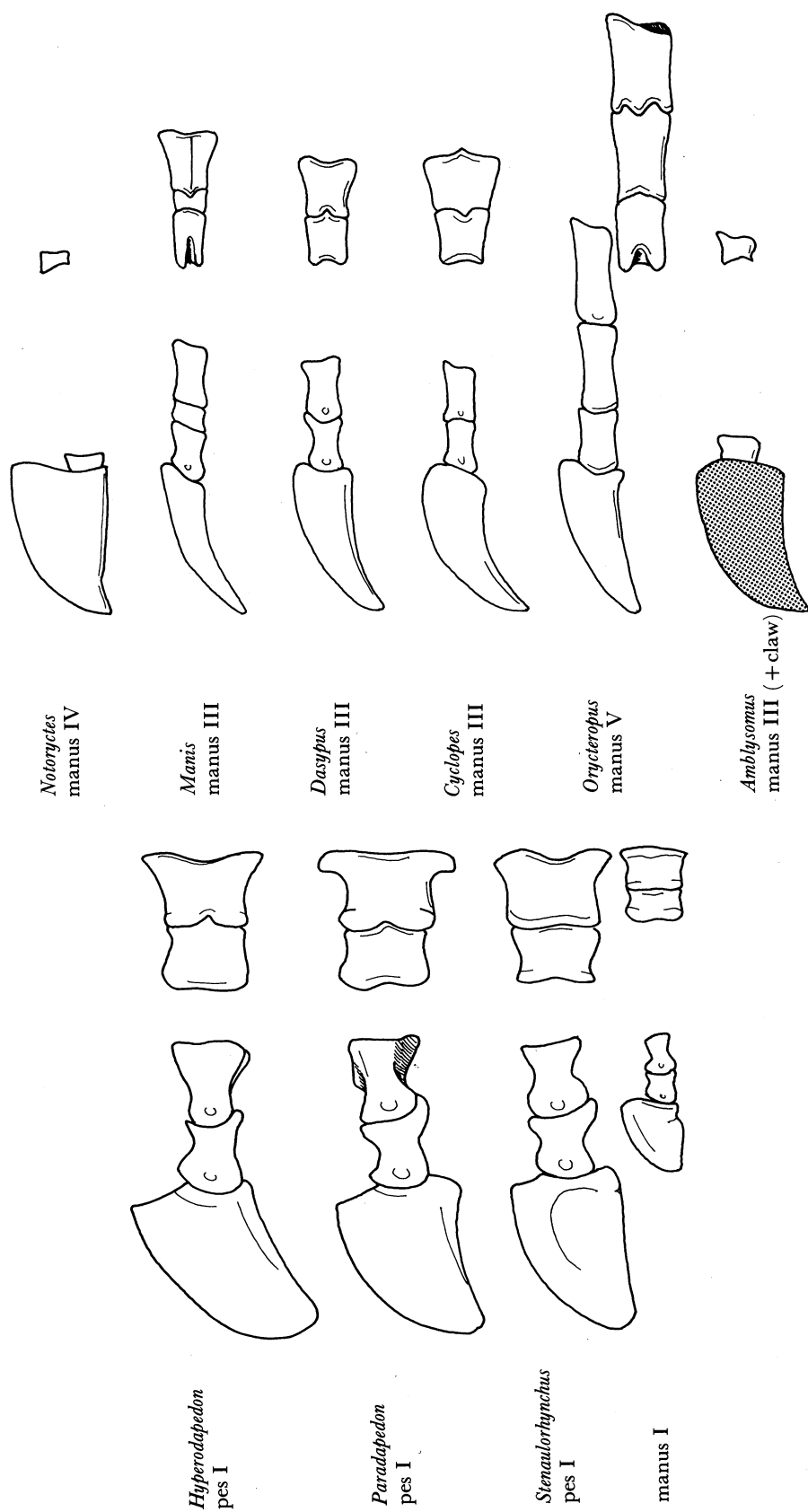
FIGURE 39. Digits of rhynchosaurs (left) and scratch-digging mammals (right). The rhynchosaur unguals and the mammal unguals are all drawn to standard lengths, and the associated phalanges of the digit are shown. Lateral and dorsal views. *Hyperodapedon* (original), *Paradapedon* after Chatterjee (1974, fig. 26d, e), *Stenaulorhynchus* after Huene (1938, pl. 18), *Notoryctes* (original), *Manis* (original), *Dasypus* after Giebel & Leche (1874, pl. 88), *Cyclopes* after Grassé (1955, fig. 1109, 1121), *Orycteropus* after Giebel & Leche (1874, pl. 84), *Amblysomus* after Hildebrand (1974, fig. 21–27).

the proximal caudal vertebrae are not particularly strong, the forequarters are heavy, and the forelimbs and manus do not appear to have been adapted to manipulative functions.

9. PALAEOBIOLOGY AND TAPHONOMY
9.1. *Restoration of the skeleton* (figure 40)

The skeleton of *Hyperodapedon* has been restored in dorsal and lateral views on the basis of all preserved remains. Relatively complete specimens (like EM 1886.3 and BMNH R699, R4782) were especially valuable. The overall length and relative proportions are based on an animal with a skull length of 180 mm, presacral length of 610 mm, sacrum length of 40 mm and tail length of 460 mm (total length 1.3 m, the commonest size group; see §2.3 above).

The head is tilted downwards slightly, as indicated by the shape of the atlas and axis, and this provides the best position for forward vision during locomotion (§4.5.7). The head would be tilted down further for use of the 'tusks' in feeding (§6.4, 5) and for examination of the ground.

The vertical curvature of the backbone (figure 40*b*) was estimated from partial series of vertebrae (e.g. BMNH R4791, R4795; figures 22*c*, 23*a*), but much of the cervical and distal caudal series had to be restored from *Scaphonyx* (Huene 1942) and *Paradapedon* (Chatterjee 1974). The horizontal curve in the backbone adds realism to the dorsal view (figure 40*a*). This feature occurs in living reptiles as an adaptation to increase stride length (Schaeffer 1941), and it has been used in restorations of other early reptiles (see, for example, Heaton & Reisz 1980). The long broad anterior dorsal ribs are shown overlapping slightly, as preserved in EM 1886.3 (figure 28; §7.5).

The shoulder girdle is set sloping back at an angle of 10°, and the forelimb is reconstructed in a sprawling pose (§8.5.1). The width of the shoulder region is uncertain, but it is based on the spacing of the interclavicle and coracoids seen in BMNH R4782 (figure 29*c*). The manus is restored from other rhynchosaurs.

The pelvic girdle is firmly united to the sacral vertebrae which fixes its position. The hindlimb is reconstructed in a semi-erect pose with the foot directed forwards (§8.6.1).

9.2. *Function and mode of life*

Several conclusions regarding function in *Hyperodapedon* have already been given. These are summarized under three headings: senses, feeding, and locomotion; and cross-references to the earlier text are given.

(*a*) *Senses*

(i) Large nasal capsule; good sense of smell (§4.5.5).

(ii) Large eye with good power of accommodation; diurnal habits (§4.5.7).

(iii) Hearing: ground-borne sounds detected via throat and hyoid apparatus, air-borne sounds via skin behind quadrate, but no tympanum (§4.6.7).

(*b*) *Feeding*

(i) Powerful tongue (§4.7).

(ii) Precision shear bite with uniform powerful force from front to rear of concentrated bite area (§§6.1.3, 6.2, 6.3, 6.4).

(iii) No normal reptilian tooth replacement, but teeth continue to grow throughout functional life (§6.1.4).

(iv) Long beak-like premaxillae, possibly for digging (§6.4.5).

(v) Hindlimb and claws of pes probably well adapted for scratch-digging (§8.6.3).

(vi) Diet consisted of tough, but not hard, plant material (possibly elements of the *Dicroidium* flora: seed ferns, equisetaleans, ginkgos, cycads and conifers) (§6.6).

(c) *Locomotion*

(i) Moderate lateral flexion of backbone possible in middle dorsal region, but very little movement between vertebrae in girdle regions. Long broad anterior dorsal ribs may have further strengthened the pectoral girdle (§7.5).

(ii) Forelimb probably held in semi-sprawling pose, with humerus rotation important in locomotion (§8.5).

(iii) Hindlimb adapted for semi-erect gait, with little femur rotation. The limb moved back and forwards close to the side of the body (§8.6).

(iv) Stride length of both forelimb and hindlimb, 20–25 cm (§§8.5, 8.6).

Thus, *Hyperodapedon* appears to have been a medium-sized active herbivore. It fed on tough vegetation, and could have dug up plant material using its 'beak' or powerful hindlimb and pes.

### 9.3. *Environment and taphonomy of the late Triassic Elgin reptiles* (figure 41)

The early Norian Lossiemouth Sandstone Formation (Warrington *et al.* 1980) (= sandstones of Lossiemouth, Spynie and Findrassie; Westoll 1951; Peacock *et al.* 1968) is distributed in several small fault-bounded blocks at Lossiemouth, Spynie and Findrassie, near Elgin. The thickness of the unit varies from 7 to 30 m. It is underlain unconformably in places by the Burghead Sandstone Formation (water-laid sandstones with pebbly and silty bands) and overlain by the (?) early Jurasic Cherty Rock (sandy limestone and chert).

The Lossiemouth Sandstones are white, buff, yellow or pinkish. Grain size is usually uniform (0.2–0.5 mm) with grains well rounded. The rock is composed of quartz, feldspar, and rare brownish chert and quartzite. Cements are usually overgrowths of secondary quartz and feldspar, but calcite and fluorspar may also occur (Peacock *et al.* 1968, pp. 69–70).

The sandstones may be finely laminated, but more usually they show large-scale cross-beds. These features, as well as the absence of pebbles, the rarity of micas and heavy minerals, strongly suggest aeolian deposition. Foreset analysis of the cross-beds indicates a prevailing southwesterly wind forming barchan dunes.

The skeletons of *Hyperodapedon*, and the other Elgin Triassic reptiles, were apparently found in the aeolian sands just above the floor of the quarry at Lossiemouth (Gordon 1892), and probably also at Spynie. This corresponds to a location near the base of the Lossiemouth Sandstone Formation, but it is not known what relationship the skeletons bore to the ancient dunes.

Peacock *et al.*(1968, p. 72) noted that the aeolian sandstone was underlain by 'a few feet of water-laid sandstone' at Lossiemouth, but they were not certain that these were equivalent to the Burghead Sandstone Formation. However, Williams (1973, pp. 11, 14) interpreted these water-laid sandstones as floodplain deposits equivalent in age to the point-bar deposits at the top of the Burghead Sandstone Formation at Burghead. Williams (1973, pp. 132–135) suggested that the dunes of the Lossiemouth Sandstone Formation consisted of reworked sand
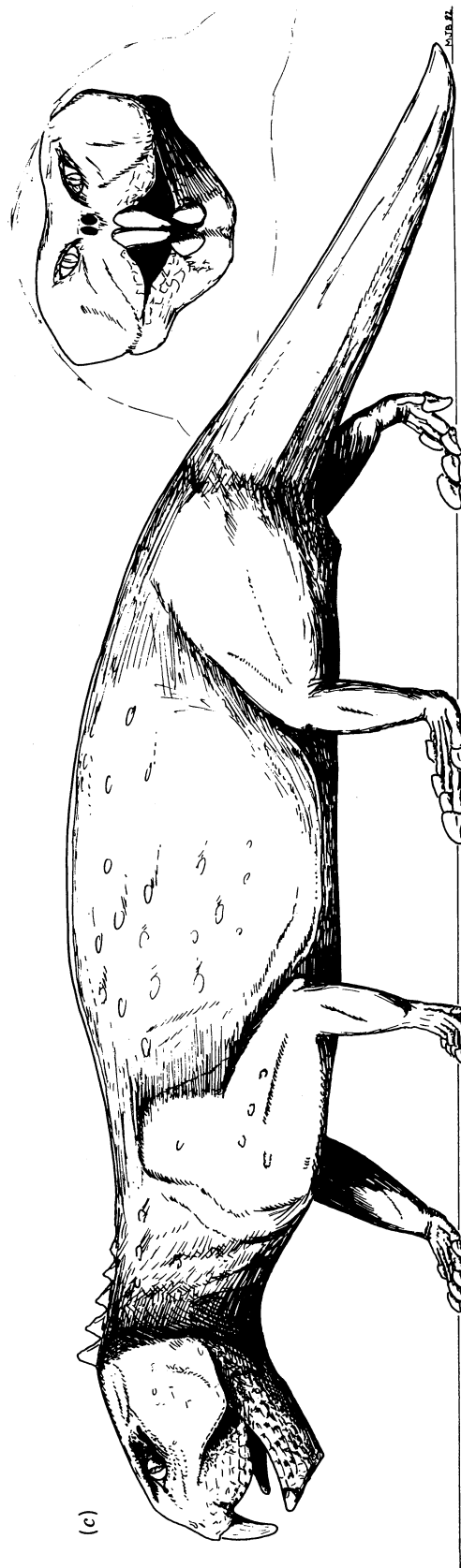
30 cm

(a)

(b)
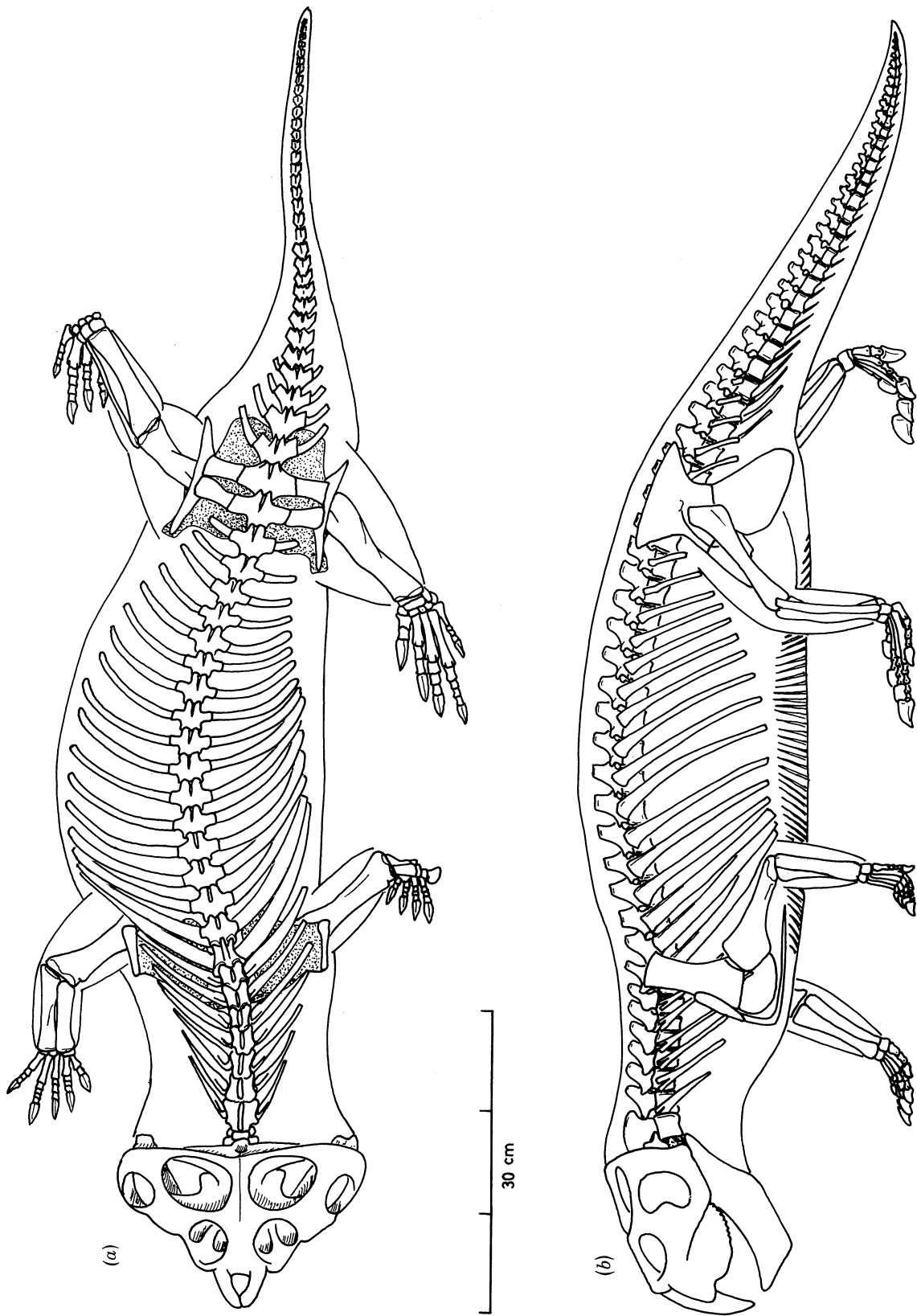
FIGURE 40. *Hyperodapedon gordoni* Huxley. Restoration of the skeleton of an individual with skull length of 180 mm, the most common size, in (*a*) dorsal and (*b*) left lateral view. (*c*) Restoration of the living animal, with sketch of anterior view of the head.

from the point bars of the Burghead Sandstone Formation. Dunes up to 20 m high migrated across the floodplain during arid periods, and the aeolian deposition was terminated by large-scale flooding and the deposition of silicified and calcareous sandstone ('Sago Pudding Sandstone' (Upper part of the Lossiemouth Sandstone Formation) (Peacock *et al.* 1968, p. 71; Williams 1973, pp. 136–143)).

The late Triassic Elgin reptiles are known only from the aeolian sands. As Walker (1961) suggested, the smaller reptiles, such as *Scleromochlus*, may have lived among the dunes, but the medium-sized herbivores like *Stagonolepis* (and *Hyperodapedon*) must have sought plants in the adjacent flood plains or around interdune pools. The bases of the late Triassic food chains at Elgin cannot be established since no plants, invertebrates or fish have been discovered. Thus, it is not possible to decide whether the flora on which *Hyperodapedon* subsisted was northern or southern in aspect. Large *Ornithosuchus* could have preyed on both *Hyperodapedon* and *Stagonolepis*.

The remains of *Hyperodapedon* are generally well preserved in an articulated state. Outline sketches of the more complete skeletons (figure 41) show that most were fossilized flattened in a horizontal plane. Only the type specimen (figure 41 *a*) lies partially on its side. The vertebral column is usually unbroken and the ribs and gastralia retain their associations. The limbs are often in a natural resting pose, with the forelimbs flexed and pointing forwards, the hindlimbs pointing forwards or backwards. The shoulder girdle and pelvis may retain their original positions, but they usually collapse. The skull is often present undamaged and in close articulation with the vertebral column. There is no evidence of disarticulation by water currents, wind or moving sand. The animals generally appear to have died naturally and to have been covered by sand fairly rapidly.

In detail, most bones are excellently preserved, and they show little sign of crushing or compression. The skull and scapulae of BMNH R4782, however, have collapsed slightly, and the shoulder girdle of RSM 1967.10.1 A is also rather compressed. This is probably the result of compaction beneath superincumbent sediment, unusual in a sandstone. In these specimens, and in others (e.g. skull, RSM 1967.10.2; hindlimb, GSM 90932/5), the bone surface is marked by fine cracks or larger fractures, probably not suncracks.

Signs of predation or scavenging are rare. Only two specimens (NUGD A, B) show broken bones that may have been caused by a large carnivore (*Ornithosuchus*). In NUGD A, an isolated skull, the parietal is broken just behind the attachment of the epipterygoids, and small displaced bone chips are preserved, and the top of the braincase is slightly crushed. This damage occurred before fossilization, and probably at, or after, death since the breaks are clean, but there are no tooth or claw marks on the bone. The damage was probably not caused by physical processes since sclerotic plates are preserved, only slightly displaced, in the orbit. NUGD B, found together with NUGD A, is another isolated almost complete skull. However, the braincase has been completely removed, and it is represented by only two fractured, displaced bone slivers. The atlas, axis and two anterior cervical vertebrae are preserved in articulation, but pushed in between the quadrates. Ossified hyoid elements are preserved in place, and so the disarticulation is unlikely to have been caused by sedimentary processes. Other isolated elements (e.g. maxillae: EM 1926.6; BMNH R3151, R4781; MM L8272) may have been broken up by water or wind, scavenging, or collecting. Walker (1964, pp. 129–131) described similar features in a specimen of *Ornithosuchus*. An articulated skeleton of a large individual had been crushed and broken in certain areas, and this was also almost certainly caused by a predator or scavenger.
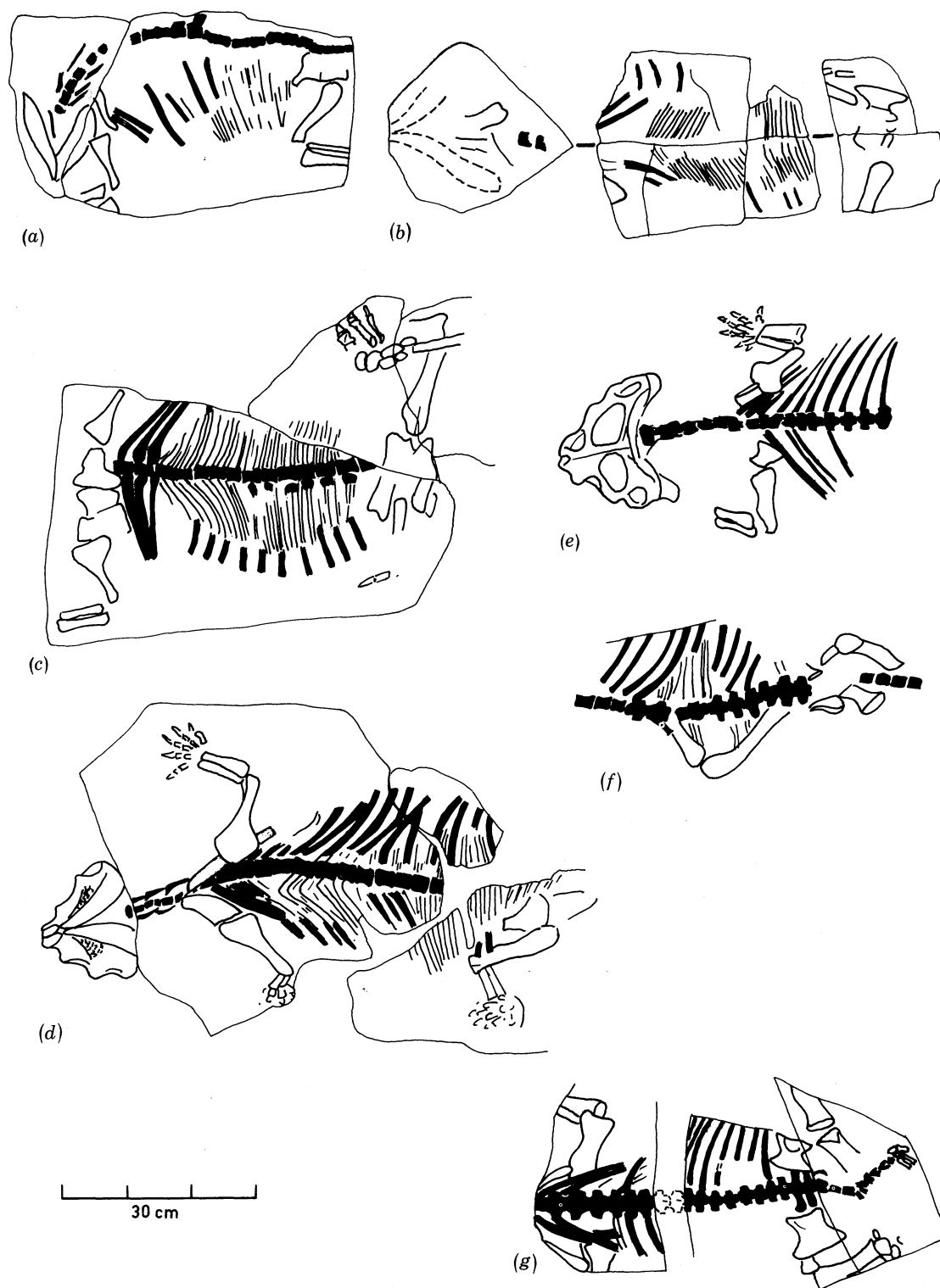
FIGURE 41. Skeletons of *Hyperodapedon* as preserved. Vertebrae and ribs are shaded black, and all other elements are shown in outline. (*a*) EM 1978.566.1–2, (*b*) EM 1978.567.1–3, (*c*) EM 1886.3 (dorsal slab), (*d*) BMNH R699 (dorsal slab), (*e*) BMNH R4782 (from casts), (*f*) BMNH R4791/4805 (from casts), (*g*) RSM 1967.10.1 (from casts).

The sedimentological and taphonomic data suggest that *Hyperodapedon* normally lived on a well vegetated lowland. During arid periods, large sand dunes migrated across the plain, and the animals seem to have died from natural causes and become entombed at the base of the aeolian unit, or they may have been overwhelmed by sand storms. The cadavers decayed, with occasional scavenging by *Ornithosuchus* (?), but all bones normally remained in articulation and the body was probably rapidly buried. The weight of sand compressed and cracked some bones. Diagenetic effects are usually minimal: the bone material often shows its original composition and structure, and it may be very soft. Occasionally, the ends of long bones, as well as cavities in teeth, may be filled with iron oxide (goethite) or crystals of fluorite.

10. RELATIONSHIPS OF THE RHYNCHOSAURS

10.1. *Classification of the rhynchosaurs*

Various schemes for the classification of the rhynchosaurs have been presented. Chatterjee (1969, 1974) and Sill (1971 *b*) divided them into three subfamilies for early, middle and late Triassic forms respectively (table 4). Chatterjee (1980 *a*) presented a different scheme, based on a suggestion of Walker (1969), which divides middle and late Triassic forms into an African–European subfamily and an American–Indian subfamily (table 5). In comparing these classifications, we must consider two questions. First, are *Noteosuchus, Mesosuchus* and *Howesia* rhynchosaurs and, if so, what do they indicate of the ancestry of the group? Secondly, what are the relationships among the middle and late Triassic rhynchosaurs?

10.2. *Relationships of Mesosuchus, Howesia and Noteosuchus*

The relationships of *Mesosuchus, Howesia* and *Noteosuchus* to each other are uncertain because of incomplete descriptions or inadequate material. They share several derived characters, but *Mesosuchus* and *Howesia* differ significantly in their dentitions and other features. *Howesia* is probably a rhynchosaur and *Mesosuchus* may be the sister group of the true rhynchosaurs.

Mesosuchus, Howesia and later rhynchosaurs share the following derived characters (information from Broom (1906, 1913, 1925), Haughton (1921, 1924), Malan (1963) and Carroll (1976 *a*)) when compared with the late Carboniferous 'eosuchian' *Petrolacosaurus*, a form considered to be near the base of later diapsid lineages (Reisz 1981):

(i)   Downturned premaxilla bearing a small number of acrodont teeth (*Mesosuchus*) or none at all – snout unknown in *Howesia*.

(ii)   Single median naris (*Mesosuchus*, later rhynchosaurs) – unknown in *Howesia*.

(iii)   Fused parietals.

(iv)   Three proximal tarsals with the centrale closely associated with the astragalus.

Other characters shared by *Mesosuchus* and *Howesia* are also present in early prolacertiforms and thecodontians, such as:

(i)   Short snout and relatively high skull.

(ii)   Absence of teeth on pterygoid, palatine and vomer.

(iii)   Dorsal vertebrae have high neural spines and less laterally placed zygapophyses than in *Petrolacosaurus*.

(iv)   Scapula is waisted and has a clear dorsal blade.

(v)   Humerus ends very much expanded.

(vi)   Acetabulum extends to pubis and ischium, as well as ilium. Pubis and ischium not massive.

TABLE 4. CLASSIFICATION OF THE GENERA OF RHYNCHOSAURS

(Based on Chatterjee (1969, 1974) and Sill (1971 b). The genera *Noteosuchus, Mesodapedon, Supradapedon* and the North American forms have been added more recently. A reorganization of the subfamily Hyperodapedontinae is described in §10.4.4.)

subfamily Mesosuchinae (early Triassic)
    Mesosuchus browni Watson, 1912
        Cynognathus Zone, South Africa (early Triassic: late Scythian)
    Howesia browni Broom, 1905
        Cynognathus Zone, South Africa (early Triassic: late Scythian)
    Noteosuchus colleti (Watson, 1912)
        Lystrosaurus Zone, South Africa (early Triassic: late Scythian)

subfamily Rhynchosaurinae (middle Triassic)
    Rhynchosaurus articeps Owen, 1842 (and other undescribed species)
        Helsby Sandstone Formation, Tarporley Siltstone Formation, and Bromsgrove Sandstone Formation,
        Midlands of England; Otter Sandstone Formation, Devon (middle Triassic: Anisian/Ladinian)
    Stenaulorhynchus stockleyi Haughton, 1932
        Manda Formation, Tanzania (middle Triassic: ?middle Anisian)
    Mesodapedon kuttyi Chatterjee, 1980
        Yerrapalli Formation, India (middle Triassic: ?early Anisian)

subfamily Hyperodapedontinae (late Triassic)
    Hyperodapedon gordoni Huxley, 1859
        Lossiemouth Sandstone Formation, Elgin (late Triassic: early Norian)
    Paradapedon huxleyi (Lydekker, 1881)
        Maleri Formation, India (late Triassic: early Norian)
    Scaphonyx fischeri Woodward, 1907
        Santa Maria Formation, Brazil (late Triassic: Carnian/Norian)
    Scaphonyx sanjuanensis Sill, 1970
        Ischigualasto Formation, Argentina (late Triassic: Carnian/Norian)
    Supradapedon stockleyi (Boonstra, 1953)
        Tanzania (?late Triassic)
    Undescribed genera
        Wolfville Sandstone, Nova Scotia (late Triassic: ?Norian); Dockum Group, Texas (late Triassic: early
        Norian)

TABLE 5. CLASSIFICATION OF THE GENERA OF RHYNCHOSAURS

(Based on Chatterjee (1980).)

subfamily Mesosuchinae (no longitudinal groove in maxilla)
    Mesosuchus, Howesia, Noteosuchus

subfamily Rhynchosaurinae (longitudinal groove in maxilla; medial dentigerous space is wider than lateral)
    Rhynchosaurus, Stenaulorhynchus, Hyperodapedon, Supradapedon

subfamily Paradapedontinae (longitudinal groove in maxilla; lateral dentigerous space is wider than medial)
    Paradapedon, Mesodapedon, Scaphonyx, undescribed North American genera

    (vii) Femur may have a greater twist than in *Petrolacosaurus*.

    (viii) Ankle shows loss of fifth distal tarsal.

    (ix) Fifth metatarsal is hooked.

Mesosuchus differs from *Howesia* and later rhynchosaurs in the following features, and these may be regarded as characters typical of the family Mesosuchidae:

    (i) *Mesosuchus* has an alternating dentition quite different from the multiple rows of 'typical' rhynchosaurs. The dentition of *Howesia* consists of multiple rows of ankylothecodont teeth, and could be regarded as a morphological predecessor to that of *Stenaulorhynchus* and later forms.

(ii) The lower temporal arcade appears to be open in *Mesosuchus*, although this is not absolutely certain. Haughton (1924, p. 24) noted that the jugal terminated in a free point in both genera and that the quadratojugal was greatly reduced. Broom (1925) strongly disagreed, and restored *Mesosuchus* with a complete lower temporal bar, and this is followed by Huene (1956) and Romer (1966).

(iii) The quadrate seems to be large, and possibly streptostylic in *Mesosuchus* (Haughton 1924; Broom 1925).

(iv) The quadratojugal is reduced.

(v) There may be a mandibular fenestra (Broom 1913, 1925).

Howesia shares several derived characters with middle and late Triassic rhynchosaurs that are absent in *Mesosuchus*:

(i) The parietal foramen is absent.

(ii) The teeth have ankylothecodont implantation.

(iii) There are batteries of functional teeth on the maxilla and dentary.

Further differences between *Mesosuchus* and *Howesia* may be seen in the more expanded humerus, the less twisted femur and the apparently more primitive pectoral girdle in the former (L-shaped lateral glenoid, heavy clavicle, posterior coracoid projection, diamond-shaped head on interclavicle), but this may be because of the sphenodontid-like reconstruction for *Howesia* given by Broom (1906). *Howesia* and later rhynchosaurs are classed as Rhynchosauroidea and the Mesosuchidae is the sister group.

Noteosuchus shares many characters with *Mesosuchus* and *Howesia* (Carroll 1976 a), but these are shared also with prolacertiforms and early thecodontians. It shows no typical rhynchosaur characters (the skull, pectoral girdle and much of the forelimb are, however, unknown) and it cannot be classed as a rhynchosaur at present.

By comparison with *Howesia*, later rhynchosaurs, the Rhynchosauridae, share the following derived characters:

(i) Loss of the supratemporal. This element has been identified in *Mesosuchus* (Haughton 1924, p. 19; Broom 1925, pp. 6–7 as 'tabular') and *Howesia* (Haughton 1924, p. 24).

(ii) Development of an interlocking groove and blade jaw apparatus.

(iii) The centrale increases in size and becomes firmly united with the astragalus.

10.3. *Diapsid classification and the origin of the rhynchosaurs*

Romer (1956, 1966) considered that diapsid reptiles divided into two major groups, each with a separate origin: the subclass Archosauria (thecodontians, dinosaurs, crocodiles and pterosaurs) and the subclass Lepidosauria (eosuchians, lizards, snakes and 'rhynchocephalians'). However, much recent work (Hughes 1968; Cruickshank 1972; Carroll 1975, 1976a–c, 1977; Wild 1978; Evans 1980; Brinkman 1981) has shown that the reptilian subclass Diapsida is probably a paraphyletic group (or monophyletic with the addition of birds), with an ancestor close to *Petrolacosaurus* from the late Carboniferous of Kansas (Reisz 1981).

Diapsids radiated widely during the Permian (Carroll 1975). These early forms, and many of those that radiated further in the Triassic, have been placed in the 'Eosuchia'. However, the 'Eosuchia' are defined on primitive characters, and the limits of the group are hard to place. Evans (1980) listed 15 families as eosuchians, but did not attempt to organize them into orders and suborders.

Recent cladistic analyses of the Permo-Triassic Diapsida (Benton 1983*c;* Evans 1983; Gauthier 1983) have produced new classifications and phylogenetic trees. During the Permian, two main lineages diverged: the Archosauromorpha (Prolacertiformes, Archosauria, Rhynchosauria) and the Lepidosauromorpha (Younginiformes, Lepidosauria). Each of these groups is defined on the basis of several shared derived characters.

The Archosauromorpha share a number of derived characters of the skull (premaxilla extends up behind naris, nares close to midline and elongate, parietal set well forward, quadratojugal mainly behind the lower temporal fenestra, loss of tabulars, stapes rod-like and without a foramen), vertebrae (non-notochordal, dorsal vertebrae have long transverse processes), forelimb (scapula tall and waisted, no entepicondylar foramen in humerus, loss of perforating foramen in the carpus) and ankle (lateral tuber on the calcaneum, complex concave–convex articulation between the astragalus and calcaneum, fifth distal tarsal lost, fifth metatarsal hooked) (Brinkman 1981; Benton 1983*c*).

The Prolacertiformes (Protorosauridae, Prolacertidae, Tanystropheidae) are characterized by very long necks (7–12 elongate cervical vertebrae) and possibly a broken lower temporal bar without streptostyly (Chatterjee 1980*b*; Wild 1980).

The earliest archosaur, *Archosaurus*, appeared in the late Permian of Russia, but the Archosauria are hard to define. Their only shared derived character is the presence of an antorbital fenestra, and even that is not a constant unique feature (Romer 1956; Wild 1978). The Pterosauria appear to have been so specialized that they may have had a separate origin from the Eosuchia and developed an antorbital fenestra as a convergent feature with archosaurs (Wild 1978).

The ancestry of rhynchosaurs has been hard to assess. They were supposed to be derived from generalized 'eosuchian' ancestors (Romer 1956), such as *Youngina* (Gow 1975; Carroll 1977; Currie 1981) or *Galesphyrus* (Carroll 1976*c*) from the late Permian of South Africa. However, *Youngina* is ruled out because of its specialized vertebrae and dermal armour, and *Galesphyrus* is rather poorly known. Rhynchosaurs have no special relationship with the sphenodontids (Osborn 1903; Carroll 1977). The supposed shared characters are either primitive (e.g. complete lower temporal bar, quadratojugal, akinetic skull, inner ear structure, 25 presacral vertebrae, vertebral shape, certain characters of limbs and girdles) or incorrect (e.g. rhynchosaurs do *not* have acrodont teeth, the 'beak-like' premaxilla of both groups is quite different in appearance, the 'tooth plate' is wholly on the maxilla in rhynchosaurs but on maxilla and palatine in sphenodontids).

The Lepidosauromorpha share several characters of the vertebrae (specialized accessory intervertebral articulations, cervical centra short) and sternum (paired sternal plates co-ossify in the adult, specialized sternal rib attachments) (Benton 1983*c*). The Younginiformes (*Youngina*, Tangasauridae) shared several derived characters, and *Youngina* can no longer be regarded as a generalized 'ancestral eosuchian' (Gow 1975; Currie 1981).

The Lepidosauria (Sphenodontidae, Squamata) share derived characters of bone growth, epiphyses, fused astragalo-calcaneum, and others (Carroll 1977). The Squamata have been defined by Evans (1980, p. 256) in such a way that the previous emphasis on an incomplete lower temporal arch and on a streptostylic quadrate is removed. These two characters need not be connected, and they occur in several non-squamate groups. The Paliguanidae, Kuehneosauridae and Gephyrosauridae are probably squamates (Evans 1983; Benton 1983*c*). Certain authors (e.g.: Robinson 1967; Halstead Tarlo 1968) also included such families as the

Askeptosauridae, Thalattosauridae, Prolacertidae and Tanystropheidae in the Squamata, but these are probably not closely related.

The classification of the diapsids is clearly in a state of flux at present (Evans 1980; Benton 1982), but an outline scheme may be presented on the basis of the recent studies already cited and the cladistic analysis (table 6).

10.4. *Interrelationships within the Rhynchosauridae*

The two classifications of middle and late Triassic rhynchosaurs (§ 10.1) will be compared. The major features of the skull and skeleton of *Stenaulorhynchus*, *Rhynchosaurus*, *Scaphonyx*, *Paradapedon* and *Hyperodapedon* are compared character by character. These are summarized in table 8 and a simple cluster analysis pairs the forms with most shared characters. Only a few comments on the dentition of *Mesodapedon* and *Supradapedon* are given since they are based on tooth-bearing elements, and the two undescribed North American forms are not considered. Much of the information is derived from the literature, but I have examined original material of all major genera.

10.4.1. *Comparison of the characters of rhynchosaurs*

The skull roof (figures 42, 43). In dorsal view (figure 42), the skulls of *Stenaulorhynchus* and *Rhynchosaurus* are longer than they are broad (ratio of length:breadth, 1.30–1.60), while the late Triassic forms have a temporal region that is broader than the mid-dorsal skull length (ratio, 0.67–0.83). *Paradapedon* has relatively the broadest skull. This change in skull proportions also changes the relative dimensions of the upper temporal fossa.

The pair of frontals in *Stenaulorhynchus* and *Rhynchosaurus* are broader than they are long, whereas they are relatively much longer in the late Triassic forms. This is correlated with a relatively very long parietal in the earlier genera. There is no difference in the posterior skull roof elements that are present. 'Epiotics' and 'tabulars' have been described in *Rhynchosaurus* (Watson 1910; Huene 1929), but these are the posterolateral wings of the parietal.

Huene (1938) suggested that the postfrontal of *Stenaulorhynchus* does not meet the parietal. However, a new reconstruction (A. D. Walker, personal communication) suggests that the postfrontal does meet the parietal as in other rhynchosaurs.

In lateral view (figure 43), the skulls of the three late Triassic genera are relatively higher than the middle Triassic forms. The prefrontal meets the maxilla in all genera, although Huene (1929, 1938) did not show this in *Rhynchosaurus* (see dashed lines on figure 43 b; A. D. Walker, personal communication). The jugal of *Stenaulorhynchus* and *Rhynchosaurus* is a slim three-pronged element without a marked ridge. The jugal of *Scaphonyx*, *Paradapedon* and *Hyperodapedon* is much broader and it has a marked diagonal ridge. Occasionally, the jugal extends back a little way above the lower temporal fossa in *Scaphonyx* (MCZ 1529), and this is not seen in the other forms.

Huene (1938, pl. 9, fig. 1) reconstructed the quadratojugal of *Stenaulorhynchus* as resting on top of the jugal, but this area of the skull was not preserved in his material. The two bones probably overlapped laterally below the lower temporal fossa as in the other genera. The squamosal in *Stenaulorhynchus* appears to have a marked double prong in Huene's figure (1938, pl. 1, fig. 1), but one of the prongs is probably part of the parietal (A. D. Walker, personal communication).

The palate (figure 44). The major differences visible in palatal view concern overall skull

TABLE 6. CLASSIFICATION OF THE DIAPSIDA IN OUTLINE

(Based on a cladistic analysis (Benton 1983 c) and references cited in the text. Standard techniques (indented list, sequencing, plesion concept) are used.)

subclass Diapsida Osborn, 1903
  plesion †Petrolacosauridae Peabody, 1952
  Diapsida *incertae sedis*:
            †family Weigeltisauridae Romer, 1933
            †family Claudiosauridae Carroll, 1981
            †family Galesphyridae Currie, 1980
  infraclass Archosauromorpha Huene, 1946
     plesion †Rhynchosauria Osborn, 1903 (Gervais, 1859)
        suborder Mesosuchidia Haughton, 1924
           family Mesosuchidae Haughton, 1924
        suborder Rhynchosauroidea Nopcsa, 1928
           family Howesiidae Watson, 1917
           family Rhynchosauridae Huxley, 1887
     plesion †Prolacertiformes Camp, 1945
           family Protorosauridae Baur, 1889 (Cope, 1871)
           family Prolacertidae Parrington, 1935
           family Tanystropheidae Romer, 1945 (Gervais, 1859)
     incertae sedis (Prolacertiformes or Thecodontia)
            †family Proterosuchidae Huene, 1908
        superorder Archosauria Cope, 1869
     plesion †Thecodontia Owen, 1859
        suborder Proterosuchia Broom, 1906/Pelycosimia Huene, 1911 (?)
           family Erythrosuchidae Watson, 1917
        ?suborder Ornithosuchia Bonaparte, 1971
           family Euparkeriidae Huene, 1920
           family Ornithosuchidae Huene, 1908
        suborder Pseudosuchia Zittel, 1890
        suborder Parasuchia Huxley, 1875
        ?suborder Lagosuchia Chatterjee, 1982
     plesion †Saurischia Seeley, 1888
     plesion †Ornithosuchia Seeley, 1888
     order Crocodylia Gmelin, 1788
     (class Aves Linnaeus, 1758)
     Archosauromorpha *incertae sedis*
            †family Trilophosauridae Gregory, 1945
  incertae sedis (Archosauromorpha or Lepidosauromorpha)
            †family Heleosauridae Haughton, 1924
            †family Monjurosuchidae Endo, 1940
         †order/infraclass Pterosauria Owen, 1840 (Kaup, 1834)
  infraclass Lepidosauromorpha nov. (Gauthier, 1983 ms.)
     plesion †Younginiformes Romer, 1933
        plesion †*Acerosodontosaurus*
        superfamily Younginoidea Currie, 1982
           family Younginidae Broom, 1914
           family Tangasauridae Camp, 1945 (Piveteau, 1926)
        superorder Lepidosauria Haeckel, 1866 (Duméril and Bibron, 1839)
        order Rhynchocephalia Günther, 1867
           family Sphenodontidae Cope, 1870
           † ?family Sapheosauridae Baur, 1895
        order Squamata Oppel, 1811
           plesion †Paliguanidae Broom, 1926
           plesion †Kuehneosauridae Romer, 1966
           suborder Sauria Macartney, 1802
           suborder Amphisbaenia Gray, 1844
           suborder Serpentes Linnaeus, 1758
        Lepidosauria/Squamata *incertae sedis*
            †family Gephyrosauridae Evans, 1980
  Diapsida *incertae sedis*
            †family Claraziidae Peyer, 1936
            †family Thalattosauridae Merriam, 1904
            †family Champsosauridae Cope, 1876 (1884?)
            †family Pleurosauridae Lydekker, 1888

FIGURE 42. Dorsal views of the skulls of (a) *Stenaulorhynchus*, (b) *Rhynchosaurus*, (c) *Scaphonyx*, (d) *Paradapedon* and (e) *Hyperodapedon* drawn to unit length ((a) after Huene (1938) and A. D. Walker (personal communication); (b) after Woodward (1907) and Huene (1929); (c) after Romer (1956); (d) after Chatterjee (1974); (e) original).

FIGURE 43. Right lateral views of the skulls of (a) *Stenaulorhynchus*, (b) *Rhynchosaurus*, (c) *Scaphonyx*, (d) *Paradapedon* and (e) *Hyperodapedon*, drawn to unit length ((a) after Huene (1938); (b) after Huene (1938); (c) after Romer (1956); (d) after Chatterjee (1974); (e) original).

proportions and dentition. The relatively long skulls of *Stenaulorhynchus* and *Rhynchosaurus* show a braincase positioned well forward of the quadrates, while the occipital condyle and quadrate condyles are nearly in line in the other three genera. The pterygoids of the earlier forms are also directed much more posteriorly than laterally. The dentition will be dealt with below (§10.4.2).
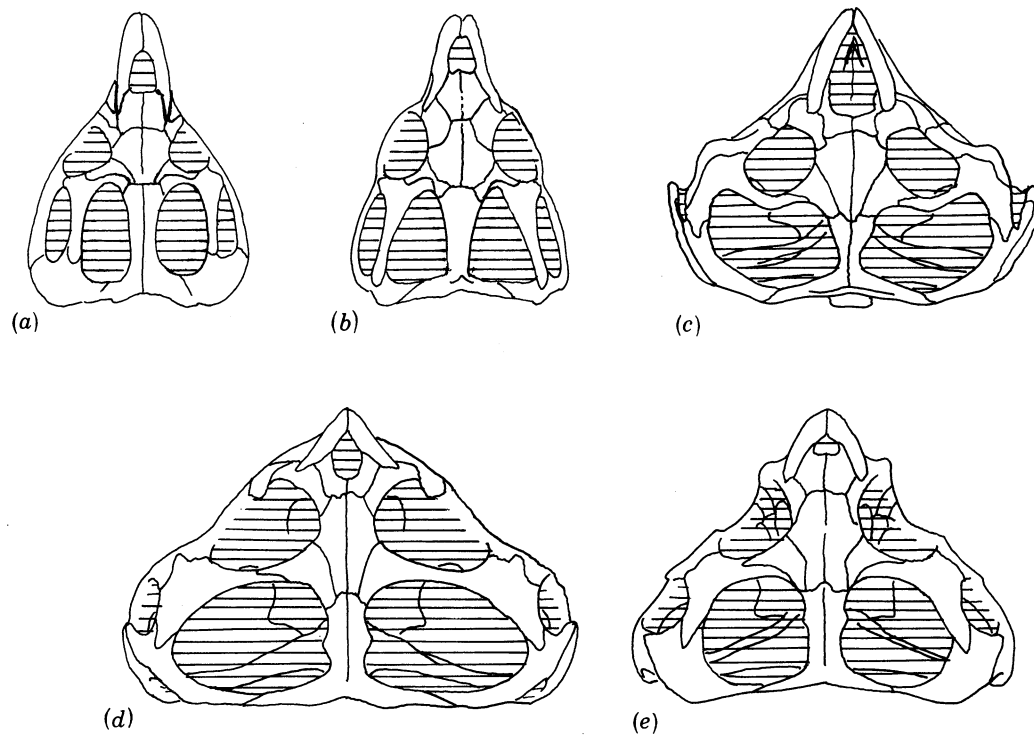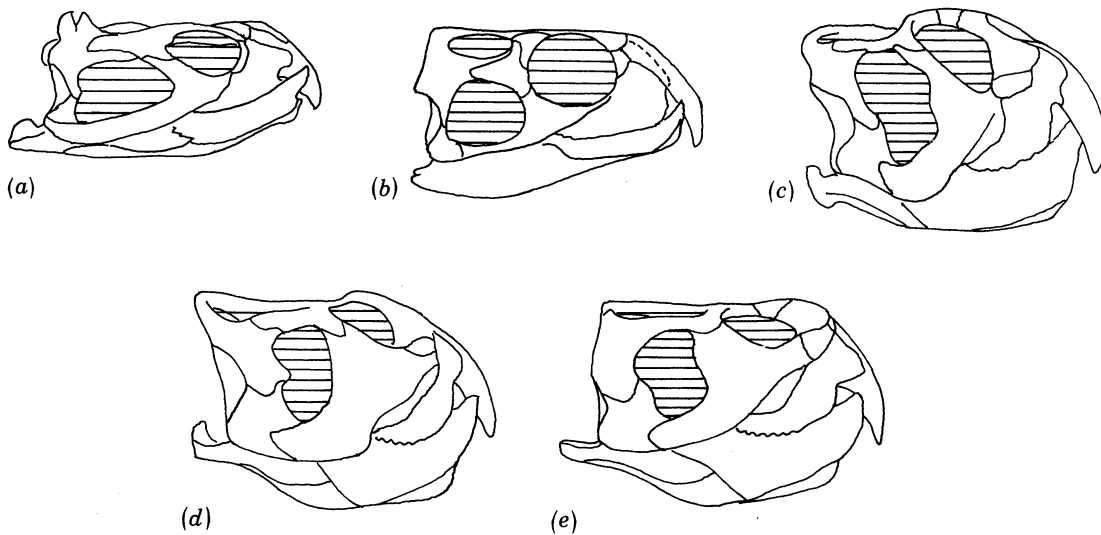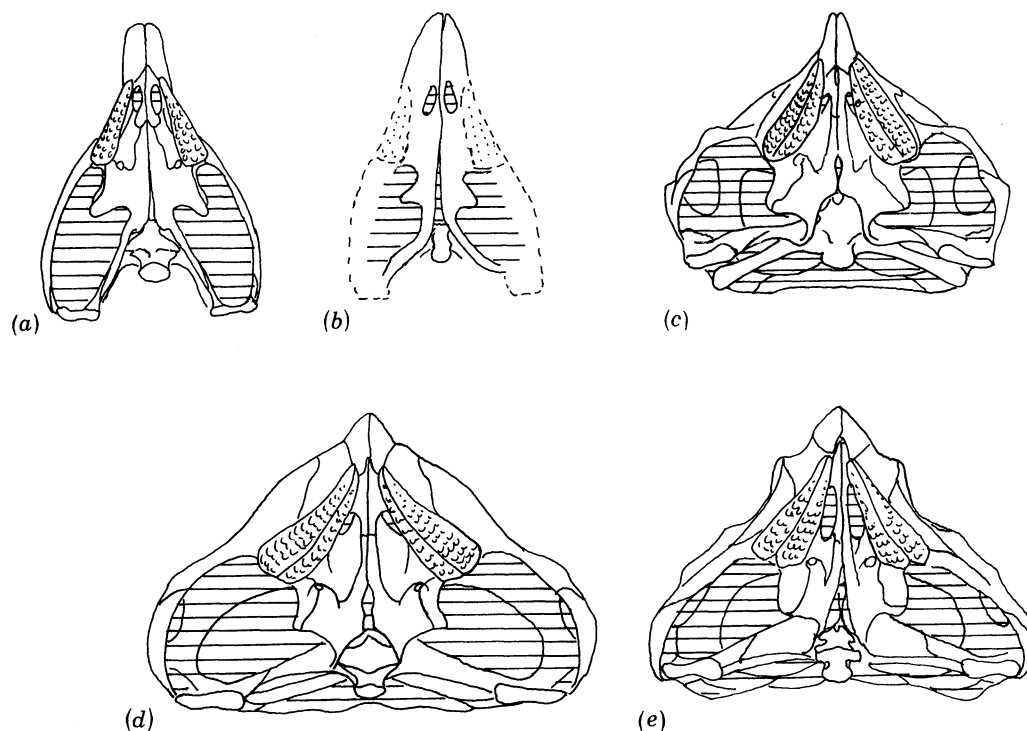

FIGURE 44. Palatal views of the skulls of (*a*) *Stenaulorhynchus*, (*b*) *Rhynchosaurus*, (*c*) *Scaphonyx*, (*d*) *Paradapedon* and (*e*) *Hyperodapedon*, drawn to unit length ((*a*) after Huene (1938); (*b*) after Watson (1910) and Huene (1938), (*c*) after Romer (1956); (*d*) after Chatterjee (1974); (*e*) original).

The braincase (figures 44–46). The endocranium of *Stenaulorhynchus* (Huene 1938, fig. 4) is quite different from that of the late Triassic forms. Since the differences are probably taxonomically important, new more detailed figures of the braincase of *Stenaulorhynchus* are given (figure 45). The braincase of *Rhynchosaurus* is poorly known (Watson 1910; Huene 1929). That of *Scaphonyx* has only been partially figured (Huene 1929, 1942) and new figures are given here (figure 46). *Paradapedon* has been well described by Chatterjee (1974, pp. 221–225) and the *Hyperodapedon* endocranium is figured above (figure 10, §4.6). These last two genera differ little from *Scaphonyx*, except that the basipterygoid processes are rather longer in *Hyperodapedon* and the spheno-occipital tubera of *Paradapedon* do not seem to be so distinct from the basisphenoid.

The basipterygoid processes of *Stenaulorhynchus* are far longer than in the late Triassic forms. In ventral view, it can be seen that the basisphenoid of *Stenaulorhynchus* is longer than the basioccipital when measured in the midline. The reverse is the case in *Scaphonyx*, *Paradapedon* and *Hyperodapedon*. The spheno-occipital tubera are not distinct in *Stenaulorhynchus* (cf. *Paradapedon*), and the large internal carotid foramina (note the asymmetric position, figure 45*a*) are set further back. The paroccipital process is directed more posteriorly than laterally in the

middle Triassic genus, and this is correlated with the more anterior position of the braincase in relation to the skull roof. In anterior view (figure 45c), the dorsum sellae of *Stenaulorhynchus* is far higher than in *Scaphonyx* (figure 46c). In posterior view, the exoccipitals do not take part in the occipital condyle of *Stenaulorhynchus* (figure 45d), but they do in the late Triassic genera (figure 46d). The spheno-occipital tubera of *Stenaulorhynchus* show a ventrolateral bifurcation that is absent in *Scaphonyx*, and the foramen magnum of the former may be relatively smaller.
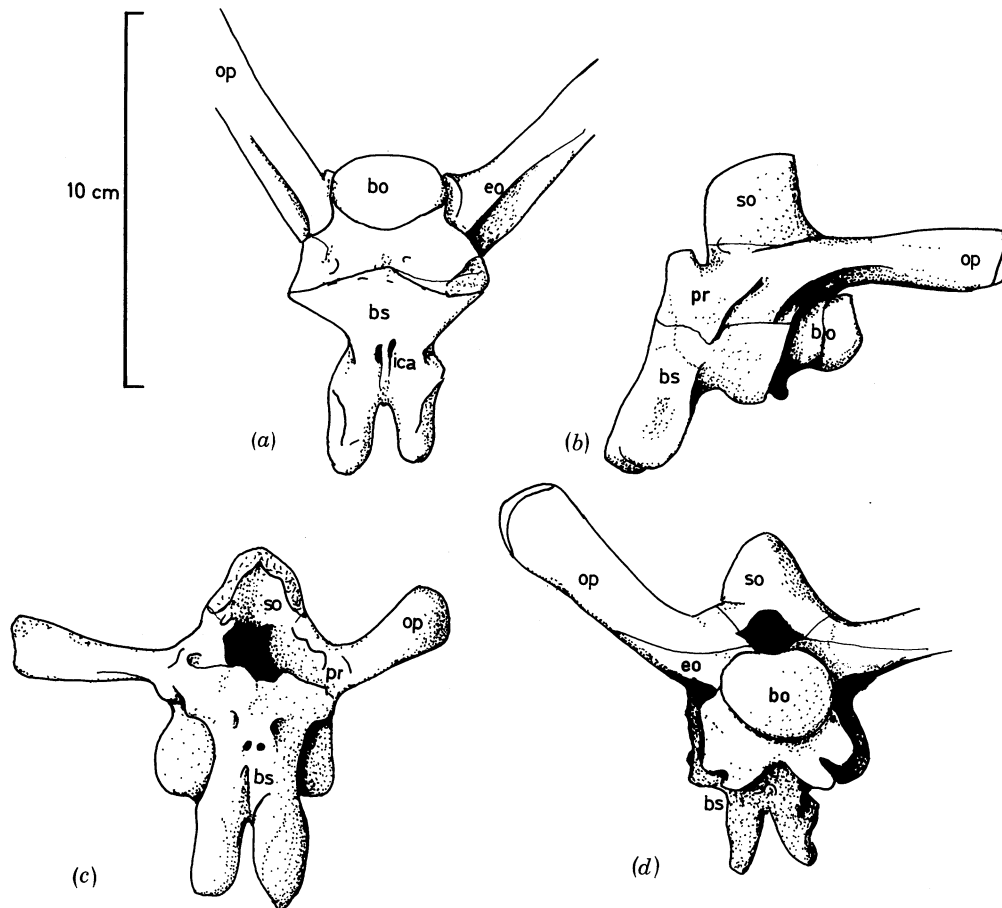
FIGURE 45. Endocranium of *Stenaulorhynchus stöckleyi*, Tübingen specimen '303e', figured by Huene (1938, fig. 4), some sutures restored. (a–d) Anteroventral, lateral, anterior and posterior views.

The lower jaw (figure 47). The mandible of *Stenaulorhynchus* is relatively less deep than in the other rhynchosaurs (*Paradapedon* seems to have the deepest). The adductor fossa extends further foward in *Stenaulorhynchus* and *Rhynchosaurus*, and the dentary is shorter and less bowed in the former than in the later forms. The symphysis is projected anteriorly on a process beyond the dentary in *Stenaulorhynchus*, and this is not seen in the other genera. The dentition is discussed below (§10.4.2).

The vertebral column. It is difficult to compare the characters of the vertebrae and ribs of rhynchosaurs because of widely differing modes of preservation. However, the atlas of *Stenaulorhynchus* (Huene 1938, pl. 10, fig. 2) has a relatively longer neural spine than in any other forms, and the cervicals all have high neural spines, which are reduced in the later genera.
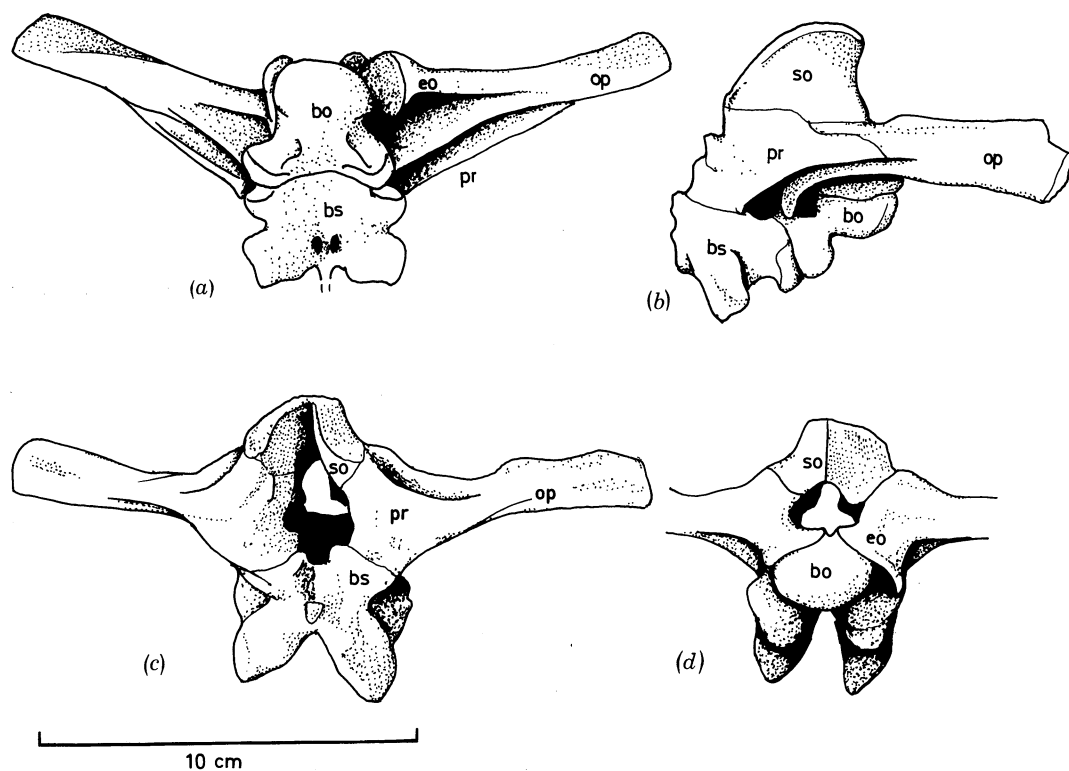
FIGURE 46. Endocranium of *Scaphonyx fischeri*, Tübingen specimen 'XIX2', figured by Huene (1942, pl. 31, fig. 1). (*a–d*) Ventral, lateral, anterior and posterior views.

FIGURE 47. The lower jaws of (*a*) *Stenaulorhynchus*, (*b*) *Rhynchosaurus*, (*c*) *Scaphonyx*, (*d*) *Paradapedon* and (*e*) *Hyperodapedon* in medial (upper) and lateral (lower) views, drawn to unit length ((*a*) after Huene (1938); (*b*) partly after Huene (1938) and specimens; (*c*) after Huene (1942); (*d*) after Chatterjee (1974); (*e*) original).

Scaphonyx and *Hyperodapedon* show a very short 8th cervical and 1st dorsal centrum (presacrals 8, 9). This is not evident in *Stenaulorhynchus* or *Paradapedon*. The remaining dorsal vertebrae are rather similar in all genera, although the rib facet (enlarged diapophysis) is rounded in *Stenaulorhynchus*, *Paradapedon* and large *Scaphonyx*, and elongate in *Hyperodapedon* and small *Scaphonyx*. The sacral vertebrae are similar, but the sacral ribs of *Stenaulorhynchus* have a more pronounced constriction of the shaft and heavier distal end than in the late Triassic forms. As far as preserved, the caudal vertebrae seem comparable in all genera.

FIGURE 48. Left shoulder girdles in lateral view of (a) *Mesosuchus*, (b), *Stenaulorhynchus*, (c) *Rhynchosaurus*, (d), *Scaphonyx*, (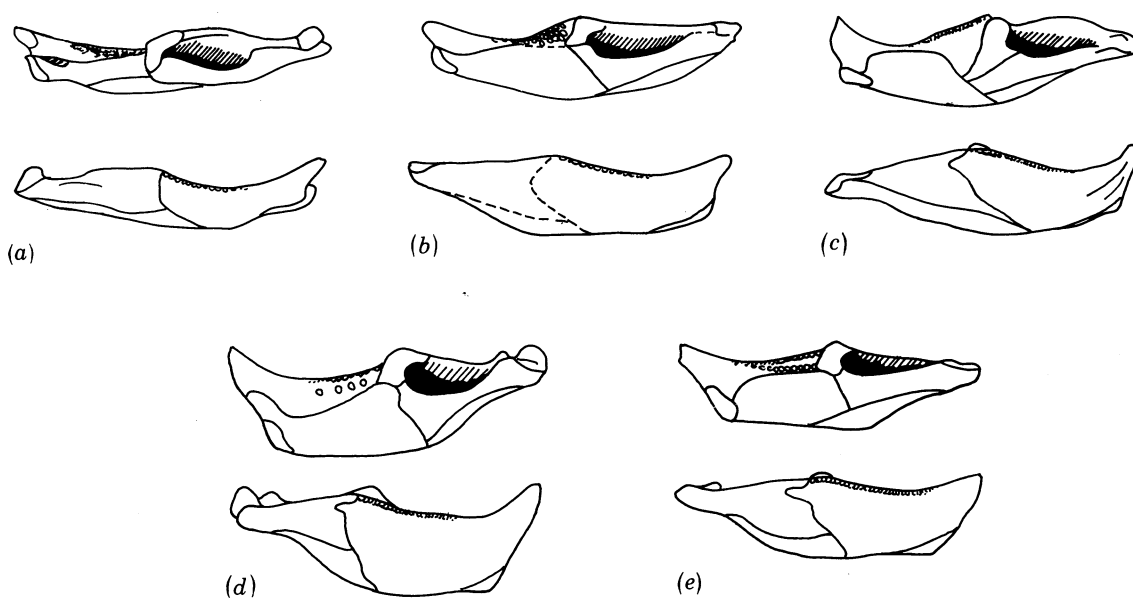e) *Paradapedon* and (f) *Hyperodapedon*, drawn to standard height ((a) after Haughton (1924); (b) after Huene (1938); (c) restored partially from Huxley (1887) and Huene (1929); (d) after Huene (1938); (e) after Chatterjee (1974); (f) original).

The ribs. All rhynchosaurs have double-headed ribs on the cervical and two most anterior dorsal vertebrae. The heads fuse and become gradually more united in posterior dorsals. Only *Hyperodapedon* has the greatly expanded anterior dorsal ribs. The chevron bones of *Hyperodapedon* are longer and more slender than those of *Stenaulorhynchus* (Huene 1938, pl. 12, fig. 10) and *Scaphonyx* (Huene 1942, pl. 32, fig. 5).

The shoulder girdle (figure 48). *Stenaulorhynchus* (Huene 1938, pp. 99–100, pl. 12, 13; Romer 1956, p. 301) has a broad interclavicle, short scapula, posterior coracoid wing and a large lateral glenoid fossa. This is more primitive in appearance than the shoulder girdles of the late Triassic forms. *Mesosuchus* (Haughton 1924, fig. 1) has a similar heavy L-shaped pectoral girdle. Broom (1906, pl. 40, figs 10, 11) reconstructed *Howesia* with an advanced sphenodontid shoulder girdle, but it was probably more like that of *Mesosuchus*.

The late Triassic forms have a slimmer interclavicle, a taller scapula, and a rounded coracoid with a reduced posterior projection. The shoulder girdle is generally lighter and less L-shaped, and the glenoid fossa faces more posteriorly in these later forms.

The shoulder girdles of *Hyperodapedon* and *Scaphonyx* are very similar in the relative size and shape of all elements and in the presence of a coracoid incisure. The glenoid fossa in *Hyperodapedon* appears to face more ventrally and posteriorly than in the other late Triassic forms, and the sharp bend and lateral ridge may also be unusual. *Paradapedon* apparently had a coracoid foramen (Chatterjee 1974, pp. 242–243), but in other respects the shoulder girdle differs little from *Hyperodapedon*. *Rhynchosaurus* seems to have been more like the late Triassic rhynchosaurs than the earlier forms in the shape and proportions of the shoulder girdle (Huxley 1887, p. 690, pl. 27, fig. 3; Huene 1929, p. 41, pl. 6, figs 5–9).
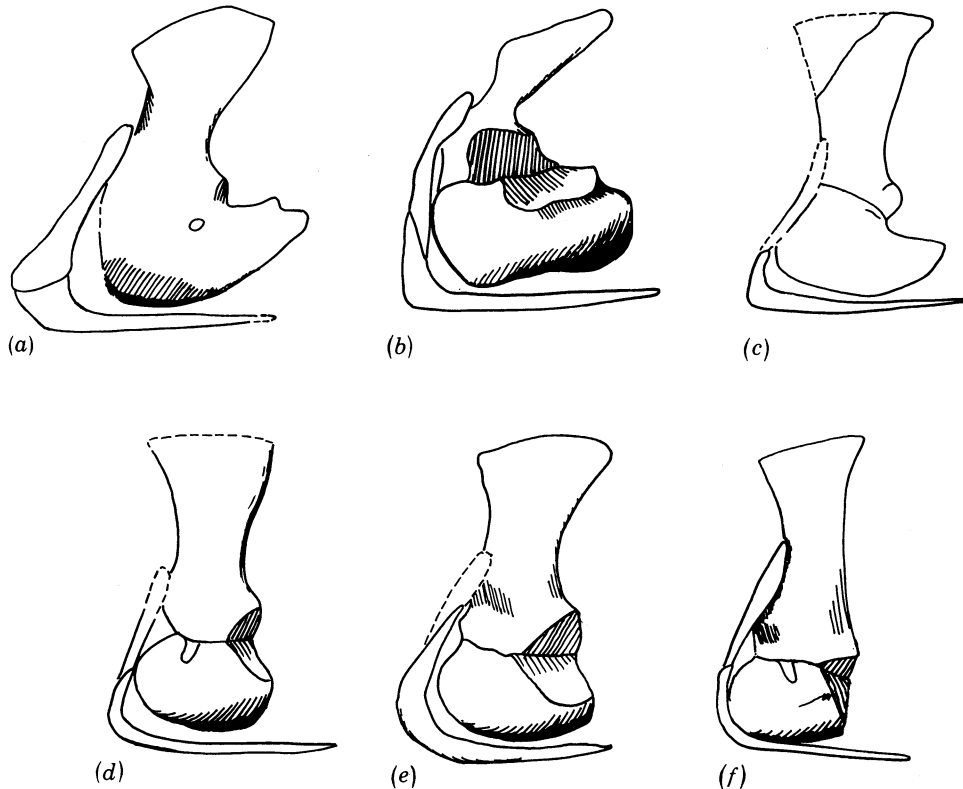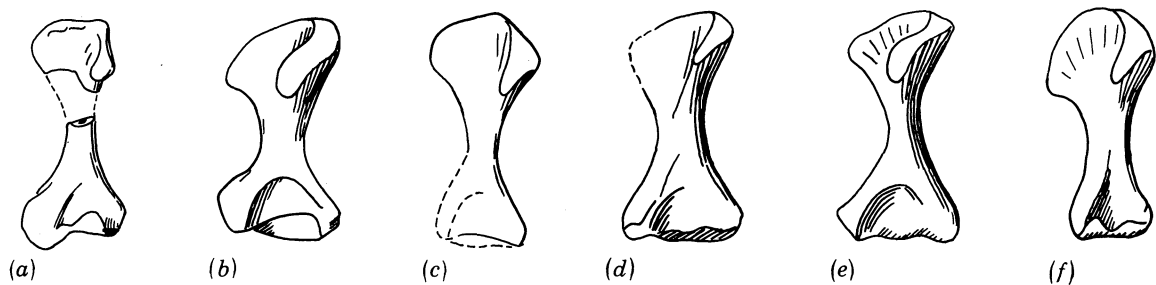

FIGURE 49. Left humeri in ventral view of (*a*) *Mesosuchus*, (*b*) *Stenaulorhynchus*, (*c*) *Rhynchosaurus*, (*d*) *Scaphonyx*, (*e*) *Paradapedon* and (*f*) *Hyperodapedon*, drawn to unit length ((*a*) after Haughton (1924); (*b*) after Huene (1938); (*c*) restored from Huxley (1887) and Huene (1929); (*d*) after Huene (1942); (*e*) after Chatterjee (1974); (*f*) original).

The forelimb. All rhynchosaur humeri (figure 49) appear essentially similar. The humerus of *Stenaulorhynchus* has a hook-like projection of the supinator crest over the ectepicondylar groove, but there is no foramen here, nor in the earlier *Mesosuchus* (Haughton 1924, p. 22). A similar hook has been observed in the Texas late Triassic rhynchosaur (R. Elder, personal communication).

The radius and ulna show no essential differences, and the hand and carpus are not well enough known for detailed comparisons. The proportions of the lengths of forelimb elements vary in different rhynchosaurs, but there is no clear trend, temporal or otherwise (table 7).

The pelvis (figure 50). All rhynchosaurs have a closed acetabulum which is formed by all three pelvic bones. *Howesia* and *Mesosuchus* have very little anterior extension to the iliac blade; this is longer in *Stenaulorhynchus*, and equals the posterior expansion in the late Triassic forms. Its shape in *Rhynchosaurus* is uncertain. The processus lateralis on the pubis seems to be directed more laterally in *Stenaulorhynchus* than in the later genera and the ischium is shorter. The pelvis of *Paradapedon* (Chatterjee 1974, pp. 245–247) differs from that of *Hyperodapedon* only in details: the iliac facet of the ischium is longer, the processus lateralis of the pubis appears to be longer, and the obturator foramen is more centrally placed in the pubis. *Scaphonyx* also seems similar, although the pelvis figured by Huene (1942, pl. 33, fig. 7) lacks the ventral median diamond-shaped space. This is probably not an important feature since it was probably filled with cartilage that ossified with age.

The hindlimb. Many of the differences in the shape of hindlimb elements between *Howesia* and *Rhynchosaurus* and the larger rhynchosaurs depend on scale effects, and are not of taxonomic
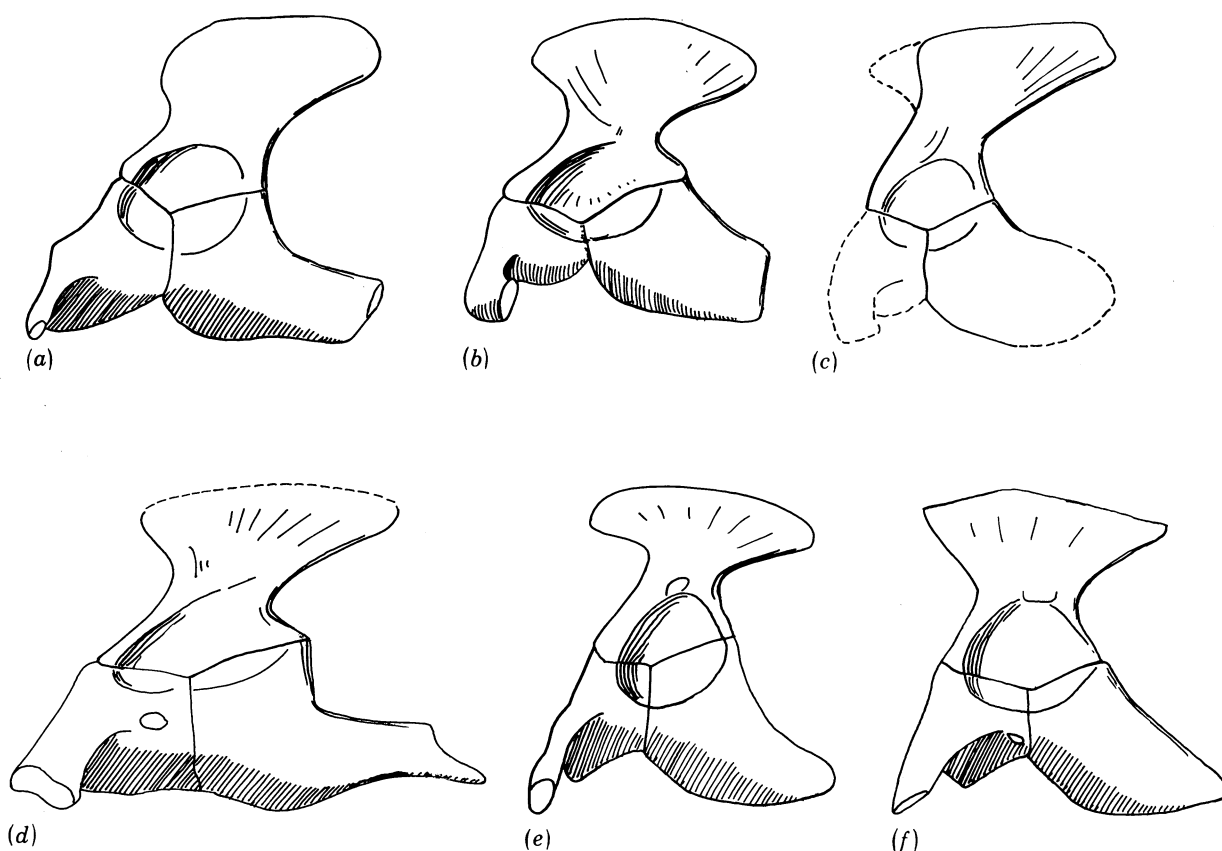
FIGURE 50. Pelvis in left lateral view of (a) *Howesia*, (b) *Stenaulorhynchus*, (c) *Rhynchosaurus*, (d) *Scaphonyx*, (e) *Paradapedon* and (f) *Hyperodapedon*, drawn to standard height. It is uncertain whether *Rhynchosaurus* had an anterior extension to the iliac blade. ((a) After Broom (1906); (b) after Huene (1938) and specimens; (c) restored from Huxley (1887) and specimens (Bath Museum M20a); (d) after Huene (1942); (e) after Chatterjee (1974); (f) original.)
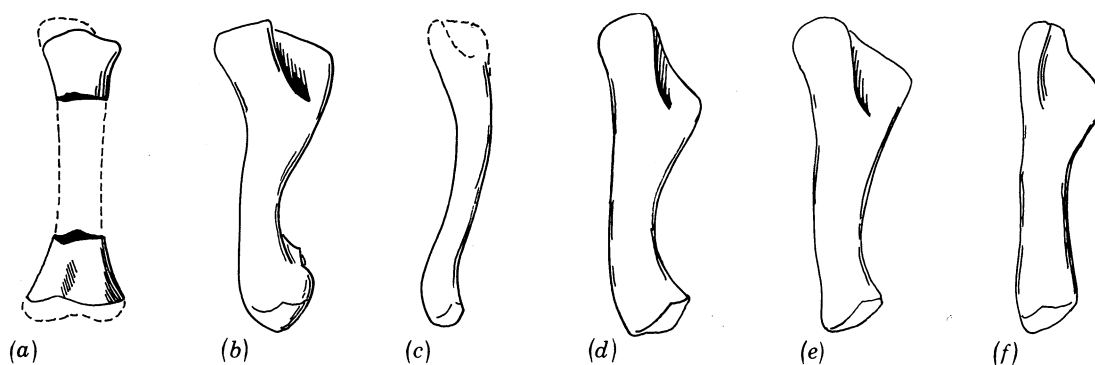
FIGURE 51. Left femur in postero-lateral view of (a) *Howesia*, (b) *Stenaulorhynchus*, (c) *Rhynchosaurus*, (d) *Scaphonyx*, (e) *Paradapedon* and (f) *Hyperodapedon*, drawn to unit length ((a) after Broom (1906); (b) after Huene (1938); (c) after Huxley (1887) and specimens; (d) after Huene (1942); (e) after Chatterjee (1974); (f) original).

value. The femur of *Rhynchosaurus* (figure 51c) is slimmer than that of other rhynchosaurs, probably because it was a much smaller animal. The femur of *Stenaulorhynchus* (figure 51b) differs from the late Triassic forms in having a relatively broader proximal end with a deep intertrochanteric fossa and a broader distal end. Some specimens of *Scaphonyx* (figure 51d) have femora like those of *Hyperodapedon* and *Paradapedon* (figure 51c, f), while other more massive

specimens (Huene 1942, pl. 37, fig. 1) have heavier elements. The femur is generally longer than the humerus, but the opposite is true in *Paradapedon* and *Hyperodapedon*, although only to a very slight extent (table 7), and measurements from various specimens of *Scaphonyx* (Huene 1942) suggest that the femur becomes relatively shorter with respect to the humerus as overall body size increases.

The scale effects just described are observed in the tibia and fibula of all rhynchosaurs. The tibia is relatively slightly longer with respect to the femur in *Noteosuchus* and *Mesosuchus* than in *Howesia* and the later rhynchosaurs (table 7).

TABLE 7. RATIOS OF LENGTHS OF VARIOUS LIMB ELEMENTS OF RHYNCHOSAURS

(Sources of measurements are given.)

	$\dfrac{\text{humerus}}{\text{radius}}$	$\dfrac{\text{femur}}{\text{humerus}}$	$\dfrac{\text{femur}}{\text{tibia}}$	$\dfrac{\text{tibia}}{\text{metatarsal 4}}$
Noteosuchus (Carroll 1976a)	—	—	1.00	2.17
Mesosuchus (Haughton 1921, 1924)	1.27	1.12	1.02	?1.75
Howesia (Broom 1906)	—	1.70	1.23	2.17
Stenaulorhynchus (Huene 1938)	1.40	1.29	1.25	1.60
Rhynchosaurus (Huene 1929)	1.39	?1.75	?1.17	1.85
Scaphonyx (Huene 1942)	1.16	1.32 1.17 1.00	1.16	1.52
Paradapedon (Chatterjee 1974)	1.45	0.99	1.16	1.73
Hyperodapedon (average, large)	1.51	0.96	1.31	2.37
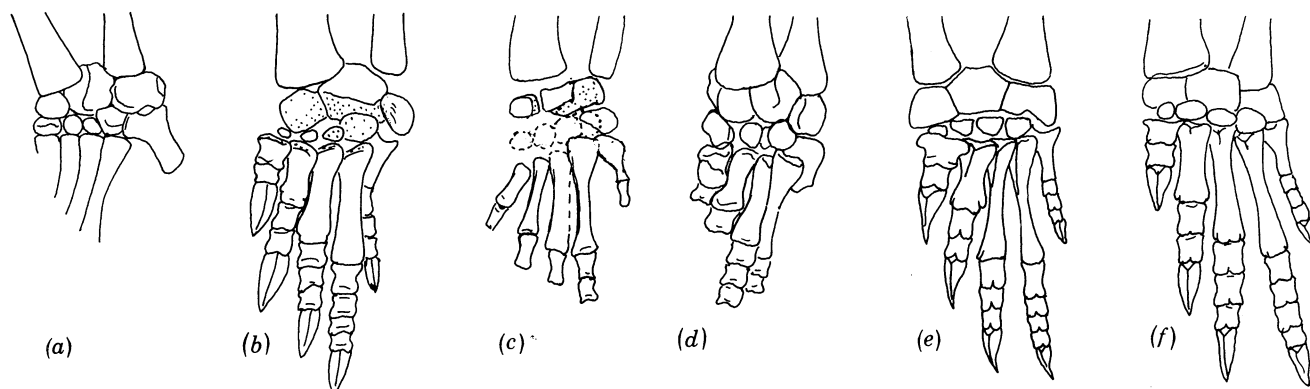
FIGURE 52. Left tarsus in anterior (extensor) view of (*a*) *Howesia*, (*b*) *Stenaulorhynchus*, (*c*) *Rhynchosaurus*, (*d*) *Scaphonyx*, (*e*) *Paradapedon* and (*f*) *Hyperodapedon*, drawn with standard ankle width ((*a*) after Carroll (1976a); (*b*) after Huene (1938) and Hughes (1968); (*c*) restored from Huxley (1887) and specimens (Bath Museum M20a); (*d*) after Huene (1942); (*e*) after Chatterjee (1974); (*f*) original).

The feet of rhynchosaurs (figure 52) all display the same characteristics: three proximal tarsal elements, four distal tarsal elements, five digits, a hooked fifth metatarsal, metatarsal length increasing from I–IV, and a phalangeal formula of 2:3:4:5:4. The centrale moves from a position between astragalus and distale 1 in *Howesia* to a more intimate association with the astragalus in later forms. The tarsus of *Rhynchosaurus* (figure 52c) is poorly known, but appears very like that of *Stenaulorhynchus* (A. D. Walker, personal communication). *Stenaulorhynchus* and the late Triassic genera show the much reduced metatarsal I, possibly characteristic of the large

digging hindfoot. The length of metatarsal 4 varies considerably with respect to the tibia length in various rhynchosaurs (table 7), but there is no clear trend through time.

10.4.2. *Rhynchosaur dentition and taxonomy* (figure 53, 54)

The dentition is reviewed in rather more detail than the remainder of the anatomy of rhynchosaurs because of its importance hitherto in classification, and because of the relative abundance of tooth-bearing bones in collections. The most recent scheme of classification has been based almost solely on the dentition (Chatterjee 1980a), but there are several shortcomings with this approach, and the characters used therein must be reconsidered.

The middle and late Triassic rhynchosaurs do not have teeth on the premaxilla. Chatterjee (1974, 1980a) reports that *Stenaulorhynchus* and *Rhynchosaurus* have a single row of teeth on the pterygoid. This is not recorded in the former by Huene (1938), but Woodward (1907) and Huene (1929, p. 40) mention these pterygoidal teeth in *Rhynchosaurus*. None of the late Triassic genera has pterygoidal teeth.

The maxilla (figure 53). The maxilla has provided the main characters used in taxonomy. All rhynchosaurs have multiple tooth rows (except *Mesosuchus*) and usually one or more grooves. *Howesia* has no groove and five rows of teeth, the middle Triassic forms (*Mesodapedon*, *Stenaulorhynchus*, *Rhynchosaurus*) have two grooves and one or more tooth rows between the grooves, and the late Triassic forms have one groove and two to six tooth rows on either side.

Chatterjee (1980a) has divided the middle and late Triassic rhynchosaurs into two subfamilies on the basis of the relative width of the dentigerous space medial to and lateral to the main groove. I do not think that this is particularly significant taxonomically since it may be variable within a single species and is often hard to determine. Chatterjee (1980a) states that the medial tooth space is wider than the lateral in *Rhynchosaurus*, *Stenaulorhynchus*, *Supradapedon* and *Hyperodapedon*, and that the reverse is the case in *Mesodapedon*, *Paradapedon*, *Scaphonyx* and the Nova Scotia rhynchosaur. From his figures (Chatterjee 1980a, fig. 1, pl. 1; here, figure 53b), it is clear that *Mesodapedon* actually falls into the first group. *Hyperodapedon* and *Supradapedon* (figure 53g, h) are difficult to assign to either group. The present study shows that, far from having a wider medial tooth space as has been assumed, *Hyperodapedon* may show equally broad segments or a wider *lateral* tooth space. In *Supradapedon* the lateral field actually appears to be wider and the number of tooth rows appears to be equal on either side of the groove. Also, in the forms with more than one groove, it may be difficult to determine which is the 'major' groove.

The number of rows of teeth in the later forms depends on the size of the individual: the larger the tooth plate, the more rows appear posteriorly. Thus, this character is not of great importance since large specimens may look quite different from younger individuals. A very large 25 cm long tooth plate of *Scaphonyx* from Brazil (Tübingen, un-numbered) looks very like the type, and only, specimen of *Supradapedon*.

The lingual surface of the maxilla of *Mesodapedon*, *Stenaulorhynchus* and *Rhynchosaurus* is covered with rows of small teeth that run down to the occlusal surface of the jaw (figure 53d). These have not been clearly reported in *Rhynchosaurus* before (cf. Chatterjee 1980a, pp. 60–61).

Variations in maxillary tooth shape may be important. In *Stenaulorhynchus* the teeth in the median row are circular in section, those in the lateral row are broader than long. The inner row of teeth on the lateral portion of the tooth plate in *Hyperodapedon*, *Paradapedon* and *Scaphonyx* are also broader than long, while all others are circular. Thus, the lateral row in *Stenaulorhynchus*
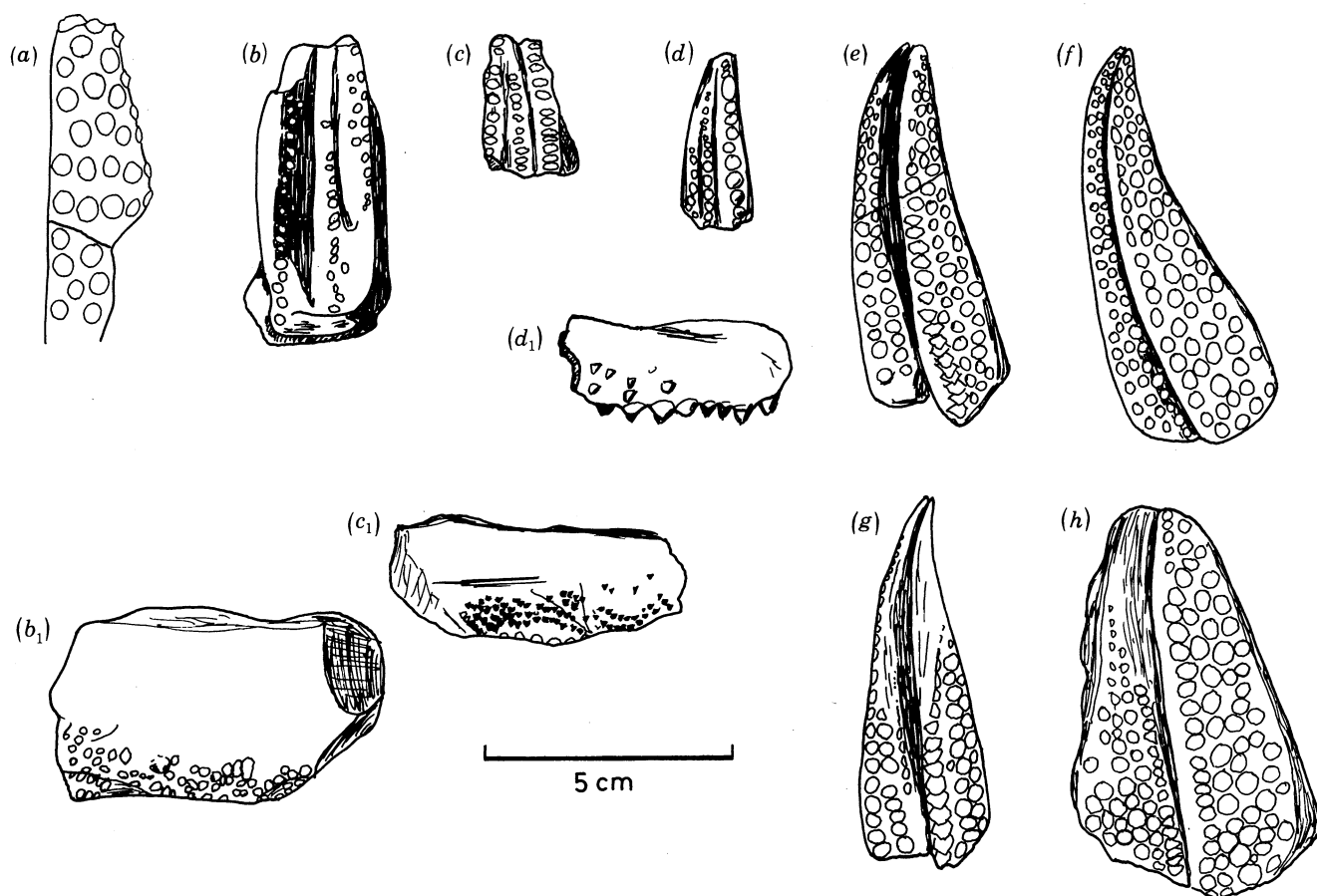
FIGURE 53. Maxillary tooth plates of (*a*) *Howesia*, (*b*) *Mesodapedon*, (*c*) *Stenaulorhynchus*, (*d*) *Rhynchosaurus*, (*e*) *Scaphonyx*, (*f*) *Paradapedon*, (*g*) *Hyperodapedon* and (*h*) *Supradapedon* in palatal view (*a–h*) and medial view (b_1, c_1, d_1). (*a*, *b*) From the right-hand side, (*c–h*) from the left. In (*a*, *b*) the medial side is on the right, in (*c–h*) on the left. ((*a*) From Malan (1963); (*b*, b_1) from Chatterjee (1980*a*); (*c*) from Huene (1938); (c_1) original (BMNH R9279); (*d*) original (GSM 59745); (d_1) original (Warwick Museum G955); (*e*) original (Tübingen 'XIX2'); (*f*) From Chatterjee (1974); (*g*) original (NUGD B); (*h*) from Chatterjee (1980*a*).)

may match the inner lateral row in the late Triassic forms, and it may be the major element controlling the pattern of the other teeth.

The dentary (figure 54). The distribution and number of teeth on the dentary generally mirrors the characters of the maxilla. The early and middle Triassic rhynchosaurs (figure 54*a–d*) have multiple rows of teeth, visible in occlusal and medial view. There is some organization into longitudinal rows in *Mesodapedon*, *Stenaulorhynchus* and *Rhynchosaurus*. The lingual rows run onto the occlusal surface, as in the maxilla, and it is not possible to distinguish numbers of occlusal and lingual rows. Woodward (1907) and Huene (1929; 1942, p. 320) recorded a single row of occlusal teeth in *Rhynchosaurus*, while Huene (1938, p. 110) suggested tentatively that there were probably several rows. The top of the dentary is divided by a groove in these middle Triassic forms, and the medial tooth rows may be lower or higher than the lateral ones. The teeth are worn flush with the bone when in occlusion.

The dentary teeth of the late Triassic forms are quite different. The lateral, buccal, teeth are always very narrow and deeply rooted, and they form a tight palisade row, while the lingual teeth, if present, are broad, thimble-shaped and spaced out. Thus the controls on tooth growth

and arrangement are quite different in the middle and late Triassic forms. *Scaphonyx* lacks lingual teeth, *Hyperodapedon* has them very well developed, and they appear to be sporadically arranged in *Paradapedon*, although perhaps not always as sporadic as suggested by Chatterjee (1974, fig. 8; cf. Lydekker 1885, pl. 2, fig. 13; Huene 1940, fig. 16) (figure 54*e–g*).

In conclusion, the classification of two geographically separate rhynchosaur subfamilies on the basis of the relative width of the two halves of the maxillary tooth plate (Chatterjee 1980*a*) cannot be accepted. The character cannot be determined in certain genera, and at least one genus is assigned to the 'wrong' subfamily. It should be regarded as one of several taxonomically significant features, but not the only one.
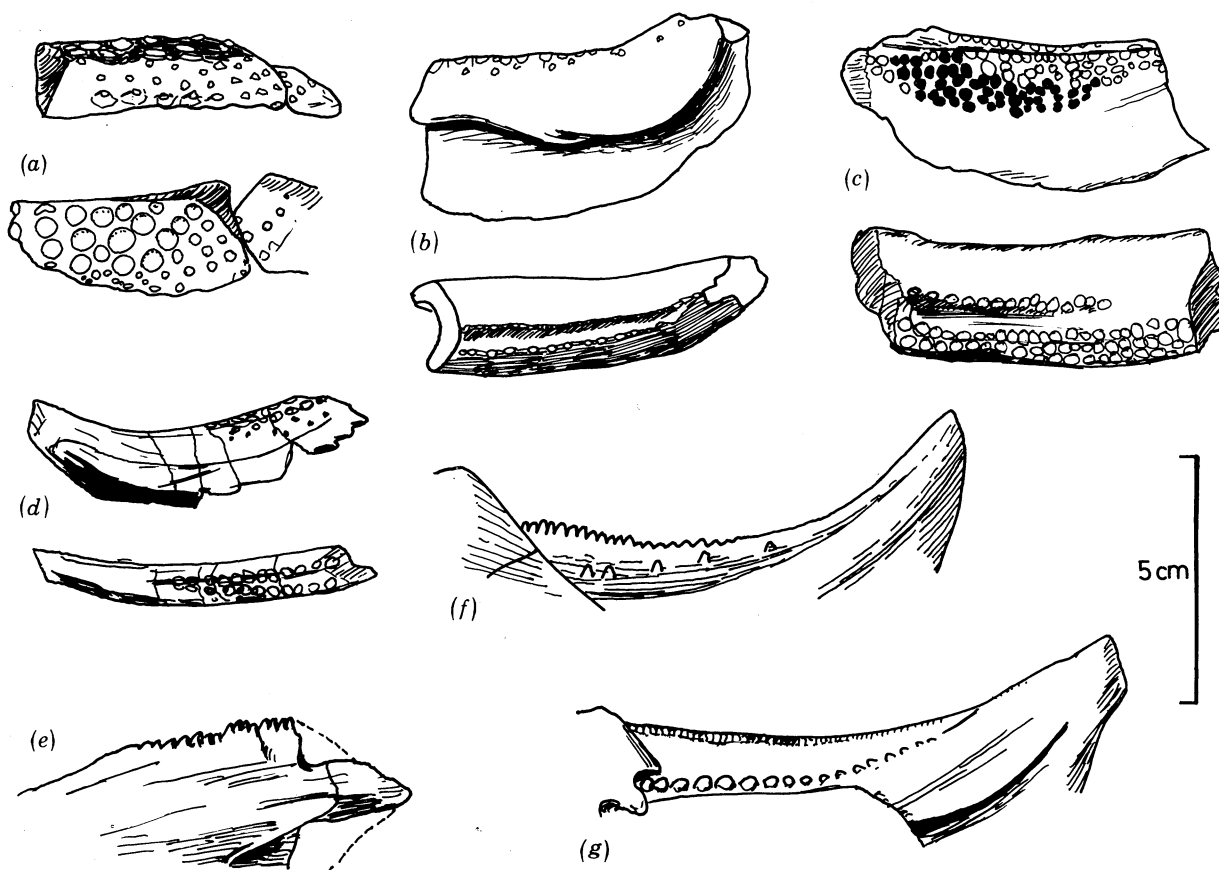
FIGURE 54. Tooth-bearing portions of the dentaries of (*a*) *Howesia*, (*b*) *Mesodapedon*, (*c*) *Stenaulorhynchus*, (*d*) *Rhynchosaurus*, (*e*) *Scaphonyx*, (*f*) *Paradapedon* and (*g*) *Hyperodapedon*. (*a–d*) Shown in medial (upper) and occlusal (lower) views, (*e–g*) in medial view only. (*d*, *e*) From right mandibles, (*a–c*, *f*, *g*) from left mandibles. ((*a*) From Malan (1963); (*b*) from Chatterjee (1980*a*); (*c*) original (BMNH R9273); (*D*) original (Warwick Museum G950); (*e*) from Huene (1942); (*f*) from Chatterjee (1974); (*g*) original (NUGD B).)

10.4.3. *Analysis of the characters of rhynchosaurs* (figure 55)

The 29 main characters discussed above (§§10.4.1, 10.4.2) are summarized in table 8. *Stenaulorhynchus* shares 21 character states with *Rhynchosaurus*, but only shares five with *Hyperodapedon* and four with *Scaphonyx* and *Paradapedon*. *Rhynchosaurus* shares seven or eight character states with each of the late Triassic forms. *Scaphonyx* shares 25 character states with *Paradapedon* and 26 with *Hyperodapedon*, and *Hyperodapedon* shares 26 character states with *Paradapedon*.

TABLE 8. A COMPARISON OF RHYNCHOSAUR CHARACTERS

(Symbols: x, present; o, absent; ?, possibly present.)

	Stenaulorhynchus	*Rhynchosaurus*	*Scaphonyx*	*Paradapedon*	*Hyperodapedon*
skull					
skull longer than broad	x	x	o	o	o
frontals longer than broad	o	o	x	x	x
postfrontal borders upper temporal fossa	o	x	x	x	x
prefrontal meets maxilla	x	x	x	?o	x
jugal has large central area	o	o	x	x	x
jugal has pronounced lateral ridge	o	o	x	x	x
parietal shorter than (nasal+frontal)	o	x	x	x	x
pterygoids directed mainly posteriorly	x	x	o	o	o
occipital condyle in front of quadrate	x	x	o	o	o
basipterygoid process long	x	?	o	o	o
basisphenoid longer than basioccipital	x	?	o	o	o
dorsum sellae high	x	?	o	o	o
exoccipitals take part in occipital condyle	o	?	o	o	o
spheno-occipital tubera bifurcate ventrally	x	?	o	o	o
mandible					
maximum depth less than ¼ length of jaw	x	x	o	o	o
adductor fossa extends more than halfway along jaw	x	o	o	o	o
dentition					
teeth on pterygoid	x	x	o	o	o
two grooves on maxilla	x	x	o	o	o
medial tooth space on maxilla wider than lateral	x	x	o	o	?
lingual teeth on maxilla	x	x	o	o	o
multiple rows of occlusal teeth on dentary	x	x	o	x	x
axial skeleton					
reduced presacral vertebrae 8 and 9	o	?o	x	o	x
appendicular skeleton					
compressed scapula	x	o	o	o	o
large lateral glenoid fossa	x	?o	o	o	o
large posterior coracoid wing	x	x	o	o	o
large anterior process on iliac blade	x	o	x	x	x
femur longer than humerus	x	x	x	o	o
reduced metatarsal I	x	o	x	x	x

This information may be simplified by means of a cluster analysis in which the genera that share most character states are paired together into progressively fewer and fewer sets until a tree is built up (the sequential agglomerative hierarchic non-overlapping clustering method (Sneath & Sokal 1973, pp. 201–245)). The analysis was done with the aid of the Clustan 1C Cluster Analysis Package (Ward's method) (Wishart 1978) on the NUMAC IBM 370/168 computer.

The results (figure 55) may be interpreted readily. The genera are plotted on the horizontal axis, and the closeness of relationship between any pair of groups may be read off the vertical axis which is divided into arbitrary units of taxonomic distance in character space. There are two clear clusters, namely *Stenaulorhynchus* and *Rhynchosaurus* on the one hand, and the late Triassic forms on the other. The genera within each cluster are clearly closely related, and the distance between clusters is very large. It should be noted that the level of similarity is less between *Stenaulorhynchus* and *Rhynchosaurus* than among the late Triassic forms which are virtually indistinguishable. All characters recorded as 'possibly present' were treated as present. When these doubtful features were treated as absent, or if they were randomized, the results were the same, although *Rhynchosaurus* did not cluster so closely with *Stenaulorhynchus*.
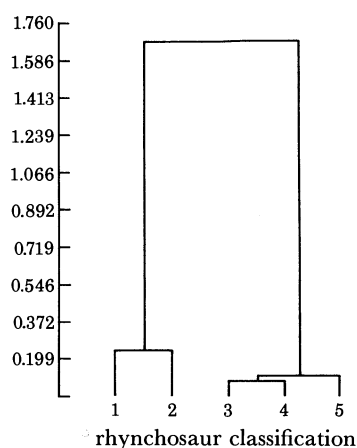

FIGURE 55. Dendrogram produced by cluster analysis of binary attributes of rhynchosaurs. The 29 characters are listed in table 8, and the analysis is described in the text (§10.4.3). Genera are numbered as follows: 1, *Stenaulorhynchus*; 2, *Rhynchosaurus*; 3, *Scaphonyx*; 4, *Hyperodapedon*; 5, *Paradapedon*. *Stenaulorhynchus* and *Rhynchosaurus* cluster closely and are quite distinct from the cluster of the late Triassic genera.

The phenetic analysis made here clearly highlights the problem of parsimony. The pattern of presence/absence for most individual characters matches the dendrogram pattern, but in 15 cases (out of 145 (29×5)) a character state does not fit. These features may be wrongly recorded, or they may represent reversals and convergence. In this example, the evidence for the classification proposed is overwhelming.

10.4.4. *Taxonomic conclusions*

The review of rhynchosaur characters and the cluster analysis clearly support a division of rhynchosaurs into a middle and a late Triassic subgroup, as proposed by Chatterjee (1969, 1974) and Sill (1971b), and gives no evidence for the classification of Chatterjee (1980a) on the basis of one tooth plate character (see §10.4.2).

Furthermore, the closeness of relationship between *Hyperodapedon*, *Paradapedon* and *Scaphonyx* is so great as to suggest that they may be congeneric. *Scaphonyx* differs from *Hyperodapedon* and *Paradapedon* only in the absence of lingual teeth on the dentary and in having a femur that is just longer than the humerus or equal to it in length. *Hyperodapedon* differs from *Paradapedon* and *Scaphonyx* in having the lateral and medial tooth-bearing areas on the maxillary tooth plate approximately equal in width, rather than the lateral wider than the medial, and *Paradapedon*

differs from the other two forms in apparently not having shortened presacral vertebrae 8 and 9. Other differences in the skull and skeleton appear to depend on the individual concerned and on the mode of preservation. This is particularly clearly shown in an examination of museum material of *Scaphonyx* specimens from the Santa Maria Formation, where a great range of proportional variation is shown which is largely dependent on age and sexual dimorphism (compare figures given by Huene (1929, 1942), Sill (1970, 1971 *a*, *b*) and Barbarena (1971)). In certain cases the chemical processes of preservation and weathering before burial can lead to massive distortion of the bones, a cause of taxonomic confusion in the past (Sill 1970).

The taxonomic options available are to retain three genera of late Triassic rhynchosaurs, to synonymize all three as species of one genus, or to synonymize two forms that are considered to be more closely related to each other than to the third form.

Although the cluster analysis shows that all three are almost equally inter-related, one character, the absence of lingual dentary teeth in *Scaphonyx*, seems to be of more than specific importance. If fossil genera are to be regarded as distinct, it must be possible to identify them unequivocally on the basis of morphology. If one was presented with a skeleton of *Hyperodapedon* and a skeleton of *Paradapedon* with no indications of provenance, it would be very difficult to tell which was which other than by the mode of preservation. It is concluded that *Hyperodapedon* and *Paradapedon* show so few morphological differences that they should be regarded as two species of one genus, *Hyperodapedon*.

When Lydekker (1885) described the Indian remains, he named them *Hyperodapedon huxleyi*. He noted several differences from *H. gordoni* (Lydekker 1885, p. 18). However, most of these differences are not relevant since he considered that the large specimens of *Rhynchosaurus* from Warwick and Devon belonged to *H. gordoni*. The remaining differences are the greater size (on average) of the Indian form (*H. gordoni*, skull length up to 210 mm (est.), average 180 mm, body length 1.3 m; *H. huxleyi*, skull length up to 420 mm (est.), average 180 mm, body length 1.4 m (Chatterjee 1974)) and the greater number of lateral than medial tooth rows on the maxillary tooth plate. Huene (1938, pp. 111–112) erected the new genus *Paradapedon* for *H. huxleyi* and gave its distinguishing features (Huene 1939*b*, 1942, 1956) as the presence of lingual teeth on the dentary. However, these are now known to be present in *Hyperodapedon gordoni*. Chatterjee (1974, 1980) gave the differences in relative widths of the medial and lateral portions of the maxillary tooth plates as the only distinguishing feature. This is not considered here to be of generic importance.

The genera and species of late Triassic rhynchosaurs (subfamily Hyperodapedontinae) are:

Hyperodapedon Huxley, 1859

    Lingual teeth on dentary; humerus longer than femur.

H. gordoni Huxley, 1859

    Lossiemouth Sandstone Formation, Elgin.

    Skull length up to 210 mm (est.); average body length 1.3 m; lateral and medial tooth-bearing areas on maxilla approximately equal in width.

H. huxleyi Lydekker, 1881 (= *Paradapedon* Huene, 1938)

    Maleri Formation, India.

    Skull length up to 420 mm (est.); average body length 1.4 m; lateral portion of tooth-bearing area on maxilla wider than medial.

Scaphonyx Woodward, 1907

    No lingual teeth on dentary; humerus shorter than, or equal in length to, femur.

S. fischeri Woodward, 1907

    Santa Maria Formation, Brazil.

    Maxillary teeth little differentiated; free edge of jugal slopes up steeply below orbit; centrale and astragalus separate.

S. sanjuanensis Sill, 1970

    Ischigualasto Formation, Argentina.

    Maxillary teeth differentiated (teeth in first lateral row rectangular, others circular in cross-section); free edge of jugal slopes up less steeply than in *S. fischeri*; centrale and astragalus possibly fused.

Supradapedon Chatterjee, 1980

S. stockleyi (Boonstra, 1953)

    (Age uncertain), Tanzania.

    Large body size; medial dentigerous space on maxilla supposedly wider than lateral (Chatterjee 1980*a*, p. 58), but this is not at all evident from photographs of the specimen. '*Supradapedon*' could be a large *Scaphonyx* or *Hyperodapedon*.

Undescribed forms

    Wolfville Sandstone, Nova Scotia.

    Dockum Group, Texas.

10.4.5. *Evolution within the Rhynchosauridae*

A comparison of the rhynchosaurs of the middle and late Triassic indicates several directions of morphological change. Some of these have been reviewed by Chatterjee (1974). The major changes are:

(i)   Skull becomes broader than it is long.

(ii)   Frontal increases in length and parietal shortens

(iii)   Skull becomes deeper, and jugal increases in area.

(iv)   Strong ridge develops on jugal.

(v)   Quadrate condyles move forward relative to braincase. Pterygoids and paroccipital processes shorten and become more laterally directed.

(vi)   Exoccipitals expand to take part in occipital condyle.

(vii) Mandible becomes deeper and adductor fossa moves back.

(viii) Palatal teeth lost.

(ix)   Multiple grooves on maxilla become one major groove.

(x)   Lingual teeth lost on maxilla.

(xi)   Simplification of teeth on dentary to one occlusal and one lingual row. The latter may be absent.

(xii) Shoulder girdle becomes more upright, glenoid faces more posteriorly, and posterior coracoid wing becomes reduced.

(xiii) Iliac blade expands.

(xiv) Femur and humerus achieve similar length.

10.5. *Diagnosis of the rhynchosaurs*

The diagnoses are based on the present work, Romer (1956), and Chatterjee (1980*a*). The position of the family Mesosuchidae was discussed in §10.2, and the subdivisions of the family Rhynchosauridae were discussed in §10.4.

Order Rhynchosauria Osborn, 1903 (Gervais, 1859)

Small to moderate-sized diapsid reptiles; broad and deep skull; generally with multiple tooth rows on maxilla and dentary, downturned toothless premaxilla, ankylothecodont tooth implantation; single median naris, lacrimal retained, fused parietals; splenials form entire jaw symphysis, reduced coronoid; primitive massive limbs and girdles; T-shaped interclavicle, single coracoid with incisure, scapula with acromion; no foramina in humerus; iliac blade extends back, large processus lateralis on pubis; three proximal tarsals with centrale closely associated with the astragalus.

Suborder Mesosuchidia Haughton, 1924
Family Mesosuchidae Haughton, 1924
      (*Mesosuchus*)
Premaxillae downturned and bear acrodont teeth, alternating 'zig-zag' tooth row, parietal foramen present, lower temporal arcade open (?), quadrate large and possibly streptostylic (?), quadratojugal reduced, mandibular fenestra (?).

Suborder Rhynchosauroidea Nopcsa, 1928

Parietal foramen absent, teeth have ankylothecodont implantation, batteries of functional teeth on maxilla and dentary.

Family Howesiidae Watson, 1917
      (*Howesia*)
Tooth-bearing elements rounded and without grooves.

Family Rhynchosauridae Huxley, 1887

Temporal region broad and skull deep, loss of supratemporal, development of groove and blade jaw apparatus, reduced retroarticular process, large centrale firmly united with astragalus.

Subfamily Rhynchosaurinae Nopcsa, 1923 (nom. transl. ex Huxley 1887)
      (*Rhynchosaurus, Stenaulorhynchus, Mesodapedon*)
Skull longer in midline than breadth across temporal region, frontals broader than long, jugal with narrow central area; occipital condyle in front of quadrate, pterygoids directed mainly posteriorly; mandible depth less than one-quarter length of jaw; teeth on pterygoid; two grooves on maxilla, lingual teeth on maxilla; large posterior coracoid wing.

Subfamily Hyperodapedontinae Chatterjee, 1969 (nom. transl. ex Lydekker 1885)
      (*Hyperodapedon, Scaphonyx, 'Supradapedon'*, ?North American forms)
Skull broader across temporal region than length in midline, frontals longer than broad; jugal with broad central area; occipital condyle in line with quadrates, pterygoids directed mainly laterally; mandible depth more than one-quarter length of jaw; no teeth on pterygoid; one groove on maxilla, no lingual teeth on maxilla; posterior coracoid wing reduced.

REFERENCES

Alexander, R. McN. 1968 *Animal mechanics*. London: Sidgwick & Jackson.

Anderson, H. M. 1974 A brief review of the flora of the Molteno Formation (Triassic), South Africa. *Palaeont. afr.* 17, 1–10.

Anderson, H. M. 1978 *Podozamites* and associated cones and scales from the Upper Triassic Molteno Formation, Karoo Basin, South Africa. *Palaeont. afr.* 21, 57–77.

Anderson, H. M. & Anderson, J. M. 1970 A preliminary review of the biostratigraphy of the uppermost Permian, Triassic and lowermost Jurassic of Gondwanaland. *Palaeont. afr.* 13 (suppl.), 1–22.

Bakker, R. T. 1971 Dinosaur physiology and the origin of mammals. *Evolution* 25, 636–658.

Barbarena, M. C. 1971 Algunas considerações o desenvolvimento de Rincossáurios. *Anales Acad. bras. Cienc.* 43 (suppl.), 403–409.

Barnard, P. D. W. 1973 Mesozoic floras. *Spec. Pap. Palaeont.* 12, 175–188.

Bellairs, A. d'A. & Boyd, J. D. 1947 The lachrymal apparatus in lizards and snakes. I. The brille, the orbital glands, lachrymal canaliculi and origin of the lachrymal duct. *Proc. zool. Soc. Lond.* 117, 81–108.

Bellairs, A. d'A. & Boyd, J. D. 1950 The lachrymal apparatus in lizards and snakes. II. The anterior part of the lachrymal duct and its relationship with the palate and with the nasal and vomeronasal organs. *Proc. zool. Soc. Lond.* 120, 269–310.

Benton, M. J. 1977 *The Elgin reptiles*. Elgin: The Moray Society.

Benton, M. J. 1981 The Triassic reptile *Hyperodapedon* from Elgin, functional morphology and relationships. Ph.D. Thesis, University of Newcastle upon Tyne.

Benton, M. J. 1982 The Diapsida: revolution in reptile relationships. *Nature, Lond.* 296, 306–307.

Benton, M. J. 1983*a* Dinosaur success in the Triassic: a noncompetitive ecological model. *Q. Rev. Biol.* 58, 29–55.

Benton, M. J. 1983*b* Progressionism in the 1850s: Lyell, Owen, Mantell and the Elgin fossil reptile *Leptopleuron* (*Telerpeton*). *Archs nat. Hist.* 11, 123–136.

Benton, M. J. 1983*c* The relationships and early evolution of the Diapsida. In *The structure, development and evolution of reptiles* (ed. M. W. J. Ferguson). London: Academic Press. (In the press.)

Benton, M. J. & Walker, A. D. 1981 The use of flexible synthetic rubbers for casts of complex fossils from natural moulds. *Geol. Mag.* 118, 551–556.

Boulenger, G. A. 1903 On reptilian remains from the Trias of Elgin. *Phil. Trans. R. Soc. Lond.* B 196, 175–189.

Brinkman, D. 1981 The origin of the crocodiloid tarsi and the interrelationships of thecodontian archosaurs. *Breviora* 464, 1–23.

Broom, R. 1906 On the South African Diaptosaurian reptile *Howesia*. *Proc. zool. Soc. Lond.* 1906, 591–600.

Broom, R. 1913 On the South African pseudosuchian *Euparkeria* and allied genera. *Proc. zool. Soc. Lond.* 1913, 619–633.

Broom, R. 1925 On the origin of lizards. *Proc. zool. Soc. Lond.* 1925, 1–16.

Bruner, H. L. 1907 On the cephalic veins and sinuses of reptiles, with description of a mechanism for raising the venous blood-pressure in the head. *Am. J. Anat.* 7, 1–117.

Burckhardt, R. 1900 On *Hyperodapedon gordoni*. *Geol. Mag.* (4) 7, 486–492, 529–535.

Byerly, T. C. 1925 The myology of *Sphenodon punctatum*. *Stud. nat. Hist. Iowa Univ.* 11 (6), 1–51.

Carroll, R. L. 1975 The early differentiation of diapsid reptiles. *Colloques int. Cent. natn. Rech. scient.* 218, 433–449.

Carroll, R. L. 1976*a* *Noteosuchus* – the oldest known rhynchosaur. *Ann. S. Afr. Mus.* 72, 37–57.

Carroll, R. L. 1976*b* Eosuchians and the origin of archosaurs. In *Athlon, essays in palaeontology in honour of Loris Shano Russell* (ed. C. S. Churcher), pp. 58–79. Toronto: Royal Ontario Museum.

Carroll, R. L. 1976*c* *Galesphyrus capensis*, a younginid eosuchian from the *Cistecephalus* Zone of South Africa. *Ann. S. Afr. Mus.* 72, 59–68.

Carroll, R. L. 1977 The origin of lizards. In *Problems in vertebrate evolution* (ed. S. M. Andrews, R. S. Miles & A. D. Walker). *Linn. Soc. Symp. Ser.* 4, 359–396. London: Academic Press.

Charig, A. J. 1972 The evolution of the archosaur pelvis and hind-limb: an explanation in functional terms. In *Studies in vertebrate evolution* (ed. K. A. Joysey & T. S. Kemp), pp. 121–155. Edinburgh: Oliver & Boyd.

Chatterjee, S. K. 1969 Rhynchosaurs in space and time. *Proc. geol. Soc. Lond.* no. 1658, pp. 203–208.

Chatterjee, S. K. 1974 A rhynchosaur from the Upper Triassic Maleri Formation of India. *Phil. Trans. R. Soc. Lond.* B **267**, 209–261.

Chatterjee, S. K. 1980a The evolution of rhynchosaurs. *Mém. Soc. géol. Fr.* **139**, 57–65.

Chatterjee, S. K. 1980b *Malerisaurus*, a new eosuchian reptile from the late Triassic of India. *Phil. Trans. R. Soc. Lond.* B **291**, 163–200.

Chatterjee, S. K. & Chowdhury, T. R. 1974 Triassic Gondwana vertebrates from India. *Ind. J. Earth Sci.* **1**, 96–112.

Coombs, W. P. 1978 Theoretical aspects of cursorial adaptations in dinosaurs. *Q. Rev. Biol.* **53**, 393–418.

Crompton, A. W. & Hotton, N. 1967 Functional morphology of the masticatory apparatus of two dicynodonts (Reptilia, Therapsida). *Postilla* **109**, 1–51.

Cruickshank, A. R. I. 1972 The proterosuchian thecodonts. In *Studies in vertebrate evolution* (ed. K. A. Joysey & T. S. Kemp), pp. 89–119. Edinburgh: Oliver & Boyd.

Cruickshank, A. R. I. 1978 Feeding adaptations in Triassic dicynodonts. *Palaeont. afr.* **21**, 121–132.

Currie, P. J. 1981 The vertebrae of *Youngina* (Reptilia: Eosuchia). *Can. J. Earth Sci.* **18**, 815–818.

Dendy, A. 1909 The intracranial vascular system of *Sphenodon*. *Phil. Trans. R. Soc. Lond.* B **200**, 403–426.

Edmund, A. G. 1969 Dentition. In *Biology of the Reptilia*, vol. 1 (ed. C. Gans), pp. 117–200. London: Academic Press.

Evans, S. E. 1980 The skull of a new eosuchian reptile from the Lower Jurassic of South Wales. *Zool. J. Linn. Soc.* **70**, 203–264.

Evans, S. E. 1983 Permian and Mesozoic diapsids and their cladistic relationship with early lizards. *Am. Zool.* (In the press.)

Frazzetta, T. H. 1968 Adaptive problems and possibilities in the temporal fenestration of tetrapod skulls. *J. Morph.* **125**, 145–158.

Fürbringer, M. 1900 Zur vergleichenden Anatomie des Brustschulterapparates und der Schultermuskeln. IV Teil. *Jena Z. Naturw.* **34**, 215–718.

Galton, P. M. 1973 The cheeks of ornithischian dinosaurs. *Lethaia* **6**, 67–89.

Gauthier, J. A. 1983 Phylogenetic relationships of the Lepidosauromorpha and the origin of the lizards. *Am. Zool.* (In the press.)

Giebel, G. & Leche, W. 1874–1906 *Die Säugetiere.* In Bronn's *Classen und Ordnungen des Tierreichs*, vol. 6 (5). Leipzig.

Goin, C. J. & Goin, O. B. 1971 *Introduction to herpetology* (2nd edn). San Francisco: W. H. Freeman.

Gordon, G. 1892 The reptiliferous sandstones of Elgin. *Trans. geol. Soc. Edinb.* **6**, 241–245.

Gow, C. E. 1975 The morphology and relationships of *Youngina capensis* Broom and *Prolacerta broomi* Parrington. *Palaeont. afr.* **18**, 89–131.

Grassé, P.-P. (ed.) 1955 *Traité de zoologie*, vol. 17. Paris: Masson.

Haas, G. 1973 Muscles of the jaws and associated structures in the Rhynchocephalia and Squamata. In *Biology of the Reptilia*, vol. 4 (ed. C. Gans & T. S. Parsons), pp. 285–490. London: Academic Press.

Halstead Tarlo, L. B. 1968 An outline classification of the squamates. *Br. J. Herpetol.* **4**, 32–35.

Haughton, S. H. 1921 On the reptilian genera *Euparkeria* Broom, and *Mesosuchus* Watson. *Trans. R. Soc. S. Afr.* **10**, 81–88.

Haughton, S. H. 1924 On a skull and partial skeleton of *Mesosuchus browni* Watson. *Trans. R. Soc. S. Afr.* **12**, 17–26.

Heaton, M. H. & Reisz, R. R. 1980 A skeletal reconstruction of the early Permian captorhinid reptile *Eocaptorhinus laticeps* (Williston). *J. Paleont.* **54**, 136–143.

Hildebrand, M. 1974 *Analysis of vertebrate structure*. New York: Wiley.

Holmes, R. 1977 The osteology and musculature of the pectoral limb of small captorhinids. *J. Morph.* **152**, 101–140.

Huene, F. von 1929 Ueber Rhynchosaurier und andere Reptilien aus den Gondwana-ablagerungen Südamerikas. *Geol. paläont. Abh.* (n.s.) **17**, 1–62.

Huene, F. von 1938 *Stenaulorhynchus*, ein Rhynchosauride der ostafrikanischen Obertrias. *Nova Acta Leopoldina* (n.s.) **6**, 83–121.

Huene, F. von 1939a Die Lebensweise der Rhynchosauriden. *Paläont. Z.* **21**, 232–238.

Huene, F. von 1939b Die Verwandtschaftsgeschichte der Rhynchosauriden. *Physis, Augsburg* **14**, 499–523.

Huene, F. von 1942 *Die fossilen Reptilien des südamerikanischen Gondwanalandes.* Munich: C. H. Beck.

Huene, F. von 1956 *Paläontologie und Phylogenie der niederen Tetrapoden.* Jena: Gustav Fischer.

Hughes, B. 1968 The tarsus of rhynchocephalian reptiles. *J. Zool.* **156**, 457–481.

Huxley, T. H. 1859 Postscript to: On the sandstones of Morayshire (Elgin &c.) containing reptilian remains; and on their relations to the Old Red Sandstone of that county (by R. I. Murchison). *Q. Jl geol. Soc. Lond.* **15**, 435–436.

Huxley, T. H. 1869 On *Hyperodapedon*. *Q. Jl geol. Soc. Lond.* **25**, 138–152.

Huxley, T. H. 1887 Further observations on *Hyperodapedon gordoni*. *Q. Jl geol. Soc. Lond.* **43**, 675–694.

Jenkins, F. A. 1971 The postcranial skeleton of African cynodonts. *Bull. Peabody Mus. nat. Hist.* **36**, 1–216.

Jollie, M. T. 1960 The head skeleton of the lizard. *Acta Zool., Stockh.* **41**, 1–64.

Kemp, T. S. 1979 The primitive cynodont *Procynosuchus*: functional anatomy of the skull and relationships. *Phil. Trans. R. Soc. Lond.* B **285**, 73–122.

Kemp, T. S. 1980a The primitive cynodont *Procynosuchus*: structure, function and evolution of the postcranial skeleton. *Phil. Trans. R. Soc. Lond.* B **288**, 217–258.

Kemp, T. S. 1980b Aspects of the structure and functional anatomy of the Middle Triassic cynodont *Luangwa*. *J. Zool.* **191**, 193–239.

King, G. M. 1981 The functional anatomy of a Permian dicynodont. *Phil. Trans. R. Soc. Lond* B. **291**, 243–322.

Lécuru, S. 1968 Myologie et innervation du membre antérieure des lacertiliens. *Mém. Mus. natn. Hist. nat., Paris* (*Zool.*) **48**, 127–215.

Lydekker, R. 1885 The Reptilia and Amphibia of the Maleri and Denwa groups. *Palaeont. indica* (4) **1** (5), 1–38.

Malan, M. E. 1963 The dentitions of the South African Rhynchocephalia and their bearing on the origin of the rhynchosaurs. *S. Afr. J. Sci.* **59**, 214–220.

Miller, C. N. 1977 Mesozoic conifers. *Bot. Rev.* **43**, 217–280.

Newton, E. T. 1893 On some new reptiles from the Elgin sandstones. *Phil. Trans. R. Soc. Lond.* B **184**, 431–503.

O'Donoghue, C. H. 1920 The blood vascular system of the tuatara, *Sphenodon punctatus*. *Phil. Trans. R. Soc. Lond.* B **210**, 175–252.

Oelrich, T. W. 1956 The anatomy of the head of *Ctenosaura pectinata* (Iguanidae). *Misc. Publs Mus. Zool. Univ. Mich.* **94**, 1–122.

Osawa, G. 1898a Beiträge zur Anatomie der *Hatteria punctata*. *Arch. mikrosk. Anat. EntwMech.* **51**, 481–691.

Osawa, G. 1898b Beiträge zur Lehre von den Sinnesorganen der *Hatteria punctata*. *Arch. mikrosk. Anat. EntwMech.* **52**, 268–366.

Osborn, H. F. 1903 The reptilian subclasses Diapsida and Synapsida and the early history of the Diaptosauria. *Mem. Am. Mus. nat. Hist.* **1**, 449–507.

Ostrom, J. H. 1964 A functional analysis of jaw mechanics in the dinosaur *Triceratops*. *Postilla* **88**, 1–35.

Parsons, T. S. 1970 The nose and Jacobson's organ. In *Biology of the Reptilia*, vol. 2 (ed. C. Gans & T. S. Parsons), pp. 99–191. London: Academic Press.

Peacock, J. D., Berridge, N. G., Harris, A. L. & May, F. 1968 The geology of the Elgin district. *Mem. geol. Surv. U.K.* Edinburgh: H.M.S.O.

Perrin, A. 1895 Recherches sur les affinités zoologiques de l'*Hatteria punctata*. *Annls Sci. nat.* (*Zool.*) (7) **20**, 33–102.

Poglayen-Neuwall, I. 1952 Untersuchungen über die Trigeminusmuskulatur von *Hatteria*. *Z. wiss. Zool.* **157**, 57–76.

Pratt, C. W. McE. 1948 The morphology of the ethmoidal region of *Sphenodon* and lizards. *Proc. zool. Soc. Lond.* **118**, 171–201.

Reisz, R. R. 1981 A diapsid reptile from the Pennsylvanian of Kansas. *Spec. Publ. Mus. nat. Hist. Univ. Kans.* **7**, 1–74.

Retallack, G. J. 1977 Reconstructing Triassic vegetation of eastern Australasia: a new approach for the biostratigraphy of Gondwanaland. *Alcheringa* **1**, 247–277.

Rieppel, O. 1978 The throat musculature of *Sphenodon*, with comments on the primitive character states of the throat muscles in lizards. *Anat. Anz.* **144**, 429–440.

Rieppel, O. & Labhardt, L. 1979 Mandibular mechanics in *Varanus niloticus* (Reptilia: Lacertilia). *Herpetologica* **35**, 158–163.

Robinson, P. L. 1967 The evolution of the Lacertilia. *Colloques int. Cent. natn. Rech. scient.* **163**, 395–407.

Robinson, P. L. 1976 How *Sphenodon* and *Uromastyx* grow their teeth and use them. *Linn. Soc. Symp. Ser.* **3**, 43–64.

Romer, A. S. 1942 The development of tetrapod limb musculature – the thigh of *Lacerta*. *J. Morph.* **71**, 251–298.

Romer, A. S. 1944 The development of tetrapod limb musculature – the shoulder region of *Lacerta*. *J. Morph.* **74**, 1–41.

Romer, A. S. 1956 *Osteology of the reptiles*. Chicago: University Press.

Romer, A. S. 1963 La evolucion explosiva de los rhynchosaurios del Triasico. *Revta Mus. argent. Cienc. nat. Bernardino Rivadavia Inst. nac. Invest. Cienc. nat.* (*Cienc. zool.*) **8**, 1–14.

Romer, A. S. 1966 *Vertebrate paleontology*. Chicago: University Press.

Säve-Söderbergh, G. 1946 On the fossa hypophyseos and the attachment of the retractor bulbi group in *Sphenodon*, *Varanus*, and *Lacerta*. *Ark. Zool.* A **38** (11), 1–24.

Säve-Söderbergh, G. 1947 Notes on the brain-case in *Sphenodon* and certain Lacertilia. *Zool. Bidr. Upps.* **25**, 489–516.

Schaeffer, B. 1941 The morphological and functional evolution of the tarsus in amphibians and reptiles. *Bull. Am. Mus. nat. Hist.* **78**, 395–472.

Sill, W. D. 1969 The tetrapod-bearing continental Triassic sediments of South America. *Am. J. Sci.* **267**, 805–821.

Sill, W. D. 1971a Implicaciones estratigraficas y ecologicas de los rincosaurios. *Revta Asoc. geol. argent.* **26**, 163–168.

Sill, W. D. 1971b Functional morphology of the rhynchosaur skull. *Forma Functio* **4**, 303–318.

Sneath, P. H. A. & Sokal, R. R. 1973 *Numerical taxonomy*. San Francisco: W. H. Freeman.

Snyder, R. C. 1954 The anatomy and function of the pelvic girdle and hindlimb in lizard locomotion. *Am. J. Anat.* **95**, 1–46.

Throckmorton, G. S. 1979 The effect of wear on the cheek teeth and associated dental tissues of the lizard *Uromastix aegyptius* (Agamidae). *J. Morph.* **160**, 195–208.

Tucker, M. E. & Benton, M. J. 1982 Triassic environments, climates and reptile evolution. *Palaeogeogr. Palaeoclimatol. Palaeoecol.* **40**, 361–379.

Tumarkin, A. 1955 On the evolution of the auditory conducting apparatus: a new theory based on functional considerations. *Evolution* **9**, 221–243.

Underwood, G. L. 1970 The eye. In *Biology of the Reptilia*, vol. 2 (ed. C. Gans & T. S. Parsons), pp. 1–97. London: Academic Press.

Walker, A. D. 1961 Triassic reptiles from the Elgin area: *Stagonolepis, Dasygnathus* and their allies. *Phil. Trans. R. Soc. Lond.* **B 244**, 103–204.

Walker, A. D. 1964 Triassic reptiles from the Elgin area: *Ornithosuchus* and the origin of carnosaurs. *Phil. Trans. R. Soc. Lond.* **B 248**, 53–134.

Walker, A. D. 1969 The reptile fauna of the 'Lower Keuper' Sandstone. *Geol. Mag.* **106**, 470–476.

Warrington, G., Audley-Charles, M. G., Elliott, R. E., Evans, W. B., Ivimey-Cook, H. C., Kent, P. E., Robinson, P. L., Shotton, F. W. & Taylor, F. M. 1980 A correlation of Triassic rocks in the British Isles. *Spec. Rep. geol. Soc. Lond.* **13**, 1–78.

Watkinson, G. B. 1906 The cranial nerves of *Varanus bivittatus. Morph. Jb.* **35**, 450–472.

Watson, D. M. S. 1910 On a skull of *Rhynchosaurus* in the Manchester Museum. *Rep. Br. Ass. Advmt Sci.* (1909), 155–158.

Werner, G. 1962 Das Cranium der Brückenechse, *Sphenodon punctatus* Gray, von 58mm Gesamtlänge. *Z. Anat. EntwGesch.* **123**, 323–368.

Westoll, T. S. 1951 the vertebrate-bearing strata of Scotland. *18th int. geol. Congr., Great Britain* (1948), vol. **9** (11), pp. 5–21. London.

Wettstein, O. 1931 Rhynchocephalia. In *Handbuch der Zoologie* (ed. W. Kükenthal & T. Krumbach), vol. 7 (1), pp. 1–235. Berlin: de Gruyter.

Wever, E. G. 1978 *The reptile ear, its structure and function.* Princeton: University Press.

Wild, R. 1978 Die Flugsaurier (Reptilia, Pterosauria) aus der oberen Trias von Cene bei Bergamo, Italien. *Boll. Soc. paleont. ital.* **17**, 176–256.

Wild, R. 1980 Neue Funde von *Tanystropheus* (Reptilia, Squamata). *Schweiz. palaeont. Abh.* **102**, 1–43.

Williams, D. 1973 The sedimentology and petrology of the New Red Sandstone of the Elgin basin, north-east Scotland. Ph.D. thesis, University of Hull.

Wishart, D. 1978 *Clustan user manual* (3rd edn). Program Library Unit, Edinburgh University.

Wood, S. C. & Lenfant, C. J. M. 1976 Respiration: mechanics, control and gas exchange. In *Biology of the Reptilia*, vol. 5 (ed. C. Gans & W. R. Dawson), pp. 225–274. London: Academic Press.

Woodward, A. S. 1898 *Outlines of vertebrate palaeontology for students of zoology.* Cambridge: University Press.

Woodward, A. S. 1905 On some abdominal ribs of *Hyperodapedon* from the Keuper Sandstone of Hollington. *Rep. Trans. N. Staffs. Fld Club* **34**, 115–117.

Woodward, A. S. 1907 On *Rhynchosaurus articeps* (Owen). *Rep. Br. Ass. Advmt Sci.* (1906), pp. 293–229.

Wyeth, F. J. 1924 The development of the auditory apparatus in *Sphenodon punctatus*, with an account of the visceral pouches, aortic arches, and other accessory structures. *Phil. Trans. R. Soc. Lond.* **B 212**, 259–368.

KEY TO ABBREVIATIONS USED IN THE FIGURES

Skull

a	angular
aaf	anterior alveolar foramen
amf	anterior meckelian foramen
ap?	ala pro-otica (?)
ar	articular
asaf	anterior supra-angular foramen
asc	anterior semicircular canal
ba	basal aponeurosis
bo	basioccipital
bpt	basipterygoid process
brion	branch to inferior orbital nerve
brm 2	branch to maxillary nerve 2
bs	basisphenoid
bt	buccal tooth
c	coronoid
ch	choana
cJo	cartilage of Jacobson's organ
cu	cupola
d	dentary
dnv	dorsal nasal vein
ds	dorsum sellae
ec	ectopterygoid
emna	external mandibular artery
eo	exoccipital
ep	epipterygoid
f	frontal
fl	floccular recess
fo	fenestra ovalis
fve	fenestra vomeronasalis externa
hm	hyomandibular
hsc	horizontal semicircular canal
ia	inferior orbital artery
ica	internal carotid artery
if	infraorbital foramen
imna	internal mandibular artery
ina	inferior nasal artery
iof	inferior orbital foramen
ion	infraorbital nerve
j	jugal
jv	jugal vein
l	lacrimal
la	lateral ampulla
laf	lateral alveolar foramina
lc	lagenar crest
ld	lacrimal duct
len	lateral ethmoidal nerve
lhv	lateral head vein
ljf	lateral jugal foramen
lpra	lateral palatine ramus (of facial nerve)
lps	lateral palatine sinus
lr	lacrimal ridge
lt	lingual teeth
m	maxilla
m2n	maxillary 2 (+1) nerve
ma	maxillary artery
mamem	m. adductor mandibulae externus medialis
mamep	m. adductor mandibulae externus profundus
mames	m. adductor mandibulae externus superficialis
mamp	m. adductor mandibulae posterior

mc	meckelian canal
mcv	median cerebral vein
mdm	m. depressor mandibulae
mf	metotic foramen
mg	meckelian groove
mjf	medial jugal foramen
mna	mandibular artery
mnf	mental foramen
mnv	mandibular vein
mp	maxillary process (of nasal capsule)
mpla	median palatine artery
mpra	medial palatine ramus (of facial nerve)
mpstp	m. pseudotemporalis profundus
mpsts	m. pseudotemporalis superficialis
mpt	m. pterygoideus typicus
mv	maxillary vein
n	nasal
ns	nasal sinus
o	orbit
op	opisthotic
opa	ossified pila antotica
os	orbital sinus
p	parietal
pa	prearticular
paf	posterior alveolar foramen
pc	paranasal cartilage
pcv	posterior cerebral vein
pf	parietal fossa
pg	palatine ganglion
pl	palatine
pla	palatine artery
pm	premaxilla
pmf	posterior meckelian foramen
po	postorbital
popr	paroccipital process
pr	pro-otic
pra	palatine ramus (of facial nerve)
prf	prefrontal
prfv	prefrontal vein
prin	pro-otic incisure
ps	parasphenoid
psaf	posterior supra-angular foramen
psc	posterior semicircular canal
pt	pterygoid
ptf	postfrontal
pv	pterygoid vein
q	quadrate
qf	quadrate foramen
qj	quadratojugal
rf	retractor fossa
s	stapes
sa	surangular
sac	sacculus
san	superior alveolar nerve
sc	sclerotic plate
sf	suborbital foramen
so	supraoccipital
sp	splenial
sq	squamosal

sta	stapedial artery		v	vomer
ta	temporal artery		ve	vestibule
tr2	trigeminal nerve, branch 2		za	zona annularis
tso	tubera spheno-occipitale			

Postcranial skeleton

amb	m. ambiens		ilfib	m. iliofibularis
ast	astragalus		iltib	m. iliotibialis
calc	calcaneum		inttr	internal trochanter
cap	capitellum		istr	m. ischiotrochantericus
ce	centrum		lsd	m. longissimus dorsi
cent	centrale		pe	m. pectoralis
cfb	m. caudifemoralis brevis		pife	m. puboischiofemoralis externus
cfl	m. caudidemoralis longus		pifi	m. puboischiofemoralis internus
cor	coracoid		R	radius
delt	deltopectoral crest		sbsc	m. subcoracoscapularis
dsc	m. deltoideus scapularis		scha	m. scapulohumeralis anterior
dv	dorsal vertebra		spc	m. supracoracoideus
F	fibula		sup	m. supinator
ic	intercentrum		T	tibia
icl	interclavicle		tr	trochlea
ilfem	m. iliofemoralis		U	ulna

FIGURE 1. The type specimen of *Hyperodapedon gordoni*, EM 1978.566. Skull and skeleton (cervical and dorsal vertebrae, ribs, gastralia, forelimb, hindlimb) in ventral and left lateral views respectively (magn. ×0.4). The blocks are shown slightly separated since they do not fit together tightly now. Photographs by A. D. Walker.

FIGURE 2. Details of the skull and teeth. (*a*) Anterodorsal view of proximal end of the premaxilla, prefrontal and maxilla, showing bone surface textures; cast of NUGD A (magn. ×1.3). (*b*) Lateral view of a natural rock cast of the lacrimal duct, NUGD A (magn. ×3.0). (*c*) Lateral view of the right dentary and maxilla, jaws slightly open, showing complete and broken teeth, NUGD B (magn. ×1.5). (*d*) Palatal view of small left maxillary tooth plate, BMNH R3140 (magn. ×1.5). (*e*) Medial view of middle portion of a large dentary, showing buccal and lingual teeth, BMNH R4780 (magn. ×2.0).

KEY TO ABBREVIATIONS USED IN THE FIGURES

Skull

a	angular	mc	meckelian canal	sa	stapedial artery
aaf	anterior alveolar foramen	mcv	median cerebral vein	ta	temporal artery
amf	anterior meckelian foramen	mdm	m. depressor mandibulae	tr2	trigeminal nerve, branch 2
apr	ala pro otica (?)	mf	metotic foramen	rso	tubera spheno-occipitale
ar	articular	mg	meckelian groove		
asaf	anterior supra-angular foramen	mjf	medial jugal foramen	v	vomer
asc	anterior semicircular canal	mra	mandibular artery	ve	vestibule
ba	basal aponeurosis	mtf	mental foramen	za	zona annularis
bo	basioccipital	mv	mandibular vein		
bpt	basipterygoid process	mp	maxillary process (of nasal capsule)		

Postcranial skeleton

amb	m. ambiens	ilfib	m. iliofibularis
ast	astragalus	iltib	m. iliotibialis
calc	calcaneum	intr	internal trochanter
cap	capitellum	istr	m. ischiotrochantericus
cc	centrum	lsd	m. longissimus dorsi
cent	centrale	pec	m. pectoralis
cfb	m. caudifemoralis brevis	pife	m. puboischiofemoralis externus
cfl	m. caudifemoralis longus	piti	m. puboischiofemoralis internus
cor	coracoid	R	radius
dch	deltopectoral crest	sbc	m. subcoracoscapularis
dsc	m. deltoideus scapularis	srha	m. scapulohumeralis anterior
dv	dorsal vertebra	spc	m. supracoracoideus
F	fibula	sup	m. supinator
ic	intercentrum	T	tibia
icl	interclavicle	tr	trochlea
ilfem	m. iliofemoralis	U	ulna

(Note: additional Skull abbreviations follow in columns)

brion	branch to inferior orbital nerve
brm2	branch to maxillary nerve 2
bs	basisphenoid
bt	buccal tooth
c	cornutum
ca	choana
cJo	cartilage of Jacobson's organ
cu	cupola
d	dentary
dnv	dorsal nasal vein
ds	dorsum sellae
ec	ectopterygoid
ema	external mandibular artery
eo	exoccipital
ep	epipterygoid
f	frontal
fl	floccular recess
fo	fenestra ovalis
fve	fenestra vestibuli externa
hm	hyomandibular
hsc	horizontal semicircular canal
ia	inferior orbital artery
ica	internal carotid artery
if	infraorbital foramen
ima	internal mandibular artery
ina	interior nasal artery
iof	inferior orbital foramen
ion	infraorbital nerve
j	jugal
jv	jugal vein
l	lacrimal
la	lateral ampulla
laf	lateral alveolar foramen
lc	lagenar crest
ld	lacrimal duct
len	lateral ethmoidal nerve
lhv	lateral head vein
ljf	lateral jugal foramen
lpra	lateral palatine ramus (of facial nerve)
lps	lateral palatine sinus
lr	lacrimal ridge
lt	lingual tooth
m	maxilla
m2n	maxillary 2 (+1) nerve
ma	maxillary artery
mamem	m. adductor mandibulae externus medialis
mamep	m. adductor mandibulae externus profundus
mames	m. adductor mandibulae externus superficialis
mamp	m. adductor mandibulae posterior

mpla	median palatine artery
mpra	medial palatine ramus (of facial nerve)
mpsrp	m. pseudotemporalis profundus
mpsts	m. pseudotemporalis superficialis
mpt	m. pterygoideus typicus
mv	maxillary vein
n	nasal
ns	nasal sinus
o	orbit
op	opisthotic
opa	ossified pila antotica
os	orbital sinus
p	parietal
pa	prearticular
paf	posterior alveolar foramen
pc	paranasal cartilage
pcv	posterior cerebral vein
pf	parietal fossa
pg	palatine ganglion
pl	palatine
pla	palatine artery
pm	premaxilla
pmf	posterior meckelian foramen
po	postorbital
popr	paroccipital process
pr	pro-otic
pra	palatine ramus (of facial nerve)
prf	prefrontal
prfv	prefrontal vein
prin	pro-otic incisure
ps	parasphenoid
psaf	posterior supra-angular foramen
psc	posterior semicircular canal
pt	pterygoid
ptf	postfrontal
pv	pterygoid vein
q	quadrate
qf	quadrate foramen
qj	quadratojugal
rf	retractor fossa
s	stapes
sa	surangular
sac	sacculus
san	superior alveolar nerve
sc	sclerotic plate
sf	subcortical foramen
so	supraoccipital
sp	splenial
sq	squamosal